STUDIES ON NATURAL EXTRACTS AS INHIBITORS OF MILD STEEL CORROSION IN 1M HCl SOLUTION

A THESIS IN CHEMICAL ENGINEERING

Presented to the Faculty of the American University of Sharjah
Collage of Engineering
in Partial Fulfillment of
the Requirements for the Degree of

MASTER OF SCIENCE

by
ALAA SHANABLEH
B.S. 2009

Sharjah, UAE
January 2011

We approve the thesis of *Alaa Shanableh*

Date of signature

Dr. Taleb Ibrahim Associate Professor, Chemical Engineering Thesis Advisor	
Dr. Nabil Abdel Jabbar Professor, Chemical Engineering Thesis Co-Advisor	
Dr. Mohamed Abou Zour Sr. Technical Consultant External Advisor	
Dr. Zarook Shareefdeen Associate Professor, Chemical Engineering Graduate Committee	
Dr. Sofian Kanan Associate Professor, Chemistry Graduate Committee	
Dr. Dana Abouelnasr Associate Professor of Chemical Engineering Program Director	
Dr. Hany El-Kadi Associate Dean College of Engineering	
Dr. Yousef Al Assaf Dean College of Engineering	
Dr. Gautam Sen Vice Provost for Research and Graduate Studies	

STUDIES ON NATURAL EXTRACTS AS INHIBITORS OF MILD STEEL CORROSION IN 1M HCl SOLUTION

Alaa Nidal Shanableh, Candidate for the Masters of Science Degree

American University of Sharjah, 2010

ABSTRACT

The inhibitive action of the aqueous plant leaves extracts and their mixtures toward the corrosion of mild steel in 1M HCl solution is investigated using different standard corrosion measurements. Inhibitors used are extracted from Figs, Olives, Rosemary and Cypress plants. Corrosion weight loss technique is applied on mild steel plates to evaluate inhibition efficiency in the presence of these plant extracts as corrosion inhibitors. Electrochemical techniques including Linear Polarization Resistance (LPR), Electrochemical Impedance Spectroscopy (EIS) and Cyclic Sweep are used in order to validate and support inhibition efficiencies from the weight loss technique and confirm the inhibition properties and mechanisms of the extracted plants. A detailed study of the experimental results is reported for each of the tests conducted. Moreover, the adsorption film isotherm is determined from the experimental data obtained and the kinetics are found to follow Langmuir isotherm.

The results showed that the extracts serve as excellent corrosion inhibitors for the tested system. It was observed in all tests that the inhibition efficiency increases as the plant extract concentration increases. The electrochemical analysis also confirmed that the corrosion current density decreases as the concentration of

the extract increases, causing a reduction in the corrosion rate of the mild steel specimen. It was also found that the inhibitors explored in this study act as mixed-type inhibitors. Moreover, Nyquist plots from EIS also proved that as the concentration of plant extracts increases, the charge transfer resistance increases and the double layer capacitance decreases. The inhibitive action of the plant extracts demonstrates that the adsorption of plant extracts is spontaneous, and the physical adsorption follows Langmuir adsorption isotherm.

The inhibition efficiency of these plant extracts is explained thoroughly in this study. The evaluation looks at inhibition performances under different test conditions, especially the more relevant oil and gas production conditions. The inhibition of the plant extracts is studied at 25^{o}C as well as elevated temperatures of 45^{o}C and 55^{o}C. The inhibition efficiency decreases as the temperature increases causing an increase in the corrosion rate of the mild steel sample. The decrease in the inhibition efficiency with the rise in temperature and activation energy, in presence and absence of inhibitor, suggests the formation of an adsorption film of a physical nature. The maximum inhibition efficiency was obtained when using pure fig inhibitor extract. However, the result changes for conditions of elevated temperatures.

A comparison is made between some commercial inhibitors and the studied plant extracts. Electrochemical analysis is applied at 25^{o}C and at concentrations of 400 and 1000 ppm in 1M HCl solution. The study showed that the inhibition efficiencies of commercial inhibitors are comparable to the one's obtained by natural inhibitors. This study demonstrates high inhibitive action of the plant extracts used. All tests performed proved similar trends in inhibitive action of the extracts. An insight about the formation of a protective film on the mild steel specimen is clarified by electrochemical analysis. The film formation caused by adsorption causes the reduction of the corrosion rate in such media.

TABLE OF CONTENTS

LIST OF FIGURES

Figure	Page #

LIST OF TABLES

Table	Page

ACKNOWLEDGEMENTS

The author takes this opportunity to express his sincere appreciation to his major professor and advisor; Dr. Taleb Ibrahim, for his guidance, insight and genuine contribution to this thesis. The author is grateful for the financial support on this project that was generously bestowed by his advisor. The author would like to thank the Department of Chemical Engineering for their funding and assistantship offered throughout the accomplishment this thesis. Furthermore, particular gratitude is expressed to Dr. Nabil Abdel Jabbar for his continuous support and encouragement. The author would also like to show his appreciation to Dr. Abou Zour for his special assistance and insight throughout the entire work. Special thanks to Mr. Ricardo De Jesus from the Manufacturing Lab for helping in preparing the specimens used. I extend my sincere recognition to the committee members for their cooperation and feedback in this thesis.

Last, but not least, the author would like to thank his family in Jordan, his parents, sister and his brother in Oklahoma for their support and inspiration during the achievement of this conducted study.

Chapter 1: Introduction

Mild steel is the main metallurgy used for the various industries, especially the oil and gas industry due to its availability and relatively inexpensive cost. However, corrosion has had a great impact on all the industries, which makes it a crucial obstacle that needs to be solved. The need for corrosion inhibitors is sometimes a must in order to control unacceptably high corrosion rates. The use of inhibitors is one of the most efficient methods for protection against corrosion especially in acid solutions to avoid metal dissolution [1]. In addition to selecting corrosion resistance alloys and using internally lined pipes and/or vessels, chemical inhibition is a commonly used approach to control internal corrosion reactions due to the various corrosive environments. Corrosion inhibitors have been used massively in industry in order to reduce the corrosion rate of many metals. The few thousands of articles and publications issued about corrosion and its prevention every year makes one understand the importance of corrosion prevention.

Many investigations been conducted in the field of finding the suitable corrosion inhibitors. However, most of the corrosion inhibitors are synthetic chemicals that could be difficult to synthesize, and as a result incur relatively higher manufacturing costs. Moreover, and most importantly, these inhibitors can also be of a great threat to the environment and the public since they can be hazardous and toxic or carcinogenic in many cases [2]. This makes the investigation and the ongoing trend of finding safe and eco-friendly corrosion inhibitors of crucial importance to many industries. Natural or Green Inhibitors are considered a promising field of research as these natural chemistries pose much lower risks in terms of handling and impact on humans and the environment. Furthermore, due to their natural availability, they are easier to produce and cheaper to buy.

The inhibition of different plant extracts are studied and investigated thoroughly on a mild steel specimen sheet of the following dimensions (50 x 25 x 1.5 mm) in aqueous 1M HCl solution. The composition of the mild steel sheet is 0.79 Mn, 0.18% C 0.03% Cu, 0.02% Cr, 0.21% Si and the rest is Fe. The investigation is

conducted at room temperature as well at elevated temperatures such as 45^0C and 55^0C. Naturally produced inhibitors are extracted from four plants which are Fig, Olive, Rosemary, and Cypress. The study uses these four plants as pure extracts, in addition to a mixture of Fig and Olive leaves. Extracts are isolated from these plant leaves, which are available at a low cost and do not affect the food industry. Corrosion weight loss technique is applied on each plant separately, in addition to a mixture of fig and olive extracts, to evaluate inhibition efficiency in the presence of these plant extracts as corrosion inhibitors. Electrochemical techniques, including Linear Polarization Resistance (LPR), Electrochemical Impedance Spectroscopy (EIS and cyclic sweeps, are used to validate and confirm information from the weight loss technique. These techniques also help give additional information about the inhibition properties and mechanisms of the extracted plants. A detailed study of the experimental results is reported for each of the tests conducted. Moreover, the adsorption film isotherm and thermodynamic properties are determined from the experimental data obtained.

The results obtained are explained and studied systematically. The extracted naturally-produced, green inhibitors are then to be compared in order to attain and determine the maximum inhibition efficiency and the minimum effective inhibitor concentration (MIC).

The main objective of this thorough investigation is to widen the scope on some highly inhibitive properties of some green extracts to be used as corrosion inhibitors. The plants to be used in the extraction of green inhibitors are Fig, Olive, Cypress, Rosemary and mixtures of Fig and Olive leaves. These inhibitors are to be evaluated to find the inhibitive properties on mild steel sheets in hydrochloric acid, a corrosive media. There are literature studies conducted in this field [3–12]; however, few been studied thoroughly and under various conditions. The investigation is also to be extended in order to understand the effect of temperature on the inhibitive properties of these green inhibitors using weight loss, impedance, cyclic sweep and potentiostatic polarization methods.

The thesis is divided into five chapters, where the problem statement, proposed work and the aim of the proposed work are discussed in Chapter 1. A general literature review of corrosion along with chemical inhibitors, natural

inhibitors, inhibition efficiency, adsorption of inhibitors and adsorption of corrosion inhibition, studies conducted and related to the conducted work are outlined in Chapter 2.

In Chapter 3, the testing methodology and the experimental work is discussed. Following that is the determination of testing method, specifications of the methods used, experimental preparations and procedure, instrumentations, weight loss method, and electrochemical test cell. Moreover, potensiostat analysis which includes LPR, EIS and cyclic sweep tests are also discussed in Chapter 3.

In Chapter 4, the preliminary results obtained from the experimental work are discussed in detail. Results and analysis of weight loss method, electrochemical analysis and adsorption isotherm is also considered in this chapter. Finally, a brief conclusion and recommendations are outlined in Chapter 5.

Chapter 2: LITERATURE REVIEW & BACKGROUND

This chapter represents an overview of the corrosion processes. Corrosion is described in terms of definition, Types, effects and prevention. Then, an insight about inhibitors, their types, inhibition efficiency, advantages and challenges of common inhibitors is given. The importance adsorption and different types of adsorption are illustrated in this chapter. A detailed literature review of different natural inhibitors studied in literature is summarized and explained. Last but not least, a background on the importance of corrosion inhibition is discussed by the end of this chapter.

2.1 Corrosion

Many structural metals and alloys can undergo a surface phenomenon called corrosion. This phenomenon appears whenever these metals and alloys are subjected to an attack by its environment. Such environments are air, water, soil or any corrosive media that may cause this attack. A reaction of the metal with its environment to produce a more stable compound causes that metal to corrode [13].

Corrosion is commonly defined as the wearing a way of metals due to chemical reactions, but in more scientific meaning is a physiochemical interaction between any exposed metal and its surrounding oxygen that results in the formation of an oxide and salts. It appears as rust, such as etching or staining. Rust is the accordance of a combination between iron, water and oxygen and usually forms if humidity is over 30% [13]. Rust is scientifically known as oxidized metal, meaning that it occurs when we have long contact between air and the metal to form an oxide [13].

Metallic corrosion is an important effect that must be studied for different reasons. Corroded media are more available than before because of water and air pollution. Moreover, oil and gas are still the main sources of energy and are usually produced and stimulated using highly acidic media and erosive mud. Furthermore, produced fluids and gas environments are very corrosive due to the production of acid

gases, organic acids together with associated water. Additionally, the vast technology development, in most cases, depends on various types of metals. Moreover, metals used in industries related to the field of nuclear energy or producing energy in general are very expensive, and replacing them once they corrode is very costly.

2.1.1 Corrosion Types and Effects

Many industries are threatened by corrosion such as the chemical processing industries for stainless steel tanks, pipelines and flanged joints. Moreover, nuclear power generation and onshore/offshore oil and gas industries are highly affected.

In some cases, corrosion occurs when two different metals electrically contact each other and are immersed in an electrolyte. This is called galvanic corrosion. It depends on the presence of an anode and a cathode metal; for example, Zinc could be the anode for steel. This steel is found in many pipelines and naval ships so this galvanic corrosion is an economical problem for marine and water industries [14].

In other cases, pitting corrosion can happen when low levels of oxygen and an anion such as chloride is present. This type of contact results in the reformation of a film (passivating film) that can cause a break in the metal if high pressure is applied on it. Furthermore, it can form holes, or pits, in the pipes and alloys [14]. Another form of corrosion is called high temperature corrosion, which is a chemical corrosion of a material subjected to conditions with very high temperatures as well as oxygen, sulfur or other oxidizing compounds [14].

Methods all over the world are used to reduce the activity of the exposed surfaces to surrounding oxygen in air, water supplies and or any corrosive medium; this is because corrosion is an industrial and economical problem to human populations and societies. In 2002, the U.S. Federal Administration released a break-through of a 2-year study on the direct costs of metallic corrosion in every industry sector in the states starting from infrastructure and transportation and ending in production and manufacturing. Results of the study showed that the total annual cost of corrosion in the U.S. is approximately 276 billion dollars and is increasing every year [15].

In the process of evaluating costs of corrosion, scientists discovered various methods to inhibit its occurrence. The methods included the use of corrosion inhibitors, either chemical or natural (inorganic or organic). When they are added in small amounts (usually ppm levels) to a fluid or gas, they decrease the corrosion rate of a metal or an alloy. These inhibitors can also be used as a painted layer or coated on the metal. This was designed to increase the ability to protect human safety and the environment.

2.2 Inhibitors

2.2.1 General Overview

Corrosion inhibitors are organic or inorganic species which are added at low concentrations to a corrosive solution in order to reduce the corrosion rate [16].

Corrosion inhibition can function in three different ways [16]:-

1. The reagent forms a precipitate or catalyzing the formation of a passive layer on the metal; examples are hydroxyl ion, phosphate, carbonate and silicate.
2. Oxidants shift the surface potential of the metal in the positive direction until the passive zone. However, if the oxidants are not available in sufficient amounts the metal surface will stay in the active zone.; for example, nitrite and chromate
3. A reagent which will be absorbed on the metal surface diminishing the metal dissolution or reduction.

Screening out the inhibitors is an initial step of eliminating undesired candidates. This might lead to elimination of some inhibitors that can perform well in the medium studied. However, the main aim of the elimination is that some inhibitors perform poorly in some systems studied, and limited sources make it almost impossible to examine all possible inhibitors.

When choosing an inhibitor one must investigate:

1. The inhibitor phase needed (liquid state or solid state)
2. Physical properties such as flash, melting or freezing points

3. The solubility of the inhibitor
4. Compatibility with material of construction
5. Environmental and hazardous impacts on humans and environment
6. The amounts needed of that specific inhibitor
7. The inhibition efficiency and persistency of the selected inhibitor.

All these crucial points are major points in choosing the inhibitor to be used in a certain environment or system. A researcher should consider take these points seriously in order to save time and resources in any study or investigation.

2.2.2 Chemical Inhibitors

Corrosion inhibitors are added to coolants, fuels, boiler water or fluid and many other fluids used in industry. They are also added as coatings. Various types of corrosion inhibitors are present and some include hexamine, phenylenediamine, polyaniline, sodium nitrite. The types can be divided into the following groups: Anodic, Cathodic or mixed. These chemicals are either surface active chemicals or non surface active chemicals [14,15].

Chromates are an example of anodic inhibitors, which form a passivity layer on aluminum and steel to prevent the oxidation of the metal. However, they are known to be carcinogenic to humans. Therefore, the use of this inhibitor has been extremely reduced. A less active chemical mixture for surface treatment of aluminum is a solution of sodium dichromate and chromic acid. Entrapped solutions of this mixture are less likely to corrode metal surfaces than chromic acid inhibitor solutions. Nitrite is another anodic inhibitor. If anodic inhibitors are used at low concentrations, they can form pitting corrosion, because they form a non uniform layer. Another anodic inhibitor is called pertechnetate. It is interesting, because it has a higher radioactivity than uranium and may be used only in very safe areas such as reactors [14].

Cathodic inhibitors such as zinc oxide reduce corrosion by inhibiting the reduction of water to hydrogen gas. Other examples are volatile amines. They are present in steam, usually used in the boilers. They increase the pH; as such, they make

proton reduction less favorable. Additionally, the amines can form a protective film on the steel surface and act as an anodic inhibitor [15,16].

An inhibitor that acts both in a cathodic and anodic manner is termed a mixed inhibitor. Hydrazine and ascorbic acid (vitamin C) both help reduce the rate of corrosion in boilers by removing the oxygen from water. Unfortunately, hydrazine is also a highly toxic carcinogen [15,16].

Benzalkonium chloride, imidazolines, fatty acids, phosphonates, their mixtures and derivatives are commonly used in the oil and gas industry. They are categorized as organic type inhibitors/filmers and have various mechanisms to give steel the inhibition needed to resist the various corrosive and aggressive environments [15,16].

2.2.3 Inhibition Efficiency

In one study done on copper corrosion inhibitors, higher inhibitor concentration and longer exposure of copper in the inhibitor solution led to an increase in the inhibition efficiency [17]. It was noticed that higher inhibition efficiency is achieved by applying organic compounds more than inorganic. Thiazoles, benzotriazole, triazoles provide good protection, except in strongly acidic media, and tetrazoles and imidazoles are revealed to be effective [17]. These materials function by the process adsorption. The organic molecule attaches to the solid surface, which prevents the corrosive entity from accessing the surface. The attachment does not need total electron transfer. Furthermore, the adsorbed layer can be formed all over the surface, either in a single layer or as a multilayer. The more complete the coverage, the better inhibitive action. As for fuels, they also need anti-corrosive commercial inhibitors such as the ones used in jet fuels, power plants, motor gasoline and pipelines systems [17].

In another study on chemical corrosion inhibitors for protection of metallic fiber reinforcement in fibrocement composites**,** the corrosion inhibitors, viz. calcium nitrite and tannic acid, were used, and the corrosion efficiency and rate were calculated [18]. However, only almost 1% of both the inhibitors give very high efficiency and a corresponding low corrosion rate. The dose gives a sufficient degree

of protection to the metallic fabric, which is termed inhibitory efficiency [18]. The study also concluded that the high efficiency and low corrosion rate exhibited by both the inhibitors improves their potential in controlling the corrosion. Long term studies are needed to determine whether this dose is recommended [17, 18].

2.2.4 Natural Inhibitors

Most of the effective corrosion inhibitors are synthetic chemicals with high cost. At the same time, the use of such synthetic compounds can cause harm to public and environment. Fortunately, most of the naturally-occurring substances are safe and can be extracted by simple and inexpensive procedures [2].

The field of extracting eco-friendly corrosion inhibitors has been promising and effective. Comparisons have been made through the years between the toxic chemical inhibitors, such as chromates, and the natural inhibitors. It has been observed that the natural inhibitors could potentially serve as an effective substitute for the chemical inhibitors, since some studies showed that their inhibition efficiency is significantly better than that of synthetic inhibitors. Recent studies have tested different extracts for corrosion inhibition applications. The examples are numerous such as Henna, Olive, Ferula Harmonis, natural honey, Onion, Ficus and many oils extracted from different parts of plants. Some are extracted from plant leaves and fruits. Many of these natural substances proved their ability to act as corrosion inhibitors for the corrosion of different types of metals [2,4].

Natural corrosion inhibitors have been studied using different plant extracts. Buchweishaija and Mhinzi have studied the gum exudates from Acacia seyal var. seyal as an inhibitor for mild steel corrosion in drinking water systems [19]. It was found that the gum exudates can block the electrochemical processes taking place on the steel undergoing corrosion in water. It reduces both the rate of cathodic and anodic reactions. Moreover, it shifts the open corrosion potentials towards less negative values. These factors suggest that the Acacia. seyal var. seyal inhibitor acts as anodic type corrosion inhibitor. The product was found to efficiently inhibit the corrosion of mild steel up to 75% [19].

Satapathy *et al*. have investigated the effect of Justicia gendarussa extract (JGPE) on mild steel, with dimensions of 1.0 x 4.0 x 0.2 cm in 1M HCl medium [20]. Weight loss and electrochemical methods were used in the investigation at room temperature and at 50-70°C. The maximum inhibition efficiency was found to be around 93% using mixed inhibitor type. A concentration of 150 ppm was added to the studied solution in order to achieve this efficiency at room temperature. The inhibitor used was considered a mixed type inhibitor since there was a change in both the cathodic and anodic tafel constants. However, it can be noticed that the cathodic change is predominant. The cathodic current-potential curves were parallel lines, which mean that the hydrogen evolution did not change by the addition of the inhibitor. The surface area available for hydrogen ions was reduced by the adsorption of the inhibitor on the studied surface. The adsorption mechanism acts as a barrier for hydrogen evolution reaction.

It can be noticed from the anodic polarization curves recorded by Satapathy *et al* that a uniform anodic corrosion is taking place. The film blocking the corrosion on the surface was found to be an oxide film and traces of the green inhibitor. The addition of the inhibitor showed a decrease in the corrosion current density, which indicates a decrease in the corrosion rate caused by the corrosive media [20]. The EIS reveals a decrease in the corrosion rate. The radius of the semicircle of the real impedance axis increases as the inhibitor is added. This proves a decrease in the corrosion current density and the corrosion rate. It can also be seen that the resistance of the charge transfer is increasing as the inhibitor is added to the corrosive media. This indicates a decrease in the current transferred and the corrosion occurring. It was found that adsorption obeys Langmuir isotherm. An increase in the activation energy of the corrosion process in presence of the green inhibitor indicated a physical adsorption is occurring [20].

El-Etre investigated the inhibition of the aqueous extract of olive leaves on carbon steel, with dimensions of 1.0 x 1.0 x 0.5 cm in 2M HCl media [21]. The study was conducted using potentio-dynamic polarization, cyclic sweep and weight loss methods at 25^{o}C. The inhibition efficiency was found to be 93%. The inhibitor adsorbs to surface and reduces charge transfer which reduces corrosion. It was established that as the concentration of the inhibitor increases the inhibition efficiency increases. The maximum inhibition efficiency was found to be at a concentration of

900 ppm. It was observed in the adsorption test that as the inhibitor is added the surface coverage increases where it reaches a maximum value of 0.91 when the maximum concentration of the olive extract is added to the corrosive media. It can be seen that the inhibition efficiency is directly proportional to the surface coverage of the adsorbed inhibitor. This indicates that the adsorption obeys Langmuir isotherm model. The constant of adsorption (k) was obtained from the plots of Langmuir model and used to find the standard energy of adsorption. The obtained value of standard energy of adsorption was found to be -8.74 kJ/mol. The negative sign indicates that the adsorption of the olive extracts is a spontaneous and also suggests a strong physical adsorption process, since it is less than -40 kJ/mol [21].

The polarization studies were conducted at a scan rate of 5mV/s. The polarization curves indicate a shift towards more negative potential values and less current density, which indicates an increase in the inhibition efficiency by the addition of olive extract inhibitor. The corrosion current density decreases, where the Tafel slopes increase upon the addition of the inhibitor. Moreover, the presence of inhibitor decreases the charge density passing in the solution [17]. As the temperature of the media increases, the inhibition efficiency decreases to almost 7% at the maximum studied temperature [21].

Abiola *et al* studied the effect of the extract of phyllwnthus amarus leaves on corrosion of aluminum in 2M NaOH using weight loss and electrochemical methods. The maximum inhibition efficiency obtained was 76% at a concentration of 20% volume composition. It was found that this experiment was conducted at 30^{o}C and the adsorbed film obeyed Langmuir isotherm [22]. The immersion time for each coupon used was for a period of six hours, which is not an accurate measure, since the weight loss is known to be a long term test. Therefore, the immersion time should be more than an hour in order to obtain more accurate results. The specimen used was cleaned for an hour by immersing it in a concentrated nitric acid solution and then washing with water. The specimen is then dried and weighed again [22]. A zero-order kinetics relationship was obtained in the presence and absence of the green inhibitor. The maximum surface coverage obtained by the inhibitor was recorded to be 0.76 of the specimen used. It was seen that as the concentration of the inhibitor used increases, the inhibition efficiency increases until it reaches its maximum. The adsorption of the

inhibitor on the metal surface blocked the corrosion sites on the specimen which resulted in reducing corrosion [22].

Okfor *et al*. investigated the inhibitive action of leaves, seeds and a combination of both on mild steel corrosion in HCl and H_2SO_4 at different concentrations and at room temperature and 40°C. The maximum efficiency found was about 94%, and the experiment obeyed Temkin isotherm [5]. The weight loss test was conducted at a temperature of 30°C and 40°C for the hydrogen evolution measurements. The results obtained show that the weight loss increases with time and decreases as the inhibitor concentration increases. This indicates an increase in the inhibition efficiency. The corrosion rate measured was found to be less in HCl media compared to H_2SO_4 solutions. The values obtained followed first-order kinetics. The half life was obtained from the values of rate constants. The recorded half life showed an increase with increasing the concentration of the green inhibitor [5].

The inhibition of the mild steel specimen used with the increase of the inhibitor concentration can be explained by the adsorption of the inhibitor components used on the metal surface. The results obtained from the paper shows that the inhibition efficiency increases with the addition of the inhibitor as well by increasing the temperature of the environment. This study also indicates that the inhibition action is due to chemical adsorption of the inhibitor composed components on the surface of the metal. The experimental data obtained followed Temkin isotherm model. The negative values of the interaction parameters obtained indicated strong repulsive interactions between the adsorbed components of the inhibitor. The adsorption constant values show an increase with increasing temperature, which indicates a chemical adsorption. The inhibitor used provided good inhibition for mild steel in both environments investigated in the study [5].

El-Etre and El-Tantawy investigated the inhibition of Ficus extract on carbon steel, Ni, Zn of size 5.0 x 1.0 x 0.2 cm in 0.1M HCl, 0.1M NaOH and 3.5% NaCl media [23]. The investigation was performed at room temperature. Using weight loss and polarization technique, the maximum efficiency was found to be 86%, and it obeyed Langmuir isotherm. The negative value of the standard free energy of adsorption indicated the spontaneity of the process. It was found that the inhibition efficiency increases as the inhibitor is added to the corrosive media. The highest

inhibition efficiencies were obtained in alkaline media, where the lowest were obtained in the acidic media. The tafel constants changes in both the cathodic and anodic region indicating that the inhibitor used is a mixed type inhibitor. The pitting potential at which the current suddenly increases was shifted to less active region as the inhibitor is added to the studied media [23].

Pandian *et al*. studied the inhibition of black pepper extract on mild steel of size 3.0 x 1.0 x 0.21 cm in 1M H_2SO_4. The methods used were weight loss, potentio-dynamic polarization and impedance tests [24]. The maximum efficiency obtained was 90%, and it obeyed Temkin isotherm. The study was conducted at two temperatures, 303K and 323K. In the weight loss method, the specimens used were exposed to 100 mL of the solution for about two hours and the final weight was recorded. However, the exposed time is not that enough for such a long term test. This can yield errors in the result. The inhibition efficiency was found to increase as the inhibitor is added until it reaches the maximum value obtained. This result indicates that as the inhibitor is added, the molecules of the inhibitor block the active sites, protecting the metal from the corrosive environment. The inhibition efficiency increased as the temperature increased. This suggests the strong adsorption of the black pepper extracts [24].

The electrochemical impedance test shows a reduction in the charge transfer and an increase in the resistance in the charge transfer, which indicates a decrease in the corrosion rate [24]. The depression in the semicircles recorded indicates the irregularity and in- homogeneities of the used media. The results show a decrease in the values of the double layer capacitance indicating a decrease in the corrosion current density and in the corrosion rate as the inhibitor is added. The tafel polarization test shows that, as the inhibitor is added to the solution used, the current value decreases, indicating a decrease in the corrosion attack. The study shows a good inhibition of mild steel using black pepper plant extracts [24].

Al-Sehaibani studied the inhibition of water extract of Henna on steel, Al of size 2.0 x 5.0 x 2.0 cm in different media. It was found using weight loss and potentio-dynamic polarization tests that the maximum inhibition efficiency is around 96% [25]. The leaves extracts were used to study the inhibition on steel and aluminum

in different media. The maximum inhibition efficiency was recorded in this study at a concentration of 20 g of plant extract in 1 liter solution.

Weight loss tests for few days showed an inhibition efficiency of 96% for steel in acidic media and 99.8% inhibition efficiency in the case of aluminum in base media. However, the study showed no inhibition efficiency in the case of aluminum and steel in salt solution. The inhibition efficiency decreased with increasing corrosive concentration. On the other hand, the inhibition efficiency increases with increasing extract concentration. This occurs due to the adsorption process occurring on the metal surface [25]. It is proven that the process follows a chemisorption process. The active components of the plant extract were recorded to be 18% by weight of the extract produced. The cost of all of henna extracts used are considered to be inexpensive and proven to reveal good inhibition efficiency on the metal used.

Pandian and Sethuraman researched the inhibition of Datura Stramonium extract on mild steel of size 3.0 x 1.0 x 0.21 cm in 1M HCl and 1M H_2SO_4 at different temperatures. It was found that the maximum inhibition efficiency obtained is 88.07% for HCl at 50°C and 91.46% for H_2SO_4 at 50°C. The weight loss test, electrochemical tests and impedance were constructed under the previous conditions. The studied temperatures were 303, 313 and 323 K. In the weight loss test, the inhibition efficiency increases as the green inhibitor is added. The maximum inhibition efficiency was obtained at a concentration of 20 ppm. Moreover, the inhibition efficiency increases as the temperature increases, suggesting chemisorption on the metal surface. Adsorption obeys Temkin isotherm [26].

It is shown in the Nyquist plots obtained that the semicircles are depressed. This is due to some in-homogeneities in the solution. The value of the charge transfer resistance increases with the addition of the green inhibitor, while the value of the double layer capacitance decreases. This indicates that there is more resistance to corrosion since less charge is being transferred through the solution [26]. The tafel polarization test showed that the value of the current density decreases as the inhibitor is added. Moreover, the shift in the potential was in the anode and the cathode parts, proving that the green inhibitor acts as a mixed inhibitor in both environments [26].

The use of natural products as corrosion inhibitors has been investigated. These include acid extracts of seeds, leaves and bark from the Figus virens plant,

Datura metel , Allium sativum, Olive, Zenthoxylum alatum ,and juice extracts of Magnifera indica (mango). It was found that all the plant materials act as good corrosion inhibitors for metal corrosion in acidic media. They act by forming a protective film on metal surfaces by coordinating with metal ions through O, S or N atoms of the functional groups present [27]. Polar organic compounds containing O, S, and N are good corrosion inhibitors as they may be responsible for the formation of a film layer which blocks discharge of hydrogen ions and dissolution of metal ions. Also, acid medium inhibitors containing organic N, amine, S, and OH groups inhibit corrosion in a similar fashion [27].

2.2.5 Film Forming Inhibitor

Film forming inhibitors are divided into passivating inhibitors and precipitation inhibitors [16]. Passivating inhibitors are the type of inhibitors that promote the formation of passive films on the surface of a metal. Passivating inhibitors are divided into two classes [16]:-

1. Oxidizing inhibitors: inorganic chromates and niratess that can passivate steel.
2. Non oxidants: such as phosphate that requires the presence of oxygen to passivate steel.

Precipitation inhibitors are species that undergo a precipitation reaction with the metal surface forming a barrier complex film on the surface of the metal. This does not involve adsorption on the metallic surface [16].

According to the electrochemical reaction, inhibitors in general may be specified as anodic, cathodic or mixed inhibitors. Inhibitors used in this thesis are considered organic and a mixed type inhibitors since they experience both cathodic and anodic electrochemical reactions.

2.2.6 Adsorption Inhibitors

Depending on the nature forces between the adsorbate and adsorbent, adsorption can be either physical or chemical adsorption:-

a) Physisorption

In physical adsorption, the attraction forces existing between the molecules of the adsorbate and the adsorbent are van der Waals' type, known to be weak in strength. The process of physical adsorption can be easily reversed by applying heat or decreasing the adsorbate pressure. This is due to the weak forces attaching them [28].

b) Chemisorption

In chemical adsorption, the molecules form chemical bonds with the molecules on the surface. The forces of attraction between the adsorbate and the adsorbent are considered very strong [28].

Table 1: Differences between chemical and physical adsorption.

Physisorption	Chemisorption
Forces of attraction are Vander Waals' forces	Forces of attraction are chemical bond forces
Low enthalpy of adsorption (20-40 kJ/mole)	High enthapy of adsorption (200-400 kJ/mole)
This process is observed under conditions of low temperature	This process takes place at high temperatures
not specific	highly specific
Multi-molecular layers may be formed	Generally, monomolecular layer is formed
This process is reversible	This process is irreversible

Adsorption inhibitors are known to form a chemisorptive bond with the metal surface avoiding any undesired electrochemical reaction. Chemisorption is a sub-class of adsorption, driven by a chemical reaction occurring at the exposed surface. A new chemical species is generated at the adsorbant surface (e.g. corrosion, metallic oxidation). The strong interaction between the adsorbate and the substrate surface creates new types of electronic bonds - ionic or covalent, depending on the reactive chemical species involved [28]. The types of adsorption are dependent on certain factors such as the chemical structure of the metal surface, chemical composition of the solution and electrochemical potential between the metal and the solution [28].

2.2.7 Importance of Corrosion Inhibition

Corrosion education and training in the United States and other parts of the world includes degree programs, certification programs, company in-house training, and general education and training. Also there are few national universities that offer courses in corrosion and corrosion control as part of their engineering curriculum.

Professional organizations such as the National Association of Corrosion Engineers (NACE) and the Society for Protective Coatings (SSPC) offer courses and certification programs from basic corrosion to coating inspector and cathodic protection specialist. These all are indications on the importance of corrosion control and economical impact on the world [13].

Corrosion damage can be classified under four types according to their causes. These types are: (1) negligible damage, (2) damage repairable by patching, (3) damage repairable by insertion, and (4) damage that requires replacement of parts [13, 15].

On the other hand, scientists have tried to control corrosion rate by reducing the tendency of the metal to oxidize. The methods are by reducing the aggressiveness of the medium or by isolating the metal from the fluid by coating the metal with a non-corroding material. The latter is widespread, but its effect may not be permanent because of breaks in the coating over time. Furthermore, in some systems, coating might interfere with the process and the equipment, because it can change the heat transfer properties.

There are two important reasons why scientists and engineers are interested in methods to control or inhibit corrosion by the use of corrosion inhibitors. The first is the issue of safety since industrial corrosion can lead to process breakdowns that could cause explosions or the release of chemicals that are dangerous to human health. The second reason is that there is the matter of cost as explained before; damage caused by corrosion was estimated in a previous study to be around 300 billion dollars in the year 2002 [14, 15].

Chapter 3: Testing Methodology & Experimental Work

This chapter represents an overview of the conducted study. The testing methodology is divided in terms challenges, types and importance. Then, material specifications, experimental preparation, experimental procedures and electrochemical cell are introduced in this chapter. The different used tests are described in details starting with the weight loss test and moving on the electrochemical analysis. Finally, a background on adsorption isotherms, the Linear Polarization, Impedance and Cyclic Sweep tests is thoroughly investigated.

Green inhibitors were extracted from plant leaves and used as corrosion inhibitors. The plants selected were Fig, Olive, Rosemary, Cypress and mixtures of Fig and Olive leaves. In the process of preparation, the plant leaves were collected and subjected to a drying process of two hours for each batch. After drying the leaves, they were grounded into fine powder and kept for storage. Each of the plants fine powder was subjected to an extraction process, in which 30 g of the material were added to 600 mL of double distilled water which was prepared ahead of a time. The inhibitor solution of each inhibitor was used in the different tests performed in this thesis. The inhibition properties were studied using different techniques and tests. This was applied on a mild steel sheet (50 x 25 x 1.5 mm) for the weight loss method and an average composition of mild steel. The corrosive environment chosen was 1M HCl solution, as is the case in many industries and applications.

The weight loss method is applied using the different plant extracts at different concentrations: 50, 100, 200, 400, 600, 800 and 1000 ppm, where each plant extract is subjected to this test for a period of one week. The inhibition efficiency and corrosion rate were calculated at each concentration, after which all plant extracts were compared and studied in detail.

Potentiostatic Polarization test was performed on the same specimen at the same concentrations mentioned, but with an exposed area of 1 cm^2 of mild steel. The Cyclic sweeps and the Impedance tests were applied in the same manner. These tests were performed to validate findings from weight loss and LPR tests. The tests were

also performed to understand the behavior of the adsorption film formed on the mild steel specimen, mainly which adsorption isotherm rule is obeyed.

The previous analysis was repeated at elevated temperatures. The temperatures examined were 25°C, 45°C and 55°C. After the suitable adsorption isotherm was determined for the experimental data obtained, the thermodynamic properties of the adsorption process were explored for all plant extracts to understand the behavior of the reaction taking place in the study.

3.1 Determination of the Testing Method

The challenge behind choosing the experimental method to be used in evaluating the inhibitors is that the test conditions used should simulate real operating conditions, such as process in oil and gas industry. The investigations where the tests are carried out should be of severe conditions. This is in order to determine how well this inhibitor can perform in such a corrosive medium. An investigation performed should not be limited to average conditions.

There are some variables that should be specified and changed when performing any of the well known tests in this area such as temperature, velocity, environment media and the metal used

3.2 Specifications

The environment of study:-

1M HCl solution which is considered an aggressive corrosion media.

Table 2: Specimen specifications and properties.

Material of Construction	Mild steel Sheet
Dimensions	50x25x1.5mm for weight loss 1 cm^2 of exposed surface area for electrochemical analysis
Composition	0.79 Mn, 0.18% C 0.03% Cu, 0.02% Cr, 0.21% Si and the rest is Fe

3.3 Experimental Preparations and Procedure

3.3.1 Materials

3.3.1.1 Preparation of plant extracts

The fresh leaves of Olive & Fig plants were washed under running water, shade dried, powdered into tiny pieces and the powdered leaves were extracted consecutively with boiling in double distilled water. After that, boiling takes place in a reflux heater where the amount of time needed depends on the plant extract used. The solution is then cooled followed by vacuum filtration to extract the green inhibitor solution without any solid particles. The concentration of the inhibitor is then found to know the amount of inhibitor available in the solution. For example a volume of 1.1 ml of fig inhibitor extract is added to contribute for a concentration of 50 ppm.

3.3.1.2 Preparation of the specimen

Mild steel specimens of dimension 50 x 25 x 1.5 mm and 1 cm^2 exposed surface area are used for weight loss and electrochemical analysis, respectively. The specimens were polished with 1/0 to 6/0 emry papers, rinsed with double distilled water, degreased with ethanol, immersed in 10% HNO_3 for 2 minutes, washed with double distilled water, wash with ethanol, washed with double distilled water and then dried [29].

3.3.1.3 Preparation of the electrolyte

About 1 M HCl solutions were prepared by diluting 37% HCl using double distilled water. The concentration range of extracts used was varied from 50 ppm to 1000 ppm and the electrolyte used was 600 ml for each experiment.

3.4 Testing Methods and Instrumentations

3.4.1 Weight Loss Method

Metal loss methods or weight loss method is actually the simplest test that can be performed. However, the problem with this test compared to other test performed is that:-

1. The time duration of the test is longer.
2. The accuracy is less due to human and instrumentation errors when weighing the specimen before and after the test.

Mild steel specimens of dimension 50 x 25 x 1.5 mm were immersed in 600 ml of electrolyte (1 M HCl) at 25^{o}C with and without the addition of different concentrations of the extracts ranging from 50 ppm to 1000 ppm. The time period of the tests was optimized and performed for a week at 25 ^{o}C (error $\pm$ 5%). At the end of the tests, weights were recorded, but after specimens were cleaned according to ASTM G-81.

The inhibition efficiency IE% was calculated using the following equation:

$$IE\% = \left(\frac{w - w_i}{w}\right) X\ 100 \qquad (3.1)$$

where w and w_i are the weight loss of the mild steel in the presence and absence of inhibitor, respectively.

3.4.2 The Electrochemical Test Cell

A photograph of an electrochemical cell used for experimental

electrochemical tests on a sheet of mild steel specimen is shown in Figure 1.

In most electrochemical cells, the cell is composed of three electrodes all immersed in the electrolyte solution: working electrode, reference electrode and the auxiliary electrode. The mild steel specimen with an exposed area of 1 cm^2 functions as the working electrode, where the anodic and cathodic reactions take place on the surface of the metal.

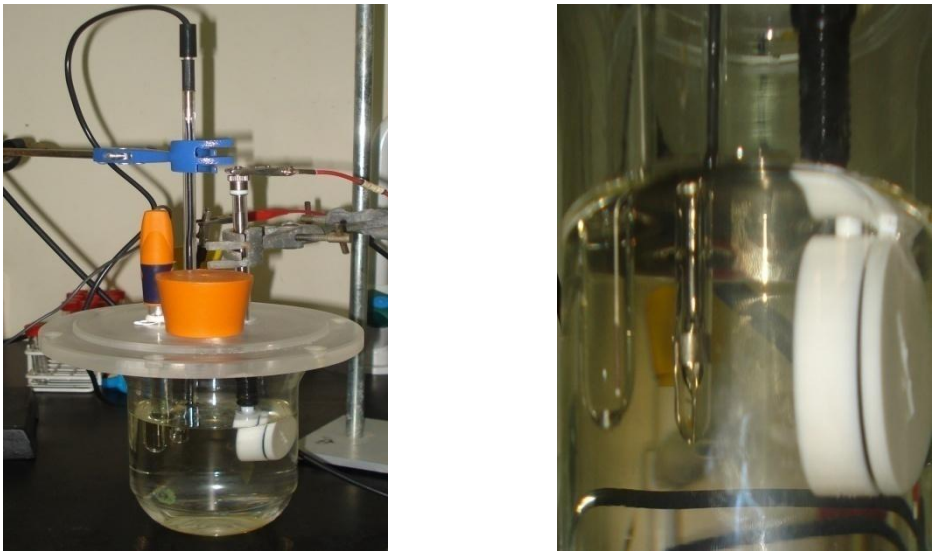

a b

Figure 1: a) Electrochemical cell used in electrochemical analysis. b) The three electrodes used; one as a reference, the other as an auxiliary electrode and the Teflon working electrode.

The current flowing at the working electrode is supplied by the auxiliary electrode. A reference electrode is utilized such that the potential between the working and reference electrodes is controlled by the potentiostat [30]. The auxiliary electrode is made out of platinum, while the reference electrode is a saturated calomel electrode. The three electrodes should be at equal distance from each other.

3.4.2.1 Working Electrode Holder

The mild steel sample should be held with a Teflon holder that assures electrical contact with the specimen. The holder is a stainless steel rod that is in direct contact with a circular stainless steel joint, which allows the installment of the mild steel specimen. The circular joint is coated by Teflon to avoid any contact with the electrolytic solution. On the other hand, a 1 cm^2 hole is made through the Teflon to allow direct contact between the specimen and the solution. An O-ring is placed before the insertion of the specimen and just before fastening the Teflon cover of the holder in order to assure no leakage. Moreover, the stainless steel rod is covered up with glass to avoid any contact with the corrosive environment.

3.4.2.2 Cell Measurement

The potential difference between the reference and working electrodes is controlled by a potentiostat, which is an electronic device used in most electrochemical tests. The potentiostat in Figure 2 records the equilibrium potential, assumed by the metal in the absence of applied electrical connections, and the current flow between the reference and working electrodes as an external potential [31]. A potentio-dynamic scan, which represents the previous point, is mostly used in electrochemical studies, because it can follow the behavior of the metal during the formation or breakage of protective oxide films [31]. It measures the potential versus current continuously. Potential measurements are important in the implementation of corrosion investigations

Figure 2: A Potentiostat sequencer (Gill AC Serial no 1094- Sequencer).

3.4.3 Potentiostat Analysis

3.4.3.1 Linear Polarization Resistance

The linear polarization resistance (LPR) experiment can be used to measure the polarization resistance (Rp). It is the resistance of the metal to oxidation when an external potential is applied to the cell [21]. LPR is carried out by a scan from approximately -10mV to +10mV *vs*. OC. The collected polarization resistance data are then graphed as a plot of the external potential versus the current. The Rp value is simply the slope of the straight line fit to the linear polarization data [31].

$$Rp = \Delta E/\Delta I \qquad (3.2)$$

Where E is the potential in mV and I is the corrosion current density mA/cm^2.

Polarization resistance tests are more common than other electrochemical tests due to the fact that the test measures the potential versus current very rapidly. Moreover, during Rp methods the metal specimen is exposed to very small potential ranges. As such the test does not significantly alter the surface of the specimen. Such an advantage allows the specimen to be used again in other experiments [31,32,33].

3.4.3.2 Impedance Test

Impedance test is crucial in accurately determining the corrosion rate by deducting the input of the solution resistance to an overall cell resistance. Furthermore, impedance test also helps in studying the effect of the film formed on the metal surface to avoid corrosion.

3.4.3.3 Anodic and Cathodic Tafel Tests (Cyclic Sweep)

Tafel plots that are produced by the cyclic sweep electrochemical test are used in calculating the cathodic and anodic Tafel constants (β_A and β_C). The tafel constants measured contributes in calculating the corrosion rate. The cathodic tafel plot is scanned on one steel sample from approximately 0 to -300mV vs. OC while the anodic tafel plot is completed on a second sample of the same composition from approximately 0 to +300mV *vs.* OC [19]. The tafel data are graphed as external potential versus the logarithm of the measured current as shown in Figure 3.

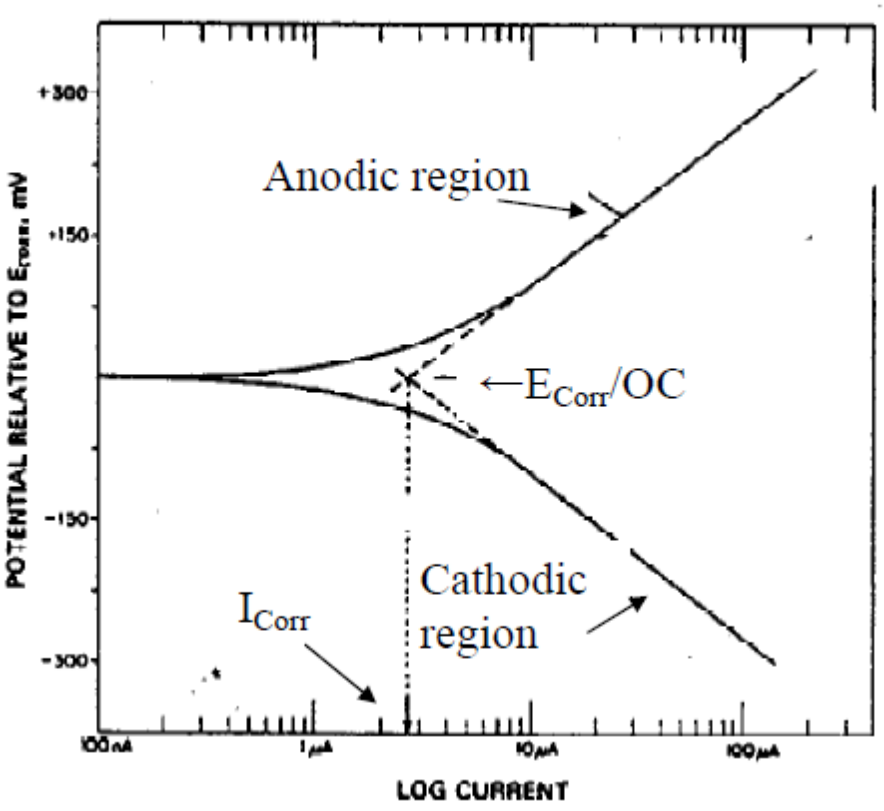

Figure 3 : The ideal tafel plot is a graph of the applied potential vs. log current data [32,33].

When the Tafel scan of the impedance test is finished, a straight line can be superimposed along the linear portion of each curve. The potential value at the intersection of the 2 slopes can be determine and used to calculate the corrosion rate. The current at that intersection gives an approximate estimate of the corrosion current, which is used in the calculation of the corrosion rate. The slope of the straight line fits of the linear regions of the anodic and cathodic tafel gives the tafel constants, β_A and β_C [21].

$$I_{corr}= \frac{\beta_A \beta_C}{2.303 Rp (\beta_A + \beta_C)} \quad (3.3)$$

Where the anodic and cathodic tafel β_A and β_C respectively. Rp is the resistance polarization [34].

The corrosion current calculated should be in agreement with the corrosion current measured in other corrosion electrochemical tests.

The corrosion rate can then be calculated using the corrosion current measured as follows [31,32]:-

$$\text{Corrosion Rate} = \frac{(M - Mi)}{t} \quad (3.4)$$

Where the corrosion rate is in grams per year (gpy), M and Mi are the specimen weight in grams before and after immersion, respectively. T is the time of immersion.

3.4.4 Comparison of Electrochemical and Mass Loss Corrosion Determinations

The linear polarization electrochemical tests are performed to study the initial effects of corrosion occurring at the surface of non corroded metal specimens in order to estimate the long-term rate of corrosion [31]. As a matter of fact, electrochemical methods are best used for the study of the initial corrosion of metal specimens, whereas weight loss tests are better in determining long term effects on the metal specimen. Additionally, the main difference between the two tests is that, in the calculation of the corrosion rate, the weight loss test is considered a long term test. It may take weeks to determine the corrosion rate in weight loss tests, while electrochemical tests require hours at most to determine the corrosion rate of a metal specimen. However, in our case both tests are accurate in the determination of corrosion rate. Moreover, excellent correlation can be made between corrosion rates obtained by both tests [33].

3.4.5 Adsorption Isotherms

The process taking place, specific adsorption, is the adsorption of inhibitors or species in the inhibitor at the metal surface. The adsorbed layer acts like a barrier between the metal surface and the electrolyte or the corrosive solution. The degree of adsorption depends on the concentration of the inhibitor as well as the concentration of the electrolyte. Three isotherms are usually considered in modeling adsorption [16, 21]:-

1. Langmuir Isotherm

It is assumed that there is no interaction between the adsorbed species on the surface of the metal and the surface is smooth and saturated. The relationship is explained as [16,21]:-

$$\frac{C}{\theta} = \frac{1}{k} + c \quad (3.5)$$

Where θ is the surface coverage $= \frac{IE}{100}$, C is the extract concentration and k is the adsorption constant [5,11]:-

$$\ln k = \ln \frac{1}{1000000} - \frac{\Delta G°ads}{RT} \quad (3.6)$$

Where $\Delta G°_{ads}$ is the standard free energy of adsorption and 1/1000000 stands for the molarity of water.

2. Temkin Isotherm

It considers the adsorption as function of the degree of coverage according to [16,21]:-

$$Ti = \frac{RT}{g} \ln (\beta i\, a_{i,\infty}) \quad (3.7)$$

$$\frac{\theta}{1-\theta} = \beta i\, a_{i,\infty} \quad (3.8)$$

Where Ti the excess of species i, g is a parameter that treats the interaction energy between the adsorbed species, βi the energetic coefficient of proportionality and $a_{i,\infty}$ is the activity of species I in the bulk solution [16,21].

3. Frumkin Isotherm

It considers the reaction as follows [21]:-

$$\beta i\, a_{i,\infty} = \frac{Ti}{Ts - Ti} \exp \frac{2gTi}{RT} \quad (1)$$

Where Ti is the maximum surface excess.

Chapter 4: RESULTS AND DISCUSSION

Mild steel is used in a wide range of industries due to its cheaper cost and easy availability. The main setback for this metal is its tendency to corrode easily in acid environment. Acids like HCl and H_2SO_4 are used for drilling operations in oil exploration, de-scaling operations and in many industrial applications. Since the above said acids cause corrosion of mild steel, several protective measures are taken, one of them being the use of inhibitors. Synthetic organic inhibitors are toxic in nature and this has lead to the use of natural products which are eco-friendly and harmless. Several green inhibitors were extracted from Fig, Olive, Cypress and Rosemary leaves. The corrosion inhibition of mild steel in 1 M HCl medium was investigated. The main objective of this thorough investigation is to widen the scope on some highly inhibitive properties of some green extracts to be used as corrosion inhibitors. The investigation is also to be extended in order to understand the effect of temperature on the inhibitive properties of these green inhibitors using weight loss, impedance, cyclic sweep and potentio-static polarization methods. Moreover, at the end of this chapter a comparison is made with some commercial inhibitors used in industry in order to confirm the inhibitive action of plant extracts studied.

4.1 Results and Analysis of Weight Loss Method

The specimens were immersed in beakers filled with a 1M HCl solution, and the inhibitor was injected at different concentrations. The weight loss test of the metal specimen was run at a specific concentration for a week. Both the initial and the final weight of the specimen were determined and recorded in the results analysis section. After all the weight loss experiments were performed for the various inhibitors and concentrations, the inhibitive action was compared. The results were recorded and interpreted in the following sections.

The inhibitor was added to the corrosive environment in this manner:- Blank , 50, 100, 200, 400, 600, 800, 1000 ppm. The corrosion rate was calculated in millimeter per year on the basis of the apparent surface area. The inhibition efficiency

measurements were based on the weight loss at the end of the measuring period. The percentage efficiency was calculated using Equation 3.1. The maximum inhibition efficiency and the minimum corrosion rate were obtained at a concentration of 1000 ppm of the inhibitor extract.

Figure 4 shows that the inhibition efficiency obtained when adding 50 ppm of the green inhibitor is about 89%. The jump that appears when adding a low concentration of the inhibitor can be explained by the formation of a protective layer on the mild steel sheet that acts as barrier between the specimen and the corrosive media. Figure 5, on the other hand, depicts the decrease in the corrosion rate as the green inhibitor is added to the blank system. The corrosion rate decreases dramatically. It is reduced from a value of 2.914 mm/yr in the blank system to a value of 0.320 mm/yr as 50 ppm of pure olive inhibitor is added to the system. This is almost nine times less than the corrosion rate obtained in the blank system. The inhibition efficiency increases gradually when adding the green inhibitor. It can be noticed that the maximum inhibition efficiency is obtained when adding 1000 ppm of Olive leaves extract and has a value of 93.63%. The corrosion rate decreases gradually as the inhibitor is added to the system to reach a value of 0.186 mm/yr, when 1000 ppm of the inhibitor is injected in the system. The gradual increase in inhibition efficiency at higher concentrations can be explained by the fact that the more sites of the exposed metal surface become covered with inhibitor components causing the reduction in corrosion rate. These results show the highly inhibitive behavior of olive leaves extracts and how efficient they are at reducing the corrosion rate of the mild steel sheets used in the tests.

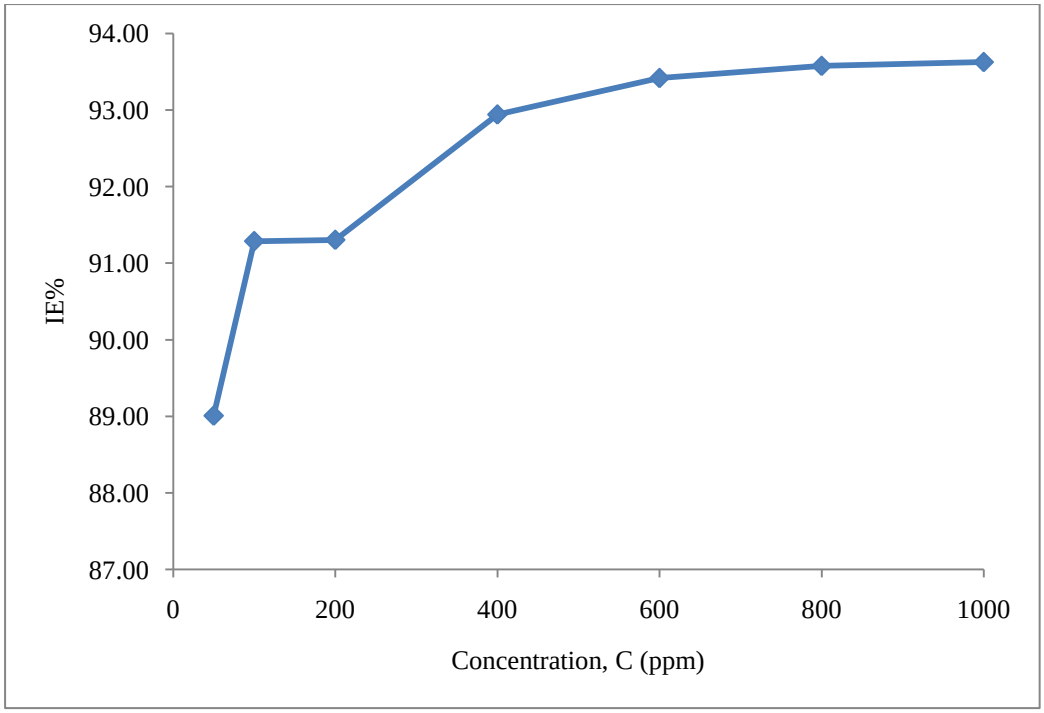

Figure 4: Inhibition Efficiency Vs Inhibitor Concentration using Olive leaves extract.

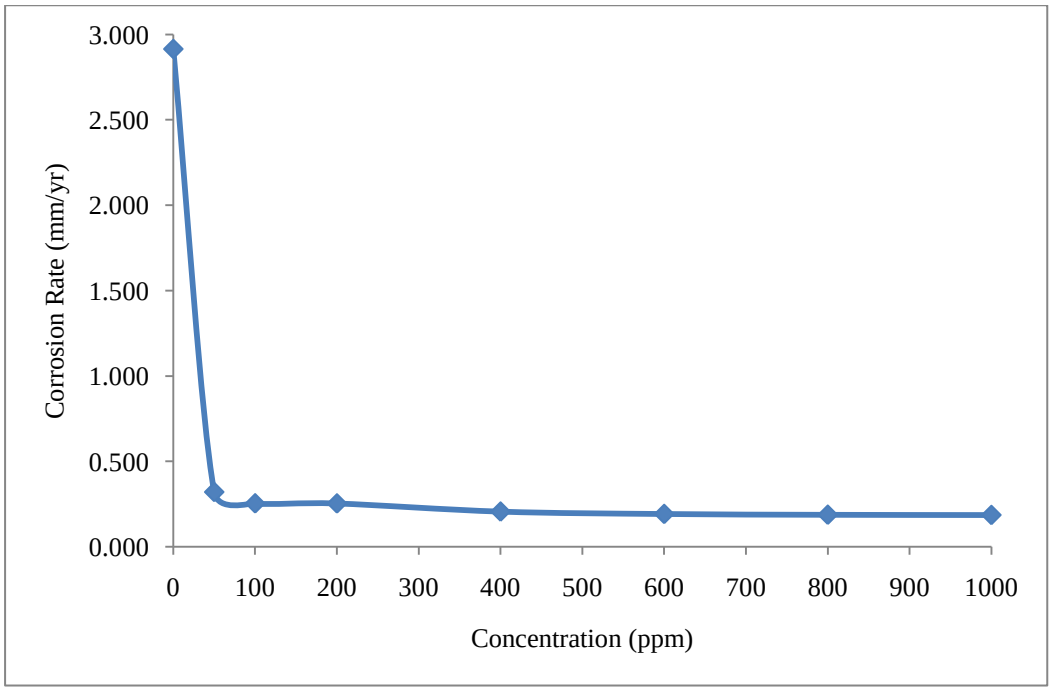

Figure 5: Corrosion Rate Vs Inhibitor Concentration using Olive leaves extract.

In Figure 6, a plot of the inhibition efficiency versus the inhibitor concentration shows that the inhibition efficiency obtained, when adding 50 ppm of

the fig extracts, is about 90.99%. Figure 7 illustrates the gradual decrease in the corrosion rate as the inhibitor extract is added to the blank system. It first decreases from almost 2.933 mm/yr to 0.264 mm/yr, which is almost 1/11 of the corrosion rate recorded in the blank 1 M HCl solution. The jump that arises in the plot of inhibition efficiency and corrosion rate indicates the formation of an adsorption layer that protects the metal from the surrounding environment. This protective layer is strengthened by the addition of the inhibitor. Therefore, the inhibition efficiency increases gradually until 300 ppm of inhibitor is added. After that, the inhibition efficiency increases slowly until it reaches 95.11 % at 1000 ppm, corresponding to a corrosion rate of approximately 0.143 mm/yr. This shows the highly inhibitive behavior of fig leaves extracts which reduces the corrosion rate of the mild steel sheet used.

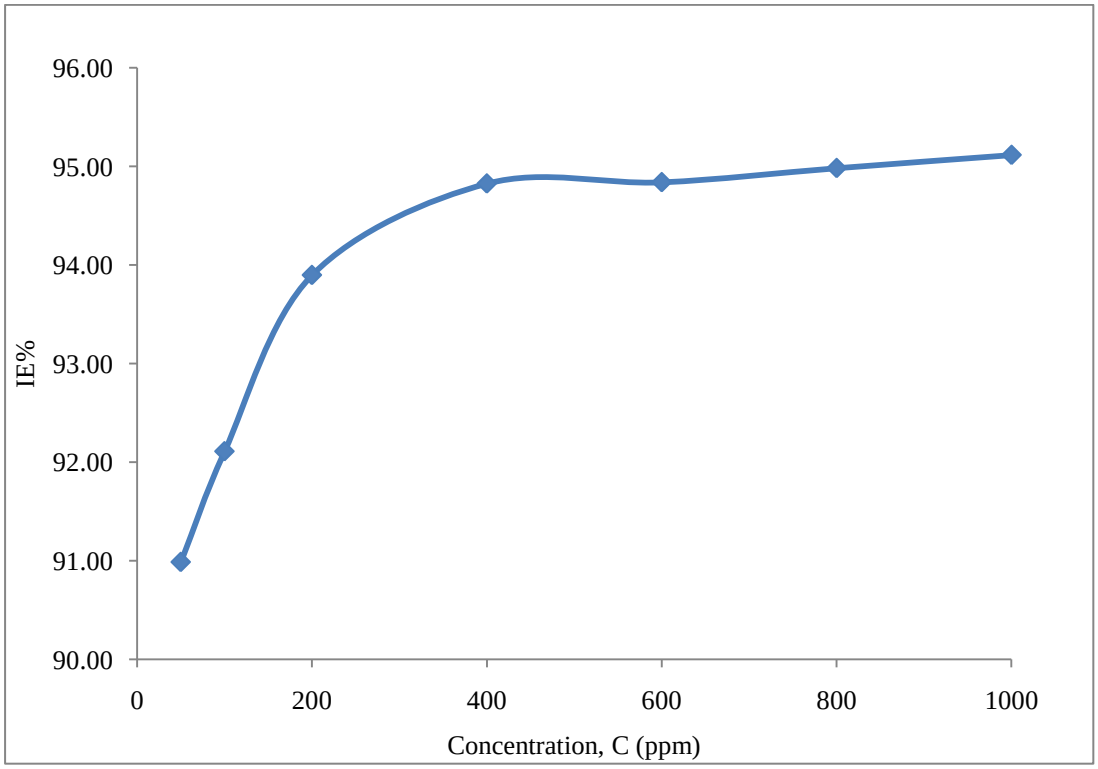

Figure 6: Inhibition Efficiency Vs Inhibitor Concentration using Fig leaves extract.

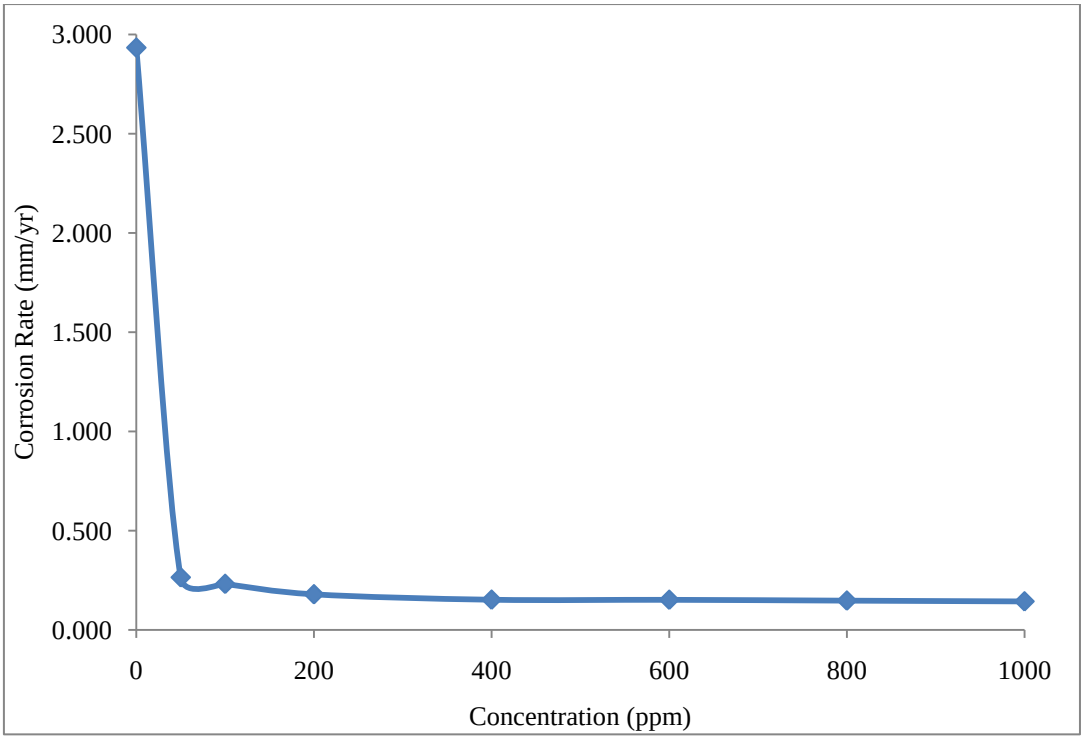

Figure 7: Corrosion Rate Vs Inhibitor Concentration using Fig leaves extract.

The plot of the inhibition efficiency versus the concentration of the green inhibitors added in Figure 8 shows that the inhibition efficiency obtained when adding 50 ppm of (1:1) Olive & Fig leaves mixture is 90.14 %, which is relatively lower than the inhibition efficiency obtained when adding 50 ppm of a single fig inhibitor. However, the inhibition efficiency obtained is quite good and only almost 1% more than the values obtained when adding pure green olive inhibitor. The corrosion rate, as illustrated in Figure 9, decreases gradually as the inhibitor solution is added to the system. The value is 2.904 mm/yr in the blank system, and is reduced to 0.184 mm/yr when adding 1000 ppm of the inhibitor mixture. The inhibition efficiency increases until 200 ppm of inhibitor is added, after which the inhibition efficiency increases slowly until it reaches 93.56 % at 800 ppm and a corrosion rate of approximately 0.187 mm/yr. It can be also noticed that the minimum corrosion obtained is almost 0.184 mm/yr at an addition of 1000 ppm of the mixture of green inhibitors. This shows that as the inhibitor is added to the solution, inhibitor components get adsorbed on the corrosion exposed sites, and as a result causing a reduction in the corrosion rate that starts with a sudden increase as soon as the inhibitor is presented to the solution. This shows the highly inhibitive behavior of both Fig and Olive leaves extracts which

reduces the corrosion rate of the mild steel sheet used and shows that mixtures of green inhibitors can also be used to reduce the corrosion rate.

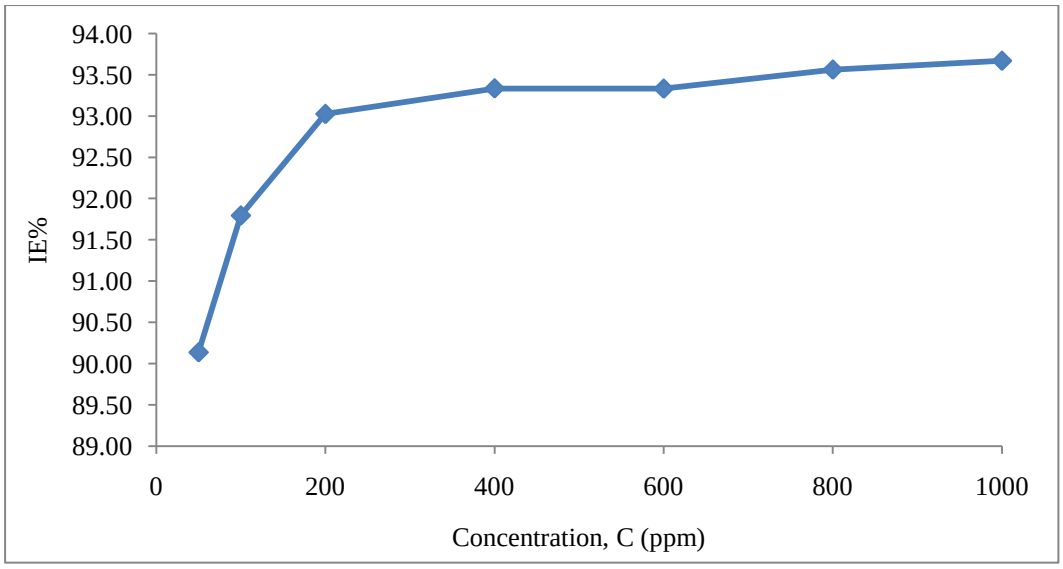

Figure 8: Inhibition Efficiency Vs Inhibitor Concentration using a mixture (1:1) Fig and Olive leaves extract.

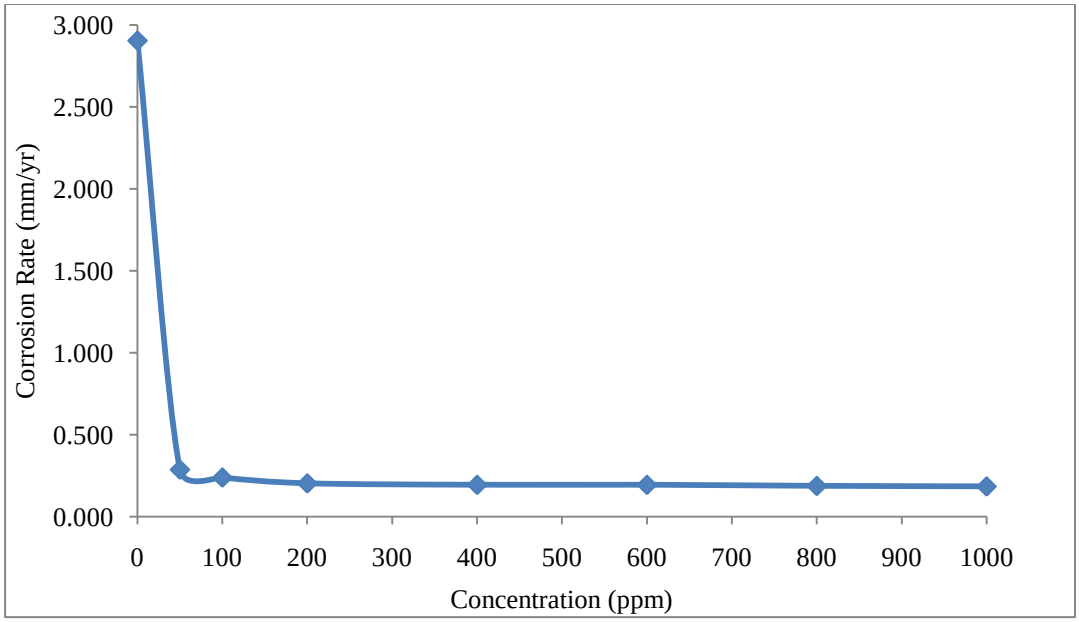

Figure 9: Corrosion Rate Vs Inhibitor Concentration using (1:1) Fig and Olive leaves extract.

In Figure 10, the inhibition efficiency for (1:7) Fig & Olive leaves mixture was plotted against concentration. It can be seen that the inhibition efficiency obtained when adding 50 ppm of is 89.74 %, which is lower than that of a (1:1) mixture. Figure 11 demonstrates the significant decrease in the corrosion rate as the inhibitor extract is added to the acidic system. It goes from 2.914 mm/yr in the blank system to 0.197 mm/yr when adding 800 ppm of the inhibitor mixture. The inhibition efficiency increases gradually until it reaches its maximum at 800 ppm with a calculated value of 93.24 and a corrosion rate of 0.197 mm/yr. The sharp increase in inhibition efficiency is introduced at a concentration range of 50-200 ppm. After that, the protective layer formed on the mild steel sheet gets strengthened by the addition of the inhibitor up to 800 ppm.

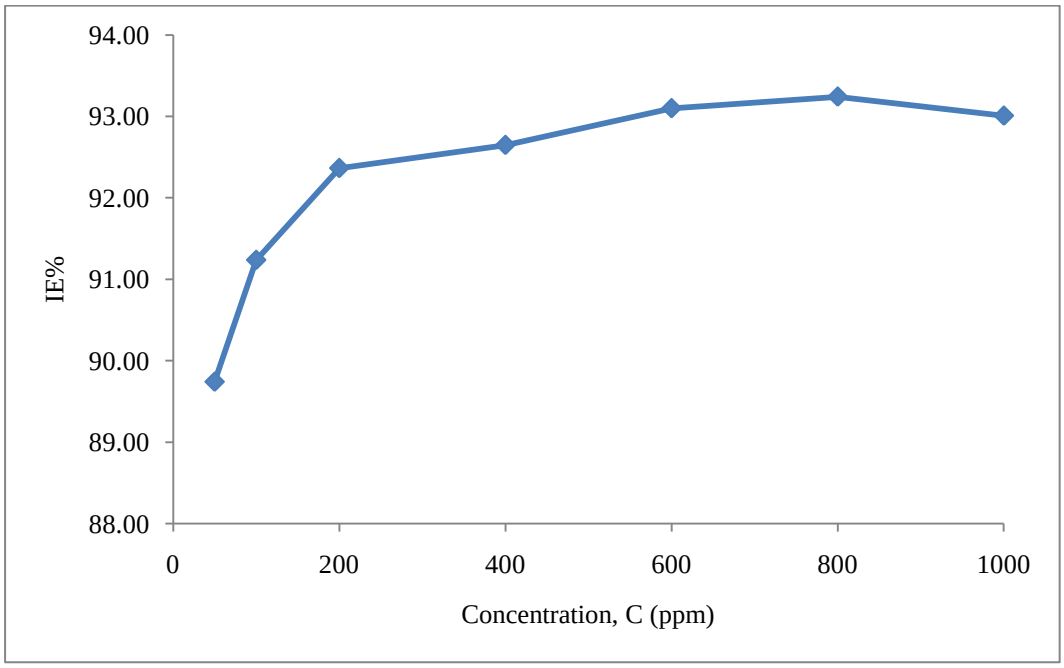

Figure 10: Inhibition Efficiency Vs Inhibitor Concentration using a mixture (1:7) Fig and Olive leaves extract.

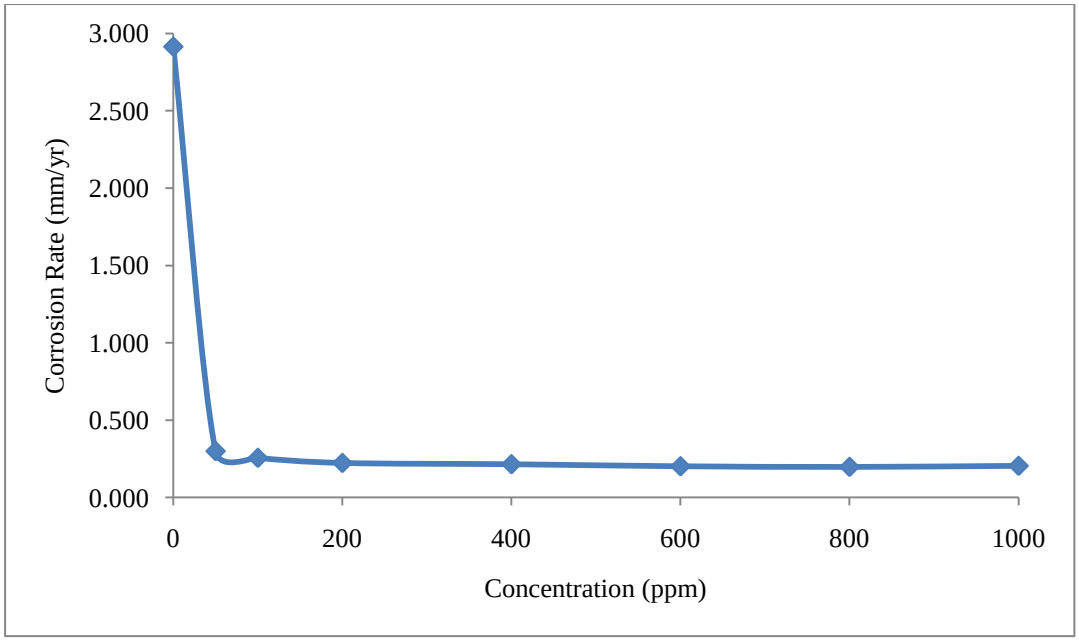

Figure 11: Corrosion Rate Vs Inhibitor Concentration using (1:7) Fig and Olive leaves extract.

As can be seen in Figure 12, the inhibition efficiency obtained when adding 50 ppm of (7:1) Fig & Olive leaves mixture is almost 90.20 %, which is the highest among the mixtures studied. The behavior differs than that of the (1:7) mixture. The inhibition efficiency increases more rapidly in the range of 50 to 200 ppm. The corrosion rate also shows a dramatic decrease in Figure 13 as the inhibitor is added at a concentration of 50 ppm. It decreases from a value of 2.890 mm/yr in the blank system to a value of 0.283 mm/yr as 50 ppm of the mixture inhibitor extract is added to the system. However, following that, the inhibition efficiency increases gradually until it reaches its maximum at 1000ppm with a recorded value of 93.52% and a corrosion rate of almost 0.187 mm/yr, as shown in Figure 13, which is approximately fifteen times less than the corrosion rate recorded in the blank 1M HCl system. This shows the high inhibitive action of the mixture used, which causes the formation of a protective barrier between the sheet surface and corrosive environment.

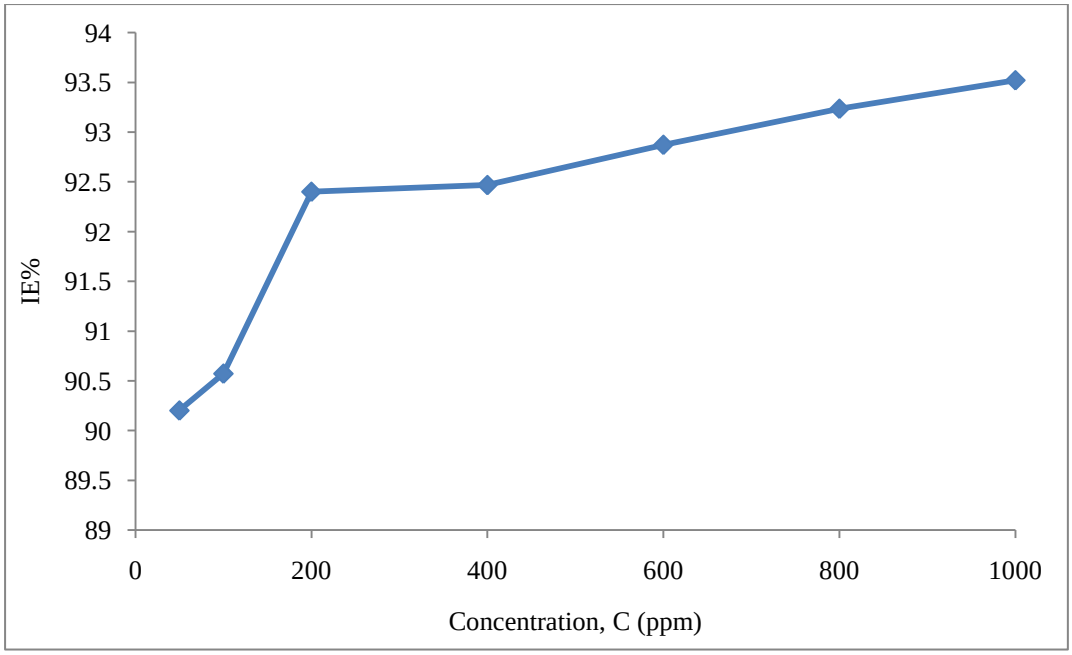

Figure 12: Inhibition Efficiency Vs Inhibitor Concentration using a mixture (7:1) Fig and Olive leaves extract.

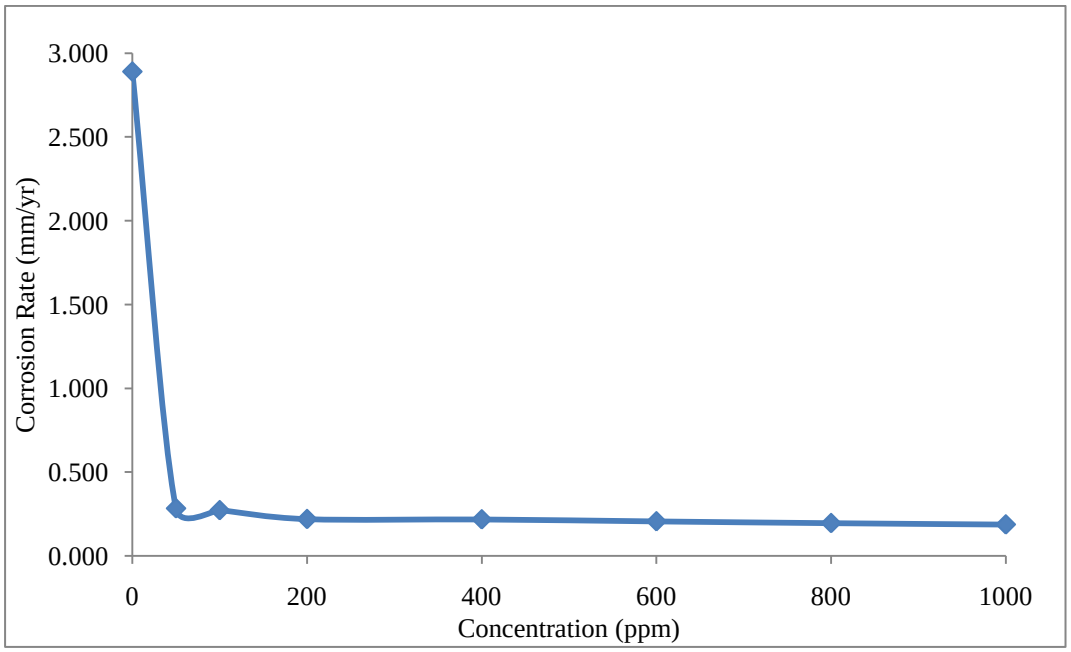

Figure 13: Corrosion rate Vs Inhibitor Concentration using (7:1) Fig and Olive leaves extract.

It can be seen in the plot of the inhibition efficiency versus the inhibitor concentration in Figure 14 that the inhibition efficiency obtained when adding 50 ppm of the Cypress leaves is about 83.85%, which less in efficiency than any of the previous runs. However, it is considered a good result, since the Cypress extract reduced the corrosion rate by a factor of 6, from 2.902 mm/yr to almost 0.469 mm/yr, as shown in Figure 15. The inhibition efficiency increases to 87.66% when 100 ppm of the inhibitor is added. It continues to increases slowly until it reaches its maximum with a reading of 95.33 % at 1000 ppm and a corrosion rate of approximately 0.135 mm/yr. This can be explained the protective layer of adsorbed component on mild steel surface is weaker than the ones formed by other studied extracts. This causes the change in inhibition efficiency of the inhibitor to be less than other extracts.

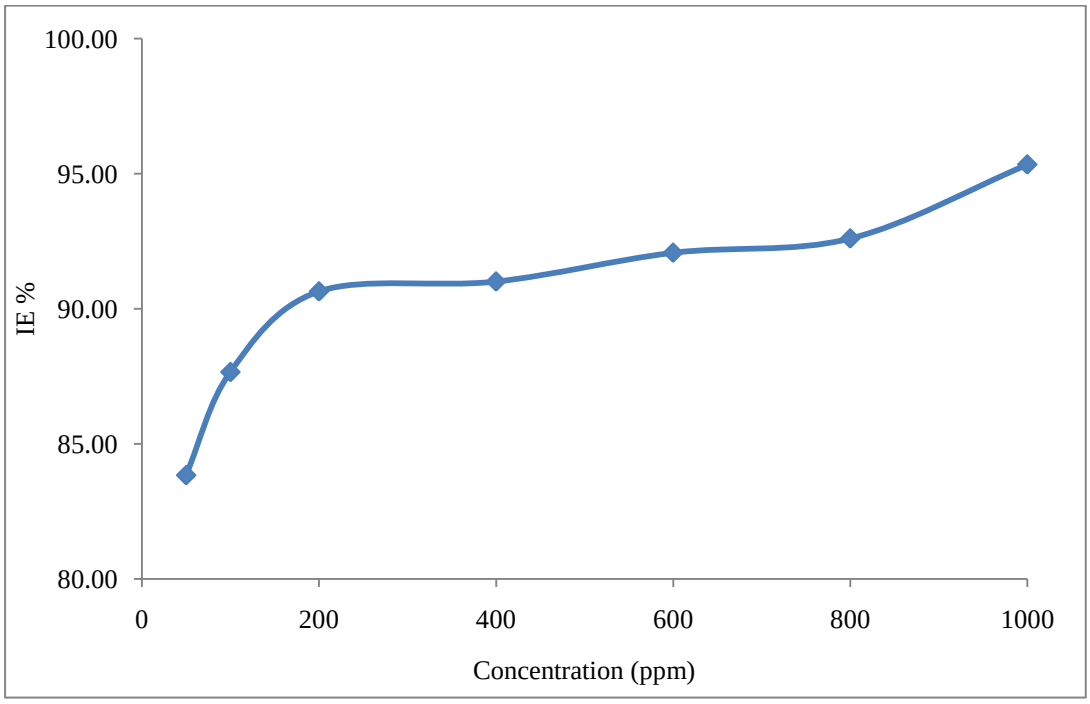

Figure 14: Inhibition Efficiency Vs Inhibitor Concentration using Cypress leaves extract.

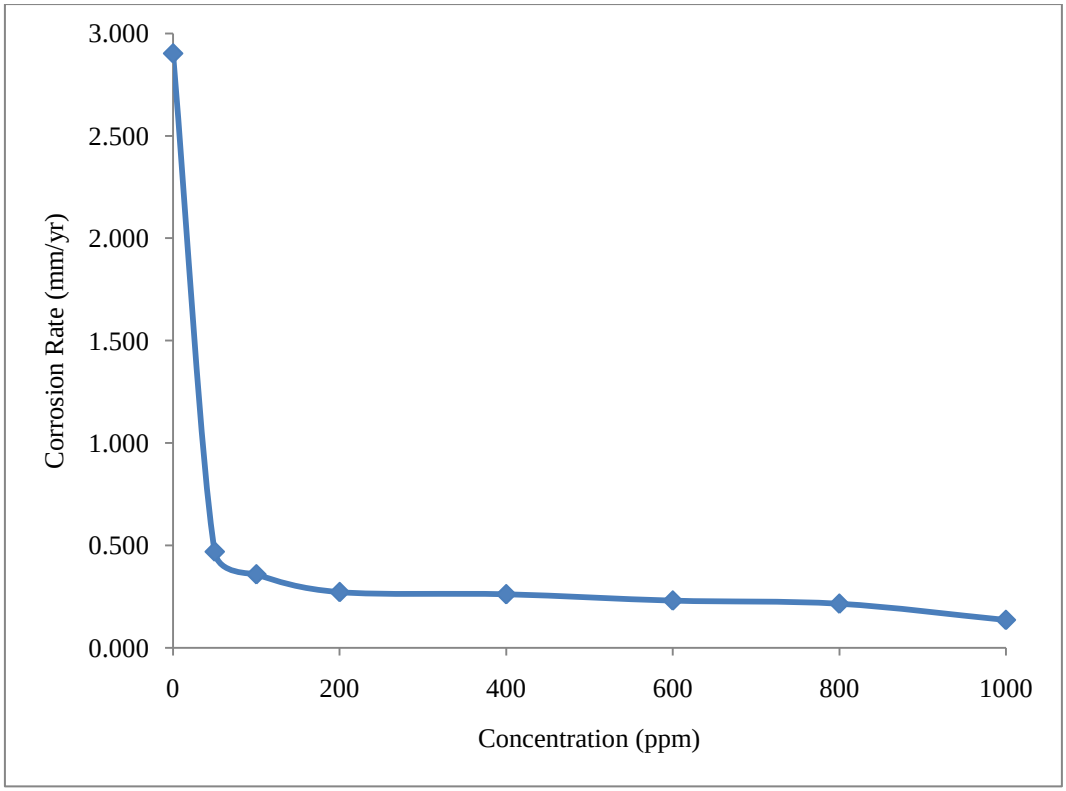

Figure 15: Corrosion Rate Vs Inhibitor Concentration using Cypress leaves extract.

Figure 16 shows how the inhibition efficiency for Rosemary extracts increases more rapidly than the other runs to reach a maximum value of 94.11% at the addition of 1000 ppm of the green inhibitor to the 1M HCl solution. The inhibition first is seen in Figure 17 to dramatically reduce the corrosion rate from 2.906 mm/yr to 0.391 mm/yr when 50 ppm of the inhibitor is added. Next, the corrosion rate decreases to 0.244 mm/yr when 200 ppm of the inhibitor is added to the solution. Then, gradually as the inhibitor is added to the system the corrosion rate decreases to reach a value of 0.171 mm/yr when 1000 ppm of the inhibitor is injected in the system.

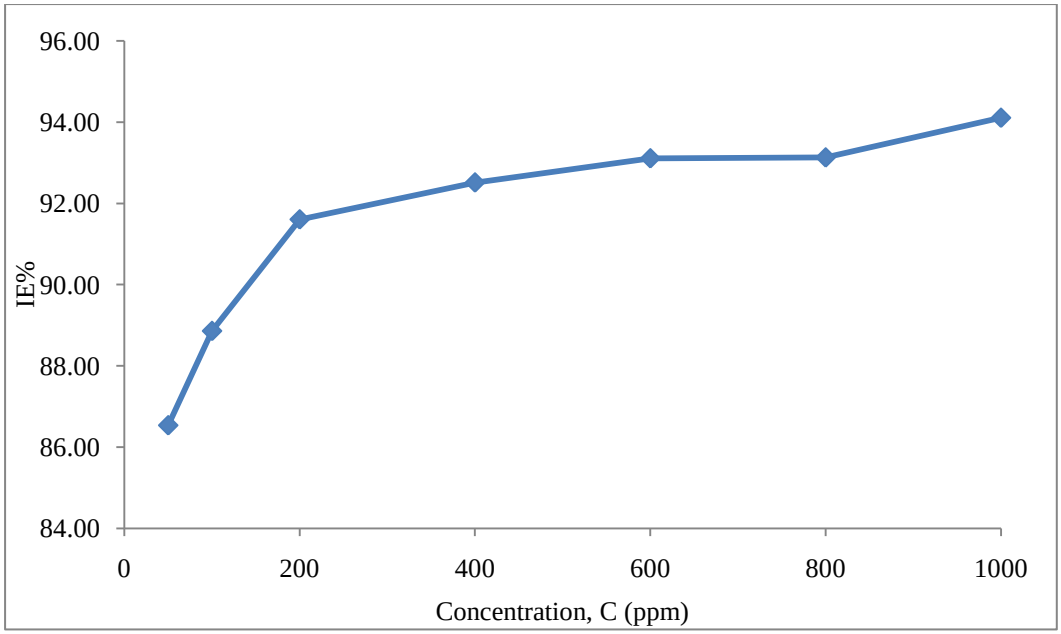

Figure 16: Inhibition Efficiency Vs Inhibitor Concentration using Rosemary leaves extract.

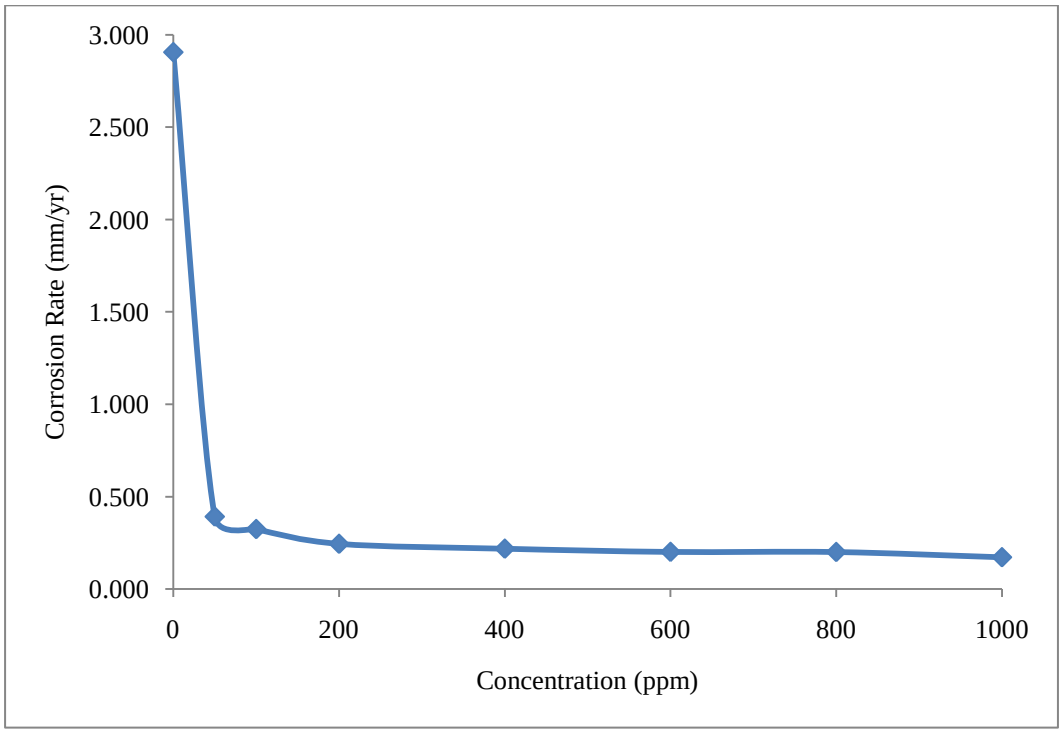

Figure 17: Corrosion Rate Vs Inhibitor Concentration using Rosemary leaves extract.

It can be noticed that by comparing the four pure inhibitors used (Olive, Fig, Rosemary and Cypress) that the maximum inhibition efficiency is achieved when

using Fig extract then Rosemary, Cypress and Olive. This observation is concluded when considering the efficiency when 1000 ppm of inhibitor is added. On the other hand, Figure 18 takes into account all concentrations and demonstrates clearly that the order of best inhibition efficiency is as follows:- Fig, Olive, Rosemary and Cypress. The inhibition efficiency of some plants intersects at some concentrations such as Olive, Cypress and Fig extracts at concentrations of 200 and 1000 ppm. Figure 18 demonstrates that the inhibition efficiency of Rosemary leaves extract is more than Cypress extract. Moreover, in all cases it is noticeable that the corrosion rate decreases to more than four times less than the corrosion rate in the blank system of 1M HCl when only 50 ppm of the inhibitor is injected in the system. This supports the inhibitive action of these green plant extracts.

The maximum inhibition efficiency obtained was when using Cypress leaves extracts with a value of 95.33 % when adding 1000 ppm of the green inhibitor. At this value, the corrosion rate is reduced to almost more than fifteen times less than the value calculated in the blank system. Most commercial inhibitors used are injected at low concentrations. Therefore, it is suggested to look at the effect of adding low concentration of the inhibitor and its effects on the tested system. Figure 18 shows the jump that occurs when adding 50 ppm of the inhibitor to the system. The inhibition efficiency jumps from 83.85% to 87.66% when 100 ppm of Cypress inhibitor extract is added to the tested system. More cases can be seen from Figure 18 regarding other pure plant extracts. The sudden increase in inhibition efficiency and the sudden decrease in corrosion rate can be explained by the formation of a protective adsorbed layer on the mild steel sheets, in which it acts as a barrier between the surface and the corrosive media. This proves that the use of pure green inhibitors reduces the corrosion rate in the 1M HCl corrosive media and that the inhibition efficiency of the tested natural inhibitors is promising. These findings are worth comparing with availability, performance, cost and environmental impact of the widely used synthetic and commercially applied corrosion inhibitors.

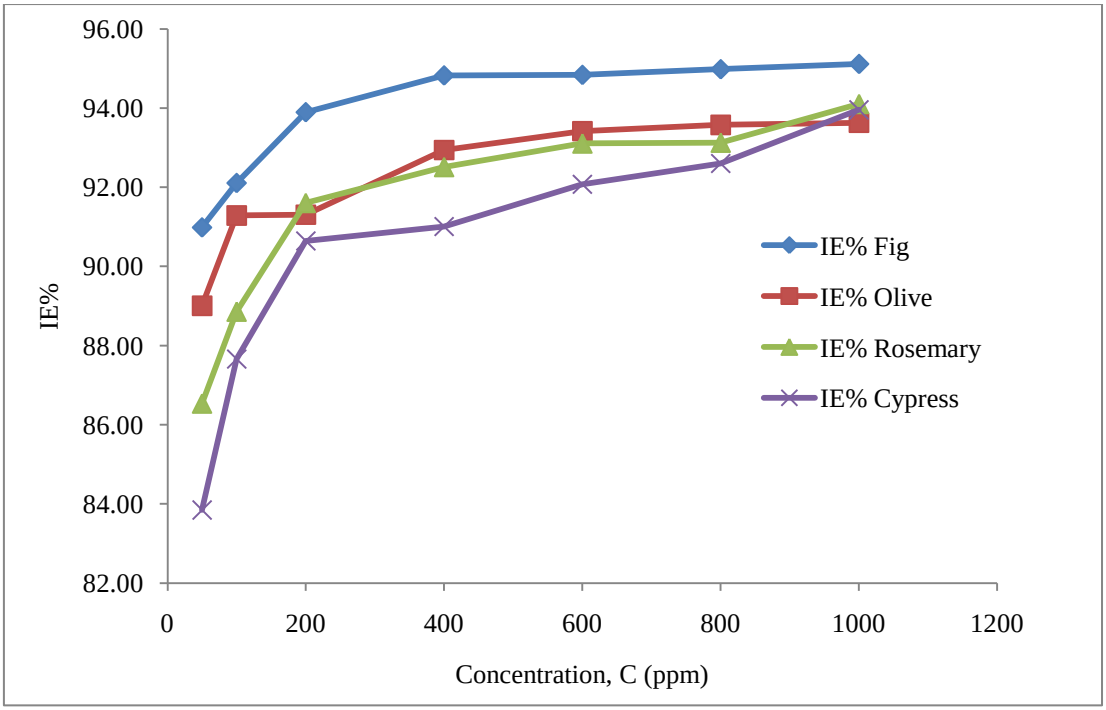

Figure 18: Inhibition Efficiency Vs Inhibitor Concentration of all runs using pure leaves extract.

Comparing the mixtures used when mixing Fig and Olive leaves inhibitors at different ratios, the mixture of (1:1) has the highest inhibition efficiency by almost 1% difference and this means that the decrease in corrosion rate is higher than when using the other two ratios.

The mixture of (1:7) Olive and Fig is higher in inhibition efficiency than the mixture of (7:1) in some cases; however, one can see that this only appears at the concentrations of 50 ppm to 800 ppm with a maximum inhibition efficiency of 93.52 %. This shows that the addition of green inhibitor mixtures reduces the corrosion rate. It also proves that the inhibition efficiency changes when changing the ratio of the mixture. This means that some inhibitors are proven to have more inhibition in corrosive media compared to other green inhibitors. This also suggests that the mixing of inhibitors may enhance the inhibitive behavior of the plant extracts.

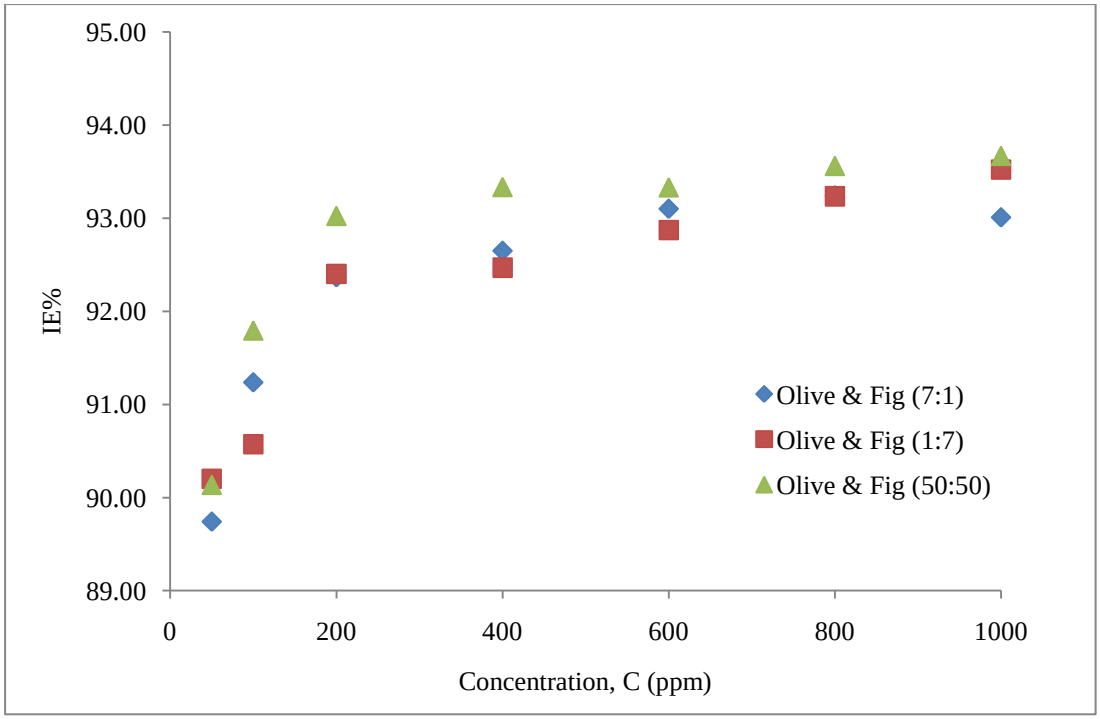

Figure 19: Inhibition Efficiency Vs Inhibitor Concentration of all runs using mixtures of Fig and Olive leaves extract.

Figure 20 demonstrates a comparison between pure and mixtures of Fig and Olive. The inhibition efficiency varies depending on the concentration of the inhibitor added. The inhibition of some inhibitors is better at certain concentrations than others. However, it is clear that the inhibition efficiency of Fig extract is the highest in all cases. This demonstrates the fact that some inhibitors work better at certain concentrations than others. The rest of the inhibitors have a similar trend. However, in terms of inhibition efficiency at the range of 50-100 ppm, pure Fig inhibitor is the highest, then (1:1) Fig & Olive mixture, (7:1) Olive & Fig mixture, and then both Olive and a mixture of (1:7) Olive & Fig mixture. At higher concentrations the order varies, but the Fig extract remains the best in inhibition efficiency and the lowest in corrosion rate.

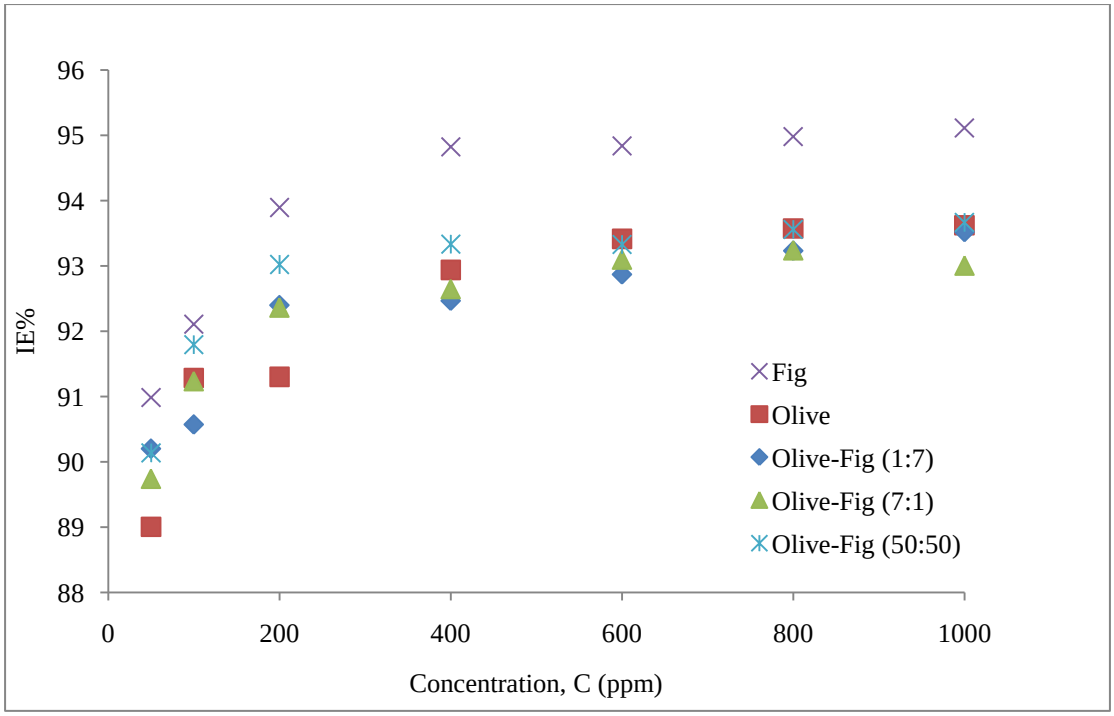

Figure 20: Inhibition Efficiency Vs Inhibitor Concentration of all runs using pure and mixtures of Fig and Olive leaves extract.

Figures 21 and 22 show a plot of the corrosion rate versus the inhibitor concentration. The trend seen in the graphs is the opposite of the trend explained before in the inhibition efficiency. As the inhibitor is injected to the system; the corrosion rate of the mild steel specimen decreases. The corrosion rate recorded in the blank system is almost 2.9 mm/yr for all cases. The corrosion rate decreases very rapidly as the first 50 ppm of the inhibitor is added to the blank system. As the inhibitor is injected to the system the corrosion rate continues to decrease, but at a slower rate. Figures 22 and 23 show the difference in corrosion rate at a closer view. The order of the best inhibitor acting or the one with higher inhibition efficiency is the one with the lowest recorded corrosion rate value. This means that the corrosion rate of the Fig inhibitor is the lowest among pure and mixed inhibitors. The value of the corrosion rate recorded when 50 ppm and 100 ppm of pure fig are added to the system is 0.264 mm/yr and 0.143 mm/yr, respectively.

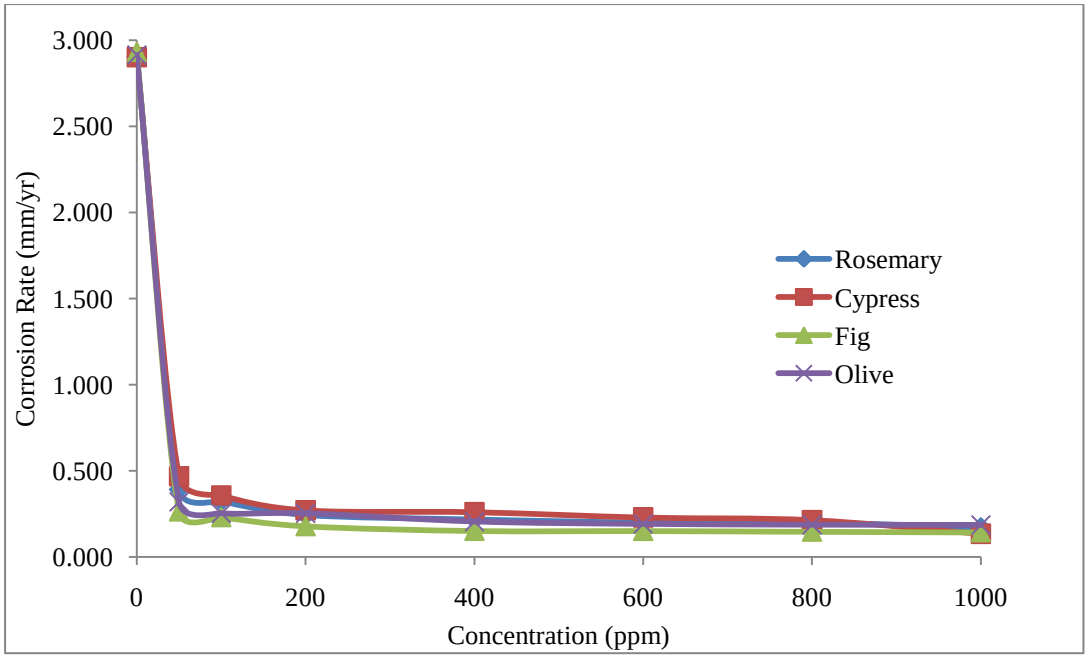

Figure 21: Corrosion Rate Vs Inhibitor Concentration of all runs using pure leaves extract.

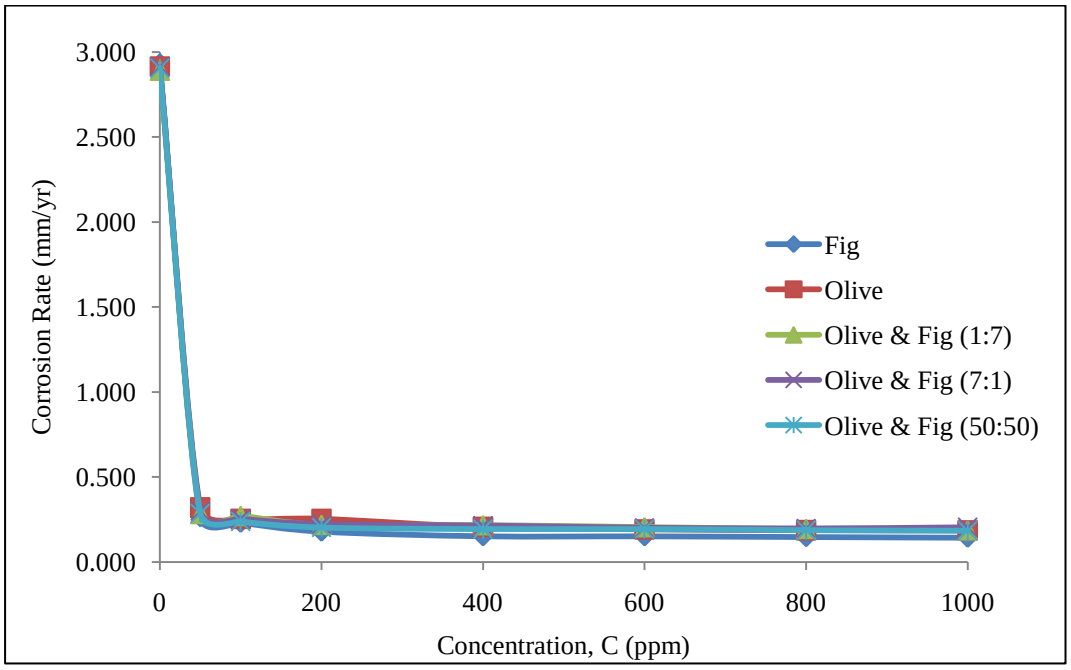

Figure 22: Corrosion Rate Vs Inhibitor Concentration of all runs using pure and mixtures of Fig and Olive leaves extract.

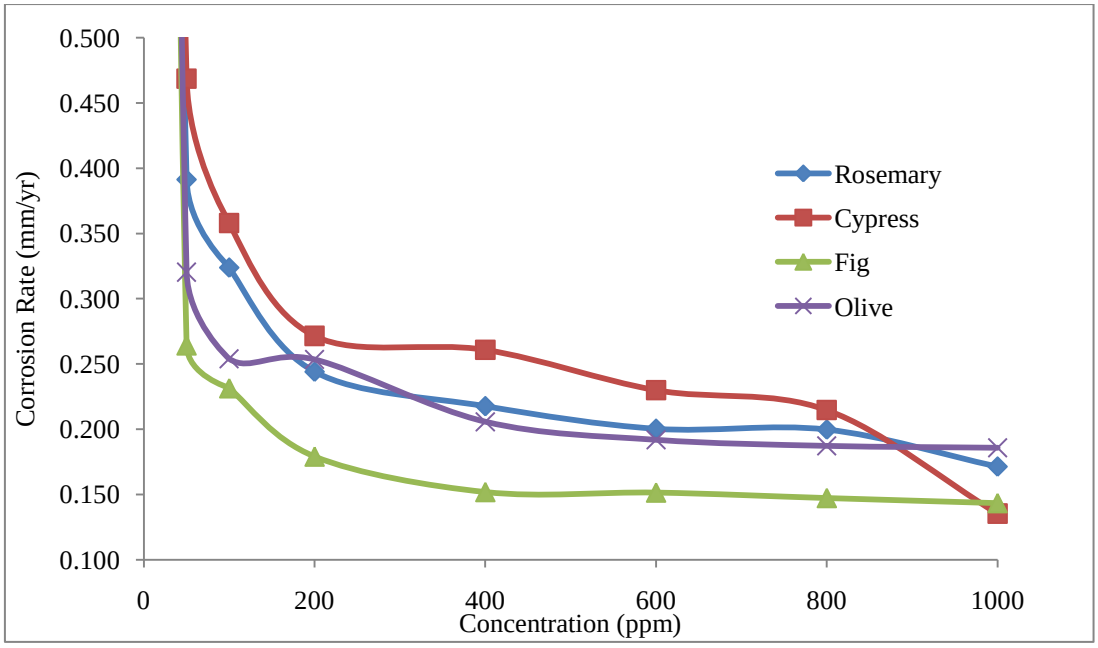

Figure 23: A closer view of the Corrosion Rate Vs Inhibitor Concentration of all runs using pure leaves extract.

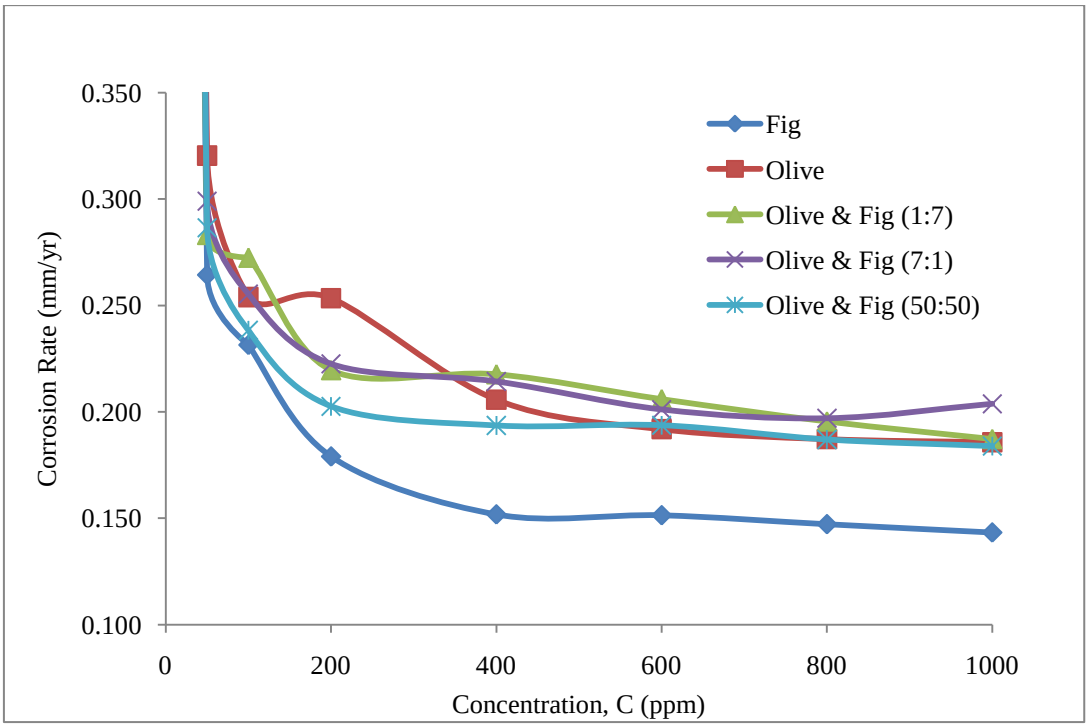

Figure 24: A closer view the Corrosion Rate Vs Inhibitor Concentration of all runs using pure and mixtures of Fig and Olive leaves extract.

4.2 Results and Analysis of Adsorption Isotherms by Weight Loss Test

Below are the results obtained in the determination of the adsorption isotherm of each of the plant extracts using the weight loss technique. The surface coverage was obtained from the data obtained by the weight loss test. It was found that the maximum surface coverage of mild steel in by plant extracts was obtained at a concentration of 1000 ppm. The kinetics obtained proved that the adsorption of inhibitors follow Langmuir adsorption model. The value of the free standard energy of adsorption indicated that physical adsorption is taking place on the mild steel specimen.

Plotting the concentration of the inhibitor versus the concentration of the inhibitor per surface coverage shows a clear linear relationship in some cases and an almost linear one in some other cases with a regression close to unity. This proves that the experimental data obtained by the weight loss method follows the Langmuir Isotherm of adsorption.

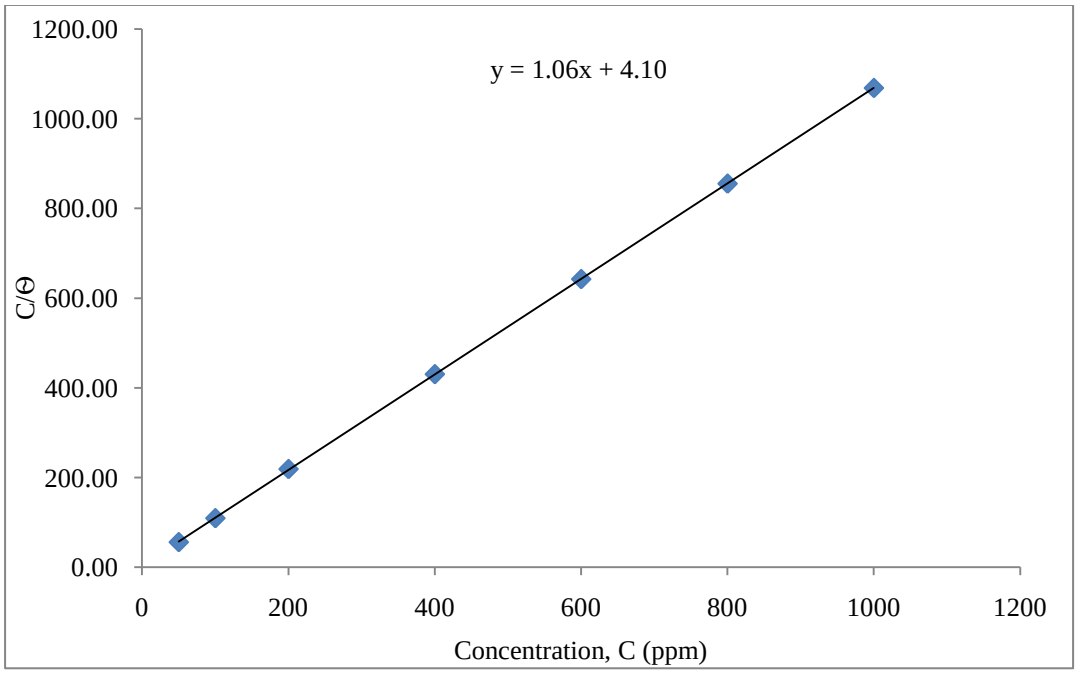

Figure 25: Concentration of the inhibitor per surface coverage versus concentration of the inhibitor of Olive leaves extract.

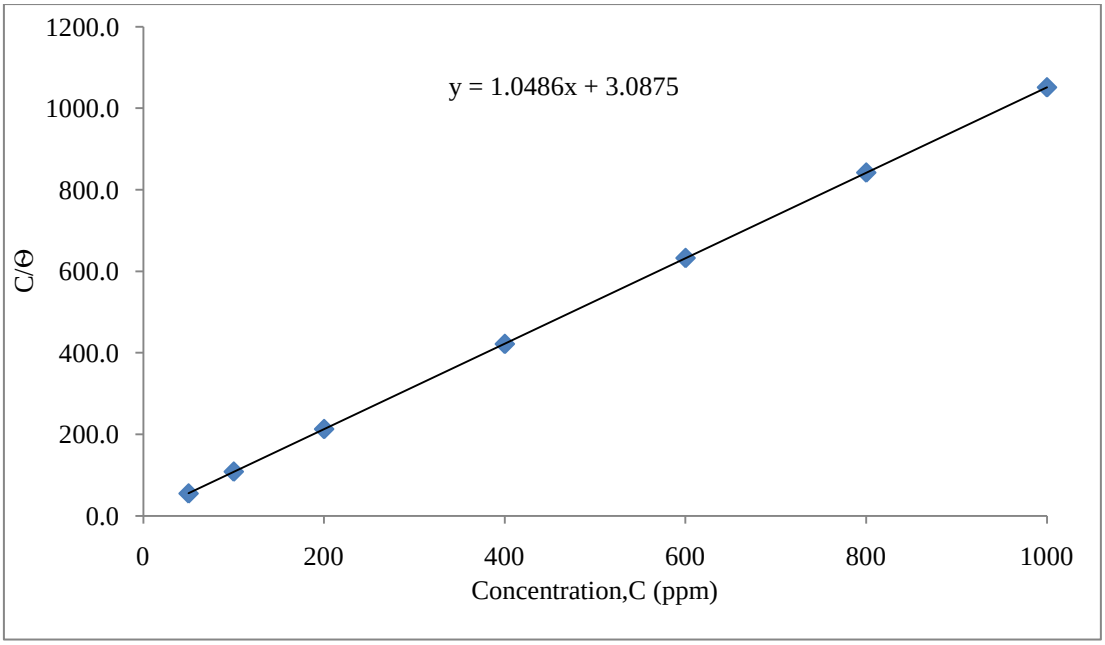

Figure 26: Concentration of the inhibitor per surface coverage versus concentration of the inhibitor of Fig leaves extract.

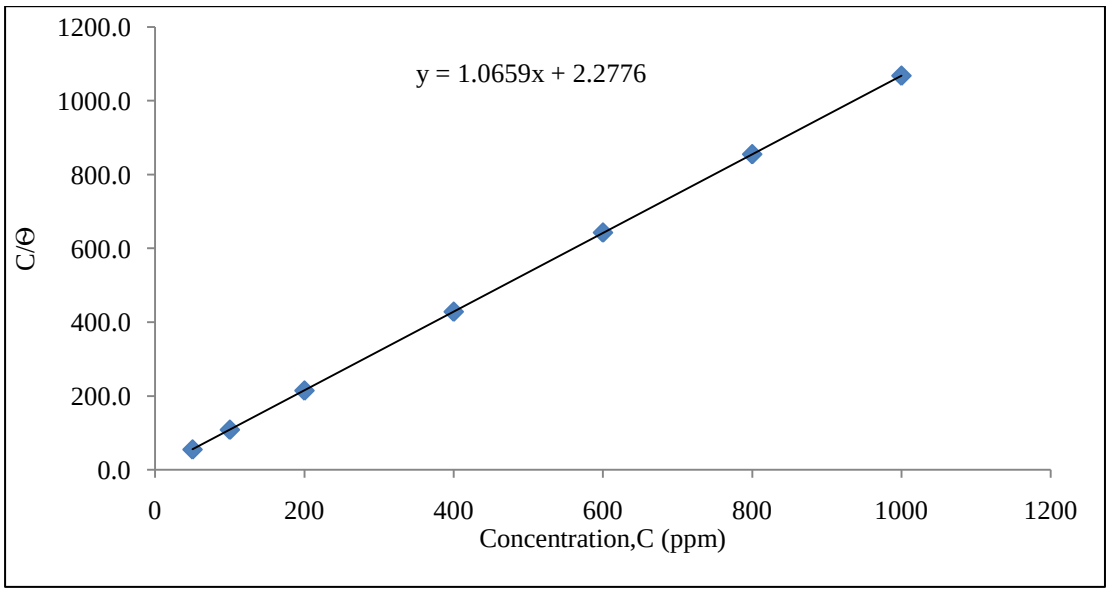

Figure 27: Concentration of the inhibitor per surface coverage versus concentration of the inhibitor of Fig and Olive (1:1) leaves extract.

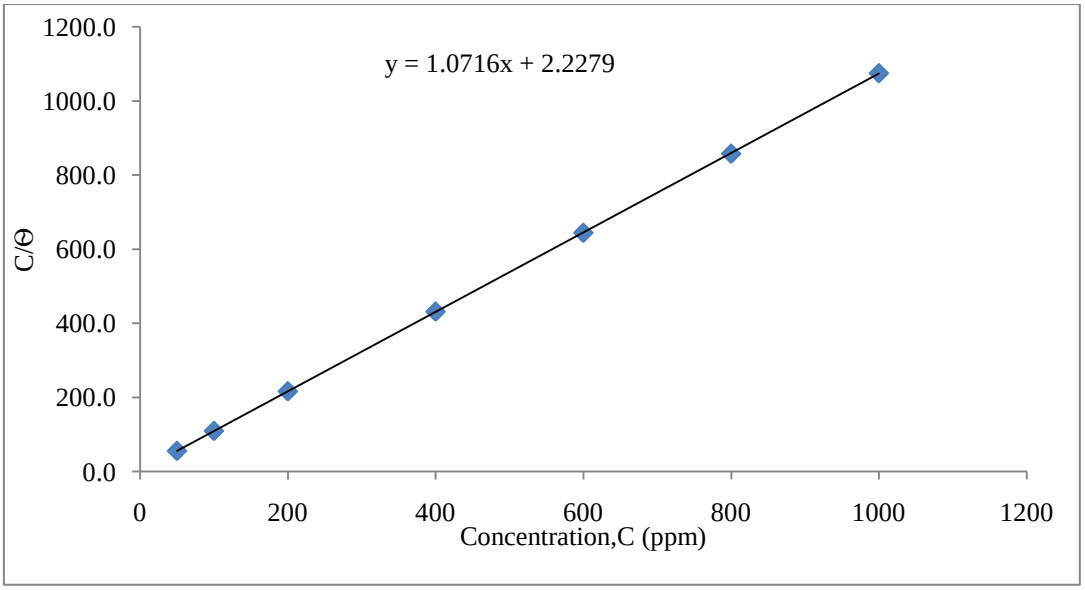

Figure 28: Concentration of the inhibitor per surface coverage versus concentration of the inhibitor of Fig and Olive (1:7) leaves extract.

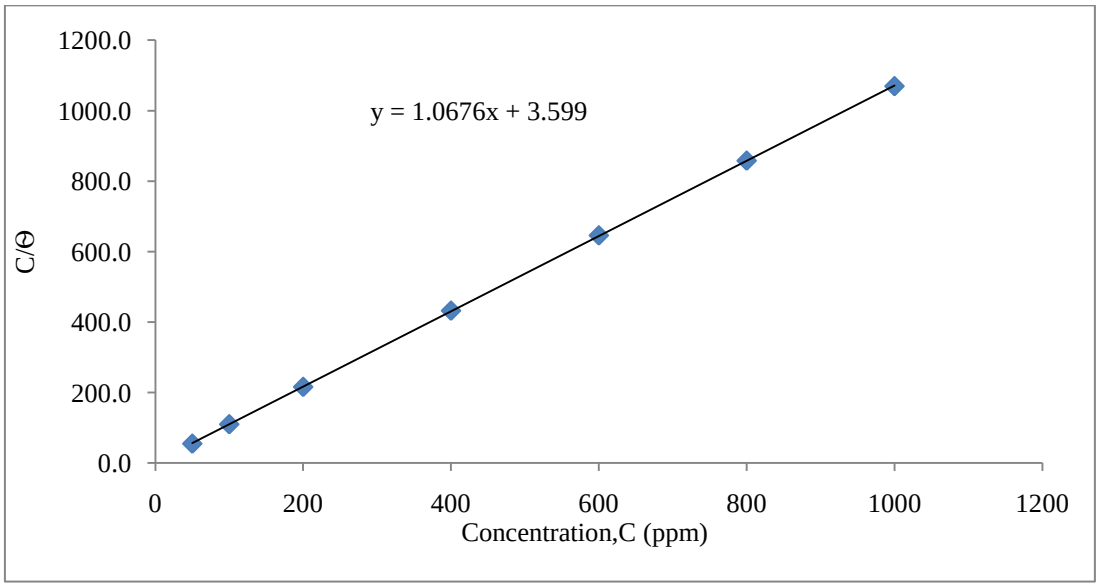

Figure 29: Concentration of the inhibitor per surface coverage versus Concentration of the inhibitor of Fig and Olive (7:1) leaves extract.

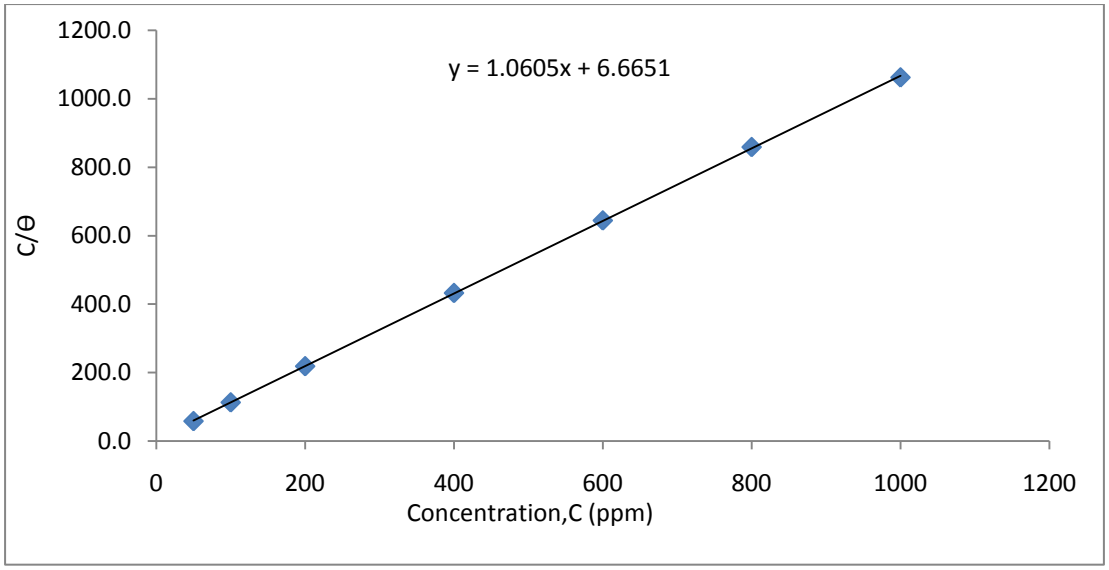

Figure 30: Concentration of the inhibitor per surface coverage versus concentration of the inhibitor of Rosemary leaves extract.

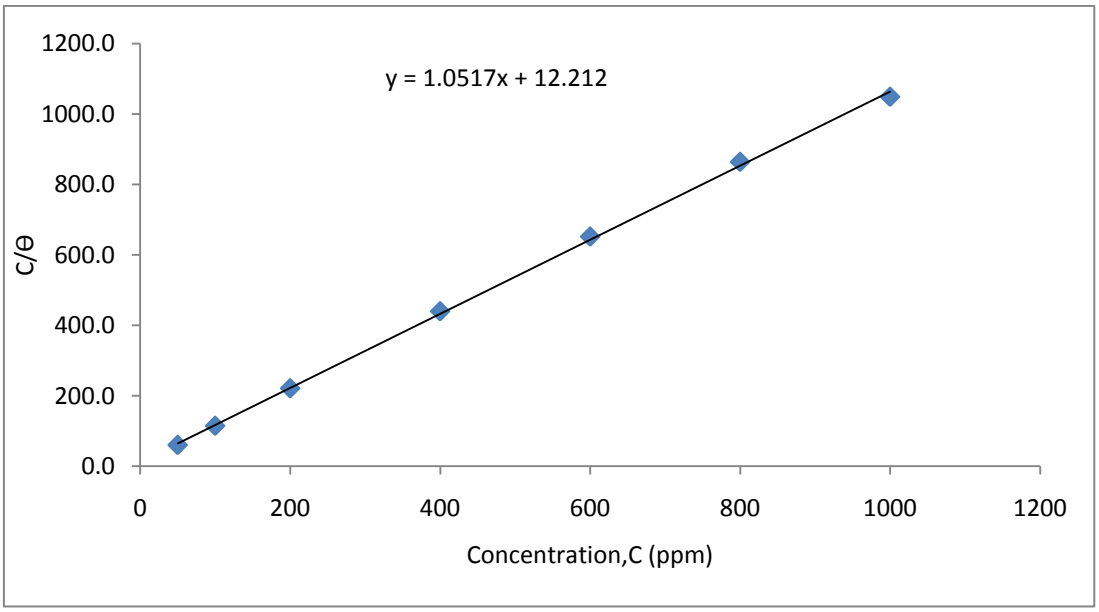

Figure 31: Concentration of the inhibitor per surface coverage versus concentration of the inhibitor of Cypress leaves extract.

The inhibitive action of green extracts towards the acidic corrosion of mild steel could be related to the adsorption of its components onto the mild steel surface. This means that the adsorbed layer acts like a barrier between the specimen surface and the corrosive solution, causing the reduction in the corrosion rate. This leads to

the fact that the inhibition efficiency is directly proportional to the surface coverage Ɵ.

As seen in the previous sections:-

It is assumed that there is no interaction between the adsorbed species on the surface of the metal and the surface is smooth and saturated. This means that the adsorbed sites don't interact with each other. The relationship is explained by Equation 3.5 [16, 21].

Where θ is the surface coverage and $\theta = \frac{IE}{100}$, C is the extract concentration and k is the adsorption constant is explained by Equation 3.6 [16,21].

The mode of variation of the surface coverage describes the adsorption isotherm that is available in the system. When the extract concentration of the green inhibitor is plotted against (c/Ɵ), a straight line is obtained with an average slope of almost unity as shown in Figures 25-31 in this section. This behavior suggests that all green inhibitors follow the Langmuir adsorption isotherm and follow Equations 3.5 and 3.6. The intercept of the plotted graphs in Figures 25-31 represents the reciprocal of the adsorption constant k. The following table represents the values of the adsorption constant and the standard free energy of all inhibitors used.

Table 3: The standard free energy of adsorption of all green plant leaves extract used at 25 ^{0}C.

Calculated value	1/k	K_{ads} (ppm^{-1})	Ln(k)	ΔG^o_{ads} (KJ/mol)
Olive	4.1000	0.2439	-1.411	-30.750
Fig	3.0875	0.3239	-1.127	-31.453
Olive & Fig (1:1)	2.2776	0.4391	-0.823	-32.207
Olive & Fig (7:1)	2.2279	0.4489	-0.801	-32.262
Olive & Fig (1:7)	3.5990	0.2779	-1.281	-31.073
Rosemary	6.6651	0.1500	-1.897	-29.546
Cypress	12.212	0.0819	-2.5024	-28.044

The calculated values of the standard free energy of adsorption have negative values. This indicates the spontaneity of the process. Values of the standard free

energy of adsorption with an order of –20 kJ/mol or higher indicate that physical adsorption is occurring. If the adsorption is in an order of -40 kJ/mol or higher, it indicates chemical adsorption process occurring [16, 21]. The measured values of ΔG^{o}_{ads} suggests a strong physical adsorption of green inhibitors leaves extract onto the surface of mild steel in 1M HCl solution. The next few sections will shed the light on the adsorption behavior and thermodynamic properties using more advances techniques.

4.3 Results and Analysis of Electrochemical Methods

The next sections record the results obtained by the electrochemical tests. The aim of the conducted tests below is to confirm the results obtained by the weight loss method. Moreover, they give a clearer insight about the film forming on the mild steel specimen. The values of the LPR, capacitance of charge transfer and the resistance of solution are all obtained by the electrochemical techniques. Last but not least, the light is shed on the effect of temperature on the inhibition efficiency and the different parameters obtained by these tests.

The maximum inhibition efficiency, linear polarization resistance and charge transfer resistance was found to be at a concentration of 1000 ppm of plant extracts. As a result, the minimum corrosion rate and corrosion current density was also obtained at a concentration of 1000 ppm of plant extracts. The change in the cathodic and anodic tafel slopes and the low shift in potential indicated that the inhibitors used are considered of mixed-type nature.

4.3.1 The Linear Polarization Resistance (LPR) Method at 25°C

A linear polarization test is carried out by a scan from approximately -10mV to +10mV. The polarization resistance can be measured by Equation 3.2. However, since the change in electrochemical potential is small the polarization resistance can be calculated from long term linear polarization resistance curves. Using the Potensiostat a long term LPR graph is obtained. This graph represents the LPR Vs time. The value of the LPR is obtained after reaching a steady value, which is

obtained after running the test at each concentration for 90 min. It can be seen from Figures 32, 34, 37, 39, 41, 43, 45 and Tables 4-10 that the resistance polarization increases as the concentration of the inhibitor added increases. As the LPR values increase, the corrosion current that passes through the solution decreases. One can notice from Equation 4.4 that as the polarization resistance increases the corrosion current decreases. It also follows that the inhibition efficiency increases as seen in Equation 4.5. Table 4 shows that the inhibition efficiency of Fig and Olive mixtures increases gradually as the concentration of the inhibitor added increases. It increases gradually until 600 ppm of inhibitor is added to the solution, where the inhibition efficiency is almost 94%. The inhibition efficiency increases after that to reach a value of 95.2 % when 1000 ppm of the inhibitor is added.

The inhibition efficiency can be calculated at each concentration from the following relationship:-

$$IE\ \% = \frac{I_{BLANK} - I_{Inhibited}}{I_{BLANK}} X\ 100\% \quad (4.1)$$

It is known that the reduction in the corrosion current causes a reduction in the corrosion rate. One can observe that by looking at equation 3.2.

Table 4: Caculations obtained using LPR method for a mixture of Fig and Olive (7:1).

Conc.(ppm)	LPR (ohm.cm²)	I_{corr} (mA/cm²)	Potential (mV)	IE%
-	63.72	0.4152	-442.80	-
50	104.02	0.0392	-377.89	90.56
100	126.74	0.0371	-374.09	91.06
200	781.86	0.0331	-421.98	92.03
400	840.45	0.0306	-416.71	92.63
600	1026.80	0.0243	-414.76	94.14
800	1128.40	0.0225	-417.32	94.58
1000	1305.80	0.0200	-425.97	95.19

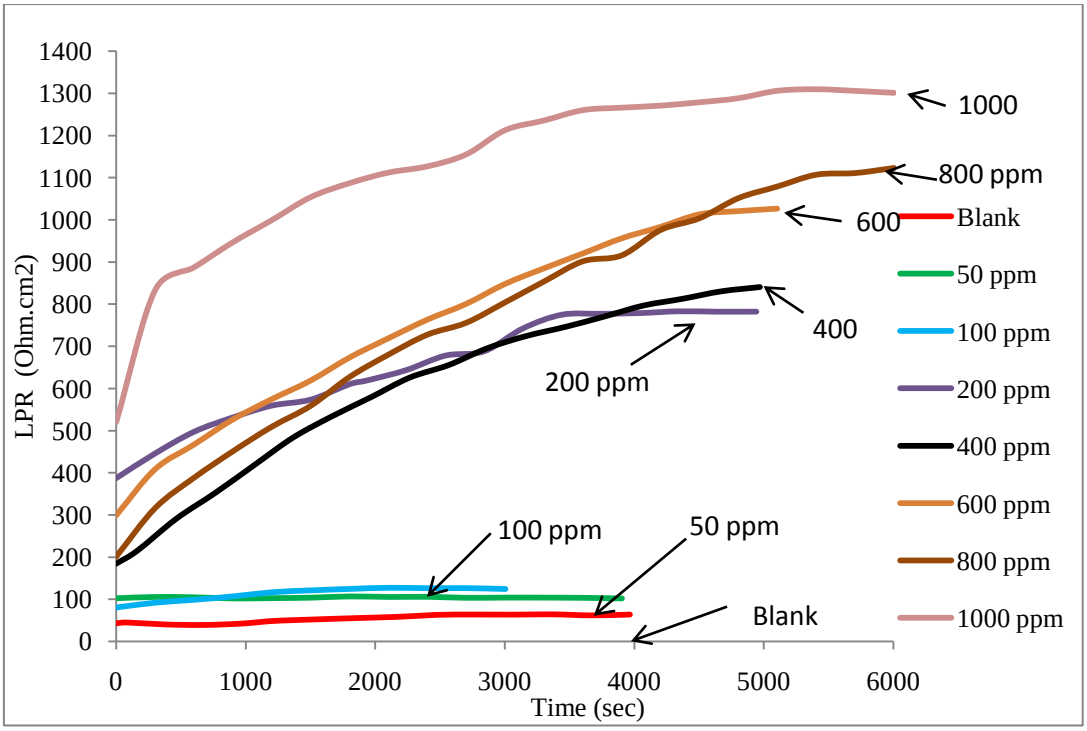

Figure 32: The LPR Vs Time of a mixture of Fig & Olive (7:1).

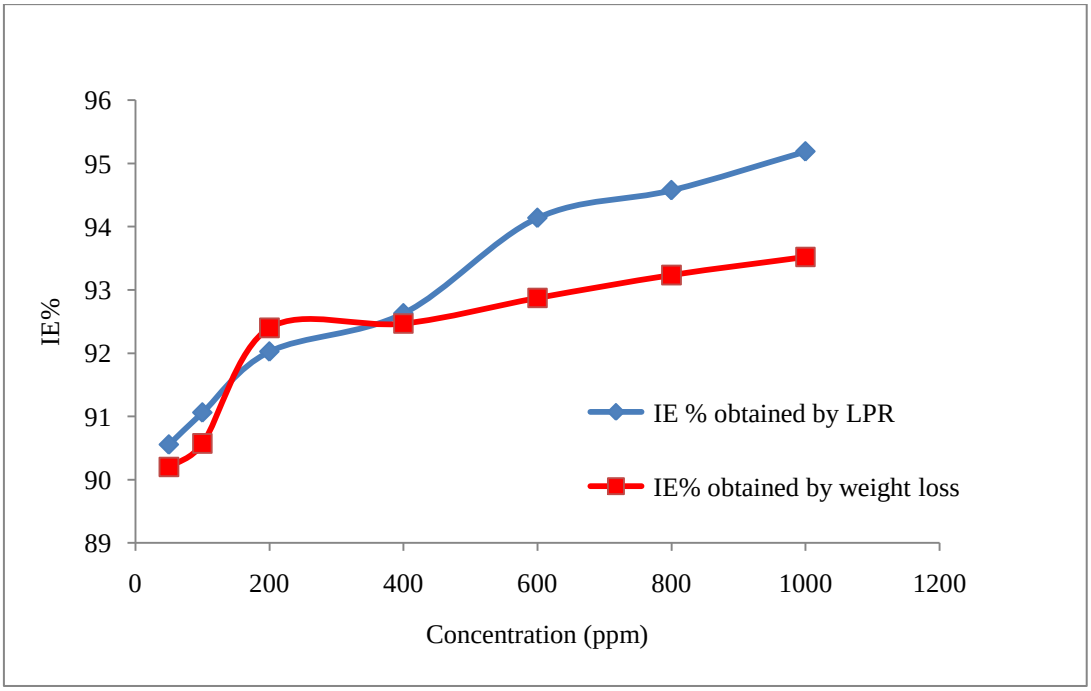

Figure 33: Inhibition Efficiency for Fig & Olive (7:1) inhibitor obtained by LPR and Weight Loss tests.

Figure 33 shows the inhibition efficiencies obtained by LPR and weight loss tests. It can be noticed that the inhibition efficiencies obtained are almost the same until 400 ppm of the inhibitor is added. It can also be noticed a 1-2 % difference in the inhibition efficiency obtained at each concentration. This is because of the errors that may occur when conducting any of the tests. However, the differences observed are very small. They come to the same conclusion, since the difference is within the margin of experimental errors. The conclusion drawn is that as the concentration of the natural inhibitor increases the corrosion rate decreases, and as a result, the inhibition efficiency of that inhibitor increases protecting the mild steel specimen from corrosion.

Table 5: Caculations obtained using LPR method for a mixture of Fig and Olive (1:7).

Conc.(ppm)	LPR (ohm.cm^2)	I_{corr} (mA/cm^2)	Potential (mV)	IE%
0	63.72	0.4152	-442.8	-
50	708.33	0.0368	-444.53	91.13
100	927.62	0.0281	-463.69	93.23
200	948.24	0.0275	-447.04	93.37
400	1023.90	0.0255	-454.34	93.86
600	1035.60	0.0252	-449.75	93.93
800	1207.40	0.0216	-448.75	94.80
1000	1740.30	0.0150	-462.95	96.39

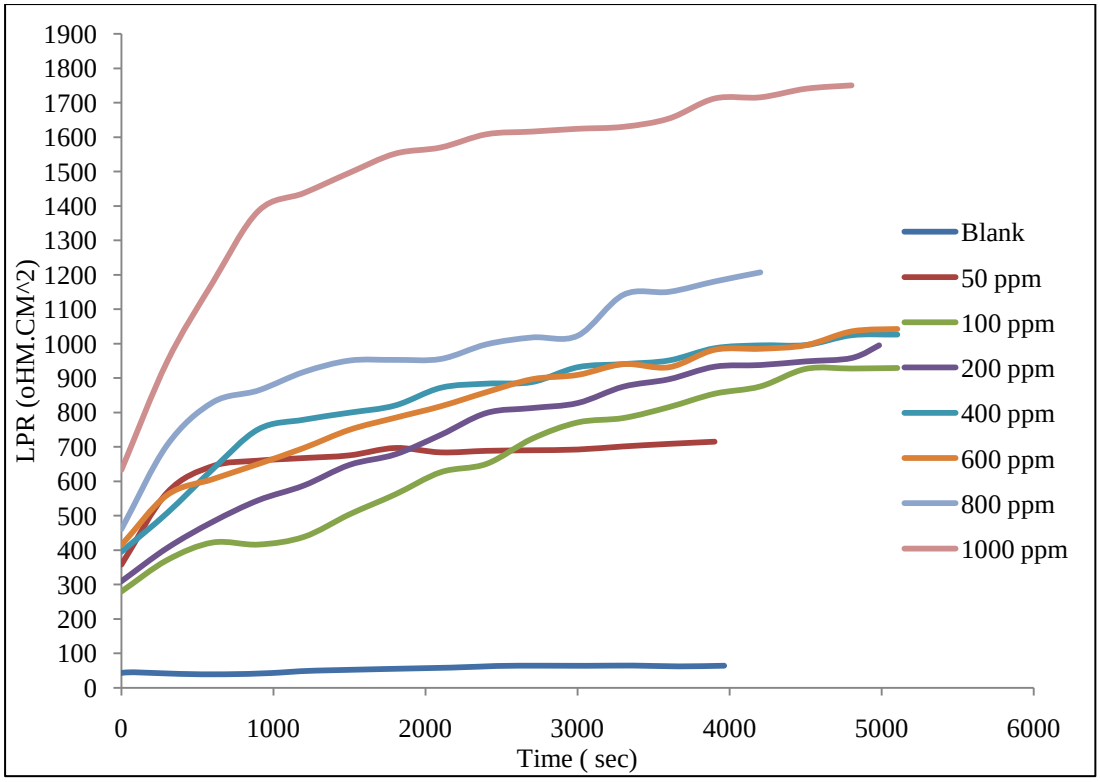

Figure 34: The LPR Vs Time of a mixture of Fig & Olive (1:7).

Figure 34 and Table 5 show that as the (1:7) Fig and Olive inhibitor is added to the solution, the long term resistance value increases gradually. This increase, after a certain amount of time, reaches a steady state value. This steady state value reads the resistance obtained after the formation of the protective film. It is obtained after running the test for approximately 90 min. As the LPR value increases, the value of the corrosion current density that passes in the solution decreases gradually. This indicates a decrease in the corrosion rate of the metal surface.

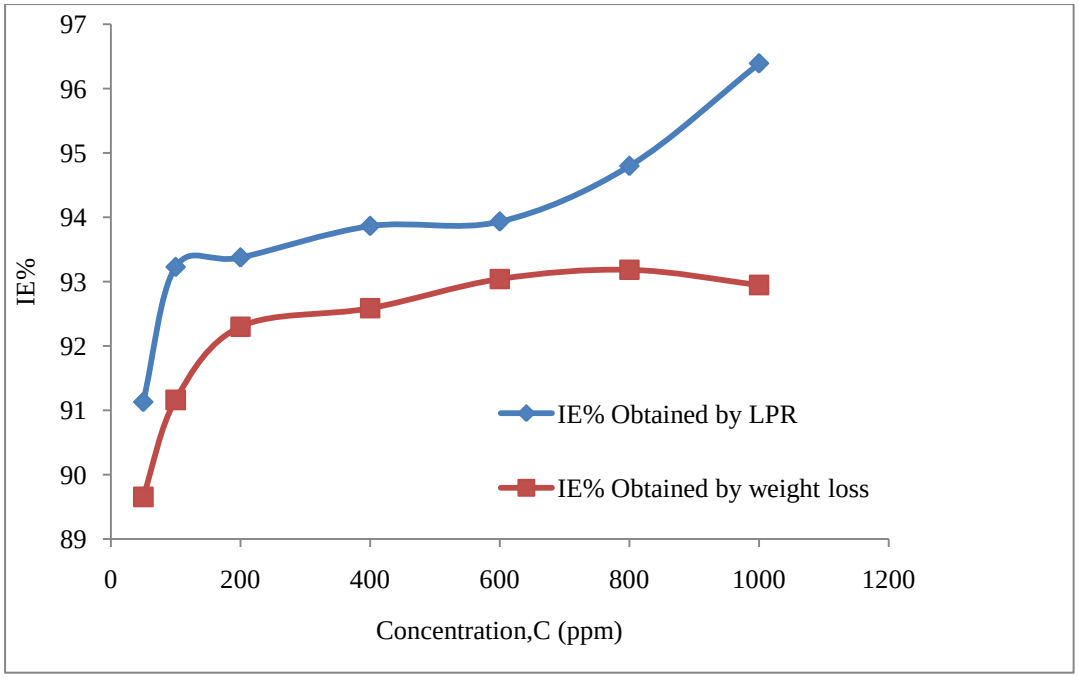

Figure 35: Inhibition efficiency for Fig & Olive (1:7) inhibitor obtained by LPR and Weight Loss tests.

Figure 35 shows the inhibition efficiency obtained by the LPR and weight loss tests for a mixture of (1:7) Fig and Olive extracts. It can be seen that both tests give the same trend. The addition of the inhibitor increases the inhibition efficiency to reach a value of 93.23 % at a concentration of 100 ppm of the inhibitor. The value of inhibition efficiency then increases to reach a value of almost 96% at a concentration of 1000 ppm. However, a slight difference can be noticed after the addition of 800 ppm of the inhibitor. This indicates that some source of error occurred. This could be explained by the inhomogeneties in the solution. However, the differences obtained from both tests indicate the same conclusion. The graph shows that as the inhibitor is added to the solution, the inhibition efficiency increases. This indicates a decrease in the corrosion rate of the metal surface.

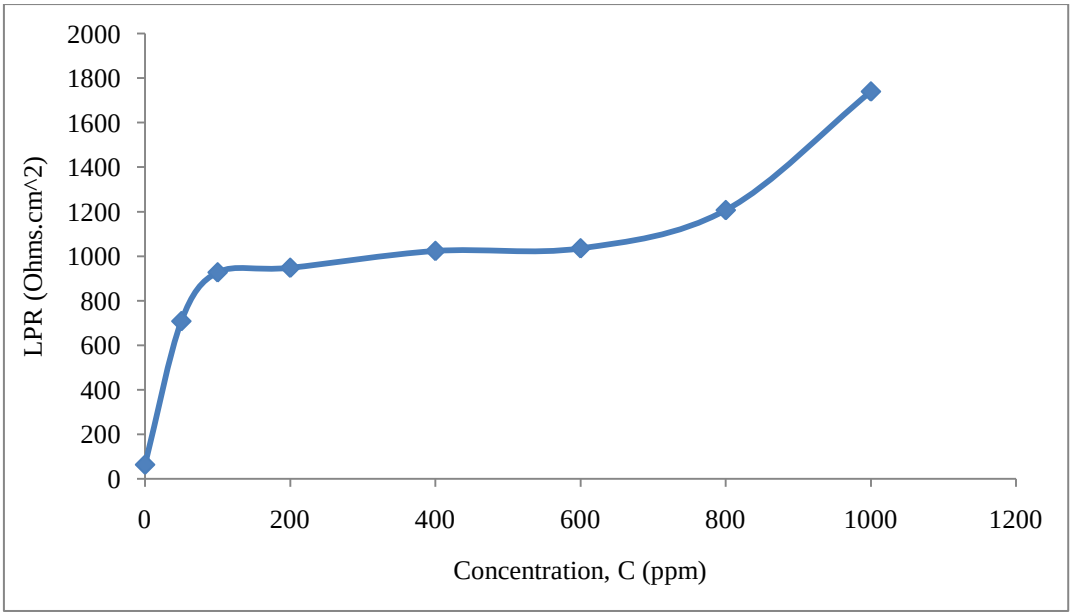

Figure 36: LPR for Fig & Olive (1:7) inhibitor Vs Concentration of the Inhibitor.

Figure 36 shows the LPR values obtained for the mixture of Fig & Olive (1:7) as the inhibitor is added to the solution. It can be seen that the LPR value increases at the concentration of 100 ppm, and then it increases gradually until 800 ppm of the inhibitor is added. The value of the LPR then increases to reach its maximum at a concentration of 1000 ppm. This results in a decrease in the current passing through the solution, proving that the corrosion rate of the metal surface decreases as the inhibitor is added to the environment.

Table 6: Caculations obtained using LPR method for a mixture of Fig and Olive (1:1).

Conc.(ppm)	LPR (ohm.cm²)	I_{corr} (mA/cm²)	Potential (mV)	IE%
0	63.72	0.4152	-442.80	-
50	623.44	0.0418	-423.84	89.92
100	982.51	0.0265	-419.75	93.61
200	1020.00	0.0256	-416.27	93.84
400	1094.80	0.0238	-419.47	94.26
600	1213.90	0.0215	-434.01	94.82
800	1258.10	0.0207	-425.80	95.00
1000	1278.80	0.0204	-427.55	95.09

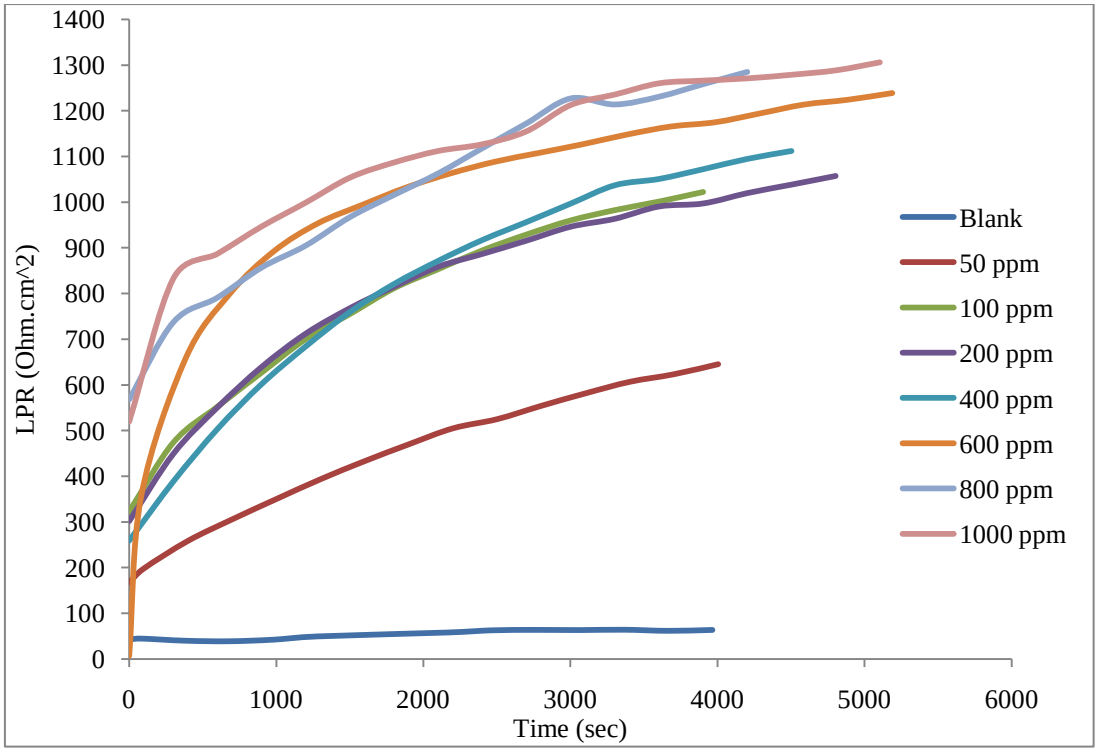

Figure 37: The LPR Vs Time of a mixture of Fig & Olive (1:1).

Figure 37 and Table 6 show the results obtained by the LPR test for a (1:1) mixture of Fig and Olive extracts. It can be seen that as the inhibitor is added to the solution, the long term resistance value increases gradually until it reaches a steady state value. This steady state value reads the long term polarization resistance obtained at the surface of the metal after the formation of the protective film and after running the test for approximately 90 min. The protective film is sustained after the inhibitor products adsorb onto the surface of the metal. It acts like a barrier between the metal surface and the corrosive environment. As the LPR value increases, the value of the current density that passes in the solution decreases gradually. This indicates a decrease in the corrosion rate of the metal surface. The addition of the inhibitor increases the inhibition efficiency to a value of 93.6% at a concentration of 100 ppm of the inhibitor. Afterwards, the inhibition efficiency increases gradually until 400 ppm. The value of inhibition efficiency then increases to reach a value of almost 95% at a concentration of 1000 ppm. This proves that the mixture of the inhibitor acts as a good inhibitor in the environment tested.

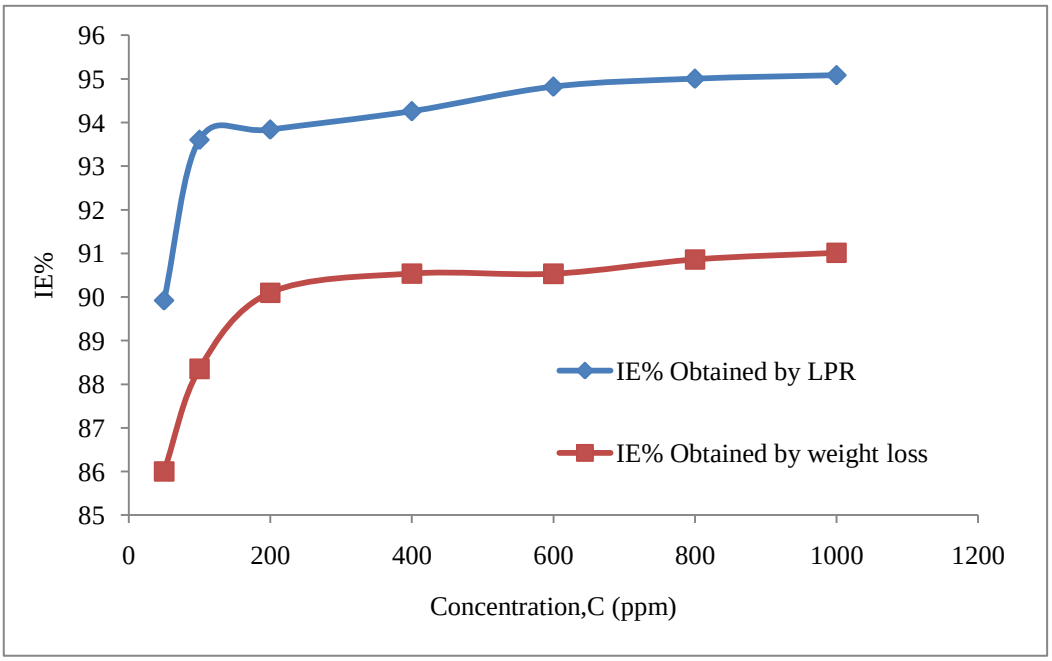

Figure 38: Inhibition efficiency for Fig & Olive (1:1) inhibitor obtained by LPR and Weight Loss tests.

Figure 38 shows the inhibition efficiency obtained by the LPR and weight loss tests for the (1:1) Fig and Olive mixture. It can be seen that both tests give the same trend. However, a slight difference can be noticed in the value of the inhibition efficiency. This small difference is approximated to be 2-4 %, which is considered within the margin of error. It could be due to the inhomogeneties in the solution. It may also be due to human errors when conducting the tests. However, the differences obtained from both tests indicate the same conclusion. The graph shows that as the inhibitor is added to the solution, the inhibition efficiency increases and so does the polarization resistance of the metal. This indicates a decrease in the corrosion current density values, as well a decrease in the corrosion rate of the metal surface. The inhibitor used shows good inhibition efficiency in the 1M HCl solution and protects the metal surface from corrosion under the severe environment.

Table 7: Caculations obtained using LPR method for pure Fig.

Conc.(ppm)	LPR (ohm.cm²)	I_{corr} (mA/cm²)	Potential (mV)	IE%
0	63.72	0.4152	-442.80	-
50	493.24	0.0528	-424.41	87.26
100	876.62	0.0297	-421.33	92.83
200	970.86	0.0268	-446.21	93.53
400	988.96	0.0263	-444.47	93.65
600	992.96	0.0260	-444.47	93.72
800	1008.50	0.0258	-414.54	93.77
1000	1060.10	0.0246	-417.67	94.07

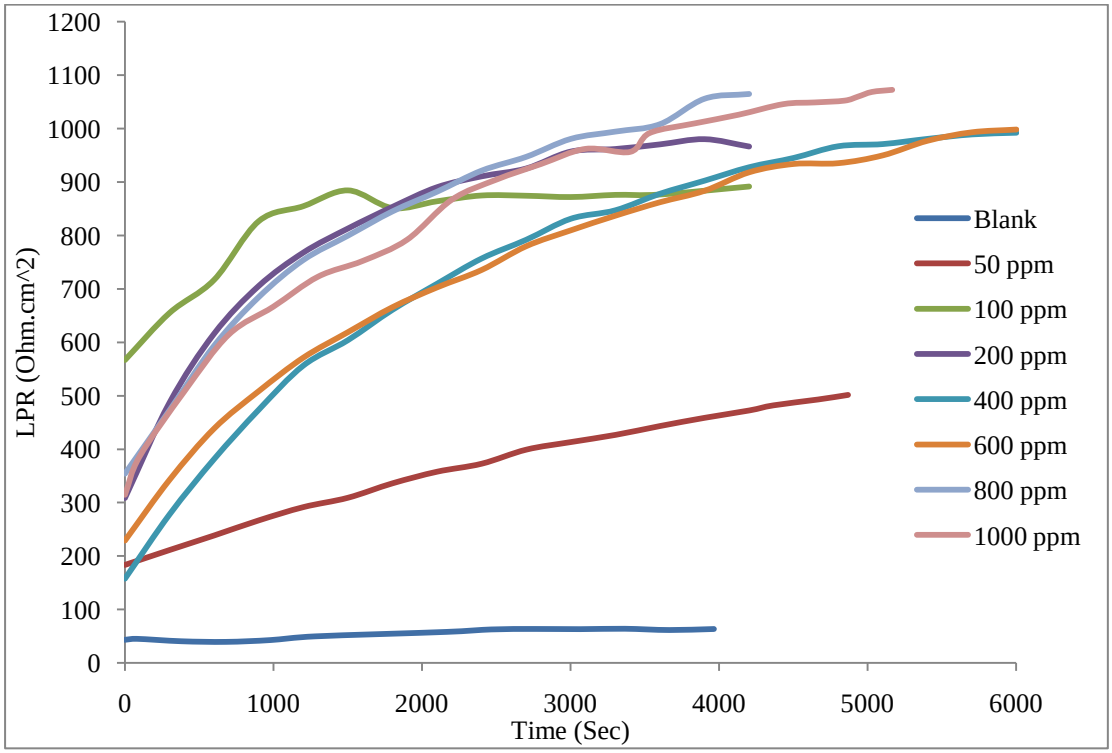

Figure 39: The LPR Vs Time of pure Fig.

Figure 39 and Table 7 show the results obtained by the LPR test for pure Fig extract. It can be seen that as the inhibitor is added to the solution the long term resistance value increases gradually until it reaches a steady state value. This steady state value reads the long term polarization resistance obtained at the surface of the metal after the formation of the protective film. This steady state value is obtained

after running the test for almost 90 min and is attained faster in some cases than others. As the LPR value increases, the value of the current density that passes decreases gradually. This indicates a decrease in the corrosion rate of the metal surface. The addition of the inhibitor increases the inhibition efficiency to reach a value of 92.83 % at a concentration of 100 ppm of the inhibitor. After that the inhibition efficiency increases gradually until it reaches its maximum at a concentration of 1000 ppm, which proves that the mixture of the inhibitor acts as a good inhibitor in the environment tested.

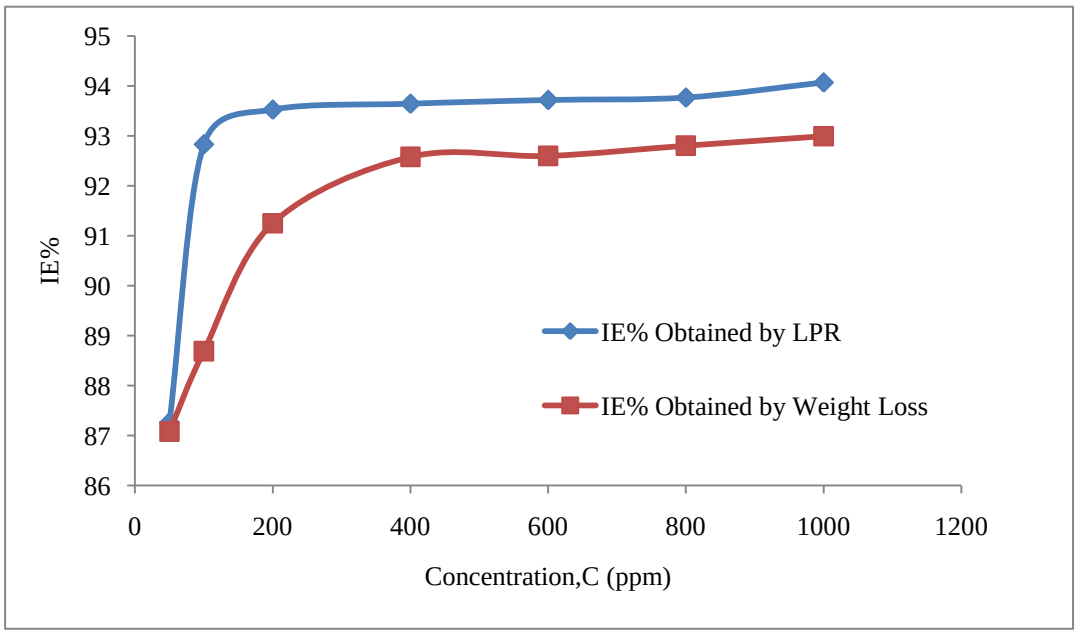

Figure 40: Inhibition efficiency for pure Fig inhibitor obtained by LPR and Weight Loss tests.

Figure 40 shows the inhibition efficiency obtained by the LPR and Weight Loss tests. It can be seen that both tests give the same trend of results. Both tests show that as the inhibitor is added to the environment the inhibition efficiency increases. However, as with the tests for the other inhibitors, there is a slight difference in the values of inhibition efficiency obtained at the different concentrations. The difference noticed is within the margin of error. The shape of both curves plotted is approximately the same. This proves that the results obtained by the LPR test agree with the one obtained by the weight loss test. This also indicates a decrease in the corrosion rate of the metal surface exposed to the environment.

Table 8: Caculations obtained using LPR method for pure Olive.

Conc.(ppm)	LPR (ohm.cm²)	I_{corr} (mA/cm²)	Potential (mV)	IE%
0	63.72	0.4152	-442.80	-
50	430.27	0.0606	-424.41	85.40
100	492.67	0.0529	-421.33	87.25
200	511.94	0.0510	-428.26	87.73
400	535.07	0.0488	-434.22	88.26
600	553.12	0.0472	-420.38	88.64
800	576.85	0.0452	-417.12	89.11
1000	627.16	0.0416	-439.09	89.98

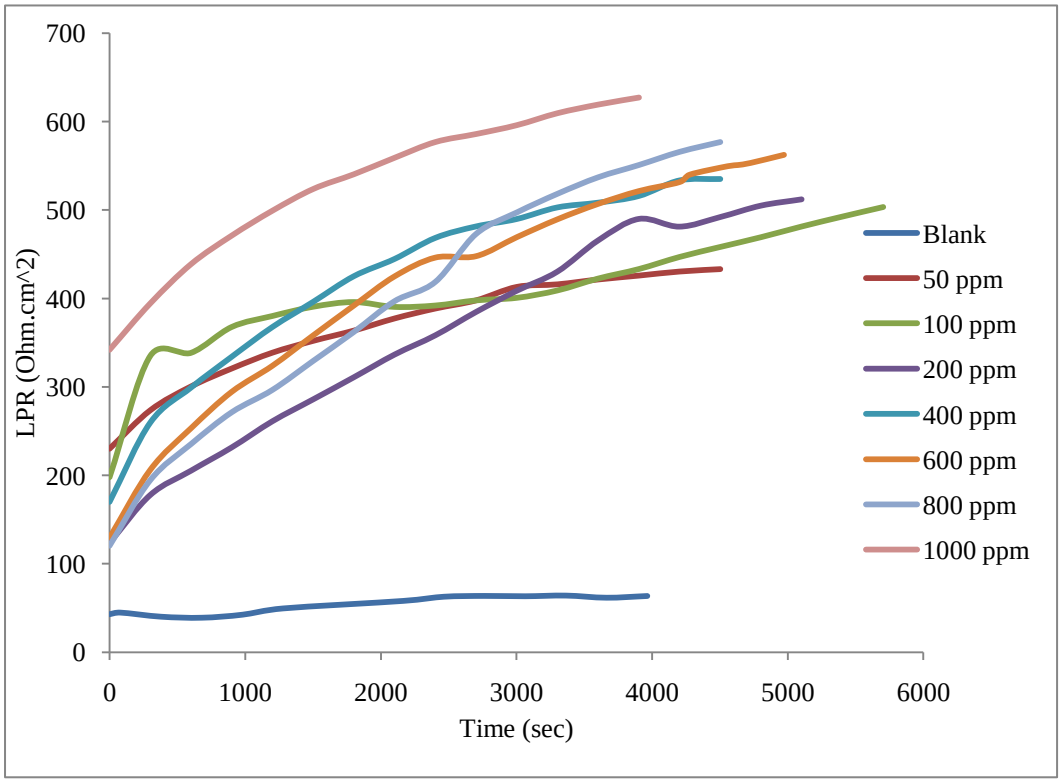

Figure 41: The LPR Vs Time of pure Olive.

Figure 41 and Table 8 show the results obtained by the LPR test for pure Olive extract. It can be noticed that the value obtained of the LPR is less than the value obtained when using a mixture of the inhibitor at certain cases. It can also be noticed that as the extract is added to the solution, the long term resistance value increases

gradually until it reaches a steady state value, which is obtained after running the test for almost 90 min. As the LPR value increases, the value of the current density that passes decreases gradually which indicates a decrease in the corrosion rate of the metal surface. The addition of the inhibitor increases the inhibition efficiency to reach a value of 87.25 % at a concentration of 100 ppm of the inhibitor. Then, the inhibition efficiency increases gradually until it reaches its maximum at a concentration of 1000 ppm.

The maximum inhibition efficiency obtained by the LPR test is less than that obtained by the weight loss test. However, the difference noticed is within the margin of error. Figure 42 shows the inhibition efficiency obtained by both test. The difference obtained is 2-4 %, which can be considered within the margin of error. Both tests have the same trend of results. Furthermore, they both prove a decrease in the corrosion rate of the metal surface.

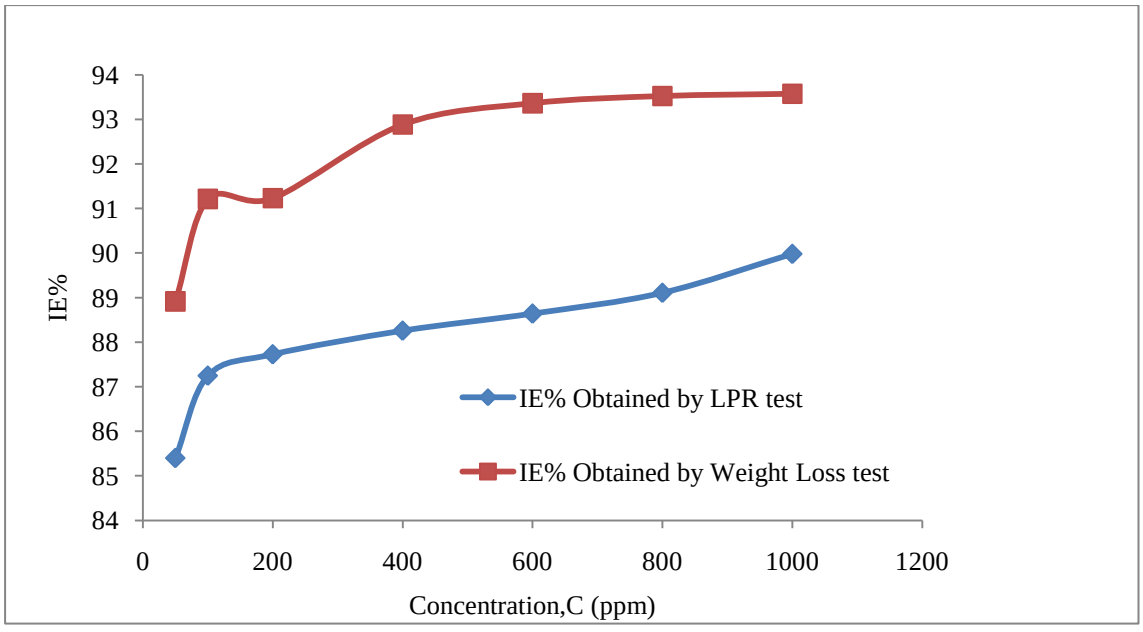

Figure 42: Inhibition efficiency for pure Olive inhibitor obtained by LPR and Weight Loss tests.

Figure 41 and Table 9 illustrate the results obtained by the LPR test for Rosemary extract. As the LPR value increases, the value of the current density that passes decreases gradually. This indicates a decrease in the corrosion rate of the metal

surface. The addition of the inhibitor increases the inhibition efficiency to reach a value of 86.83 % at a concentration of 50 ppm of the inhibitor, which is a lower value than the previous tested inhibitors. The inhibition efficiency continues to increase gradually until it reaches its maximum at a concentration of 1000 ppm, reading a value of 94.87%. This proves that the mixture of the inhibitor acts as a good inhibitor in the environment tested, though it has lower inhibition efficiency than other tested extracts.

Table 9: Caculations obtained using LPR method for pure Rosemary.

Conc.(ppm)	LPR (ohm.cm²)	I_{corr} (mA/cm²)	Potential (mV)	IE%
0	63.72	0.4152	-442.80	-
50	477.18	0.0547	-477.53	86.83
100	514.76	0.0507	-482.77	87.80
200	543.61	0.0480	-470.62	88.44
400	549.27	0.0475	-464.00	88.56
600	679.78	0.0384	-470.32	90.76
800	997.89	0.0261	-467.66	93.70
1000	1223.80	0.0213	-427.75	94.87

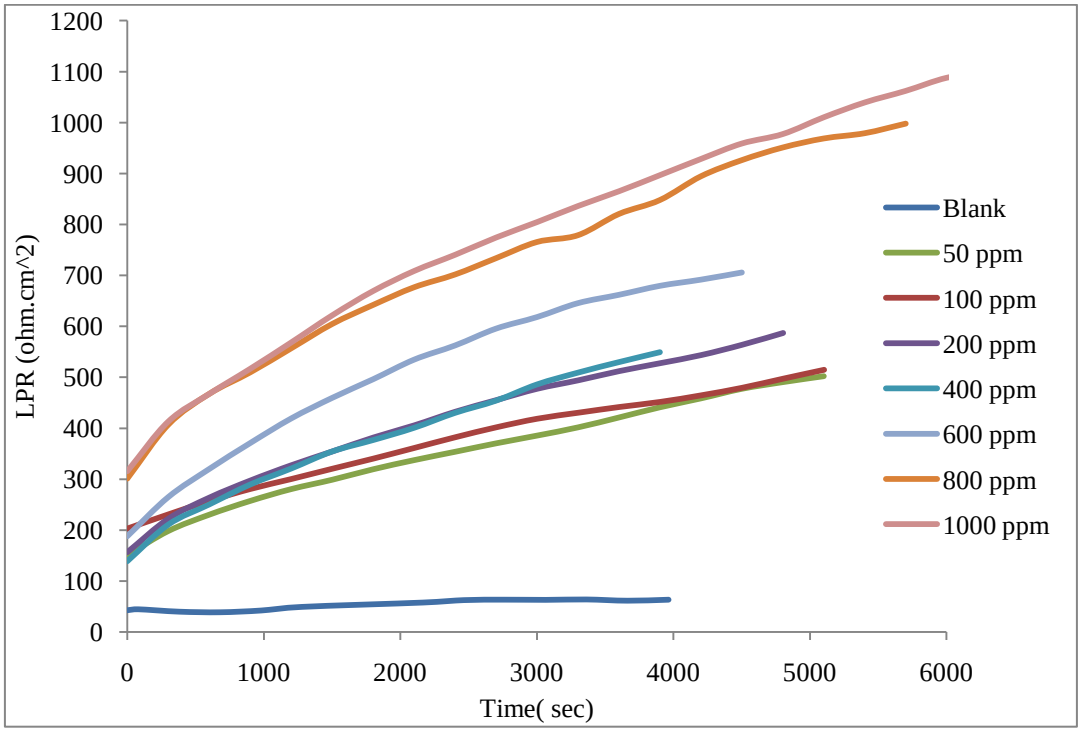

Figure 43: The LPR Vs Time of pure Rosemary.

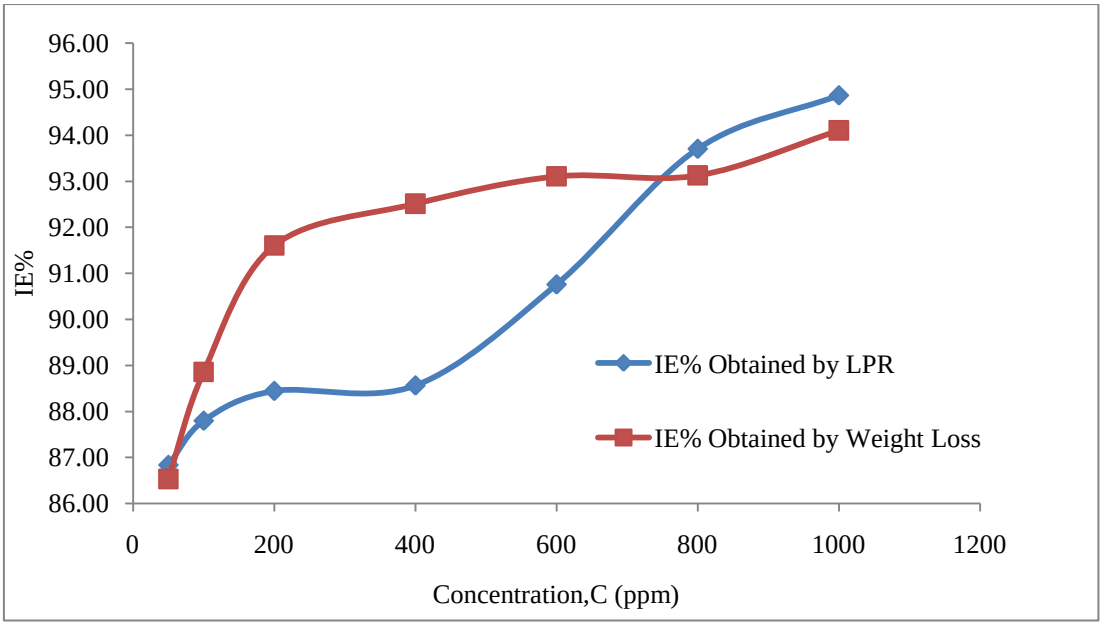

Figure 44: Inhibition efficiency for pure Rosemary inhibitor obtained by LPR and Weight Loss tests.

Figure 42 shows the inhibition efficiency obtained by the LPR and Weight Loss tests for Rosemary extract. It can be seen that both tests give the same trend of results with slight difference. Both tests show that as the inhibitor is added to the environment the inhibition efficiency increases. However, a slight difference can be noticed in the values of inhibition efficiency obtained at the different concentrations of the inhibitor. The difference noticed is within the margin of error. The shape of both curves plotted is approximately the same with a slight change at the concentrations of 200-600 ppm. This proves that the results obtained by the LPR test agree with the one obtained by the weight loss test. This also indicates a decrease in the corrosion rate of the metal surface exposed to the environment.

Table 10: Caculations obtained using LPR method for pure Cypress.

Conc.(ppm)	LPR (ohm.cm²)	I_{corr} (mA/cm²)	Potential (mV)	IE%
0	63.72	0.41523	-442.80	-
50	502.50	0.05191	-430.28	87.50
100	553.71	0.04711	-443.54	88.65
200	553.71	0.04711	-443.54	88.65
400	635.85	0.04103	-427.10	90.12
600	659.87	0.03953	-427.50	90.48
800	1024.00	0.02547	-485.46	93.87
1000	1177.50	0.02215	-429.92	94.66

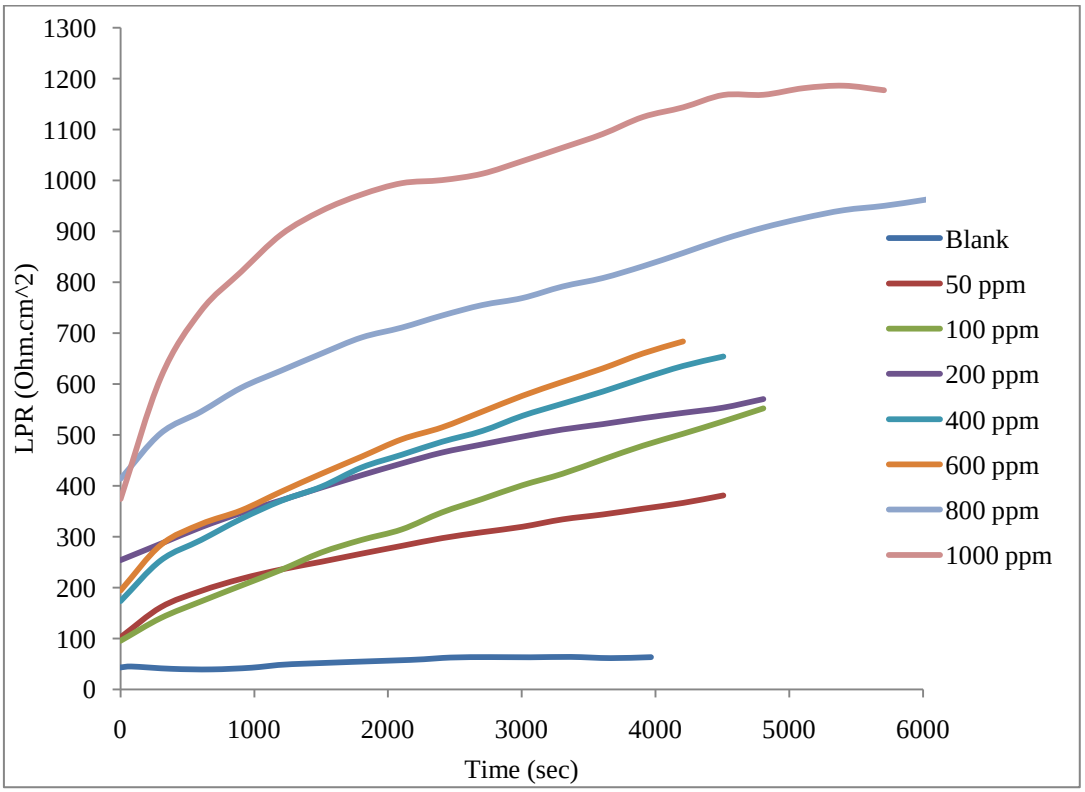

Figure 45: The LPR Vs Time of pure Cypress.

Figure 45 and Table 10 demonstrate the results obtained by the LPR test for Cypress extract. It can be seen that as the inhibitor is added to the solution the long term resistance value increases gradually until it reaches a steady state value. As the LPR value increases, the value of the current density that passes decreases gradually.

This indicates a decrease in the corrosion rate of the metal surface. This proves that the mixture of the inhibitor acts as a good inhibitor in the environment tested, though it has lower inhibition efficiency than other tested extracts.

The inhibition efficiency obtained by the LPR and Weight Loss tests for Rosemary extract is shown in Figure 46. The addition of the inhibitor increases the inhibition efficiency to reach a value of 88.65% at a concentration of 100 ppm of the inhibitor, which is a lower value than the previous tested inhibitors. The inhibition efficiency reaches its maximum of 94.66% at a concentration of 1000 ppm. It can be seen that both tests give the same trend of results with slight difference. However, the difference noticed is within the margin of error. The shape of both curves plotted is approximately the same with a slight change at a concentration of 800 ppm. This proves that the results obtained by the LPR test agree with the one obtained by the weight loss test.

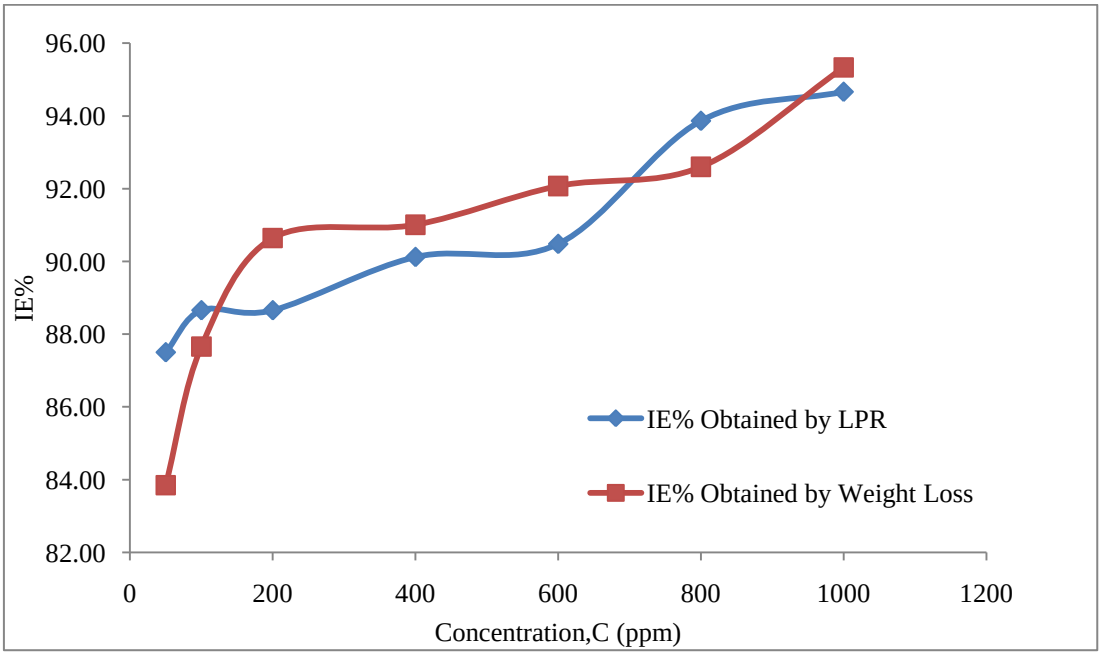

Figure 46: Inhibition efficiency for pure Cypress inhibitor obtained by LPR and Weight Loss tests.

Figures 47-50 show the values of the LPR and inhibition efficiency obtained by the LPR test for pure inhibitors and Fig and Olive inhibitors (pure and mixtures). It can be seen from the graphs that the order of efficiency is different from the one

obtained by the weight loss test. However, the difference is small and considered to be within the margin of error. Both tests are considered reliable and the weight loss results can be considered a better approach in some cases, since it is a long term test compared to the other test considered in this thesis. One can draw a clearer conclusion by looking at the results obtained by all tests.

Moreover, all results obtained by the LPR test draw the same conclusion and that is: the LPR values increase as the inhibitor extract is added to the solution. This proves that the inhibition efficiency increase and the corrosion rate of the metal decreases as the inhibitor is added to the corrosive environment. This happens as a result of the protective film formed by adsorption which acts as a barrier between the metal surface and the surrounding environment. It protects the metal surface from direct exposure to the severe environment.

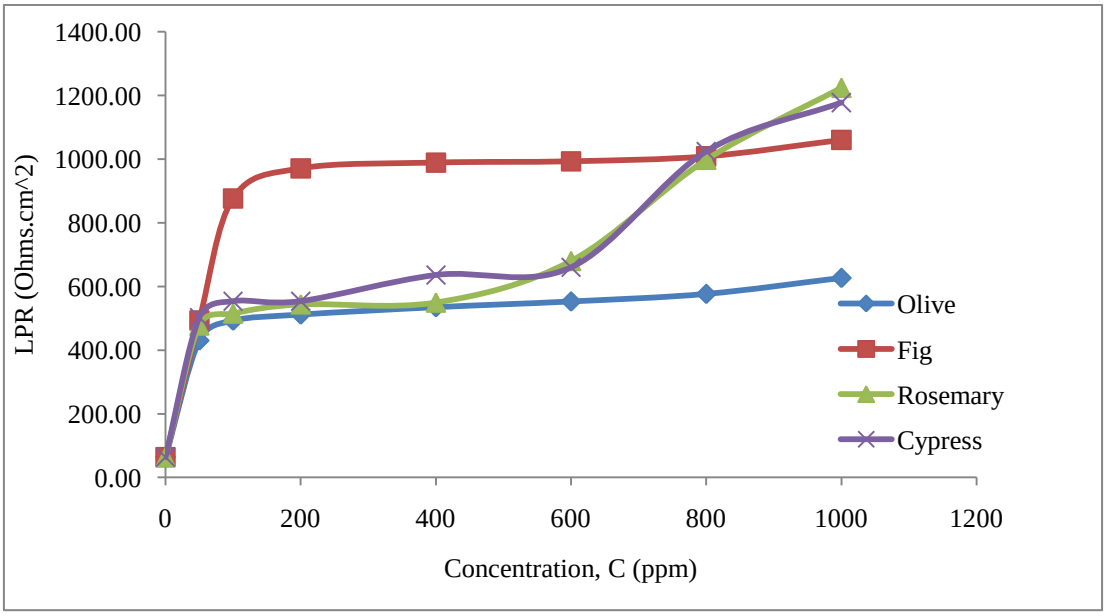

Figure 47: LPR values obtained by the LPR Test of pure plant extracts Vs the Concentration of the Inhibitor added.

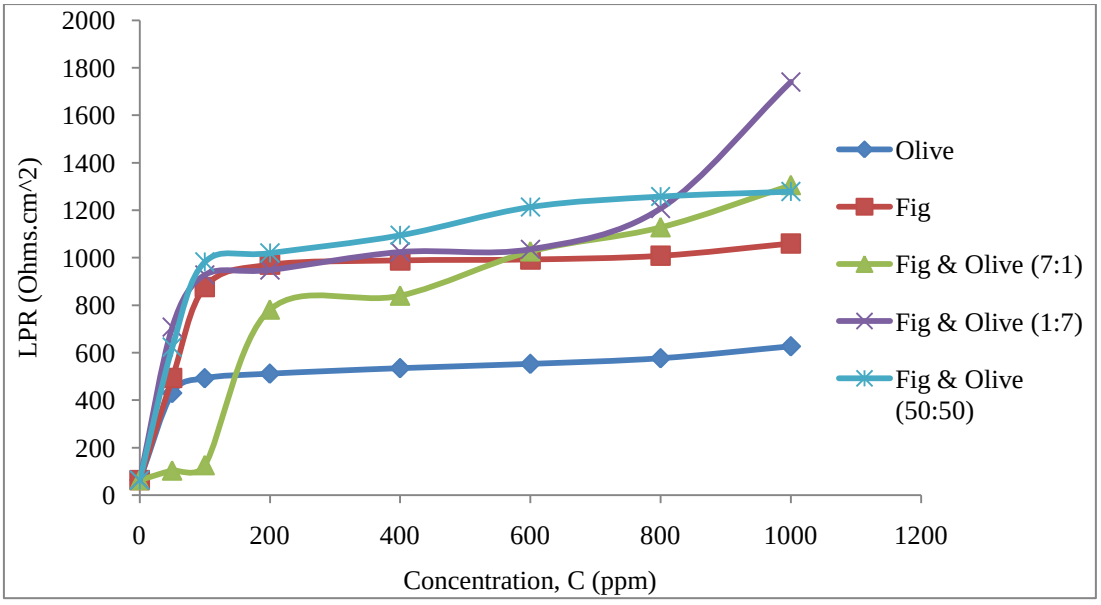

Figure 48: LPR values obtained by the LPR Test of pure and mixtures of Olive and Fig Vs the Concentration of the Inhibitor added.

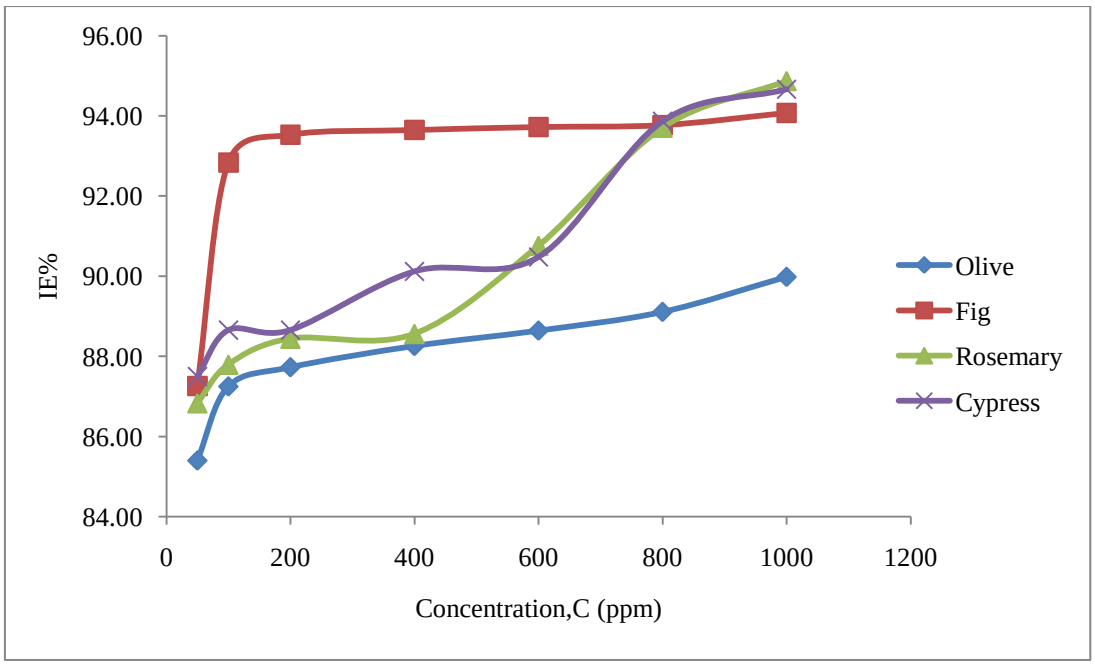

Figure 49: Inhibition Efficiency values obtained by the LPR Test of pure and plant extracts Vs the Concentration of the Inhibitor added.

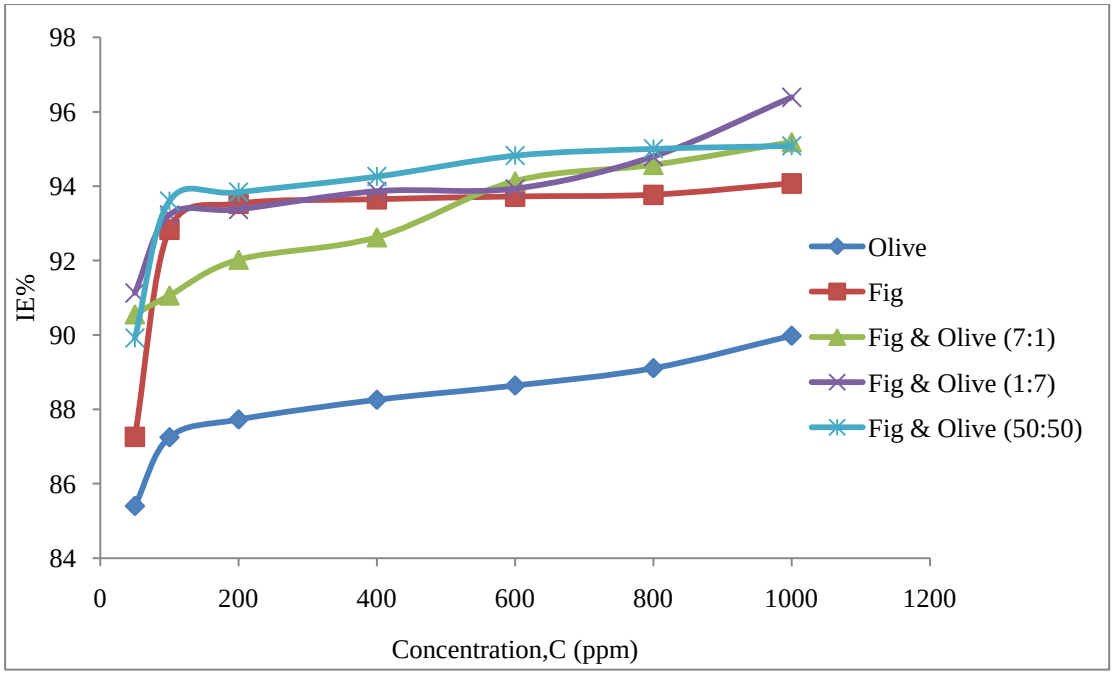

Figure 50: Inhibition Efficiency values obtained by the LPR Test of pure and mixtures of Olive and Fig Vs the Concentration of the Inhibitor added.

4.3.2 The Impedance Test

The corrosion of mild steel in hydrochloric acid solution in the presence of fig and olive (7:1) extract was investigated by EIS at 25°C after an exposure time of 20 min. Nyquist plots in uninhibited and inhibited acidic solutions containing different concentrations of plant extract are shown in Figure 51. The impedance generated from Nyquist plots can be either calculated using equation 4.2 or graphically.

$$Z = R_{sol} + \frac{R_{ct}}{1+w^2 C_{dl}^2 R_{ct}^2} - \frac{jwC_{dl}R_{Ct}^2}{1+w^2 C_{dl}^2 R_{ct}^2} \qquad (4.2)$$

Where Z is the impedance, R_{ct} is the resistance to charge transfer, R_{sol} is the resistance of the solution and C_{dl} is the double layer capacitance.

The results are similar for the other extracts, as shown in Figures 53-58. The semicircles obtained in the figures are depressed, with some plots more depressed than the others such as Nyquist plots obtained for Rosemary and Cypress plant extracts. Depression of the semicircles occurs when the curves do not continue decreasing until they reach the x-axis. This feature indicates formation of porous layers and adsorption of the inhibitor on the surface of the mild steel specimen [16,

31, 34]. It can be seen that as the inhibitor is added, the impedance increases and this indicates a reduction in the corrosion rate. This may not be clear, but if the corrosion current in Tables 11-17 is examined closely, it can be noticed that there is a decrease in the corrosion current as the inhibitor is added to the solution, which causes a reduction in the corrosion rate.

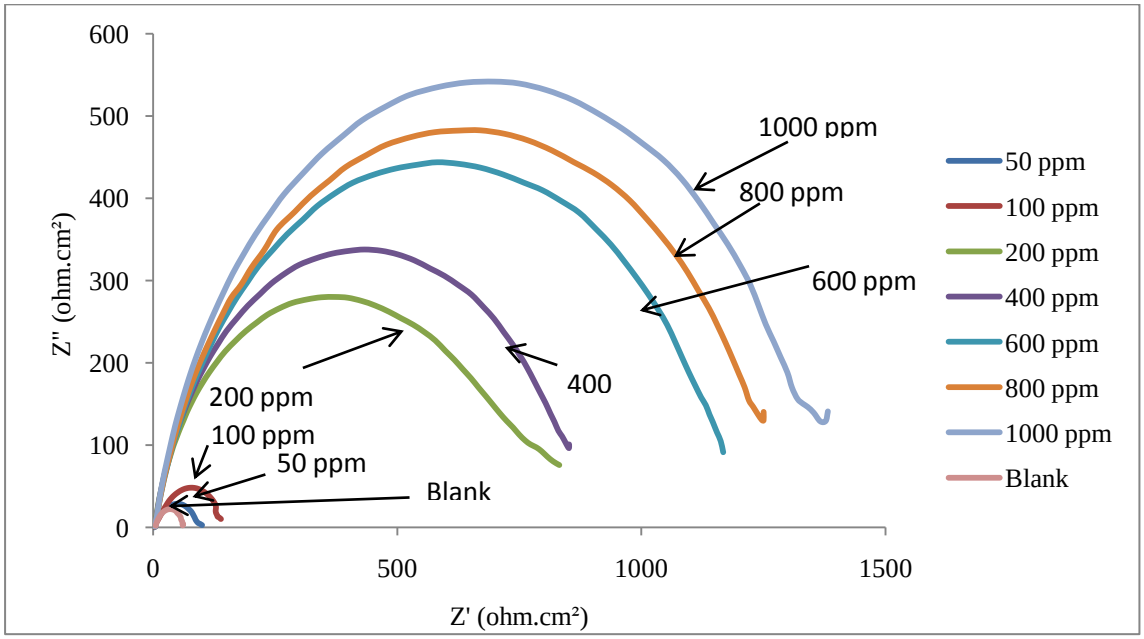

Figure 51: Nyquist plots for mild steel in a 1M HCl solution in the absence and presence of Fig & Olive (7:1) plant extract at 25°C.

Table 11: Impedance parameters and corresponding inhibition efficiency for mild steel in 1M HCl in the absence and presence of Fig & Olive (7:1) plant extract at 25°C.

Conc.(ppm)	R_{soln} (Ohms.cm^2)	R_{ct} (Ohms.cm^2)	C_{dl} (F)	I_{corr} (mA/cm^2)	IE%
-	1.542	57.07	0.000431	0.2001	0
50	2.112	452.00	0.000186	0.0222	88.90
100	2.501	521.30	0.000171	0.0185	90.75
200	2.909	872.00	0.000169	0.0148	92.60
400	3.329	886.20	0.000166	0.0128	93.60
600	3.371	1197.00	0.000102	0.0092	95.42
800	3.469	1300.00	0.000101	0.0091	95.48
1000	3.693	1416.00	0.000099	0.0090	95.50

The Nyquist plots are analyzed in terms of the equivalent circuit comprised of classic parallel capacitor (C_{dl} ; double layer capacitance) and a resistor (R_{ct} ; charge transfer resistance or R_p, where both are connected in series with the solution resistance R_s). The fitted values of R_{ct} , C_{dl} , R_s, I_{corr} and the IE% are all tabulated in Table 11. The inhibition efficiency can also be calculated as [16]:-

$$IE\% = \frac{(1/R_{ct})a - (1/R_{ct})p}{(1/R_{ct})a} \qquad (4.3)$$

Where a and p refers to the absence and presence of corrosion inhibitor respectively.

It was found that as the concentration of the inhibitor increases, R_{ct} (radius of semicircle) and R_s values increase, whereas values of C_{dl} decrease. This occurs because of the adsorption of the inhibitor molecules on the mild steel surface. R_{ct} values are as the Rp values which are inversely proportional to the corrosion rate [16, 31, 34]. The finding proves a reduction in the corrosion rate and an increase in the inhibition efficiency as the inhibitor is added to the solution.

It can be seen from Table 11 that the inhibition efficiencies obtained by the impedance method is almost the same as the one obtained by the weight loss method. It is clearer in Figure 52, which shows a slight difference (1-3%) between the two methods and in addition to the LPR method.

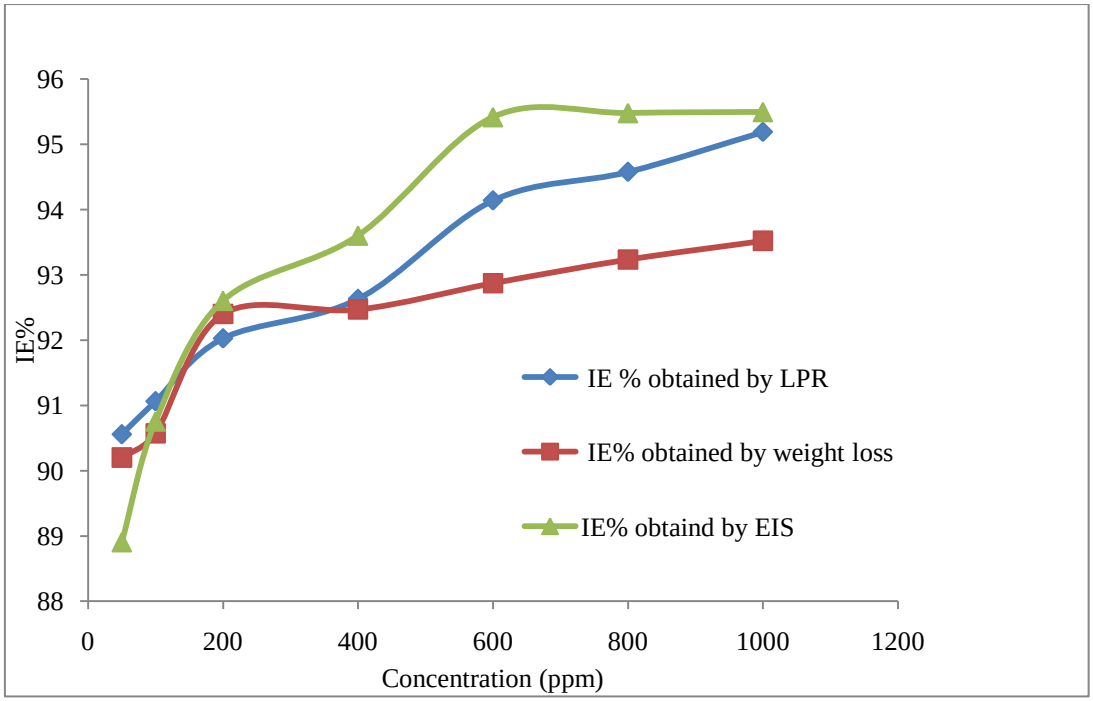

Figure 52: Inhibition efficiency for Fig & Olive (7:1) inhibitor obtained by LPR Weight loss and EIS tests.

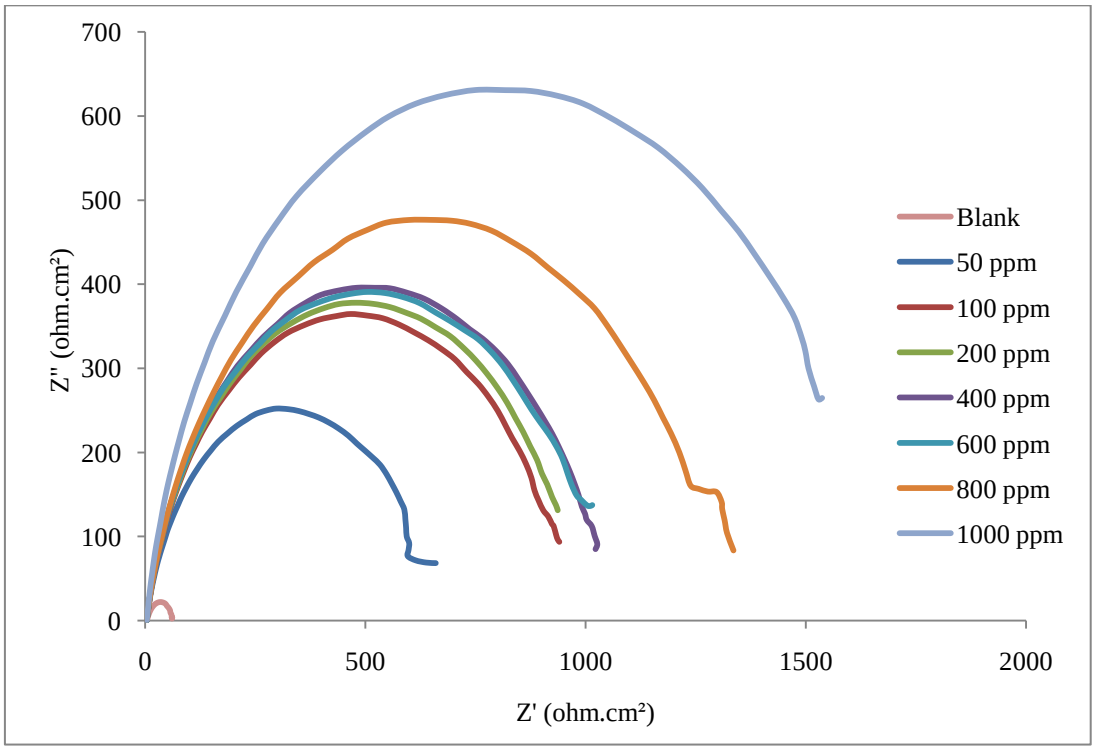

Figure 53: Nyquist plots for mild steel in a 1M HCl solution in the absence and presence of Fig & Olive (1:7) plant extract at 25°C.

Table 12: Impedance parameters and corresponding inhibition efficiency for mild steel in 1M HCl in the absence and presence of Fig & Olive (1:7) plant extract at 25°C.

Conc.(ppm)	Rsol (ohm.cm^2)	Rct (ohm.cm^2)	Cd (F)	I corr. (mA/cm^2)	IE%
0	1.542	57.07	0.000431	0.2001	
50	3.030	684.30	0.000163	0.0174	91.31
100	3.031	975.70	0.000161	0.0123	93.86
200	3.133	987.30	0.000152	0.0123	93.87
400	3.143	1052.00	0.000124	0.0116	94.21
600	3.144	1075.00	0.000104	0.0149	94.55
800	3.145	1370.00	0.000072	0.0091	95.45
1000	3.148	1649.00	0.000071	0.0076	96.22

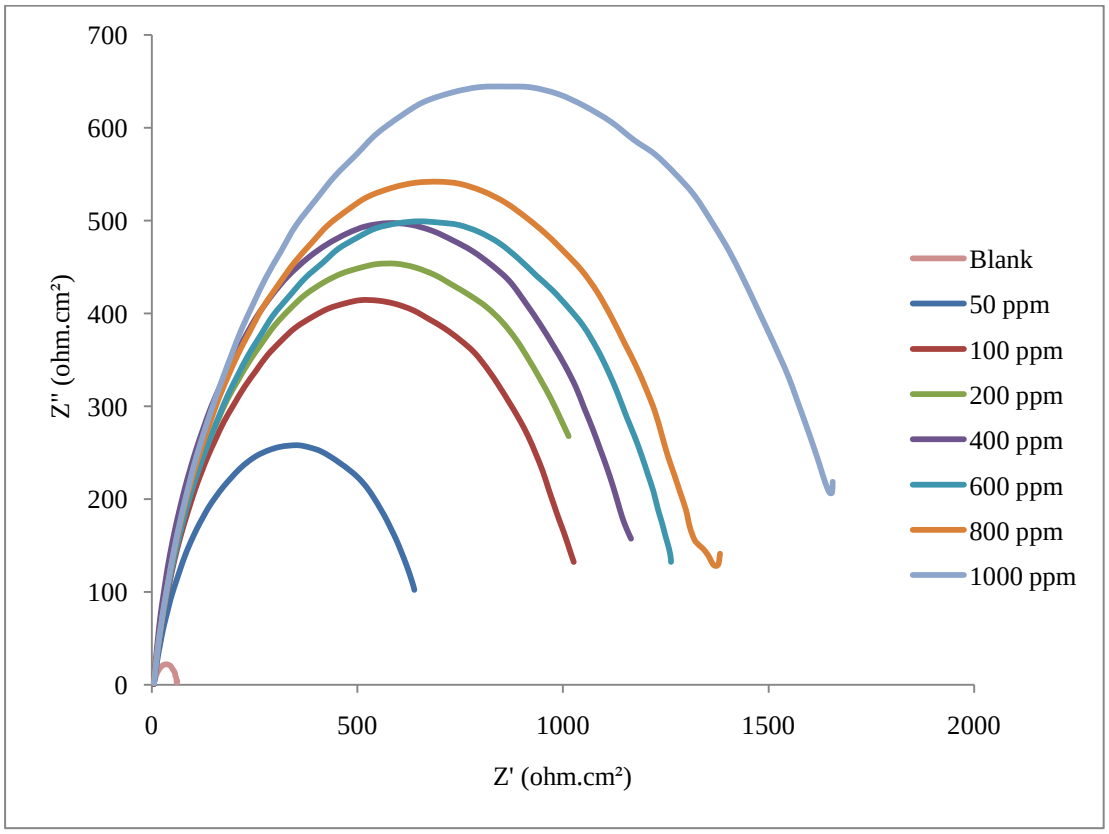

Figure 54: Nyquist plots for mild steel in a 1M HCl solution in the absence and presence of Fig & Olive (1:1) plant extract at 25°C.

Table 13: Impedance parameters and corresponding inhibition efficiency for mild steel in 1M HCl in the absence and presence of Fig & Olive (1:1) plant extract at 25°C.

Con.(ppm)	Rsol ($ohm.cm^2$)	Rct ($ohm.cm^2$)	Cd (F)	I corr. (mA/cm^2)	IE%
0	1.542	57.07	0.0004312	0.2001	
50	4.616	683.40	0.0001944	0.0143	92.85
100	4.666	1083.00	0.0001289	0.0100	94.10
200	4.700	1165.00	0.000123	0.0097	95.14
400	4.716	1226.00	0.000122	0.0093	95.38
600	4.736	1311.00	0.000858	0.0089	95.56
800	4.736	1742.00	0.000781	0.0067	96.65
1000	4.741	1842.00	0.000701	0.0067	96.66

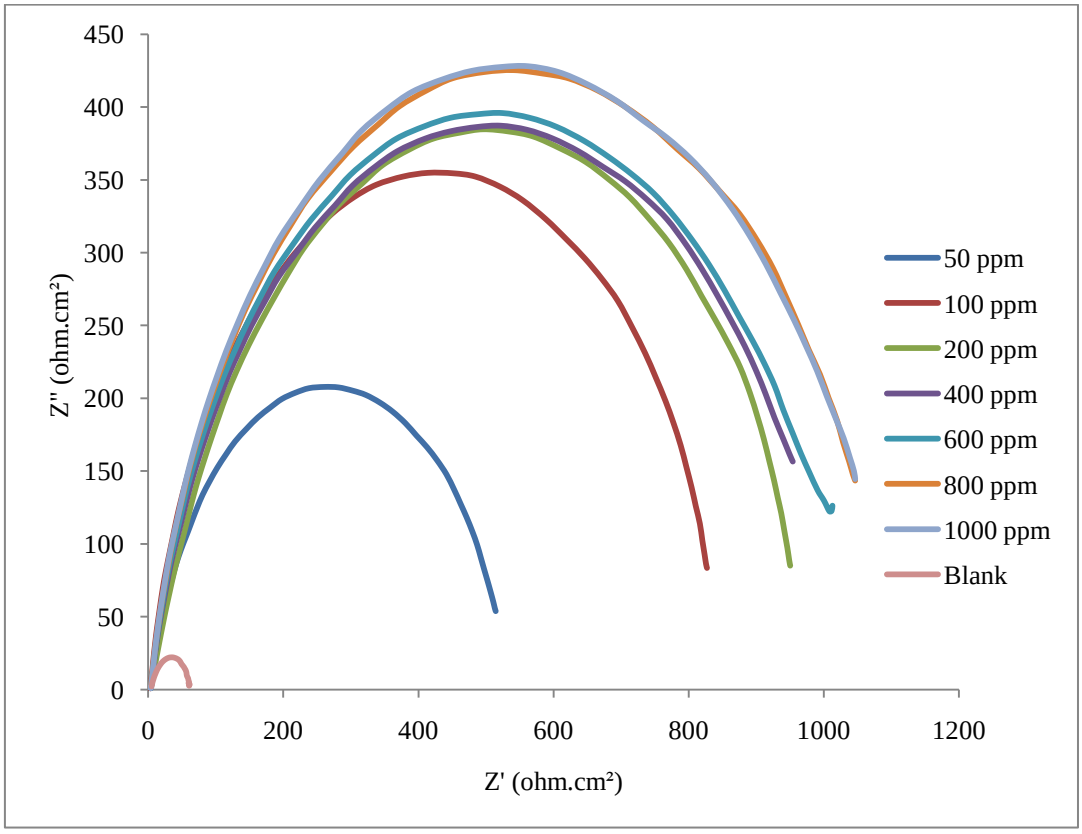

Figure 55: Nyquist plots for mild steel in a 1M HCl solution in the absence and presence of Fig plant extract at 25°C.

Table 14: Impedance parameters and corresponding inhibition efficiency for mild steel in 1M HCl in the absence and presence of Fig plant extract at 25°C.

Con(ppm)	Rsol ($ohm.cm^2$)	Rct ($ohm.cm^2$)	Cd (F)	I corr. (mA/cm^2)	IE%
0	1.542	57.07	0.000431	0.2001	
50	3.852	530.70	0.000173	0.01891	90.55
100	3.255	848.80	0.000124	0.0140	93.00
200	3.290	973.90	0.000113	0.0132	93.41
400	3.351	1016.00	0.000112	0.0129	93.57
600	3.361	1057.00	0.000111	0.0128	93.62
800	3.348	1101.00	0.000109	0.0127	93.65
1000	3.369	1105.00	0.000101	0.0124	93.80

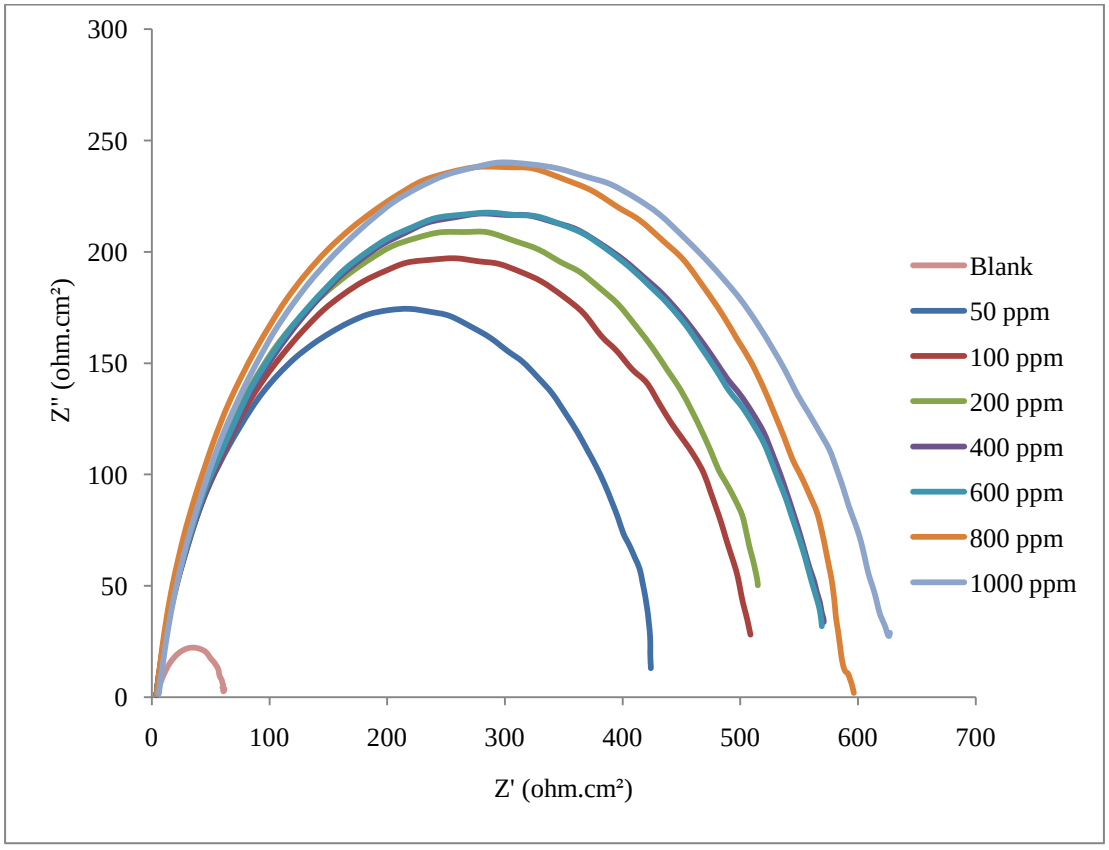

Figure 56: Nyquist plots for mild steel in a 1M HCl solution in the absence and presence of Olive plant extract at 25°C.

Table 15: Impedance parameters and corresponding inhibition efficiency for mild steel in 1M HCl in the absence and presence of Olive plant extract at 25°C.

Con.(ppm)	Rsol ($ohm.cm^2$)	Rct ($ohm.cm^2$)	Cd (F)	I corr. (mA/cm^2)	IE %
0	1.542	57.07	0.000431	0.2001	
50	3.204	424.00	0.006810	0.0201	89.95
100	3.217	514.40	0.000113	0.0175	91.24
200	3.247	528.40	0.000112	0.0174	91.29
400	3.251	579.30	0.000108	0.0174	91.31
600	3.262	579.60	0.000103	0.0174	91.32
800	3.426	593.40	8.01E-06	0.0170	91.49
1000	4.983	629.30	7.01E-06	0.0163	91.84

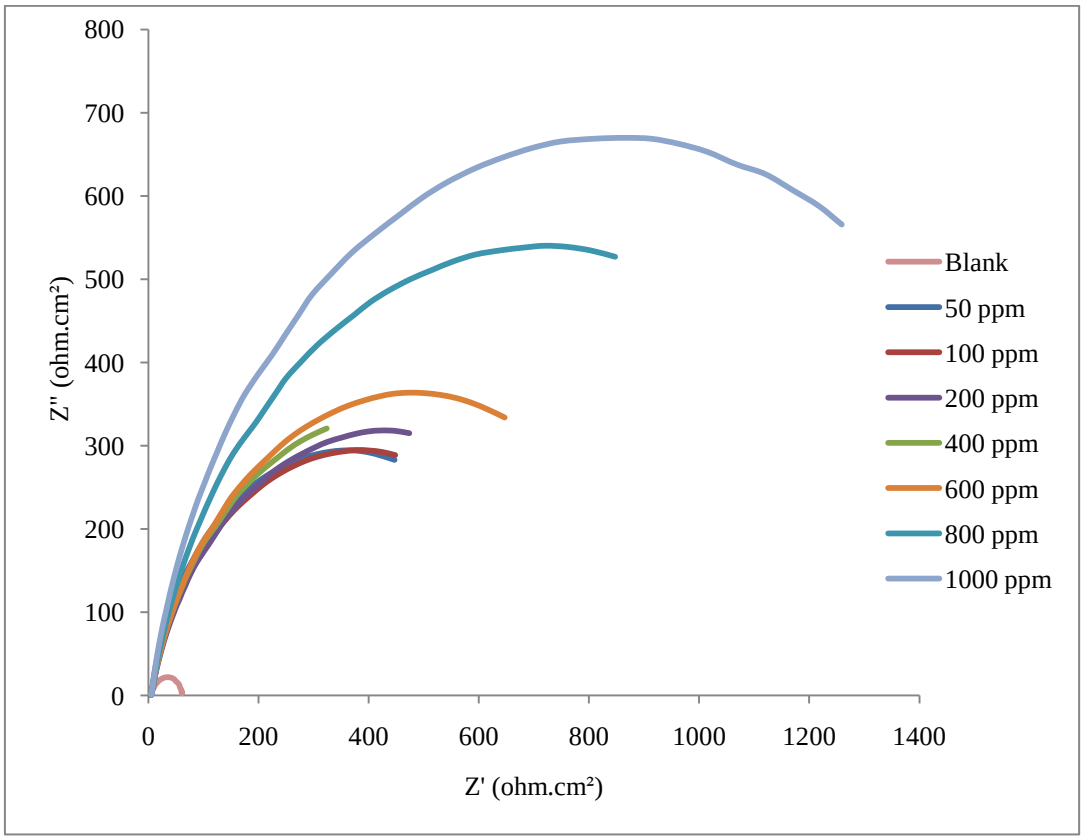

Figure 57: Nyquist plots for mild steel in a 1M HCl solution in the absence and presence of Rosemary plant extract at 25°C.

Table 16: Impedance parameters and corresponding inhibition efficiency for mild steel in 1M HCl in the absence and presence of Rosemary plant extract at 25°C.

Con(ppm)	Rsol ($ohm.cm^2$)	Rct ($ohm.cm^2$)	Cd (F)	I corr. (mA/cm^2)	IE %
0	1.542	57.07	0.00043	0.2001	
50	4.357	700.00	0.00015	0.0185	90.77
100	4.506	753.90	0.00015	0.0175	91.24
200	4.517	846.90	0.00015	0.0158	92.11
400	4.591	890.00	0.00015	0.0153	92.34
600	5.071	958.00	0.00014	0.0145	92.75
800	5.179	1425.00	0.00008	0.0100	95.00
1000	5.200	1671.00	0.00006	0.0086	95.71

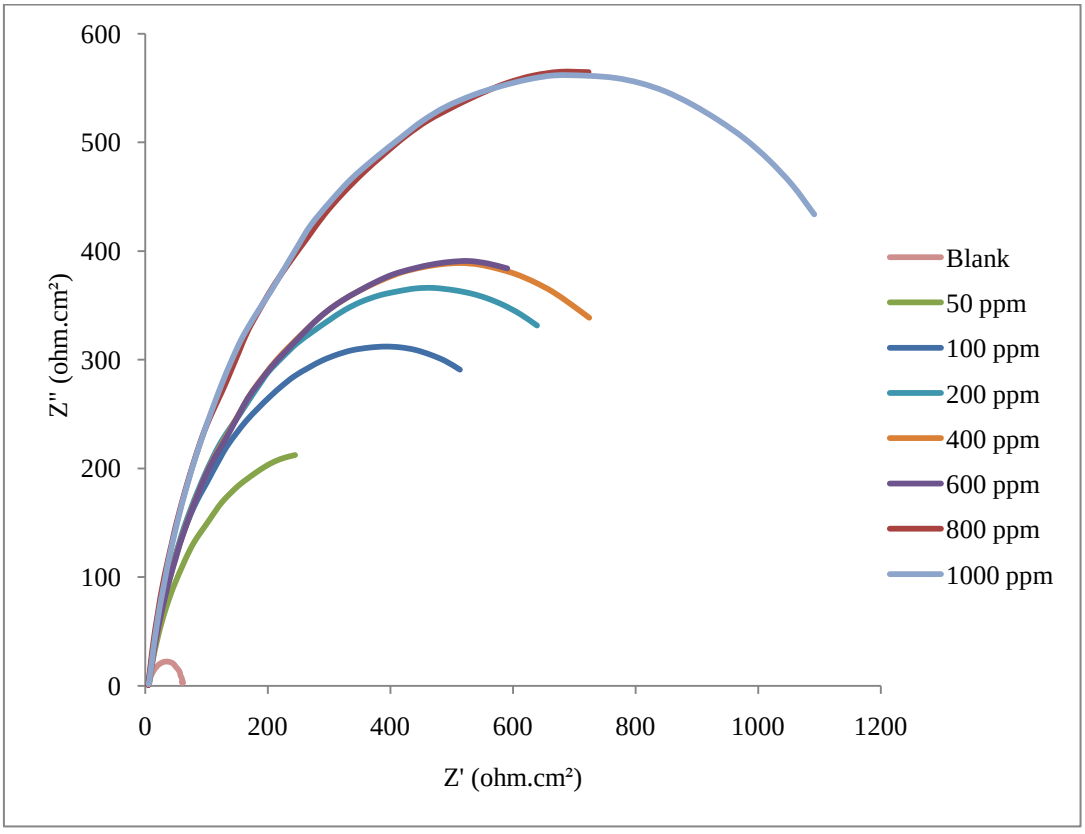

Figure 58: Nyquist plots for mild steel in a 1M HCl solution in the absence and presence of Cypress plant extract at 25°C.

Table 17: Impedance parameters and corresponding inhibition efficiency for mild steel in 1M HCl in the absence and presence of Cypress plant extract at 25°C.

Con.(ppm)	Rsol ($ohm.cm^2$)	Rct ($ohm.cm^2$)	Cd (F)	I corr. (mA/cm^2)	IE%
0	1.542	57.07	0.00043	0.2001	
50	4.363	554.00	0.00017	0.0280	86.00
100	4.531	758.90	0.00013	0.0266	86.69
200	5.089	908.70	0.00009	0.0174	91.32
400	5.155	995.80	0.00012	0.0160	92.00
600	5.250	1005.00	0.00012	0.0159	92.05
800	5.310	1379.00	0.00010	0.0118	94.12
1000	5.420	1402.00	0.00007	0.0117	94.17

Figures 59-64 show that the inhibition efficiencies obtained by the impedance method is almost the same as the ones obtained by the weight loss and LPR methods. The figures also show a slight difference (1- 4%) between the two methods and LPR method. Some plant extracts show a trend in the curve using different methods and some have slight differences. However, the difference obtained is considered small, assuring them all to be reliable.

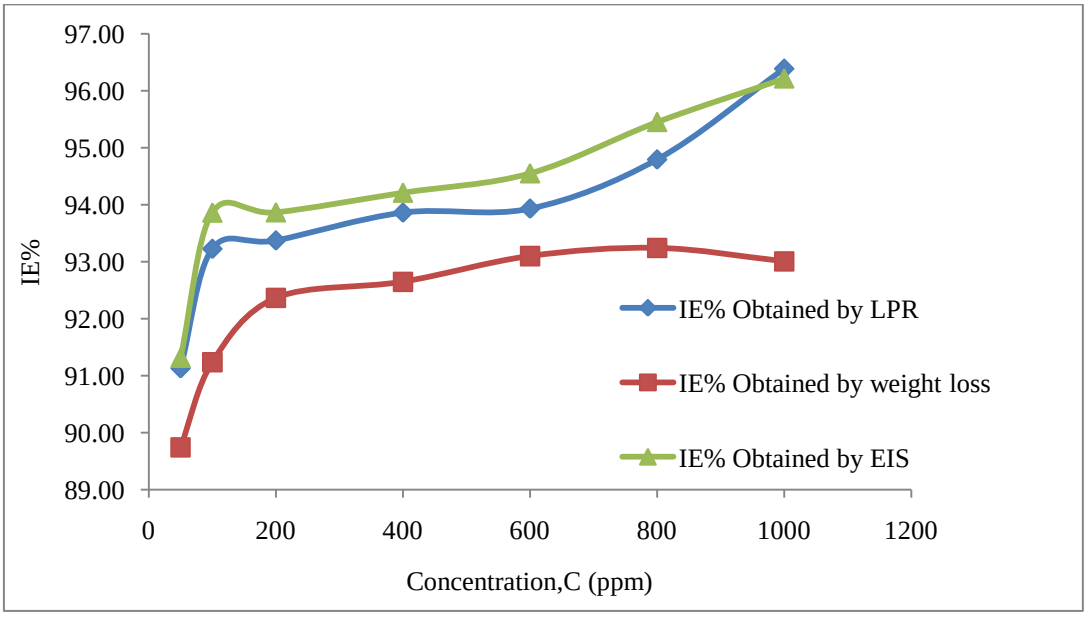

Figure 59: Inhibition efficiency for Fig & Olive (1:7) inhibitor obtained by LPR, Weight loss and EIS tests.

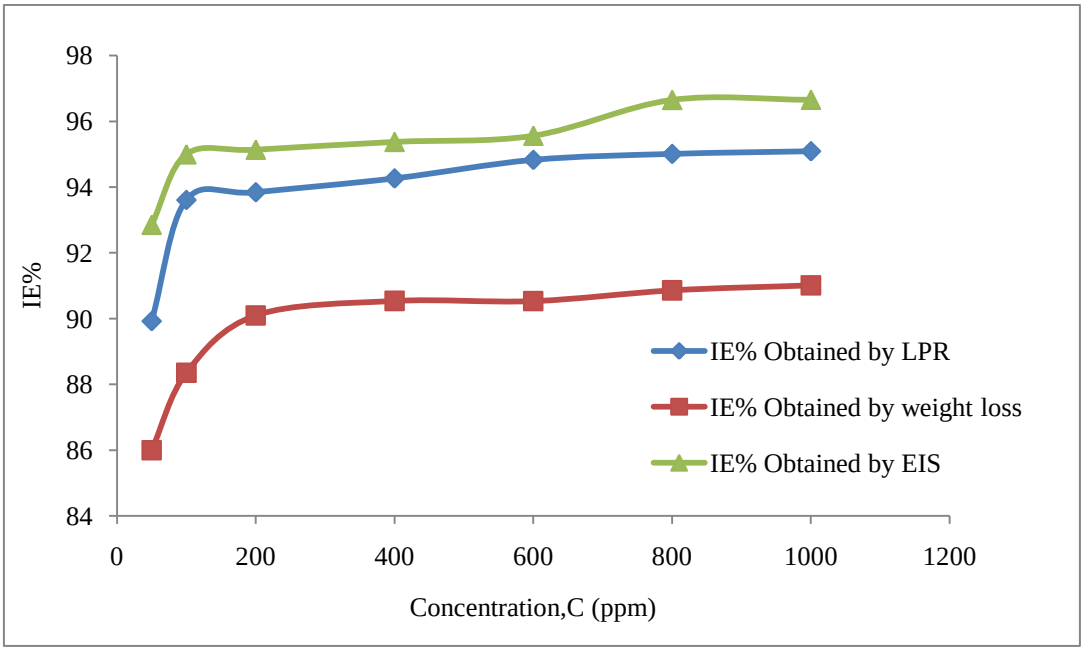

Figure 60: Inhibition efficiency for Fig & Olive (1:1) inhibitor obtained by LPR, Weight loss and EIS tests.

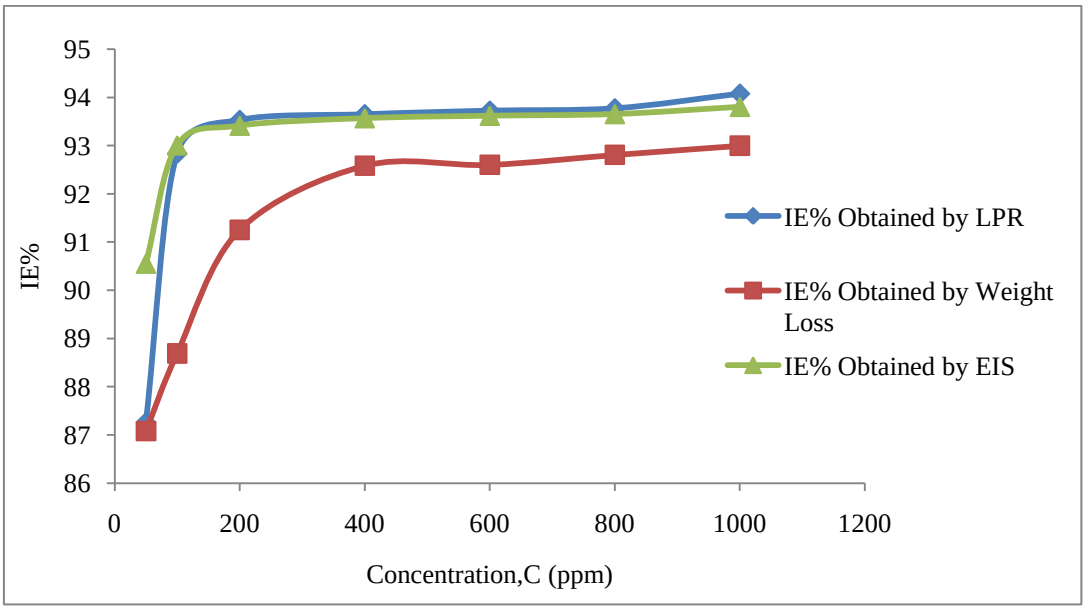

Figure 61: Inhibition efficiency of Fig inhibitor obtained by LPR, Weight loss and EIS tests.

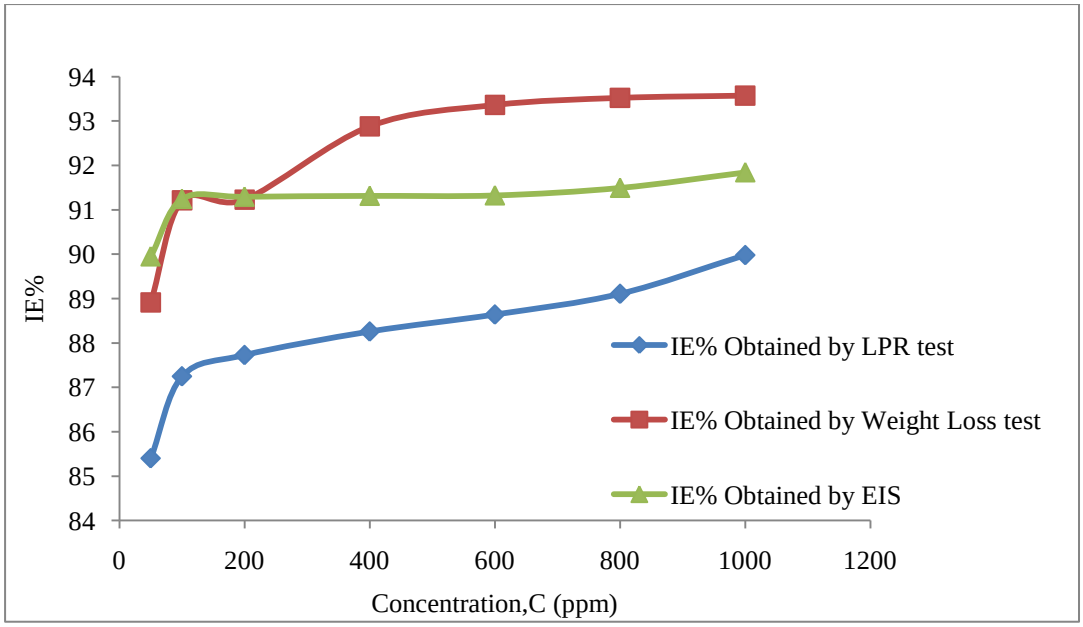

Figure 62: Inhibition efficiency for Olive inhibitor obtained by LPR, Weight loss and EIS tests.

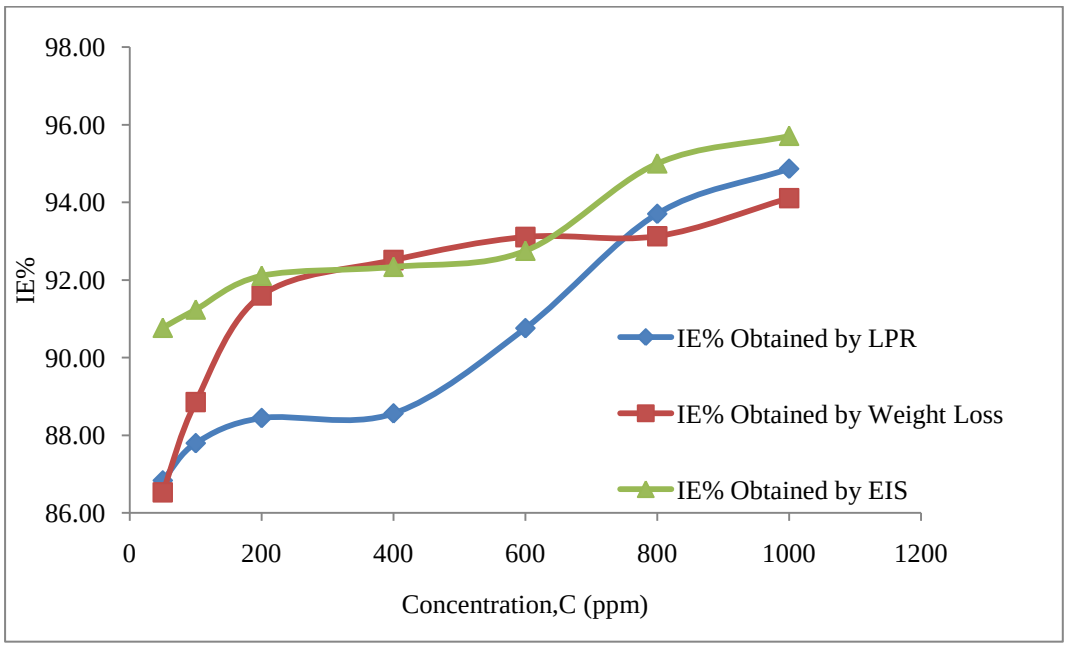

Figure 63: Inhibition efficiency for Rosemary inhibitor obtained by LPR, Weight loss and EIS tests.

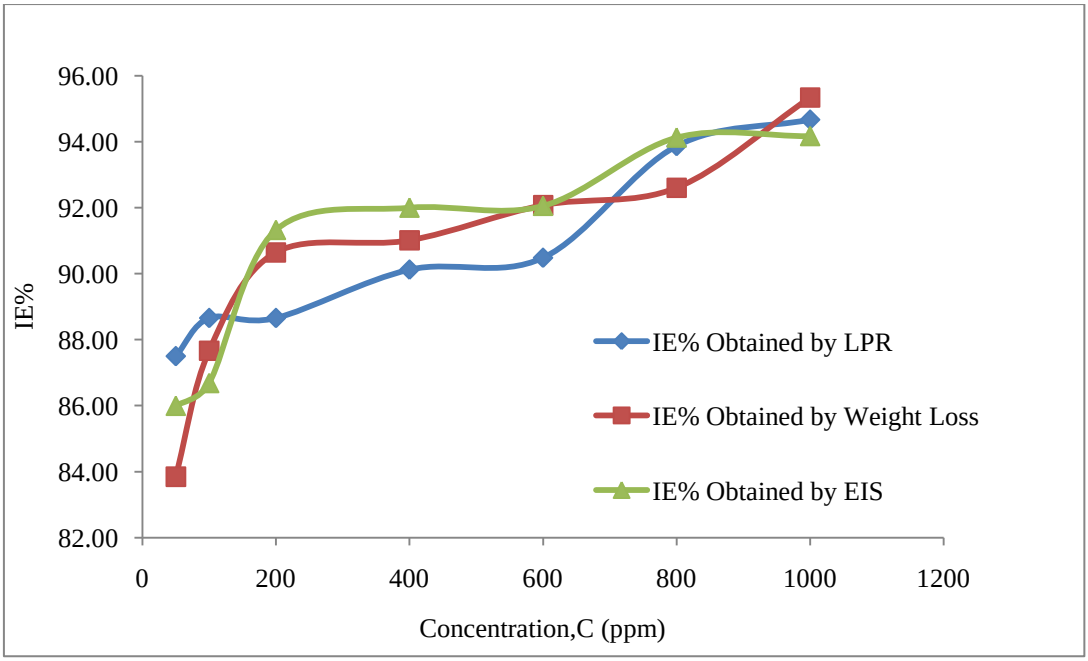

Figure 64: Inhibition efficiency for Cypress inhibitor obtained by LPR, Weight loss and EIS tests.

4.3.3 Cyclic Sweep Test

The conditions used for the cyclic sweep tests are the same as mentioned in the previous section. The corrosion current decreases shifting the curves along the x-axis. This indicates a decrease in the corrosion rate and an increase in the inhibition efficiency. It is also noticed that there is a shift in along the potential after the blank sample due to formation of a layer or an adsorption of the inhibitor on the mild steel sample. It can be seen that the cathodic part of the curve does not change. However, the anodic part changes slightly after the 100 ppm of the inhibitor is added. This indicates that the inhibitor used is a mixed type inhibitor, with a predominant cathodic effectiveness. The cathodic part of the curves gave rise to parallel lines indicating that the addition of the inhibitor to the 1M HCl solution did not modify the hydrogen evolution mechanism. The inhibitor molecules first got absorbed on the mild steel surface and blocked part of the reaction sites of the mild steel which caused a reduction in the corrosion rate [20].

The decrease in the anodic corrosion current density as the inhibitor added proves the formation of protective films containing oxide and inhibitor [20]. The

change in the shape of the anodic part of the cyclic sweeps also suggests that some form of a protective (inhibitor) layer is laid on the surface of the metal. The “S” shape is more apparent when higher contractions are used, which is an agreement with all the other test data generated by weight loss, LPR, and impedance spectroscopy. Anodic parts of the sweeps corresponding to lower concentrations as low as 50 ppm were similar to that of the blank.

Figures 65-71 explain the conclusions drawn in the previous discussion and show the inhibition of the inhibitors used on the mild steel specimen in 1 M HCl solution.

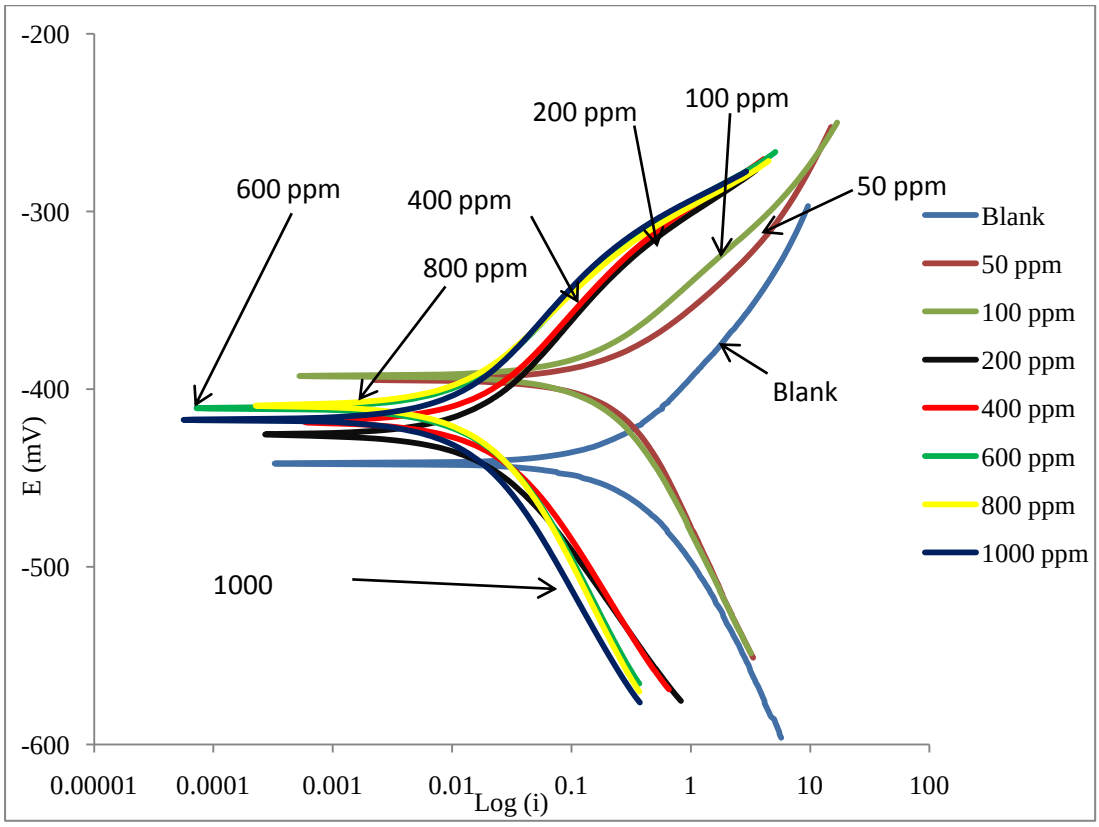

Figure 65: Potential plots of mild steel in a 1M HCl solution in the absence and presence of Fig & Olive (7:1) plant extract at 25^{o}C.

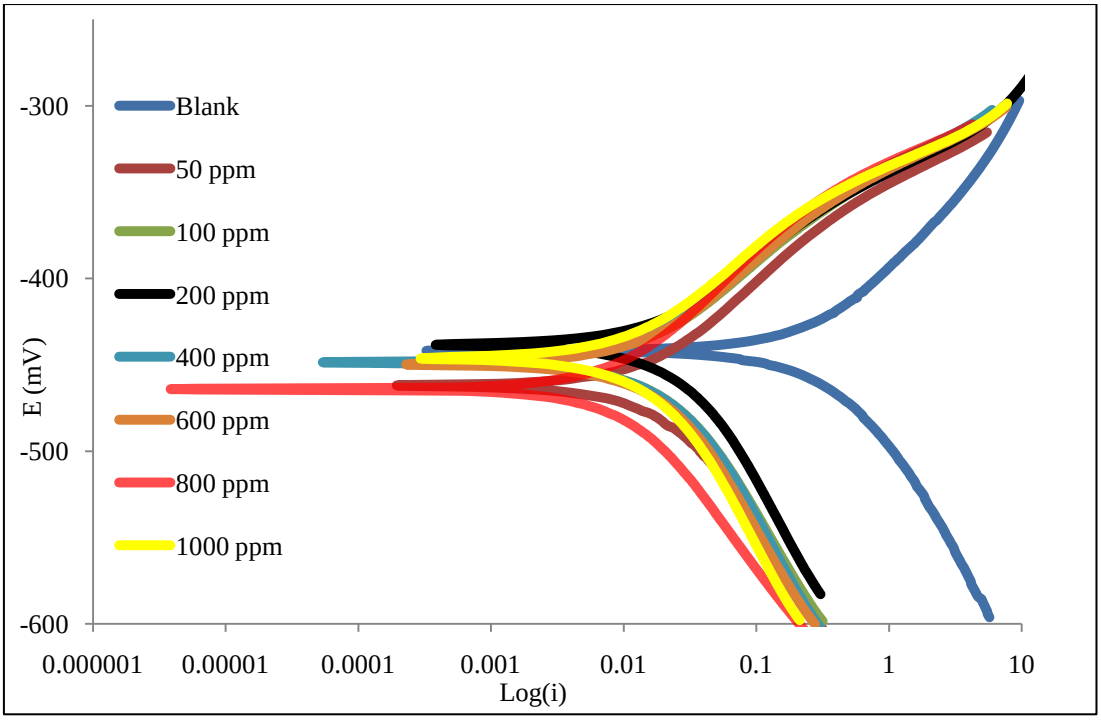

Figure 66: Potential plots of mild steel in a 1M HCl solution in the absence and presence of Fig & Olive (1:7) plant extract at 25^{o}C.

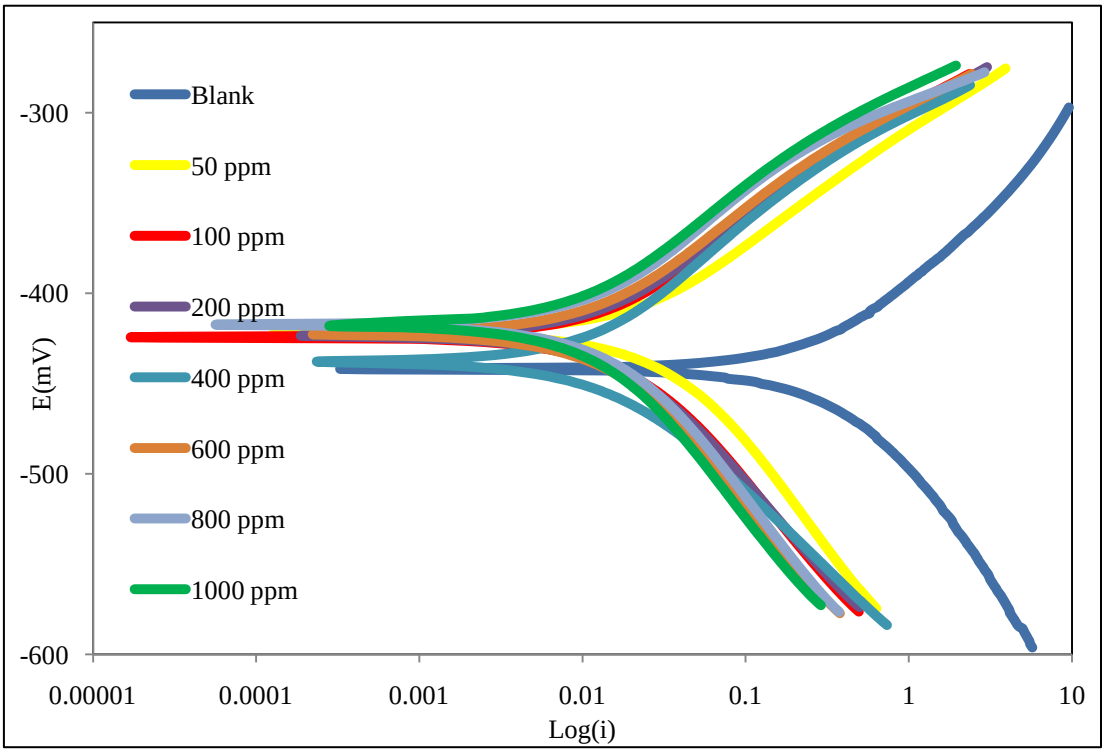

Figure 67: Potential plots of mild steel in a 1M HCl solution in the absence and presence of Fig & Olive (1:1) plant extract at 25^{o}C.

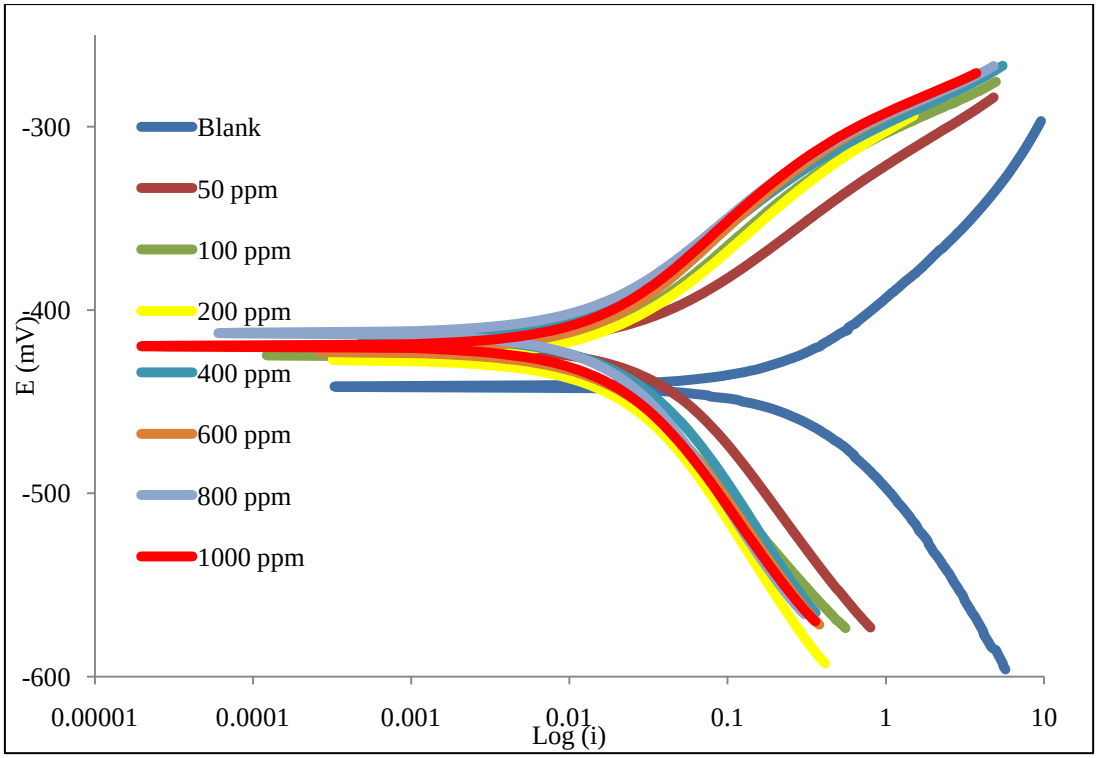

Figure 68: Potential plots of mild steel in a 1M HCl solution in the absence and presence of Fig plant extract at 25^{o}C.

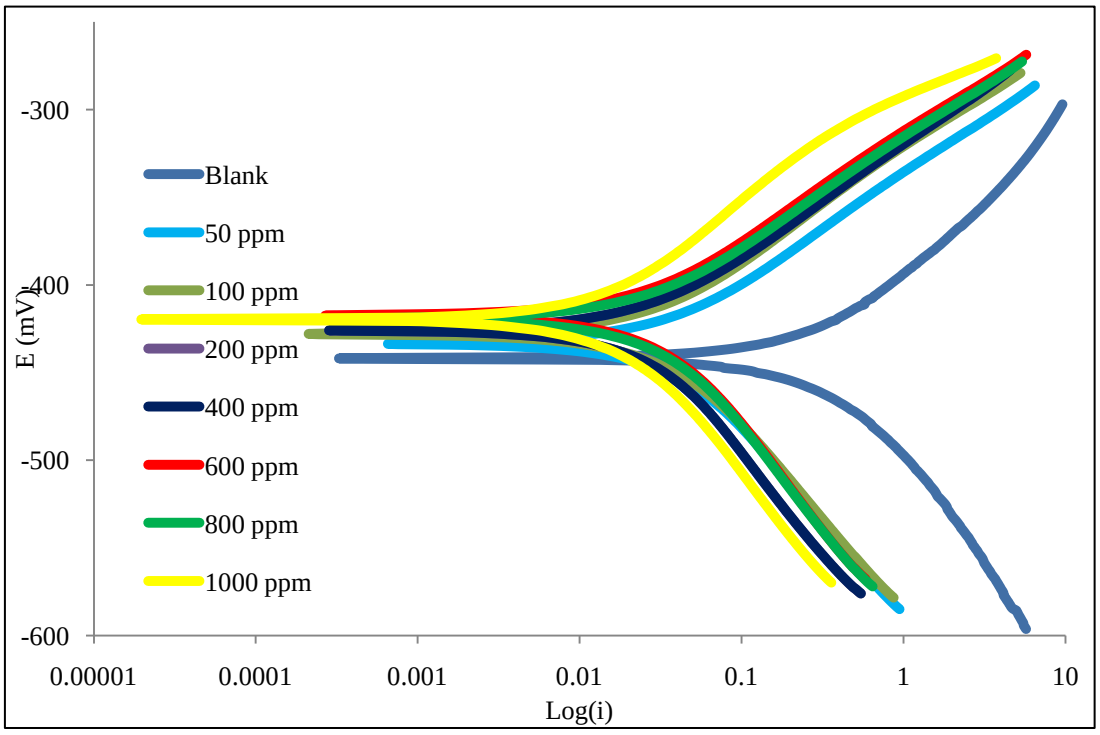

Figure 69: Potential plots of mild steel in a 1M HCl solution in the absence and presence of Olive plant extract at 25^{o}C.

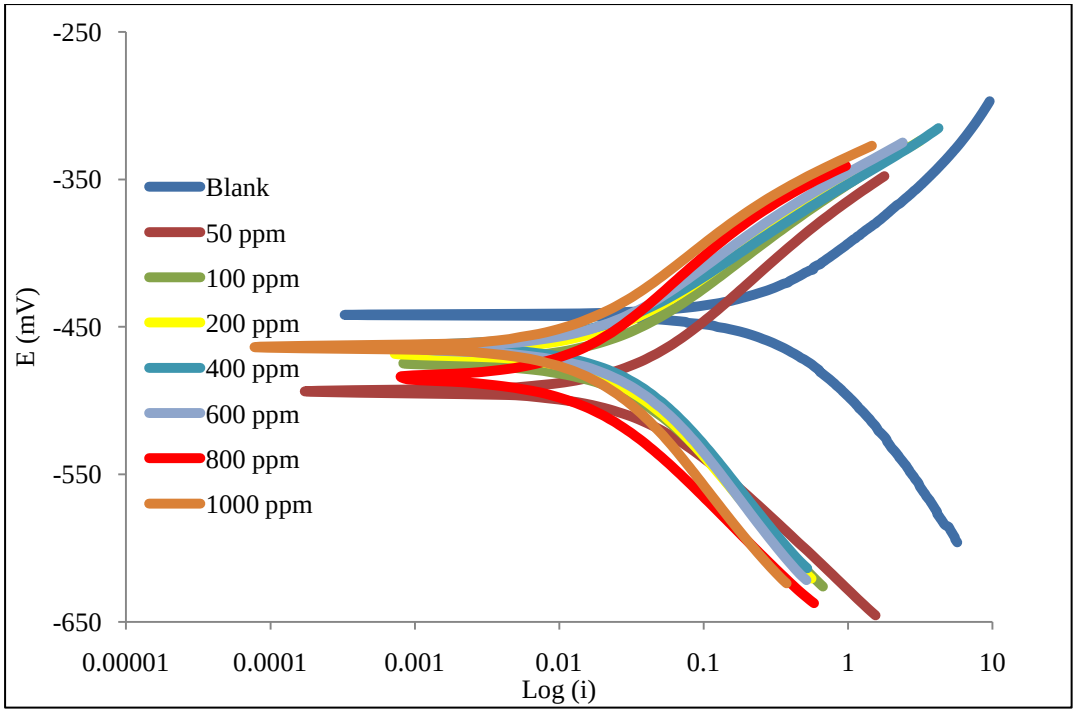

Figure 70: Potential plots of mild steel in a 1M HCl solution in the absence and presence of Rosemary plant extract at 25^{o}C.

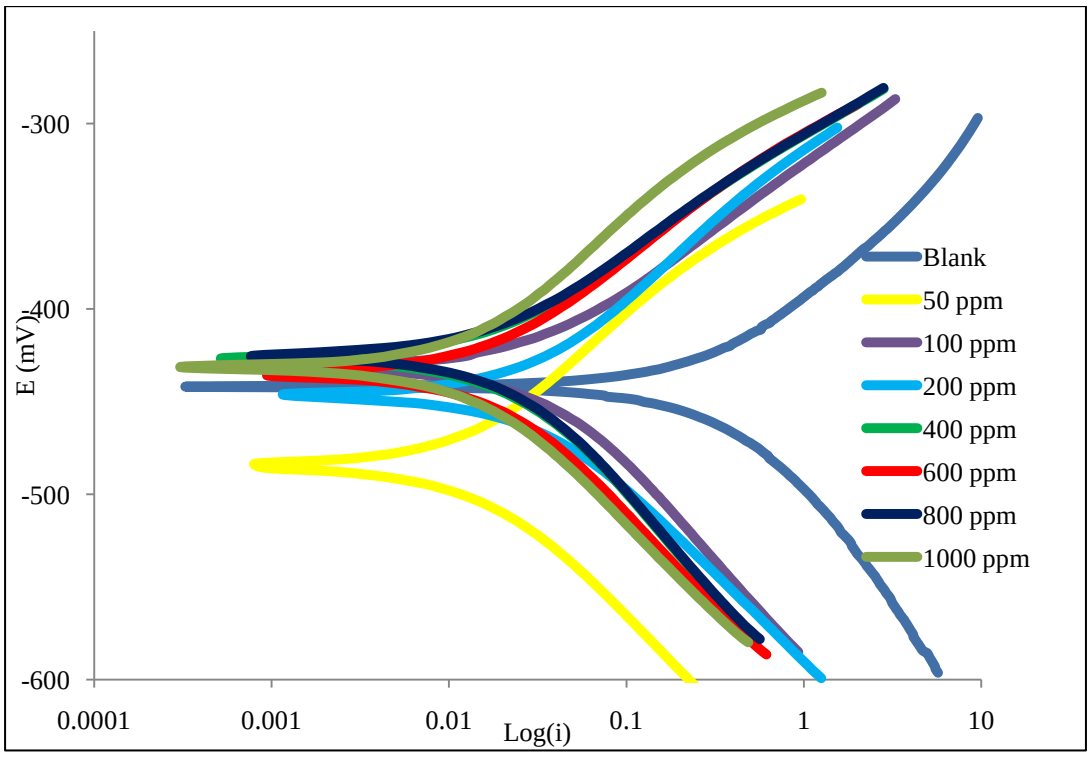

Figure 71: Potential plots of mild steel in a 1M HCl solution in the absence and presence of Cypress plant extract at 25^{o}C

4.3.4 The Linear Polarization Resistance (LPR) Method at Elevated Temperatures:-

A linear polarization test is carried out by a scan from approximately -10mV to +10mV at elevated temperatures. The polarization resistance can be measured from Equation 3.2. The maximum inhibition efficiency and LPR was obtained at a concentration of 200 ppm of plant extracts. The increase in the LPR value was caused by a decrease in the corrosion current density causing the reduction in corrosion rate. The increase in temperature cause a decrease in the inhibitive action of the inhibitors used, which resulted in an increase in the corrosion rate of the exposed mild steel sample.

The setup used in this situation is using a different type of cell. The used cell is a jacket vessel cell connected to a water bath and a pump.

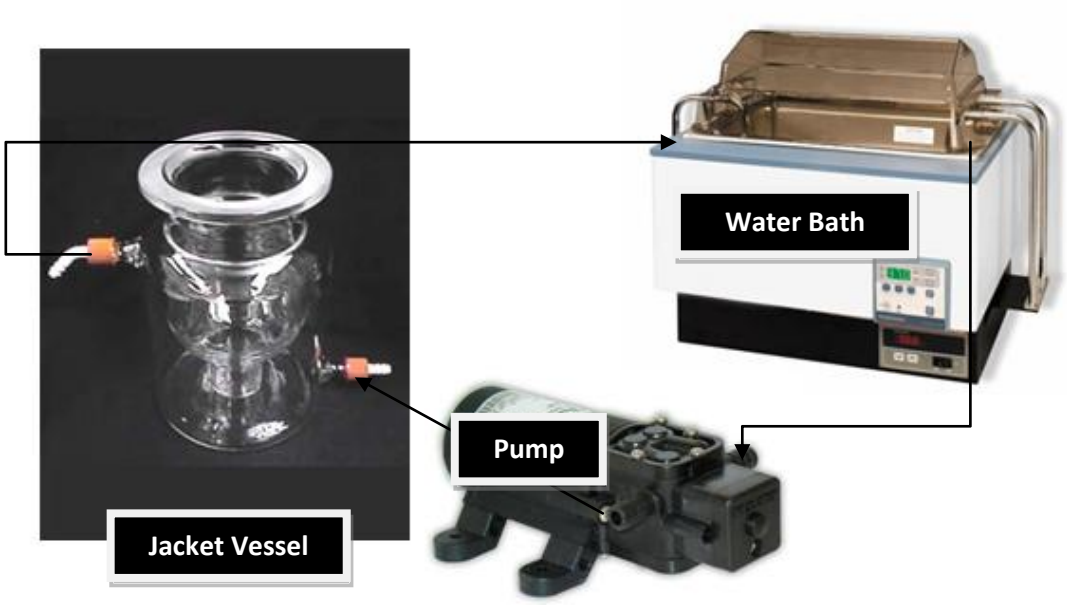

Figure 72: Experimental Set Up of Elevated Temperature Experiment.

The water bath is set to the desired temperature and then left for an hour to allow the temperature to stabilize. The water flows from the bath through the pump to the jacket vessel. The flow of hot water in the jacket vessel maintains a constant temperature inside the cell constant. To assure keeping the temperature constant, the jacket vessel is covered from outside with an insulation material. The rest of the cell setup is the same as the electrochemical cell used in the room temperature experiment.

However, a hole is added to the cell cover to install a thermometer and measure the temperature of the solution inside the cell. Holes 1-3 are used to install the specimen holder, reference and the electrode, respectively. Hole 4 is used to install the thermometer to measure the temperature. To avoid any losses of heat and to assure that the temperature inside the cell is at the desired temperature, the temperature inside the bath is set above the desired temperature by 2°C.

The change in electrochemical potential is small. The polarization resistance can be calculated from long term linear polarization resistance curves. Using the potensiostat, a long term LPR graph is obtained for all inhibitors. The value of the LPR is obtained after reaching a steady value, which is obtained after running the test at each concentration for 90 min. It can be seen from Figures 73, 76, 79, 82, 85, 88, 91 and Tables 42-59 that the resistance polarization increases as the concentration of the inhibitor added increases. As the LPR values increase, the corrosion current that passes through the solution decreases. One can notice from Equation 4.4 that as the polarization resistance increases the corrosion current decreases. The inhibition efficiency increases accordingly as seen from Equation 4.1.

The test is conducted at three different temperatures: 25°C, 45°C and 55°C. The room temperature study was recorded in the previous sections. The concentrations at which the study is conducted are 50-200 ppm. The reason behind choosing the low range of concentrations is to test the ability of the inhibition at the commercial inhibitor concentrations.

The LPR graphs are plotted for the different concentrations at the different temperatures studied. It is clear from Figures 73, 76, 79, 82, 85, 88, 91 that as the temperature increases the value of the steady state LPR decreases. This indicates that the ability of the inhibitor to form a protective film on the surface of the metal decreases. This causes an increase in the current passing through the solution, causing an increase in the rate of corrosion to which the specimen is exposed.

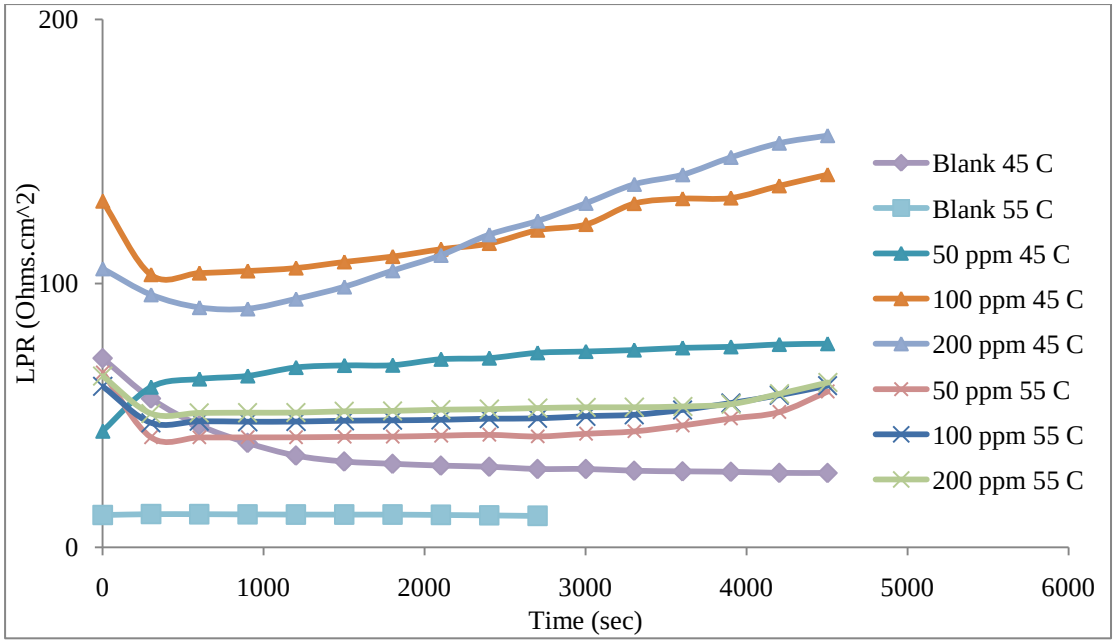

Figure 73: The LPR Vs Time of a mixture of Fig & Olive (7:1) elevated temperatures.

In Figure 73, the LPR values obtained for the mixture of Fig and Olive (7:1) are shown to increase at low concentrations. The value of the LPR increases more rapidly at low temperatures than at elevated temperatures. This results in a decrease in the current passing through the solution, which in turn proves that the corrosion rate of the metal surface decreases as the inhibitor is added to the environment. However, the inhibition is more effective at low temperatures than high temperatures. The adsorption of the inhibitor on the metal surface decreases as the temperature increases causing less resistance to corrosion.

Table 18: Caculations obtained using LPR method for a mixture of Fig and Olive (7:1) at 25°C.

Concentration (ppm)	LPR (ohm.cm²)	I_{corr} (mA/cm²)	Potential (mV)	IE%
0	63.72	0.4152	-442.80	-
50	104.02	0.0392	-377.89	90.56
100	126.74	0.0371	-374.09	91.06
200	781.86	0.0331	-421.98	92.03

Table 19: Caculations obtained using LPR method for a mixture of Fig and Olive (7:1) at 45°C.

Concentration (ppm)	LPR (ohm.cm²)	I_{corr} (mA/cm²)	Potential (mV)	IE%
0	28.18	0.9258	-499.15	-
50	77.12	0.3382	-503.16	63.46
100	136.99	0.1904	-501.13	79.43
200	153.08	0.1704	-500.78	81.59

Table 20: Caculations obtained using LPR method for a mixture of Fig and Olive (7:1) at 55°C.

Concentration (ppm)	LPR (ohm.cm²)	I_{corr} (mA/cm²)	Potential (mV)	IE%
0	12.31	2.1196	-493.28	-
50	42.06	0.6203	-504.86	70.74
100	54.68	0.4771	-506.65	77.49
200	62.46	0.4176	-495.93	80.30

Figure 74 and Tables 18-20 show that the LPR value for Fig and Olive (7:1) increases as the concentration of the inhibitor in the solution increases. After a certain period of time, a steady state value that reads the resistance obtained after the formation of the protective film is reached. The trend is noticeable at all three temperatures studied. The steady state value of the LPR at lower temperature is higher than those obtained at higher temperatures, indicating less resistance to corrosion at high temperatures. As the LPR value increases, the value of the current density that passes decreases gradually. The increase in the LPR value is more rapid at high temperatures than at low temperatures. The LPR steady state value at 25^{o}C is not achieved at a concentration of 200 ppm; it instead keeps increasing. However, it is achieved at higher concentrations.

Figure 75 with the LPR represented in the previous section, showed that the addition of the inhibitor increases the inhibition efficiency. The value of inhibition efficiency increases by almost 2%, 17% and 10% at temperatures of 25°C, 45°C and 55°C, respectively. The graph indicates that the increase in inhibition efficiency at 45°C is more rapid than the other temperatures studied. This represents the inhibition efficiency difference between the addition of 50 ppm and 200 ppm of the inhibitor

extract. The increase of the inhibition efficiency indicates a decrease in the corrosion current density and the corrosion rate.

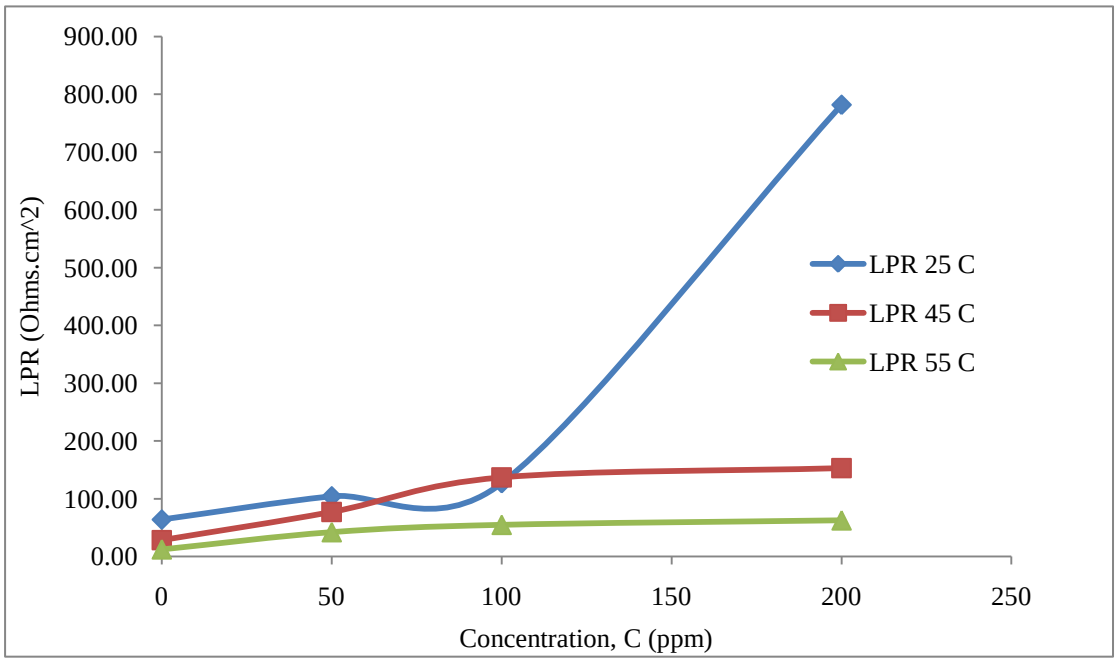

Figure 74: LPR for Fig & Olive (7:1) inhibitor Vs Concentration of the inhibitor at room and elevated temperatures.

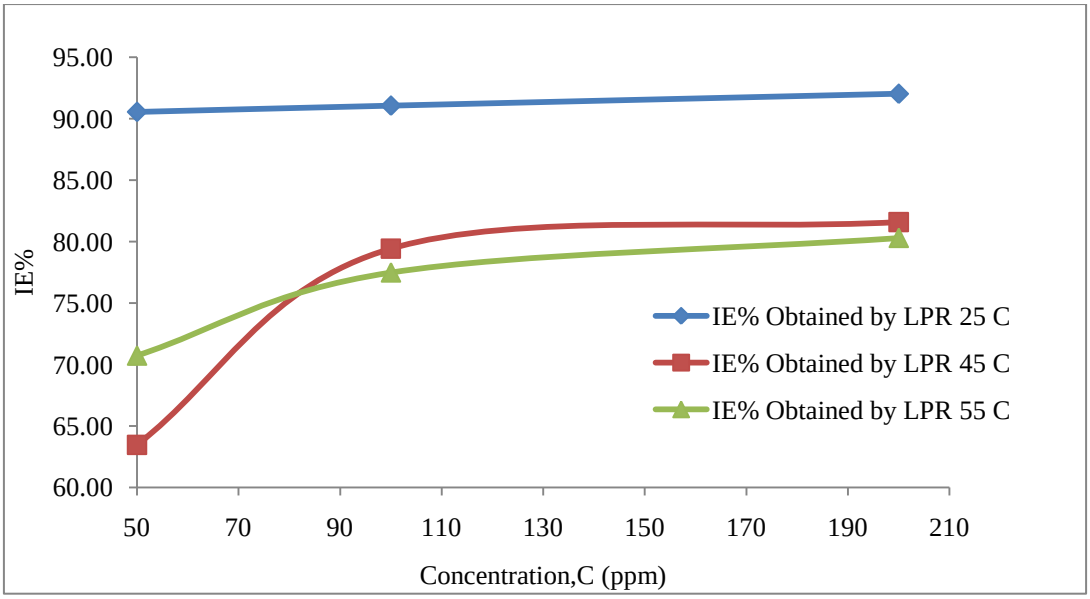

Figure 75: Inhibition efficiency for Fig & Olive (7:1) inhibitor obtained by LPR Vs Concentration of the Inhibitor at room and elevated temperatures.

Figure 76 shows the LPR values obtained for the mixture of Fig & Olive (1:7) as the inhibitor extract is added to the solution. The LPR value increases at low concentrations. The value of the LPR then increases more rapidly at low temperatures than at elevated temperatures. This results in a decrease in the current passing through the solution. As such, the corrosion rate of the metal surface decreases as the inhibitor is added to the environment. However, the inhibition is more effective at low temperatures than high temperatures. Unlike the previous mixture, the LPR curves at 25°C are much higher in value than the other two elevated temperatures studied. This can be more noticeable at concentrations of 50 and 100 ppm. The adsorption of the inhibitor on the metal surface decreases as the temperature increases causing less resistance to corrosion.

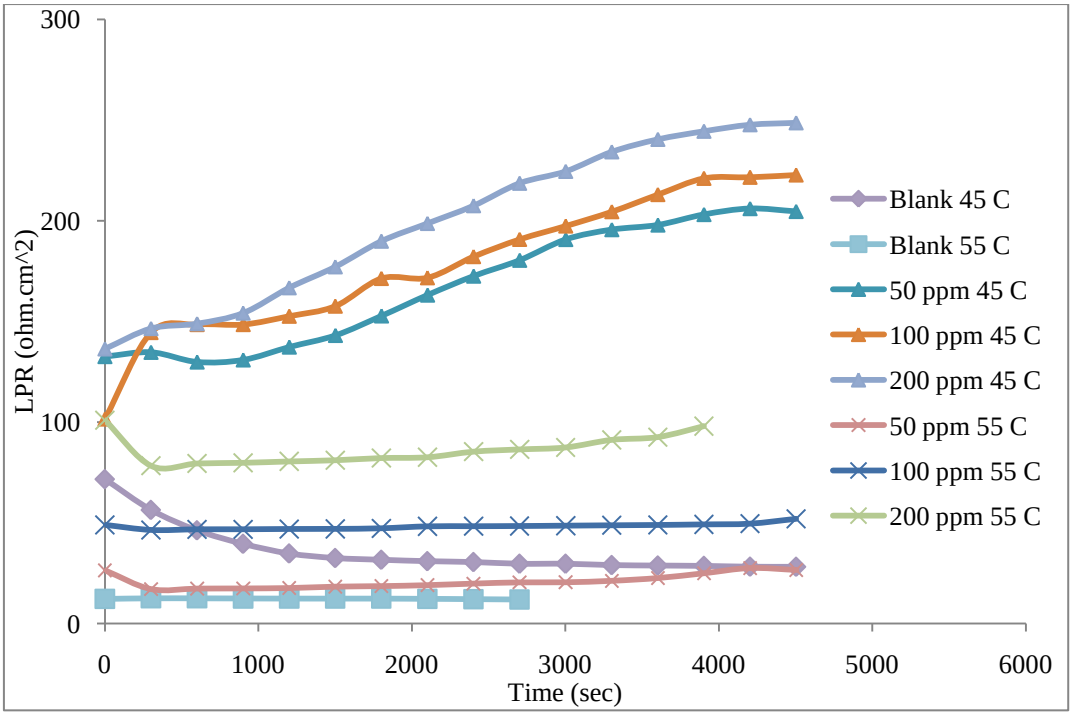

Figure 76: The LPR Vs Time of a mixture of Fig & Olive (1:7) at elevated temperatures.

Figure 77 and Tables 21-23 show that the LPR value increases as the concentration of the inhibitor in the solution increases. The result can be seen for the three temperatures studied. The increase of the LPR value reaches a steady state value after a certain amount of time (90 min). The LPR steady state value at lower temperature is higher than that recorded at higher temperatures. This indicates less resistance to corrosion at high temperatures. As the LPR value increases, the value of the current density that passes decreases gradually. This implies a decrease in the corrosion rate of the metal surface. The increase in the LPR value is more rapid at high temperatures than at low temperatures.

Figure 78 demonstrates that the addition of the inhibitor increases the inhibition efficiency. The value of inhibition efficiency increases by almost 2%, 2% and 35% at temperatures of 25°C, 45°C and 55°C respectively. The graph plotted indicates that the increase in inhibition efficiency at 55°C is more visible than the other temperatures studied. This represents the inhibition efficiency difference between the addition of 50 ppm and 200 ppm of the inhibitor extract to the solution. The increase of the inhibition efficiency implies a decrease in the corrosion current density and the

corrosion rate. The difference is due to the fact that the breakage and formation of the protective film occurs either very fast or very slow sometimes. It also depends on the components being adsorbed on the metal surface.

Table 21: Caculations obtained using LPR method for a mixture of Fig and Olive (1:7) at 25°C.

Concentration (ppm)	LPR (ohm.cm²)	I_{corr} (mA/cm²)	Potential (mV)	IE%
0	63.72	0.4152	-442.80	-
50	714.71	0.0365	-452.18	91.21
100	927.62	0.0281	-463.69	93.23
200	957.98	0.0272	-447.54	93.44

Table 22: Caculations obtained using LPR method for a mixture of Fig and Olive (1:7) at 45°C.

Concentration (ppm)	LPR (ohm.cm²)	I_{corr} (mA/cm²)	Potential (mV)	IE%
0	28.18	0.9258	-499.15	-
50	206.04	0.1266	-502.46	86.32
100	221.62	0.1177	-495.98	87.29
200	247.65	0.1053	-500.24	88.62

Table 23: Caculations obtained using LPR method for a mixture of Fig and Olive (1:7) at 55°C.

Concentration (ppm)	LPR (ohm.cm²)	I_{corr} (mA/cm²)	Potential (mV)	IE%
0	12.31	2.1196	-493.28	-
50	24.98	1.0444	-496.55	50.73
100	48.95	0.5329	-507.25	74.86
200	91.23	0.2859	-507.32	86.51

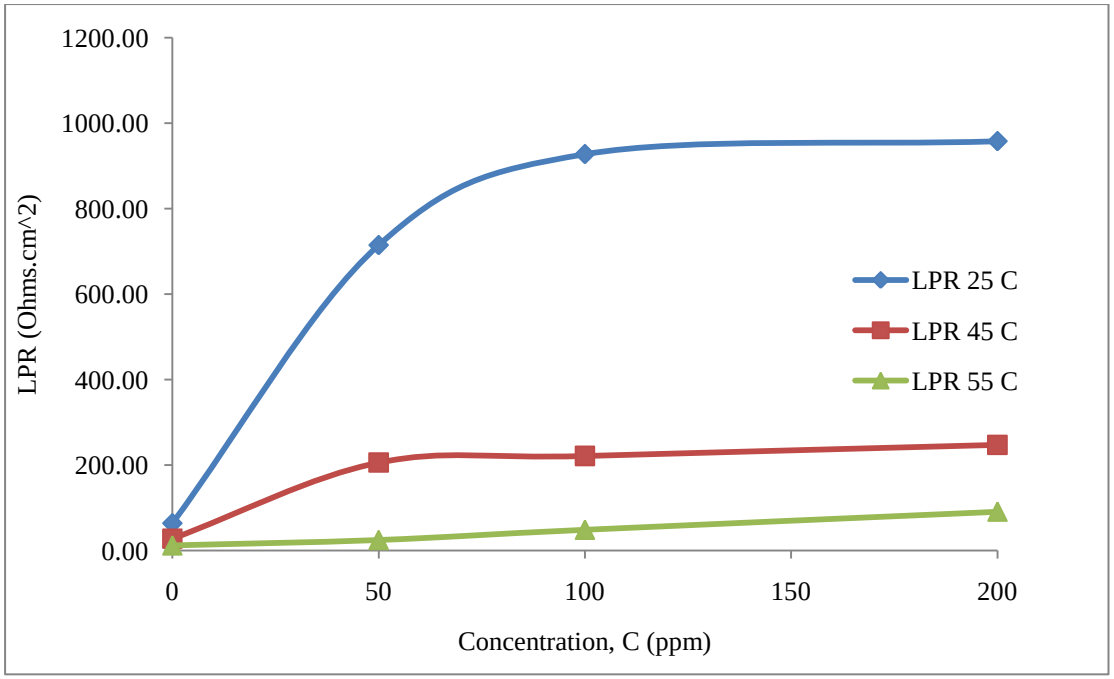

Figure 77: LPR for Fig & Olive (1:7) inhibitor Vs Concentration of the inhibitor at room and elevated temperatures.

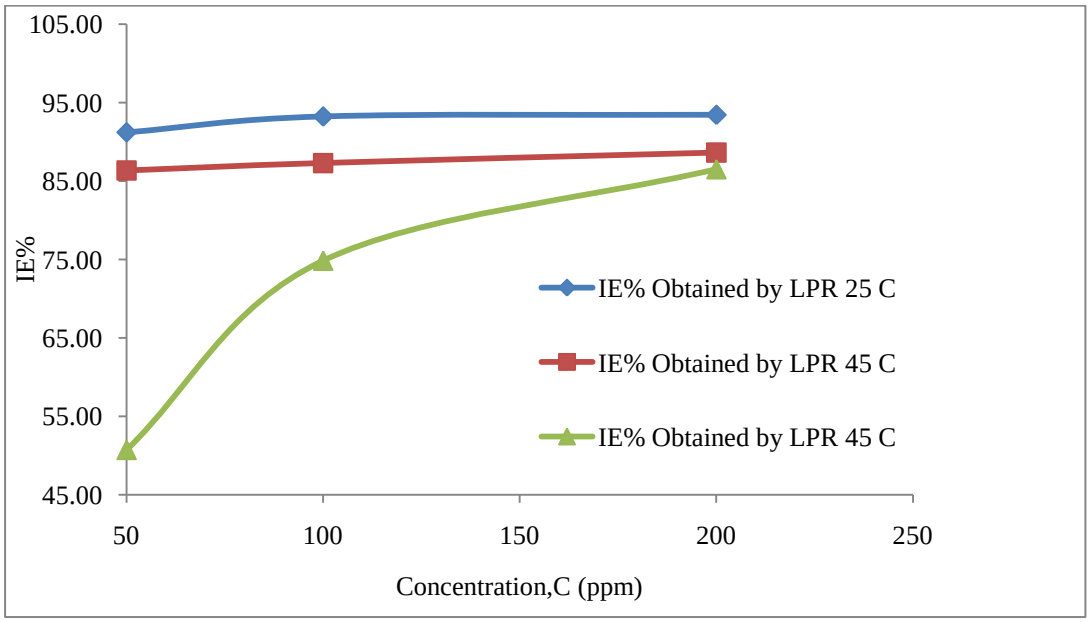

Figure 78: Inhibition efficiency for Fig & Olive (1:7) inhibitor obtained by LPR Vs Concentration of the Inhibitor at room and elevated temperatures.

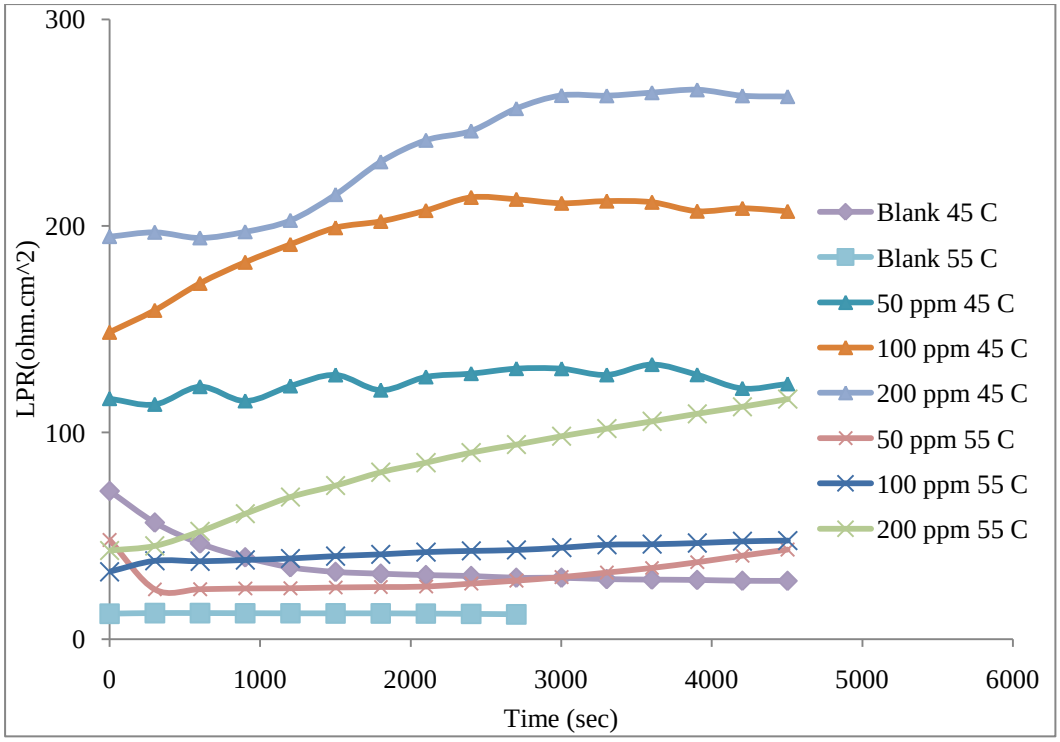

Figure 79: The LPR Vs Time of a mixture of Fig & Olive (1:1) at elevated temperatures.

Figure 79 illustrates the LPR values obtained for the mixture of Fig & Olive (1:1) as the inhibitor extract is added to the solution. The value of the LPR, similar to previous tests, increases more rapidly at low temperatures than at elevated temperatures. This results in a decrease in the current passing through the solution, signifying a decrease in the corrosion rate of the metal surface as the inhibitor is added to the environment. However, the inhibition is more effective at low temperatures than high temperatures. Unlike the two previous mixtures, the LPR curves are following the same trend and the difference is established clearly. The adsorption of the inhibitor on the metal surface decreases as the temperature increases causing less resistance to corrosion.

For the three temperatures studied, Figure 80 and Tables 24-26 explain that the LPR value increases as the concentration of the inhibitor in the solution increases. The increase of the LPR value reaches a steady state value after approximately 90 min. The trend for Fig and Olive (1:1) follows the same behavior as the previous extracts.

The speed in the breakage and formation of the protective film and the type of components being adsorbed on the metal surface causes a difference in the inhibition efficiency. The value of inhibition efficiency increases by almost 2%, 12% and 17% at temperatures of 25°C, 45°C and 55°C respectively. The graph plotted in Figure 81 indicates that the increase in inhibition efficiency at 55°C is more visible than the other temperatures studied. This represents the inhibition efficiency difference between the addition of 50 ppm and 200 ppm of the inhibitor extract to the solution. Figure 69 demonstrates that the addition of the inhibitor increases the inhibition efficiency. The increase of the inhibition efficiency indicates a decrease in the corrosion current density and the corrosion rate of the specimen studied.

Table 24: Caculations obtained using LPR method for a mixture of Fig and Olive (1:1) at 25°C.

Concentration (ppm)	LPR (ohm.cm²)	I_{corr} (mA/cm²)	Potential (mV)	IE%
0	63.72	0.4152	-442.80	-
50	645.41	0.0404	-424.01	90.27
100	1001.20	0.0261	-420.42	93.73
200	1038.60	0.0251	-416.91	93.95

Table 25: Caculations obtained using LPR method for a mixture of Fig and Olive (1:1) at 45°C.

Concentration (ppm)	LPR (ohm.cm²)	I_{corr} (mA/cm²)	Potential (mV)	IE%
0	28.18	0.9258	-499.15	-
50	126.88	0.2056	-493.6	77.79
100	208.59	0.1251	-501.05	86.49
200	262.68	0.0993	-493.69	89.27

Table 26: Caculations obtained using LPR method for a mixture of Fig and Olive (1:1) at 55°C.

Concentration (ppm)	LPR (ohm.cm²)	I_{corr} (mA/cm²)	Potential (mV)	IE%
0	12.31	2.1196	-493.28	-
50	40.38	0.6461	-431.59	69.52
100	46.52	0.5607	-433.14	73.54
200	98.21	0.2656	-489.68	87.47

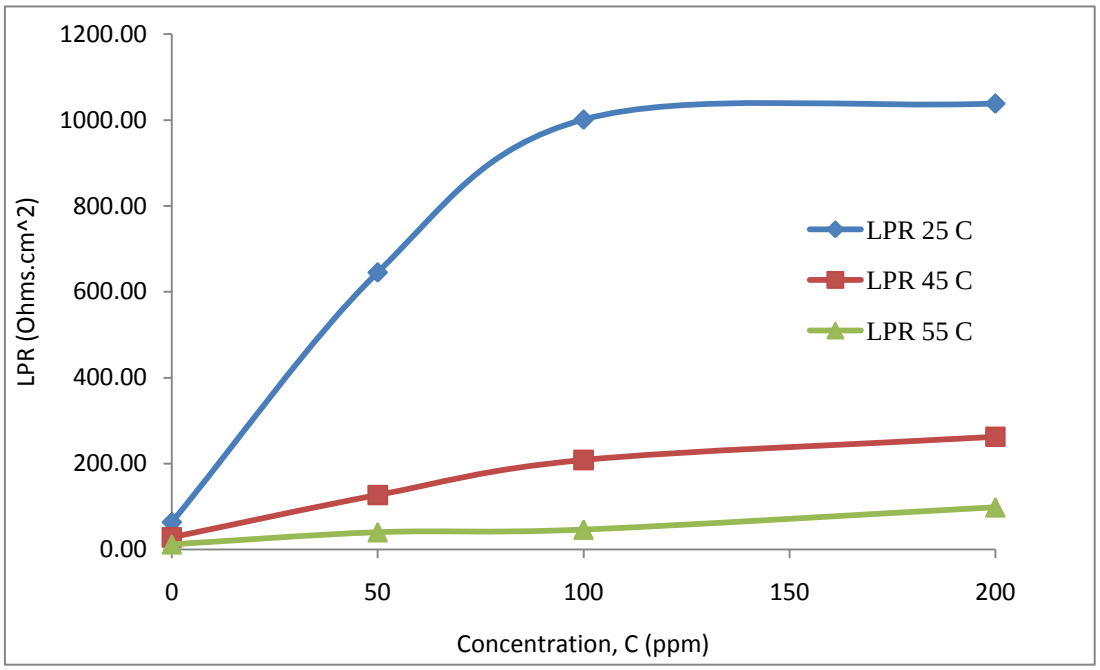

Figure 80: LPR for Fig & Olive (1:1) inhibitor Vs Concentration of the inhibitor at room and elevated temperatures.

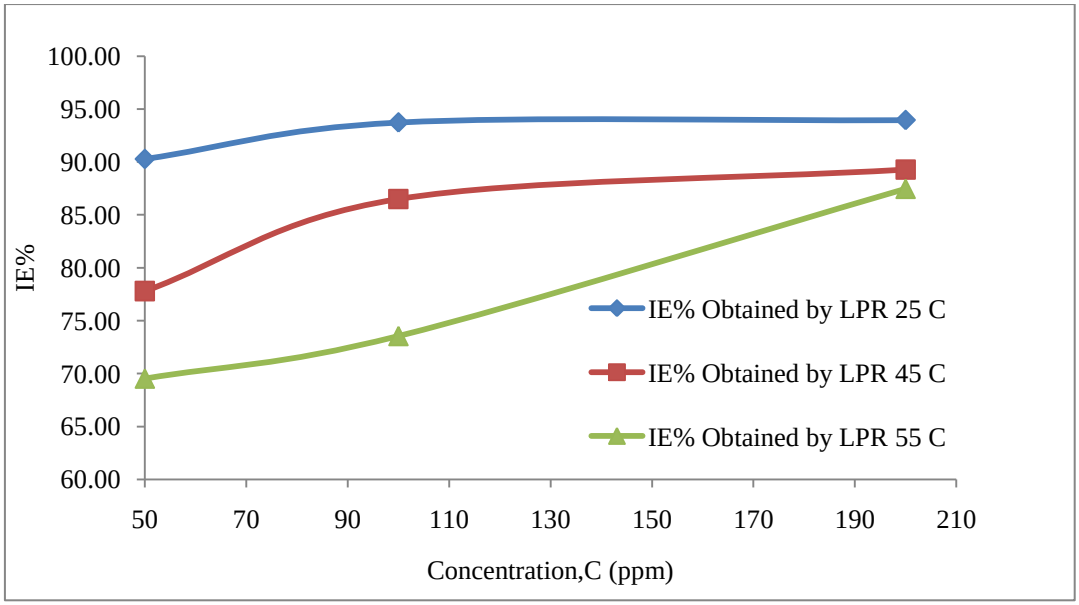

Figure 81: Inhibition efficiency for Fig & Olive (1:1) inhibitor obtained by LPR Vs Concentration of the Inhibitor at room and elevated temperatures.

In Figure 82, the LPR values obtained for Fig inhibitor with time are demonstrated. The value of the LPR increases more rapidly at low temperatures than at elevated temperatures. This results in a decrease in the current passing through the solution, which shows that the corrosion rate of the metal surface decreases as the inhibitor is added to the environment. However, the inhibition is more effective at low temperatures than high temperatures. The LPR curves at high temperatures are close to each other compared to the mixtures studied previously. This indicates a small difference in inhibition efficiency. The adsorption of the inhibitor on the metal surface decreases as the temperature increases causing less resistance to corrosion.

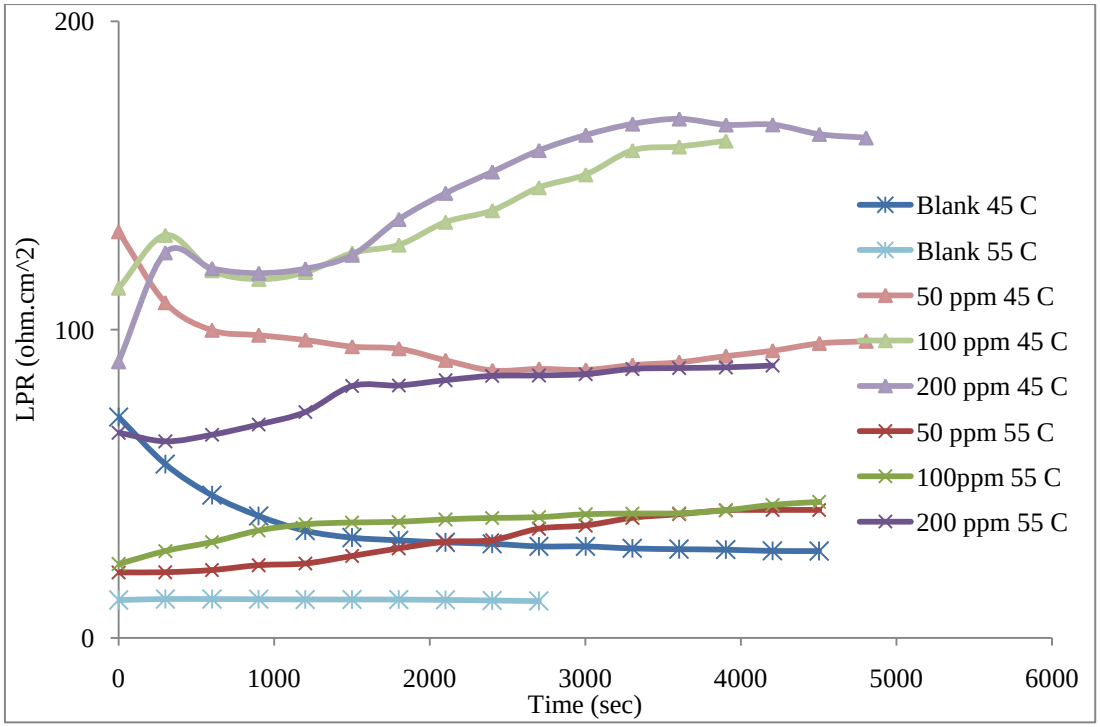

Figure 82: The LPR Vs Time of Fig at elevated temperatures.

At the three studied temperatures Figure 83 and Tables 27-29 clarify that the increase of the LPR value reaches after approximately 90 min a steady state value and this value increases with the addition of the inhibitor extract. This steady state value reads the resistance obtained after the formation of the protective film. The LPR steady state value at lower temperature is higher than the one's recorded at higher temperatures. This indicates a less resistance to corrosion is taking place at high temperatures. As the LPR value increases, the value of the current density that passes decreases steadily. This designates a decrease in the corrosion rate of the metal surface. It is clear that the increase in the LPR value is more rapid at high temperatures than at low temperatures.

The speed in the breakage and formation of the protective film and the type of components being adsorbed on the metal surface causes a difference in the inhibition efficiency. The value of inhibition efficiency increases by almost 1%, 11% and 12% at temperatures of 25^{o}C, 45^{o}C and 55^{o}C respectively. Figure 84 indicates that the increase in inhibition efficiency at 55^{o}C is more visible than the other temperatures studied. This represents the inhibition efficiency difference between the addition of 50 ppm and 200 ppm of the inhibitor extract to the solution. The trend at all temperatures

looks clearly the same compared to previous mixtures studied. The increase of the inhibition efficiency indicates a decrease in the corrosion current density and the corrosion rate of the specimen studied.

Table 27: Caculations obtained using LPR method for Fig at 25°C.

Concentration (ppm)	LPR (ohm.cm²)	I_{corr} (mA/cm²)	Potential (mV)	IE%
0	63.72	0.4152	-442.80	-
50	104.02	0.0392	-377.89	90.56
100	126.74	0.0371	-374.09	91.06
200	781.86	0.0331	-421.98	92.03

Table 28: Caculations obtained using LPR method for Fig at 45°C.

Concentration (ppm)	LPR (ohm.cm²)	I_{corr} (mA/cm²)	Potential (mV)	IE%
0	28.18	0.9258	-499.15	-
50	96.25	0.2710	-495.31	70.72
100	161.24	0.1618	-499.86	82.53
200	162.28	0.1608	-494.80	82.64

Table 29: Caculations obtained using LPR method for Fig at 55°C.

Concentration (ppm)	LPR (ohm.cm²)	I_{corr} (mA/cm²)	Potential (mV)	IE%
0	11.95	2.1832	-493.67	-
50	36.44	0.7159	-500.30	67.21
100	44.09	0.4914	-503.96	77.49
200	83.59	0.4121	-507.42	81.13

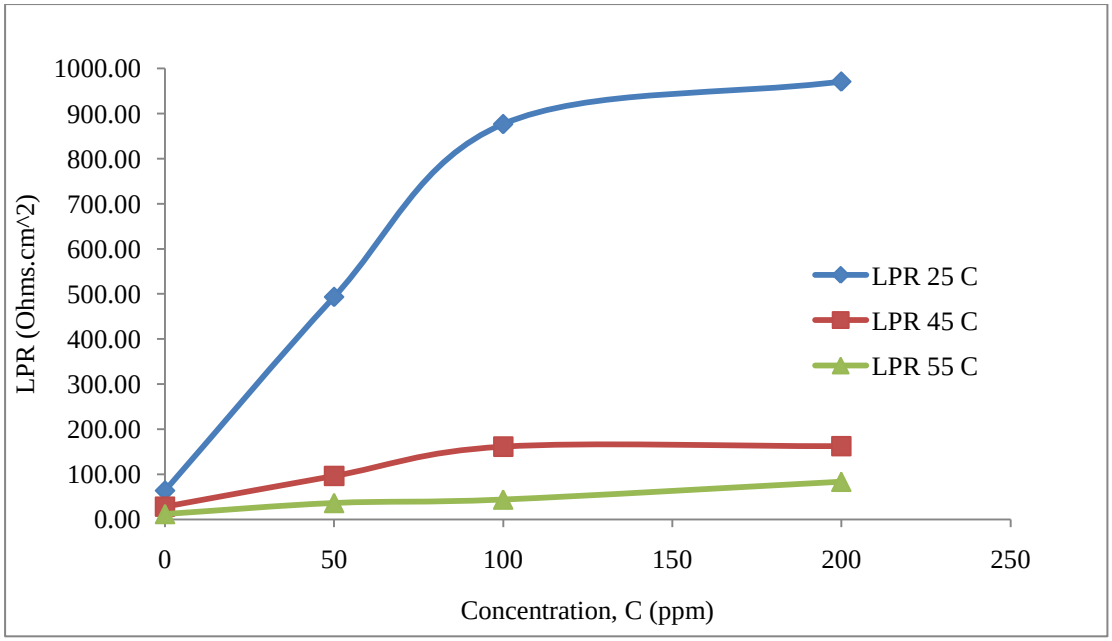

Figure 83: LPR for Fig inhibitor Vs Concentration of the inhibitor at room and elevated temperatures.

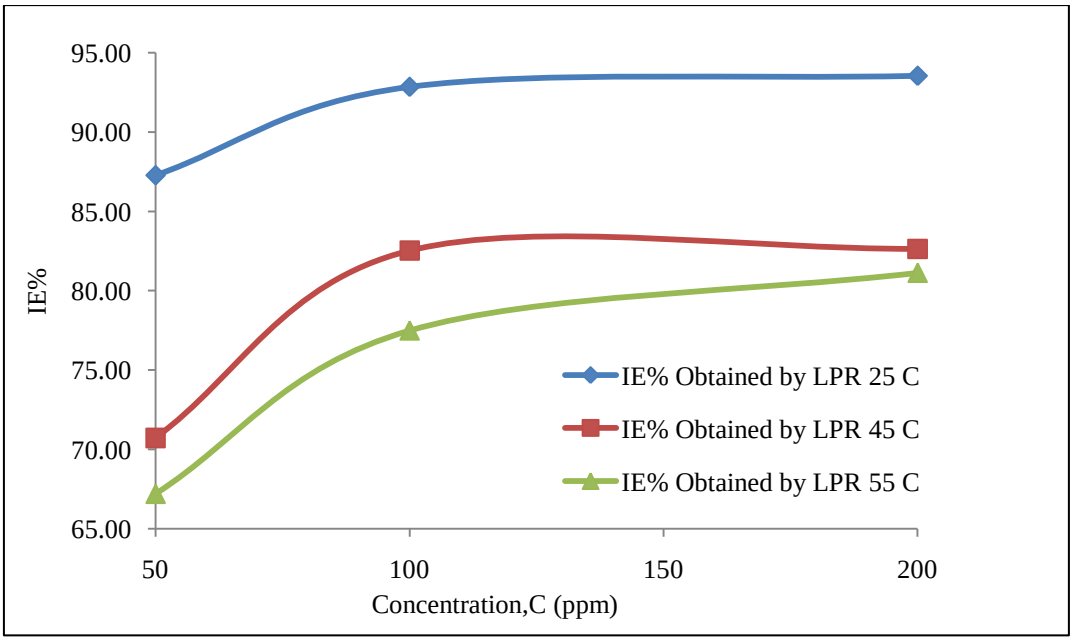

Figure 84: Inhibition efficiency for Fig inhibitor obtained by LPR Vs Concentration of the Inhibitor at room and elevated temperatures.

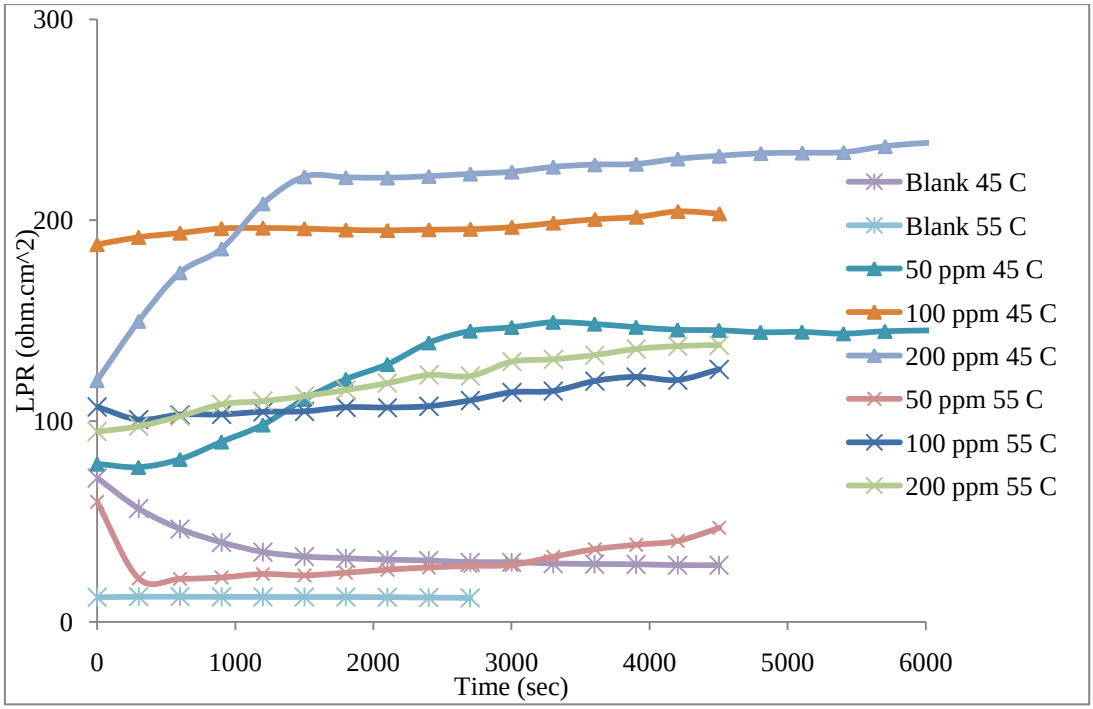

Figure 85: The LPR Vs Time of Olive at elevated temperatures.

Figure 85 demonstrates the LPR values obtained for Olive inhibitor as the inhibitor extract is added to the solution. The value of the LPR increases more rapidly at low temperatures than at elevated temperatures. In addition, both the current passing through the solution and the corrosion rate of the metal surface decrease as the inhibitor is added to the environment. However, the inhibition is more effective at low temperatures than high temperatures. The LPR curves at high temperatures are close to each other compared to the mixtures studied previously. This indicates a small difference in inhibition efficiency. The LPR curves are distributes more on the range of LPR recorded than the previous cases. The adsorption of the inhibitor on the metal surface decreases as the temperature increases causing less resistance to corrosion.

For the three temperatures studied, Figure 86 and Tables 30-32 clarify that the increase of the LPR value reaches steady state after approximately 90 min. The LPR steady state value at lower temperature is higher than that recorded at higher temperatures. This indicates less resistance to corrosion at high temperatures. As the LPR value increases, the value of the current density that passes decreases steadily.

This signifies a decrease in the corrosion rate of the metal surface. It is clear that the increase in the LPR value is more rapid at high temperatures than at low temperatures.

The increase of the inhibition efficiency indicates a decrease in the corrosion current density and the corrosion rate of the specimen studied. The speed in the breakage and formation of the protective film and the type of components being adsorbed on the metal surface cause a difference in the inhibition efficiency. The value of inhibition efficiency increases by 2%, 8% and 11% at temperatures of 25°C, 45°C and 55°C, respectively. The graph plotted in Figure 87 indicates that the increase in inhibition efficiency at 55°C is more visible than the other temperatures studied. This represents the inhibition efficiency difference between the addition of 50 ppm and 200 ppm of the inhibitor extract to the solution. Figure 87 also demonstrates that the addition of the inhibitor increases the inhibition efficiency. The trend at all temperatures looks clearly the same compared to previous mixtures studied.

Table 30: Caculations obtained using LPR method for Olive at 25°C.

Concentration (ppm)	LPR (ohm.cm²)	I_{corr} (mA/cm²)	Potential (mV)	IE%
0	63.72	0.4152	-442.8	-
50	430.27	0.0606	-424.41	85.40
100	492.67	0.0529	-421.33	87.25
200	511.94	0.0510	-428.26	87.73

Table 31: Caculations obtained using LPR method for Olive at 45°C.

Concentration (ppm)	LPR (ohm.cm²)	I_{corr} (mA/cm²)	Potential (mV)	IE%
0	28.18	0.9258	-499.15	-
50	147.37	0.1770	-493.3	80.88
100	203.29	0.1283	-494.78	86.14
200	243.85	0.1070	-492.30	88.44

Table 32: Caculations obtained using LPR method for Olive at 55°C.

Concentration (ppm)	LPR (ohm.cm²)	I_{corr} (mA/cm²)	Potential (mV)	IE%
0	12.31	2.1196	-493.28	-
50	46.87	0.5566	-506.70	73.74
100	107.36	0.3430	-501.24	83.82
200	129.55	0.3014	-503.69	85.78

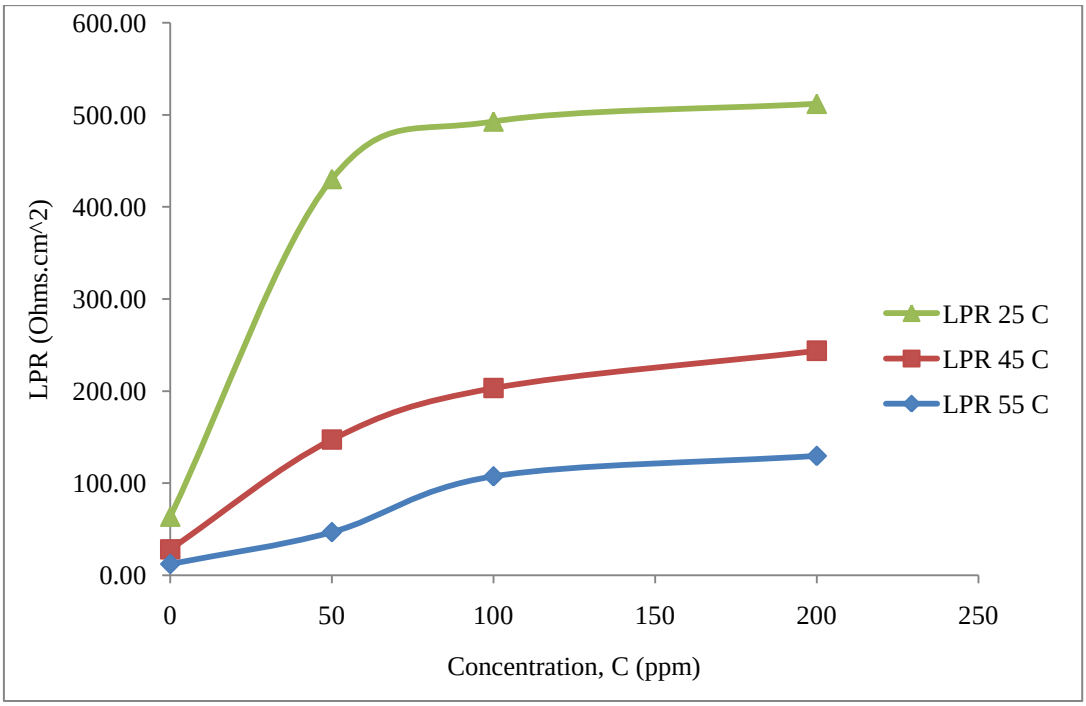

Figure 86: LPR for Olive inhibitor Vs Concentration of the inhibitor at room and elevated temperatures.

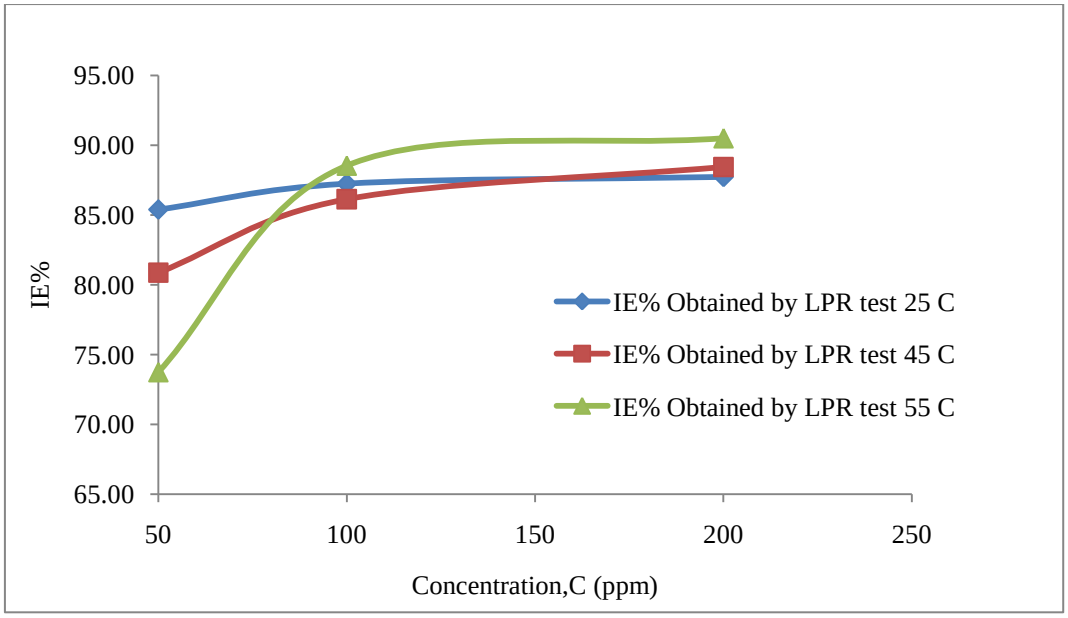

Figure 87: Inhibition efficiency for Olive inhibitor obtained by LPR Vs Concentration of the Inhibitor at room and elevated temperatures.

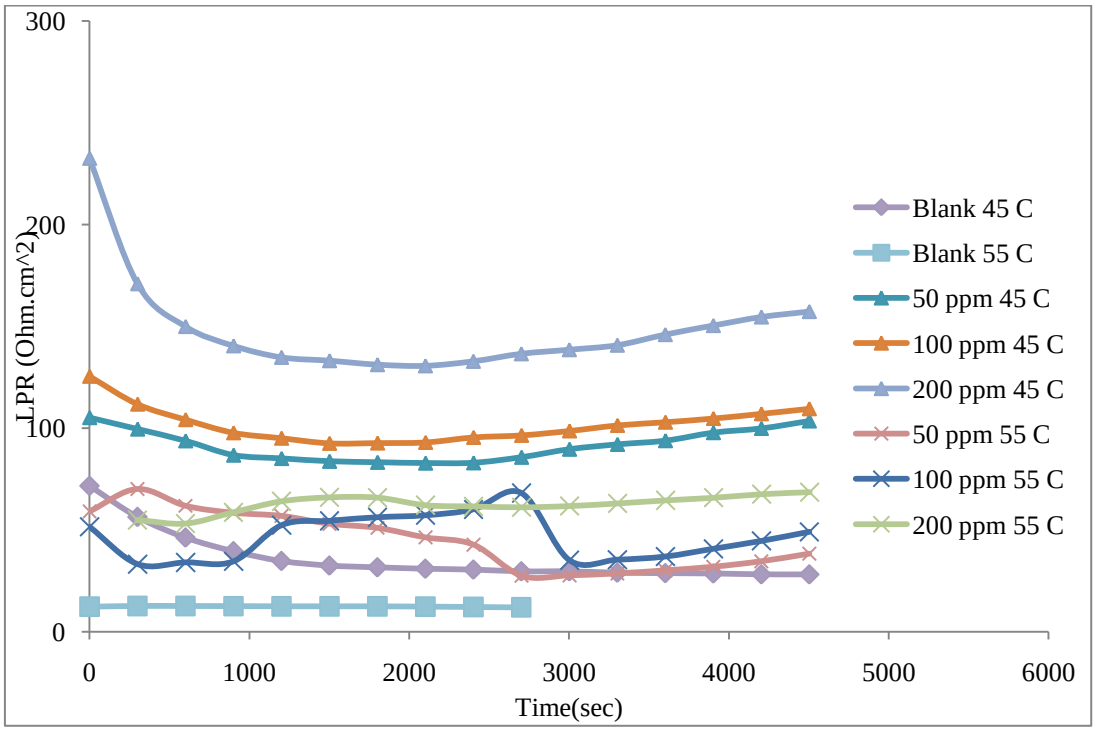

Figure 88: The LPR Vs Time of Rosemary at elevated temperatures.

Figure 88 makes obvious illustration of the LPR values obtained for Rosemary inhibitor as the inhibitor extract is added to the solution. The value of the LPR is seen

to increases as the inhibitor is added to the solution. This is more obvious at low temperatures than at elevated temperatures. An increase in the LPR values causes a decrease in the current passing through the solution and this shows that the corrosion rate of the metal surface decreases as the inhibitor is added to the environment. Though, the inhibition is more effective at low temperatures than high temperatures. The LPR curves at high temperatures are close in range to each other compared to the mixtures studied previously. This indicates a small difference in inhibition efficiency. The LPR curves are distributes more on the range of LPR recorded than the previous cases. The LPR curve at a temperature of 55^{o}C is seen to be disturbed in values. This is happening due to the breakage of the adsorption layer formed on the metal surface. The adsorption of the inhibitor on the metal surface decreases as the temperature increases causing less resistance to corrosion. The breakage of the film causes an increase in the current passing which leads to an increase in the corrosion rate and a decrease in the LPR value recorded.

Figure 89 and Tables 33-35 clarify that the increase of the LPR value reaches after approximately 90 min a steady state value and this value increases with the addition of the inhibitor extract. This steady state value reads the resistance obtained after the formation of the protective film for the three studied temperatures. The LPR steady state value at lower temperature is higher than the one's recorded at higher temperatures. This designates a less resistance to corrosion is taking place at high temperatures. As the LPR value increases, the value of the current density that passes decreases steadily. This causes a decrease in the corrosion rate of the metal surface. It is clear that the increase in the LPR value is more rapid at high temperatures than at low temperatures.

The speed in the breakage and formation of the protective film and the type of components being adsorbed on the metal surface causes a difference in the inhibition efficiency. The value of inhibition efficiency increases by almost 1%, 10% and 20% at temperatures of 25°C, 45°C and 55°C respectively. The difference is obtained higher in this case at 55°C because the low concentration of inhibitor is not sufficient enough to obtain good inhibition efficiency. On the other hand, as the inhibitor is added at higher concentration the increase in inhibition efficiency is well established. The graph plotted in Figure 90 indicates that the increase in inhibition efficiency at 55°C is more visible than the other temperatures studied. This represents the

inhibition efficiency difference between the addition of 50 ppm and 200 ppm of the inhibitor extract to the solution. Figure 90 demonstrates that the addition of the inhibitor increases the inhibition efficiency. The trend at all temperatures looks clearly the same compared to previous mixtures studied. The increase of the inhibition efficiency indicates a decrease in the corrosion current density and the corrosion rate of the specimen studied.

Table 33: Caculations obtained using LPR method for Rosemary at 25°C.

Concentration (ppm)	LPR (ohm.cm²)	I_{corr} (mA/cm²)	Potential (mV)	IE%
0	63.72	0.4152	-442.8	-
50	490.28	0.0532	-477.21	87.19
100	514.76	0.0507	-482.77	87.80
200	563.80	0.0463	-470.79	88.86

Table 34: Caculations obtained using LPR method for Rosemary at 45°C.

Concentration (ppm)	LPR (ohm.cm²)	I_{corr} (mA/cm²)	Potential (mV)	IE%
0	28.18	0.9258	-499.15	-
50	99.82	0.2613	-503.01	71.77
100	107.01	0.2438	-503.31	73.67
200	154.62	0.1687	-503.01	81.78

Table 35: Caculations obtained using LPR method for Rosemary at 55°C.

Concentration (ppm)	LPR (ohm.cm²)	I_{corr} (mA/cm²)	Potential (mV)	IE%
0	11.95	2.1832	-493.67	-
50	30.07	0.8674	-514.67	60.27
100	40.70	0.6410	-510.26	70.64
200	61.07	0.4272	-503.84	80.43

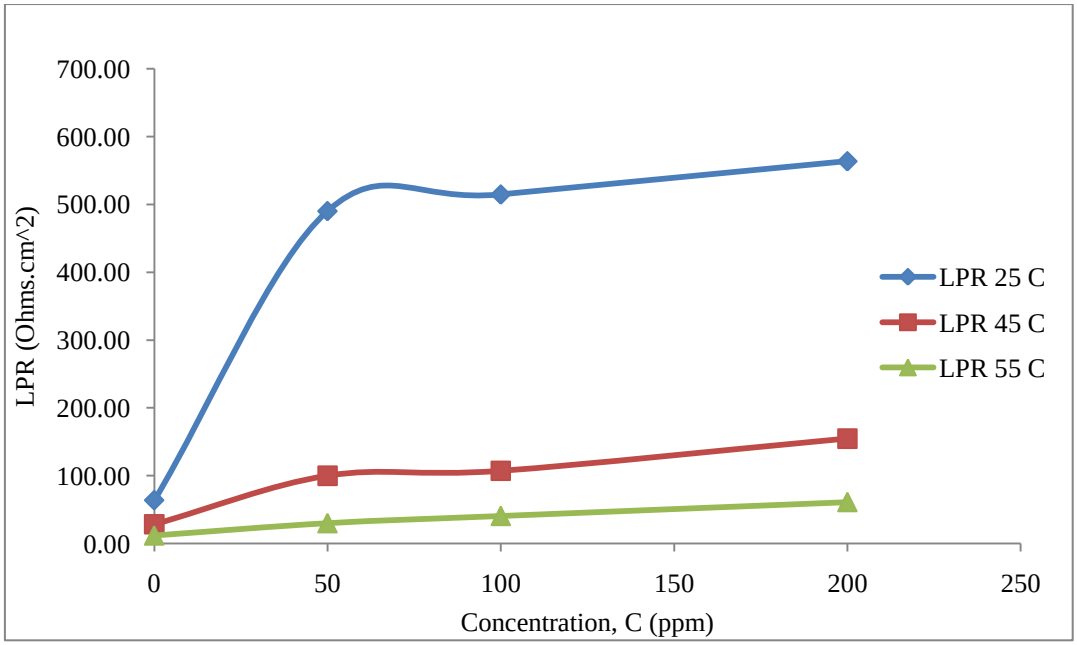

Figure 89: LPR for Rosemary inhibitor Vs Concentration of the inhibitor at room and elevated temperatures.

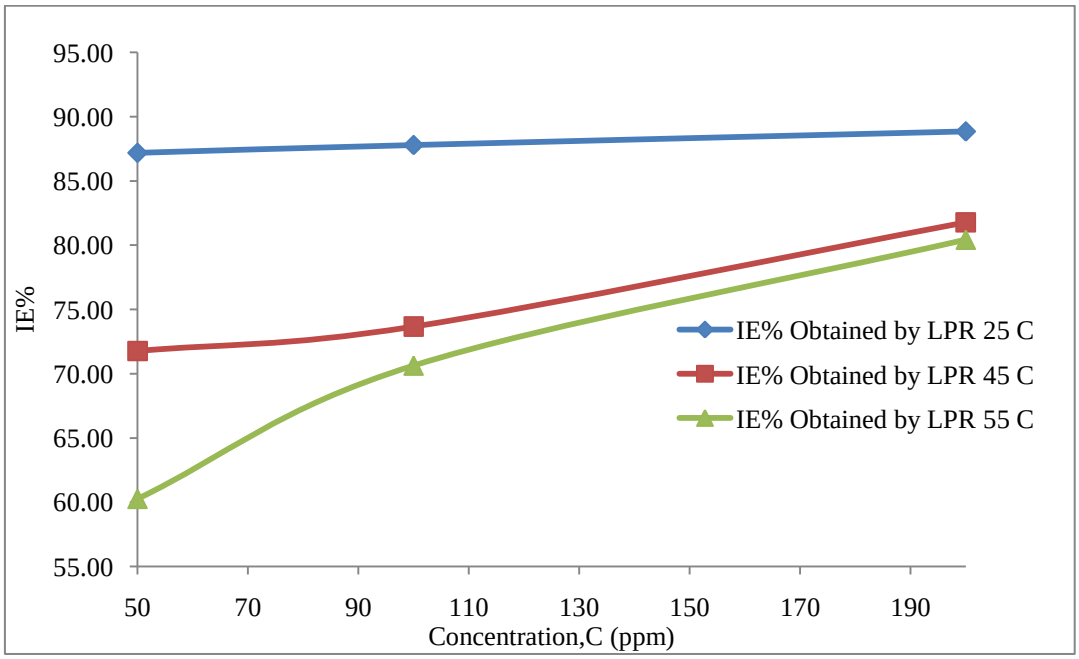

Figure 90: Inhibition efficiency for Rosemary inhibitor obtained by LPR Vs concentration of the Inhibitor at room and elevated temperatures.

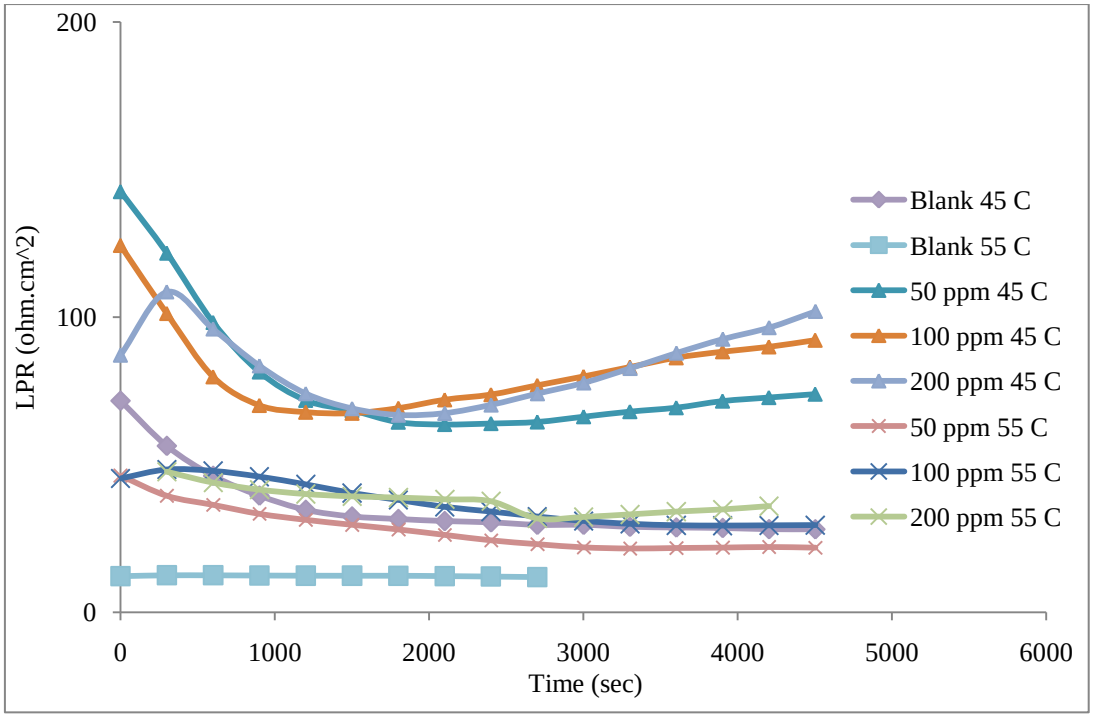

Figure 91: The LPR Vs Time of Cypress at elevated temperatures.

Figure 91 demonstrates the LPR values obtained for Cypress inhibitor as the inhibitor extract is added to the solution. The value of the LPR increases more rapidly at low temperatures than at elevated temperatures. This results in a decrease in the current passing through the solution and shows that the corrosion rate of the metal surface decreases as the inhibitor is added to the environment. The inhibition is more effective at low temperatures than high temperatures. This indicates a small difference in inhibition efficiency. The adsorption of the inhibitor on the metal surface decreases as the temperature increases causing less resistance to corrosion.

At the three temperatures studied, Figure 92 and Tables 36-38 clarify that the increase of the LPR value reaches a steady state value after approximately 90 min, which increases with the addition of the inhibitor extract. This steady state value reads the resistance obtained after the formation of the protective film. The LPR steady state value at lower temperature is higher than the ones recorded at higher temperatures. This means that less resistance to corrosion takes place at high temperatures. As the LPR value increases, the value of the current density that passes decreases steadily. This designates a decrease in the corrosion rate of the metal surface.

The increase of the inhibition efficiency indicates a decrease in the corrosion current density and the corrosion rate of the specimen studied. The graph plotted in Figure 93 indicates that the increase in inhibition efficiency at 55°C is more visible than the other temperatures studied. The speed in the breakage and formation of the protective film and the type of components being adsorbed on the metal surface causes a difference in the inhibition efficiency. The value of inhibition efficiency increases by almost 1%, 9% and 19% at temperatures of 25°C, 45°C and 55°C, respectively. This represents the inhibition efficiency difference between the addition of 50 ppm and 200 ppm of the inhibitor extract to the solution. Figure 93 demonstrates that the addition of the inhibitor increases the inhibition efficiency. The trend at all temperatures appears the same compared to previous mixtures studied.

Table 36: Caculations obtained using LPR method for Cypress at 25°C.

Concentration (ppm)	LPR (ohm.cm²)	I_{corr} (mA/cm²)	Potential (mV)	IE%
0	63.72	0.41523	-442.80	-
50	502.50	0.05191	-430.28	87.50
100	553.71	0.04711	-443.54	88.65
200	553.71	0.04711	-443.54	88.65

Table 37: Caculations obtained using LPR method for Cypress at 45°C.

Concentration (ppm)	LPR (ohm.cm²)	I_{corr} (mA/cm²)	Potential (mV)	IE%
0	28.18	0.9258	-499.15	-
50	72.77	0.3585	-498.53	61.28
100	89.99	0.2899	-501.1	68.69
200	96.46	0.2704	-496.16	70.79

Table 38: Caculations obtained using LPR method for Cypress at 55°C.

Concentration (ppm)	LPR (ohm.cm²)	I_{corr} (mA/cm²)	Potential (mV)	IE%
0	11.95	2.1832	-493.67	-
50	22.12	1.1793	-498.81	45.98
100	29.46	0.8856	-500.28	59.43
200	36.00	0.7247	-499.62	66.81

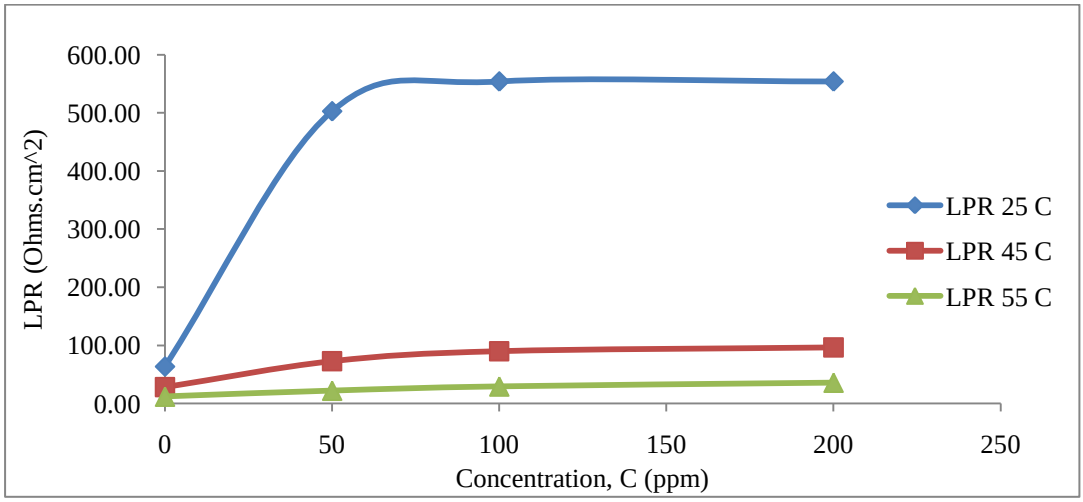

Figure 92: LPR for Cypress inhibitor Vs concentration of the inhibitor at room and elevated temperatures.

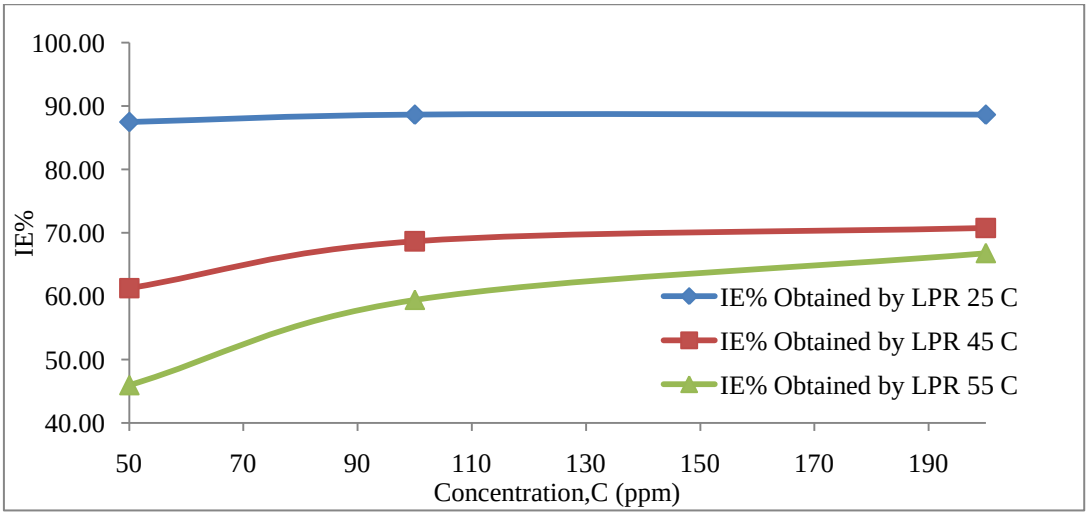

Figure 93: Inhibition efficiency for Cypress inhibitor obtained by LPR Vs concentration of the Inhibitor at room and elevated temperatures.

Figures 94-97 illustrate the values of the LPR and inhibition efficiency obtained by the LPR test for Fig and Olive using pure and mixtures of inhibitors at 45°C and 55°C. It can be seen from the graphs that the order of efficiency is different from the one obtained by the weight loss test. However, the difference is small and considered to be within the margin of error. Figures 98-101 illustrate the values of the LPR and inhibition efficiency obtained by the LPR test for pure green inhibitors at 45°C and 55°C. It can be seen that the order agrees between the two temperatures. All tests are considered reliable and the difference between the tests that some components in the inhibitor acts differently at higher temperatures. The order of the best inhibitor efficiency at a concentration range of 0-100 ppm is as follows:-

- At 45°C:- Fig & Olive (1:7), Olive, Fig & Olive (1:1), Fig and Fig & Olive (7:1).
- At 55°C:- Olive, Fig & Olive (7:1), Fig, Fig & Olive (1:1) and Fig & Olive (1:7).
- At 45°C:- Olive, Fig, Rosemary and Cypress.
- At 55°C:- Olive, Fig, Rosemary and Cypress.

The order above does not match for the cases of Figures 94-97. However, not all inhibitors act at the same inhibition efficiency at the different inhibitor concentrations studied. There is a slight difference in inhibition efficiencies that is within the margin of error.

Moreover, all results obtained by the LPR test draw the same conclusion and that is: the LPR values increase as the inhibitor extract is added to the solution. This proves that the inhibition efficiency increase and the corrosion rate of the metal decreases as the inhibitor is added to the corrosive environment. This happens as a result of the protective film formed by adsorption which acts as a barrier between the metal surface and the surrounding environment. This protects the metal surface from direct exposure to the severe environment. Moreover, inhibitor extracts act more sufficiently at lower temperatures than at elevated temperatures. This is due to the fact that the film starts to break or easier to break at higher temperature. This means that the adsorption on the surface decreases as the temperature increases causing the metal to be exposed to more corrosive media. In the following sections this will be explained in more details when studying the adsorption behavior.

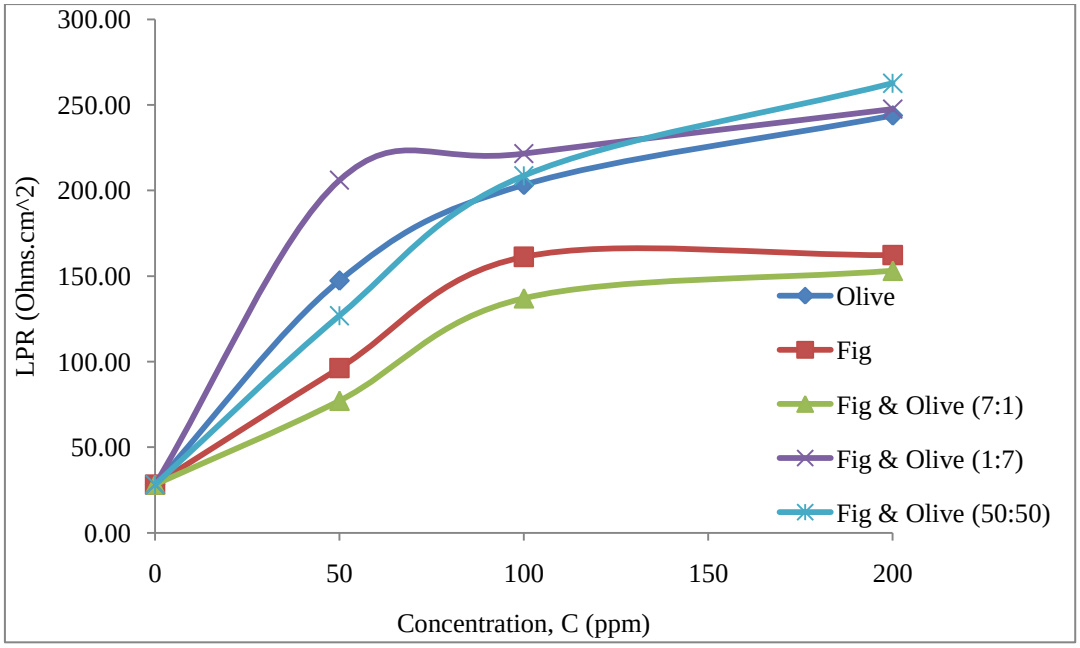

Figure 94: LPR for Fig & Olive pure & mixtures of inhibitors Vs concentration of the inhibitor at 45°C.

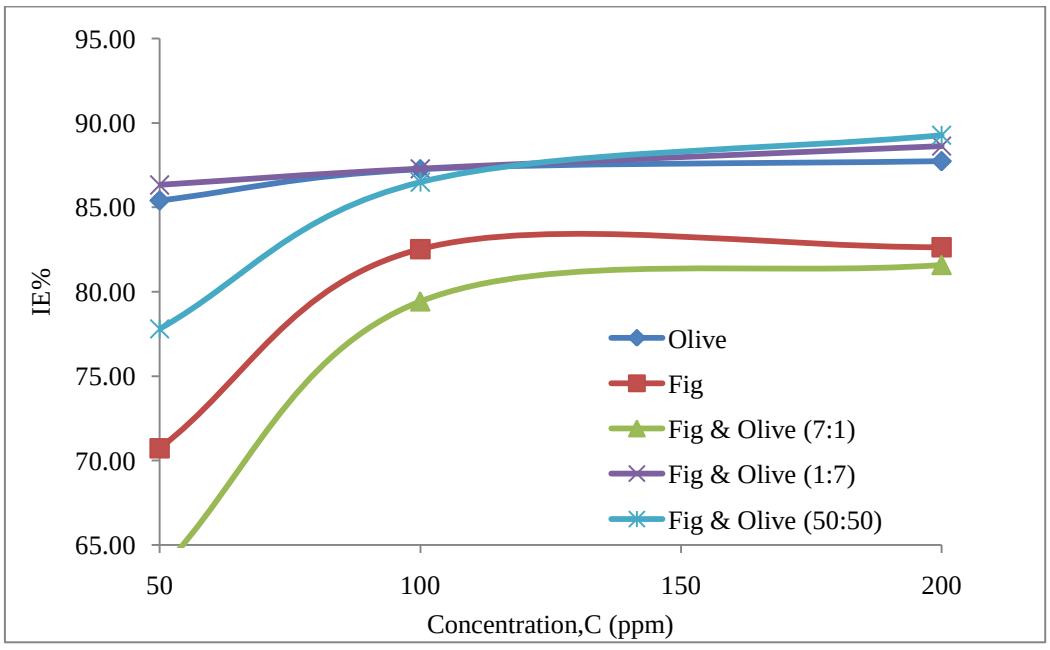

Figure 95: Inhibition efficiency for Fig & Olive pure & mixtures of inhibitors Vs concentration of the inhibitor at 45°C.

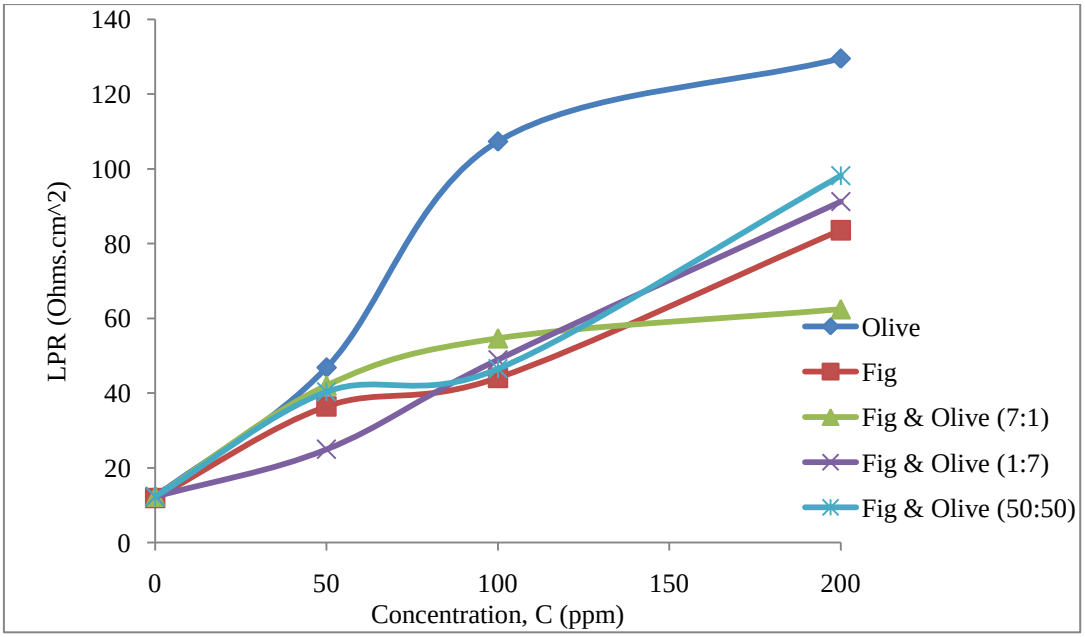

Figure 96: LPR for Fig & Olive pure & mixtures of inhibitors Vs concentration of the inhibitor at 55°C.

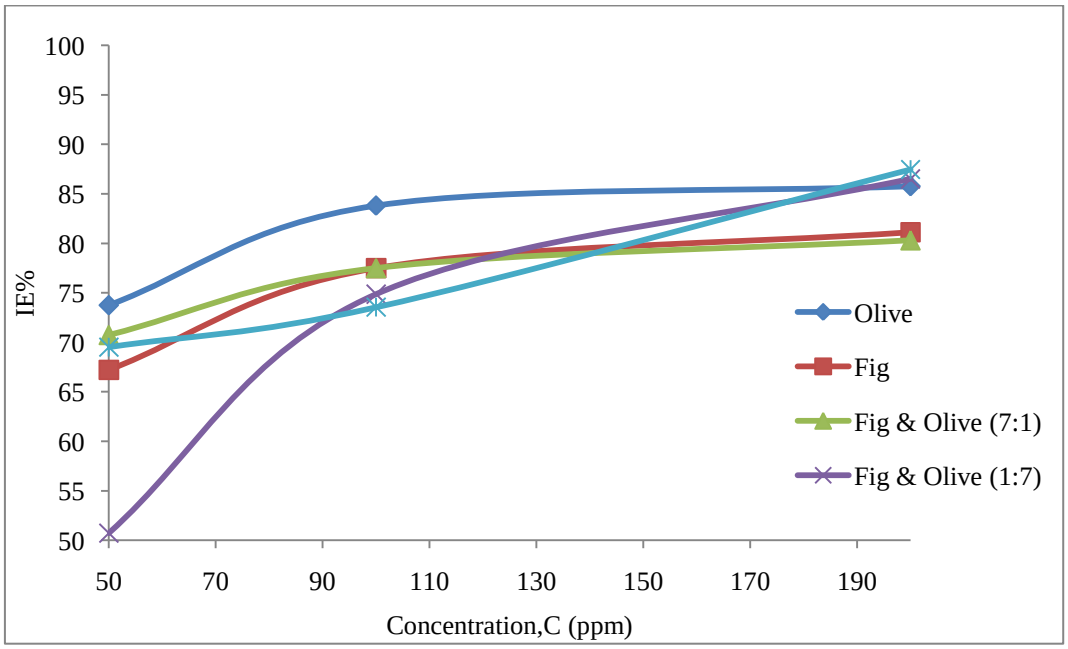

Figure 97: Inhibition efficiency for Fig & Olive pure & mixtures of inhibitors Vs concentration of the inhibitor at 55°C.

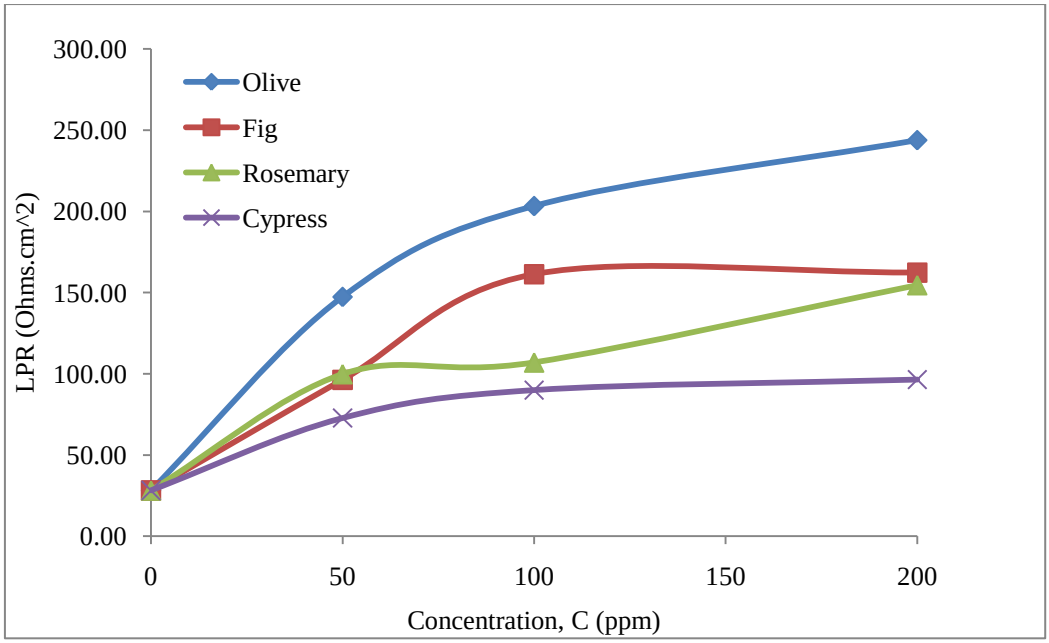

Figure 98: LPR for pure inhibitors Vs concentration of the inhibitor at 45°C.

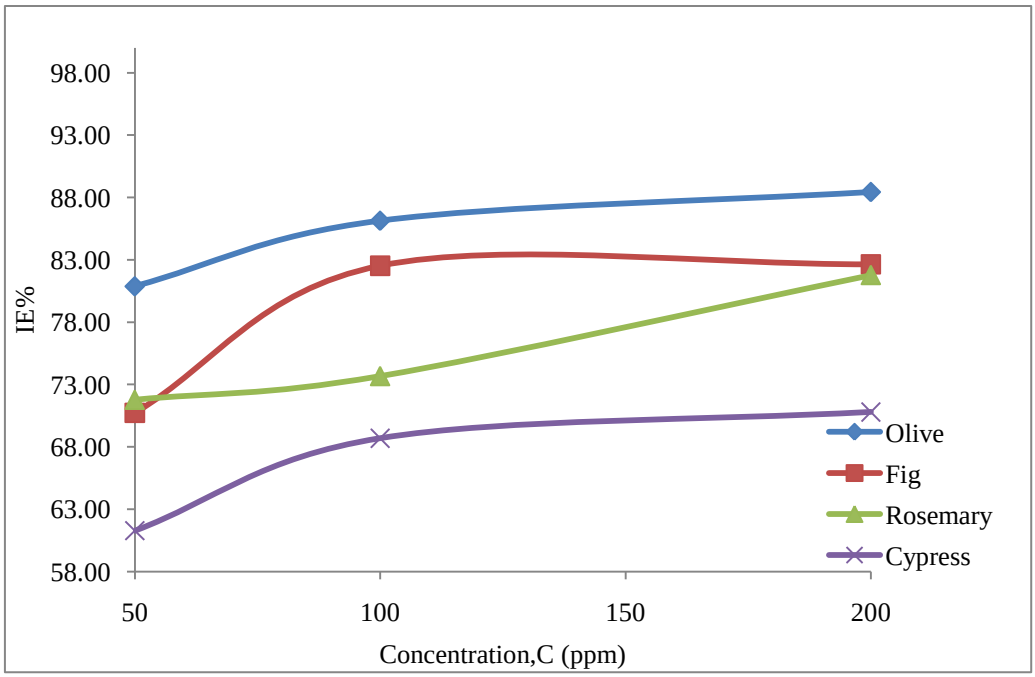

Figure 99: Inhibition efficiency for pure inhibitors Vs concentration of the inhibitor at 45°C.

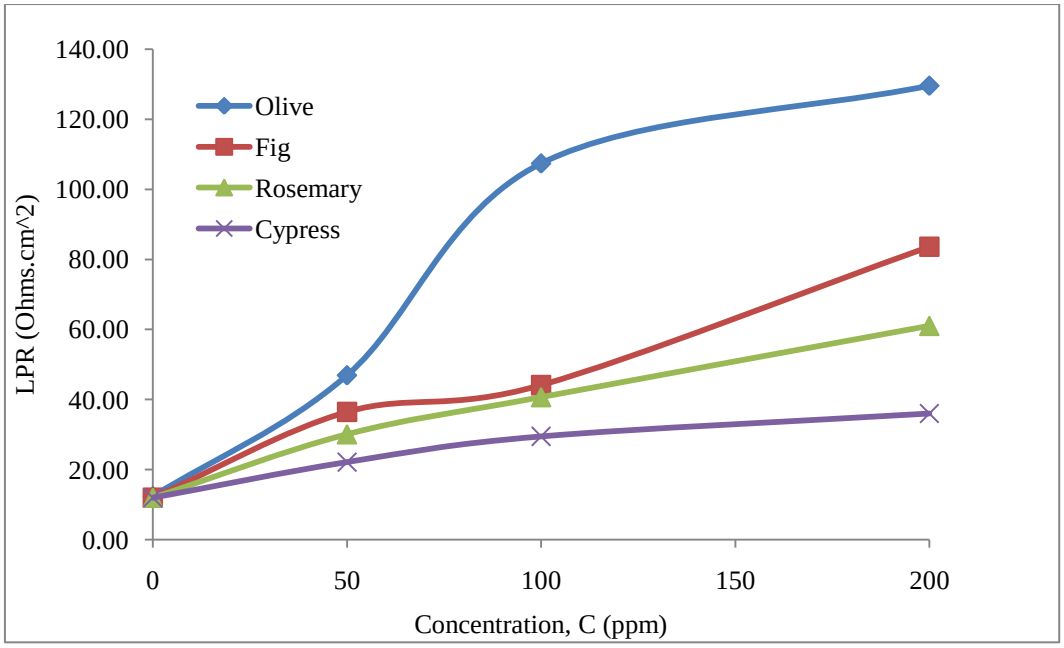

Figure 100: LPR for pure inhibitors Vs concentration of the inhibitor at 55°C.

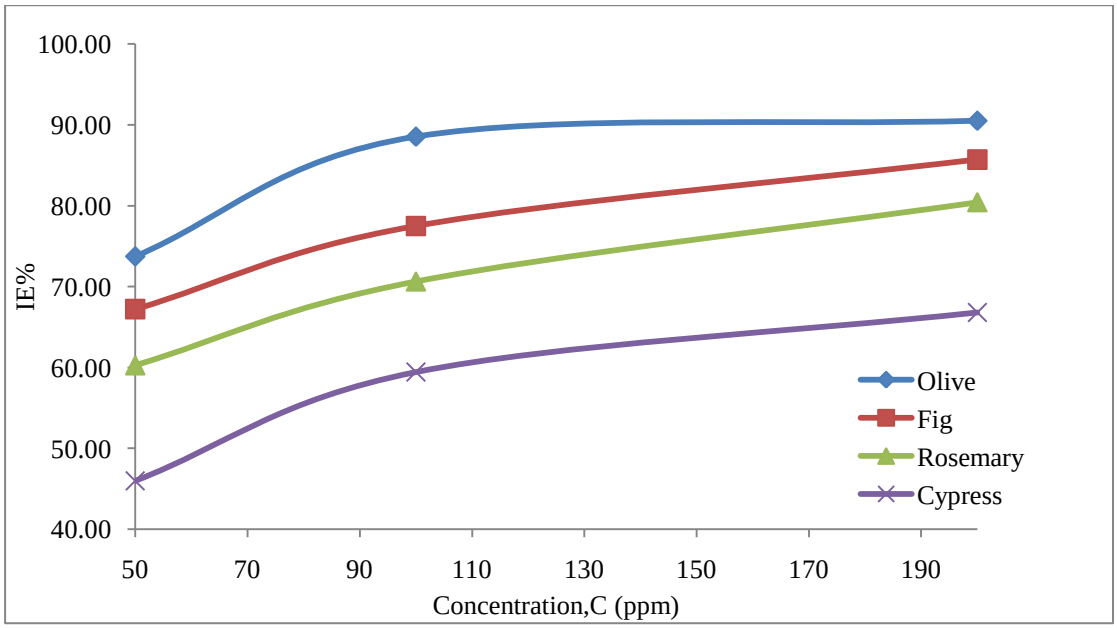

Figure 101: Inhibition efficiency for pure inhibitors Vs concentration of the inhibitor at 55°C.

4.3.5 Impedance Test at Elevated Temperatures

The corrosion of mild steel in hydrochloric acid solution in the presence of different inhibitors extract was investigated by EIS at 25°C, 45°C and 55°C after an exposure time of 20 min. Nyquist plots in uninhibited and inhibited acidic solutions containing different concentrations of plant extract are shown in Figures 102-108. The semicircles obtained in most cases are depressed [16, 31, 34]. This can be seen since the semicircles do not continue decreasing until they reach the x-axis. This feature indicates formation of porous layers and adsorption of the inhibitors on the surface of the mild steel specimen [16, 31, 34]. The depression can be noticed clearly in the case of Rosemary and Cypress plant extracts. It starts at low temperatures and almost vanishes at higher temperatures, indicating that the film starts to break. It is known that as the radius of the semicircles increases, the resistance to corrosion increases. As the inhibitor is added to the solution studied, the impedance increases and this indicates a reduction in the corrosion rate. This may not be clear, but if the corrosion current in Tables 39-59 is studied closely, a decrease in the corrosion current as the inhibitor is added to the solution can be noticed. The decrease causes a reduction in the corrosion rate. The rate at which the resistance of charge transfer increases is different from one case to another, as seen from the Nyquist plots. Some have very high resistivity relative to others. This means less corrosion occurring at the metal surface.

The Nyquist plots are analyzed in terms of the equivalent circuit comprised of classic parallel capacitor (C_{dl} ; double layer capacitance) and a resistor (R_{ct} ; charge transfer resistance or R_p, where both are connected in series with the solution resistance R_s). The fitted values of R_{ct} , C_{dl} , R_s, I_{corr} and the IE% are all tabulated in Tables 39-59. The inhibition efficiency can also be calculated from Equation 4.3.

It was found that as the concentration of the inhibitor increases, R_{ct} (radius of semicircle) and R_s values increase, where values of C_{dl} decrease. This happens because of the adsorption of the inhibitor molecules on the mild steel surface. R_{ct} values are the same as the Rp values, which are inversely proportional to the corrosion rate [16, 31, 34]. This proves a reduction in the corrosion rate and an increase in the inhibition efficiency as the inhibitor is added to the solution. It can be seen in Figure 109 that some inhibitors are higher in inhibition efficiency than others.

The Figures and tables below are the results obtained by the impedance test at the three temperatures studied with a range of concentration varying between 0 to 200 ppm. The corrosion of mild steel in hydrochloric acid solution in the presence of the inhibitor extracts is inspected by EIS at 25°C, 45°C and 55°C after an exposure time of 20 min.

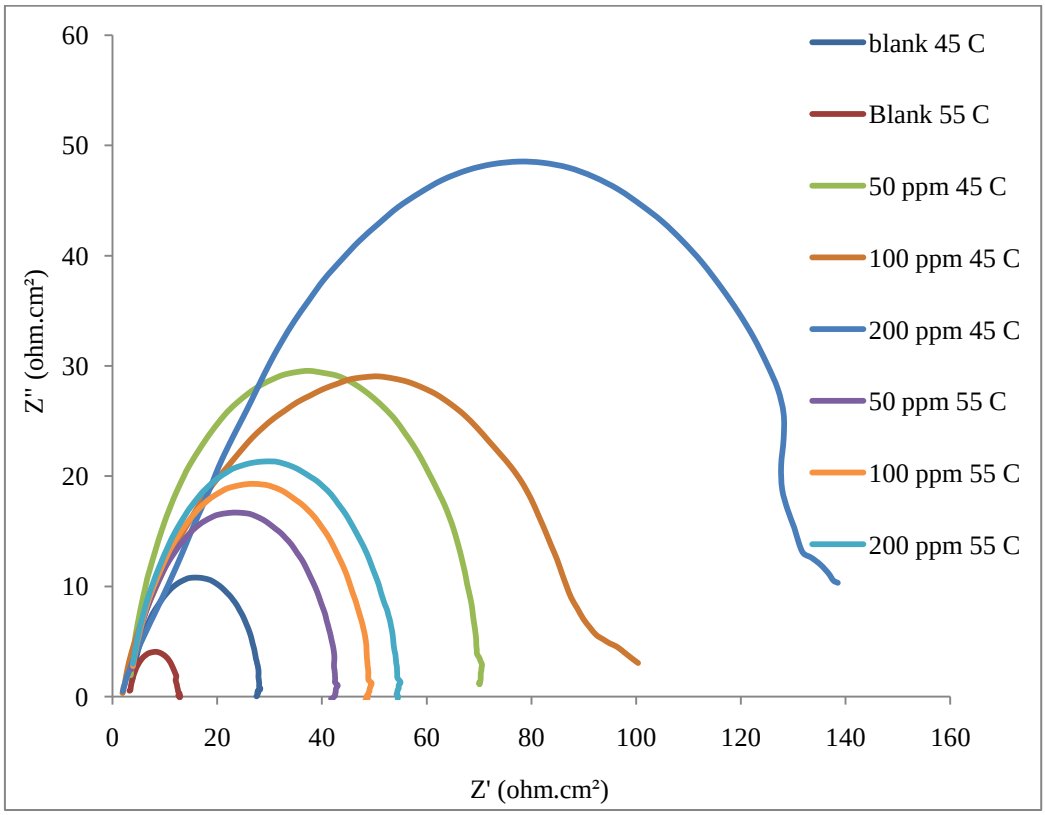

Figure 102: Nyquist plots for mild steel in a 1M HCl solution in the absence and presence of Fig & Olive (7:1) plant extract at 45°C & 55°C.

Table 39: Impedance parameters and corresponding inhibition efficiency for mild steel in 1M HCl in the absence and presence of Fig & Olive (7:1) plant extract at 25°C for specific concentrations.

Con.(ppm)	Rsol ($ohm.cm^2$)	Rct ($ohm.cm^2$)	Cd (F)	I corr. (mA/cm^2)	IE%
0	1.542	57.07	0.000431	0.2001	
50	2.112	452.00	0.000186	0.0222	88.91
100	2.501	521.30	0.000171	0.0185	90.75
200	2.909	872.00	0.000169	0.0148	92.60

Table 40: Impedance parameters and corresponding inhibition efficiency for mild steel in 1M HCl in the absence and presence of Fig & Olive (7:1) plant extract at 45°C for specific concentrations.

Con(ppm)	Rsol ($ohm.cm^2$)	Rct ($ohm.cm^2$)	Cd (F)	I corr. (mA/cm^2)	IE%
0	1.424	24.90	0.000249	0.3230	
50	3.244	145.61	0.000148	0.0821	74.59
100	3.753	174.13	0.000082	0.0704	78.21
200	3.835	204.27	0.000079	0.0639	80.23

Table 41: Impedance parameters and corresponding inhibition efficiency for mild steel in 1M HCl in the absence and presence of Fig & Olive (7:1) plant extract at 45°C for specific concentrations.

Con(ppm)	Rsol ($ohm.cm^2$)	Rct ($ohm.cm^2$)	Cd (F)	I corr. (mA/cm^2)	IE%
0	1.246	9.43	0.001120	1.2280	
50	3.168	36.82	0.000156	0.3433	74.40
100	3.267	39.95	0.000135	0.3110	76.40
200	3.316	45.76	0.000122	0.2954	79.40

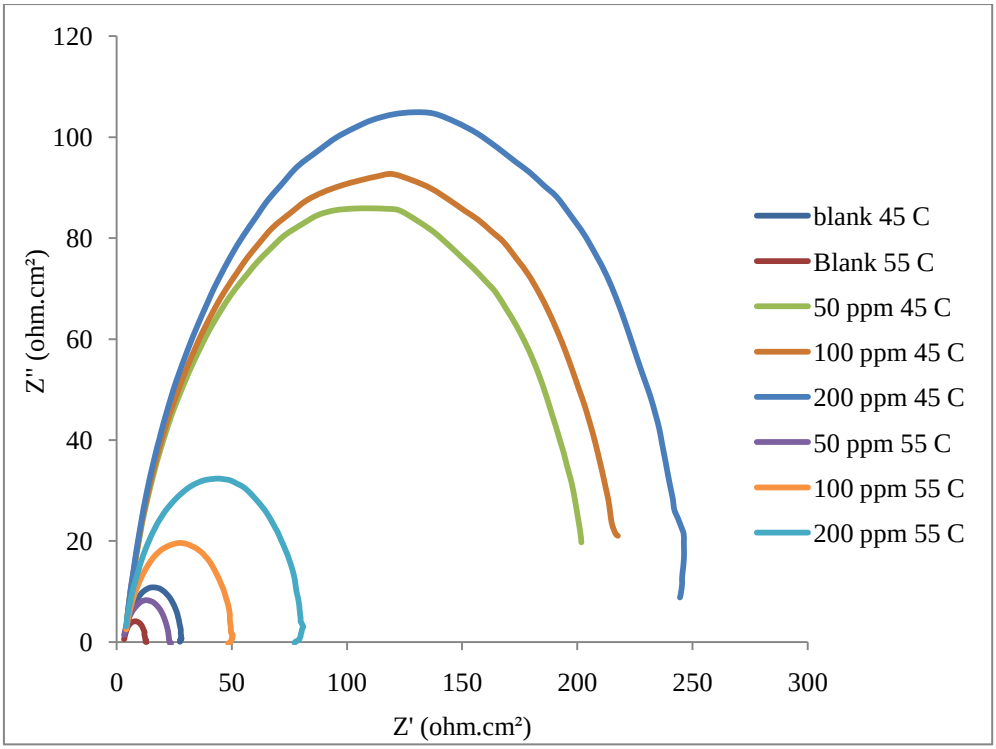

Figure 103: Nyquist plots for mild steel in a 1M HCl solution in the absence and presence of Fig & Olive (1:7) plant extract 45°C & 55°C.

Table 42: Impedance parameters and corresponding inhibition efficiency for mild steel in 1M HCl in the absence and presence of Fig & Olive (1:7) plant extract at 25°C for specific concentrations.

Con(ppm)	Rsol (ohm.cm^2)	Rct (ohm.cm^2)	Cd (F)	I corr. (mA/cm^2)	IE%
0	1.542	57.070	0.000431	0.2001	
50	3.030	684.300	0.000163	0.0174	91.66
100	3.031	975.700	0.000161	0.0123	94.15
200	3.133	987.300	0.000152	0.0123	94.22

Table 43: Impedance parameters and corresponding inhibition efficiency for mild steel in 1M HCl in the absence and presence of Fig & Olive (1:7) plant extract at 45°C for specific concentrations.

Con(ppm)	Rsol ($ohm.cm^2$)	Rct ($ohm.cm^2$)	Cd (F)	I corr. (mA/cm^2)	IE%
0	1.424	24.900	0.000249	0.3230	
50	3.616	147.248	0.000150	0.0679	83.09
100	3.713	175.356	0.000103	0.0597	85.80
200	3.671	209.067	0.000082	0.0514	88.09

Table 44: Impedance parameters and corresponding inhibition efficiency for mild steel in 1M HCl in the absence and presence of Fig & Olive (1:7) plant extract at 55°C for specific concentrations.

Con(ppm)	Rsol ($ohm.cm^2$)	Rct ($ohm.cm^2$)	Cd (F)	I corr. (mA/cm^2)	IE%
0	1.246	9.427	0.001120	1.2280	
50	2.913	37.729	0.000258	0.3479	75.01
100	3.646	40.987	0.000156	0.3418	77.00
200	3.747	47.134	0.000126	0.3040	80.00

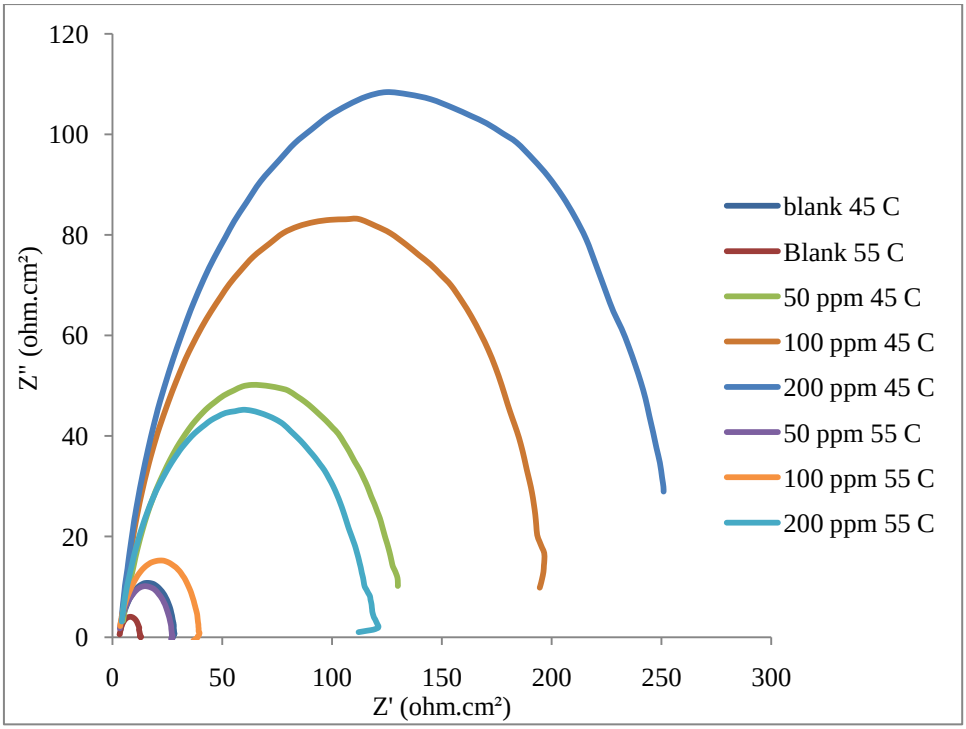

Figure 104: Nyquist plots for mild steel in a 1M HCl solution in the absence and presence of Fig & Olive (1:1) plant extract at 45°C & 55°C.

Table 45: Impedance parameters and corresponding inhibition efficiency for mild steel in 1M HCl in the absence and presence of Fig & Olive (1:1) plant extract at 25°C for specific concentrations.

Con(ppm)	Rsol (ohm.cm^2)	Rct (ohm.cm^2)	Cd (F)	I corr. (mA/cm^2)	IE%
0	1.542	57.07	0.000431	0.20010	
50	3.852	530.70	0.000173	0.01891	89.25
100	3.255	848.80	0.000124	0.01400	93.28
200	3.290	973.90	0.000113	0.01318	94.14

Table 46: Impedance parameters and corresponding inhibition efficiency for mild steel in 1M HCl in the absence and presence of Fig & Olive (1:1) plant extract at 45°C for specific concentrations.

Con(ppm)	Rsol ($ohm.cm^2$)	Rct ($ohm.cm^2$)	Cd (F)	I corr. (mA/cm^2)	IE%
0	1.424	24.90	0.000249	0.32300	
50	3.839	155.62	0.000136	0.06908	84.00
100	3.899	190.07	0.000093	0.06848	86.90
200	4.177	200.81	0.000075	0.06805	87.60

Table 47: Impedance parameters and corresponding inhibition efficiency for mild steel in 1M HCl in the absence and presence of Fig & Olive (1:1) plant extract at 55°C for specific concentrations.

Con(ppm)	Rsol ($ohm.cm^2$)	Rct ($ohm.cm^2$)	Cd (F)	I corr. (mA/cm^2)	IE%
0	1.246	9.43	0.001120	1.22800	
50	2.989	38.01	0.000200	0.30880	75.20
100	3.060	40.99	0.000163	0.30880	77.00
200	3.586	37.71	0.000141	0.30880	75.00

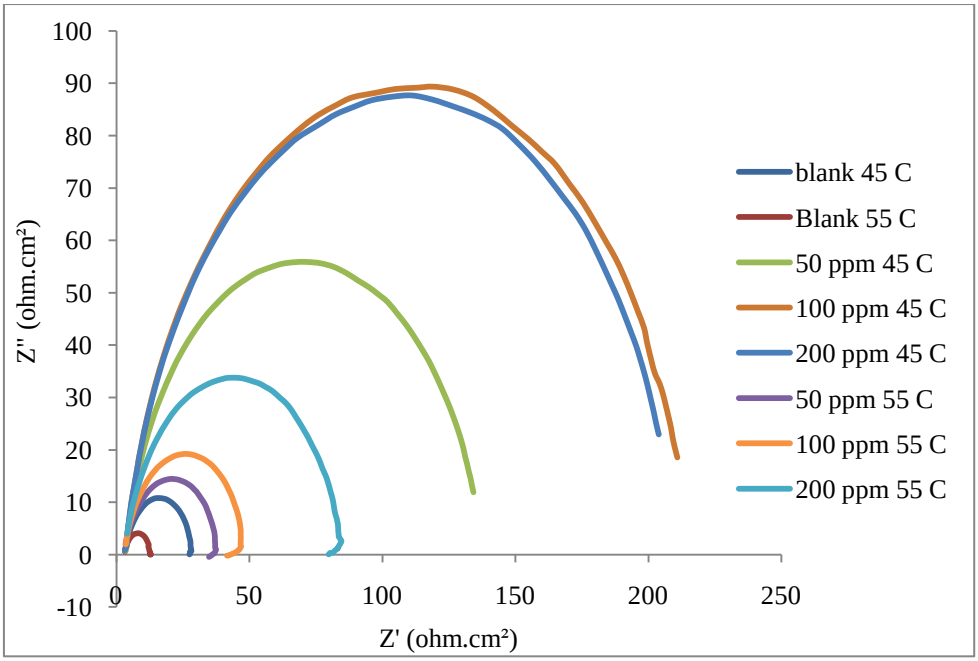

Figure 105: Nyquist plots for mild steel in a 1M HCl solution in the absence and presence of Fig plant extract at 45^{o}C & 55^{o}C.

Table 48: Impedance parameters and corresponding inhibition efficiency for mild steel in 1M HCl in the absence and presence of Fig plant extract at 25°C for specific concentrations.

Con(ppm)	Rsol (ohm.cm^2)	Rct (ohm.cm^2)	Cd (F)	I corr. (mA/cm^2)	IE%
0	1.542	57.07	0.000431	0.2001	
50	3.852	530.70	0.000173	0.0189	89.25
100	3.255	848.80	0.000124	0.0140	93.28
200	3.290	973.90	0.000113	0.0132	94.14

Table 49: Impedance parameters and corresponding inhibition efficiency for mild steel in 1M HCl in the absence and presence of Fig plant extract at 45°C for specific concentrations.

Con(ppm)	Rsol ($ohm.cm^2$)	Rct ($ohm.cm^2$)	Cd (F)	I corr. (mA/cm^2)	IE%
0	1.424	24.90	0.000249	0.3230	
50	3.153	134.30	0.000136	0.0765	81.46
100	3.168	157.60	0.000085	0.0624	84.20
200	3.191	227.90	0.000084	0.0431	89.07

Table 50: Impedance parameters and corresponding inhibition efficiency for mild steel in 1M HCl in the absence and presence of Fig plant extract at 55°C for specific concentrations.

Con(ppm)	Rsol ($ohm.cm^2$)	Rct ($ohm.cm^2$)	Cd (F)	I corr. (mA/cm^2)	IE%
0	1.246	9.43	0.001120	1.2280	
50	3.085	31.42	0.000208	0.4372	70.00
100	3.126	35.18	0.000190	0.4071	73.20
200	3.137	37.71	0.000094	0.4009	75.00

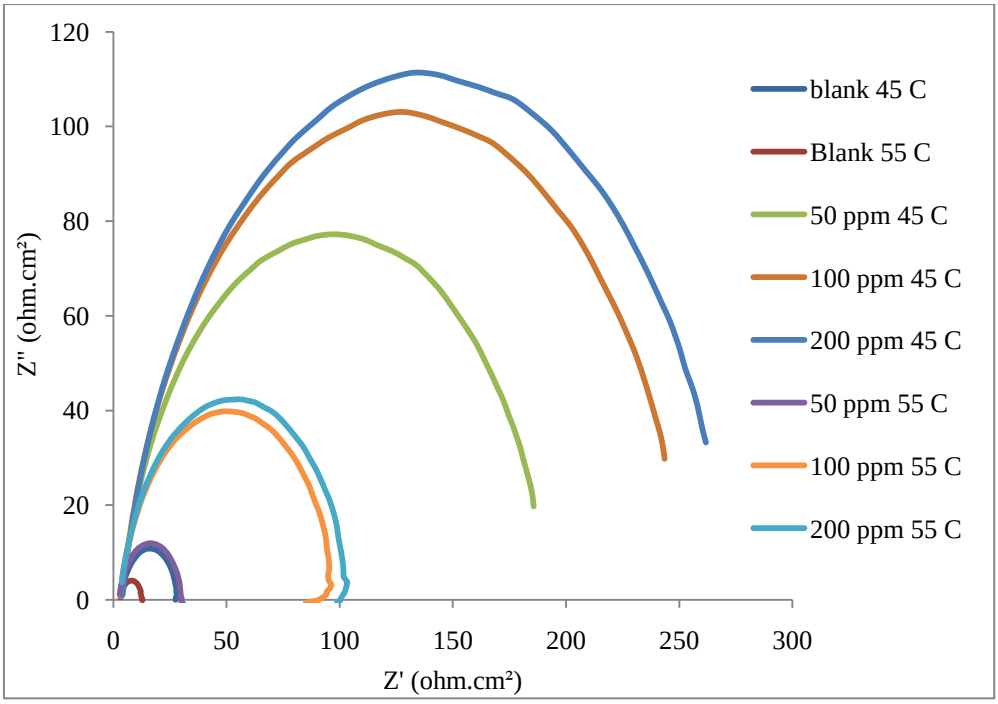

Figure 106: Nyquist plots for mild steel in a 1M HCl solution in the absence and presence of Olive plant extract at 45°C & 55°C.

Table 51: Impedance parameters and corresponding inhibition efficiency for mild steel in 1M HCl in the absence and presence of Olive plant extract at 25°C for specific concentrations.

Con(ppm)	Rsol (ohm.cm^2)	Rct (ohm.cm^2)	Cd (F)	I corr. (mA/cm^2)	IE
0	1.542	57.07	0.000431	0.2001	
50	3.204	424.00	0.006814	0.0201	86.54
100	3.217	514.40	0.000113	0.0175	88.91
200	3.247	528.40	0.000112	0.0174	89.20

Table 52: Impedance parameters and corresponding inhibition efficiency for mild steel in 1M HCl in the absence and presence of Olive plant extract at 45^{o}C for specific concentrations.

Con(ppm)	Rsol (ohm.cm^2)	Rct (ohm.cm^2)	Cd (F)	I corr. (mA/cm^2)	IE%
0	1.424	24.90	0.000249	0.3230	
50	3.58	99.60	0.000099	0.1351	75.00
100	3.613	108.26	0.000094	0.1292	77.00
200	3.688	118.57	0.000087	0.1187	79.00

Table 53: Impedance parameters and corresponding inhibition efficiency for mild steel in 1M HCl in the absence and presence of Olive plant extract at 55^{o}C for specific concentrations.

Con(ppm)	Rsol (ohm.cm^2)	Rct (ohm.cm^2)	Cd (F)	I corr. (mA/cm^2)	IE%
0	1.246	9.43	0.001120	1.2280	
50	2.617	25.48	0.000206	0.4973	59.50
100	3.009	27.77	0.000089	0.4885	60.22
200	3.155	30.54	0.000084	0.4488	63.45

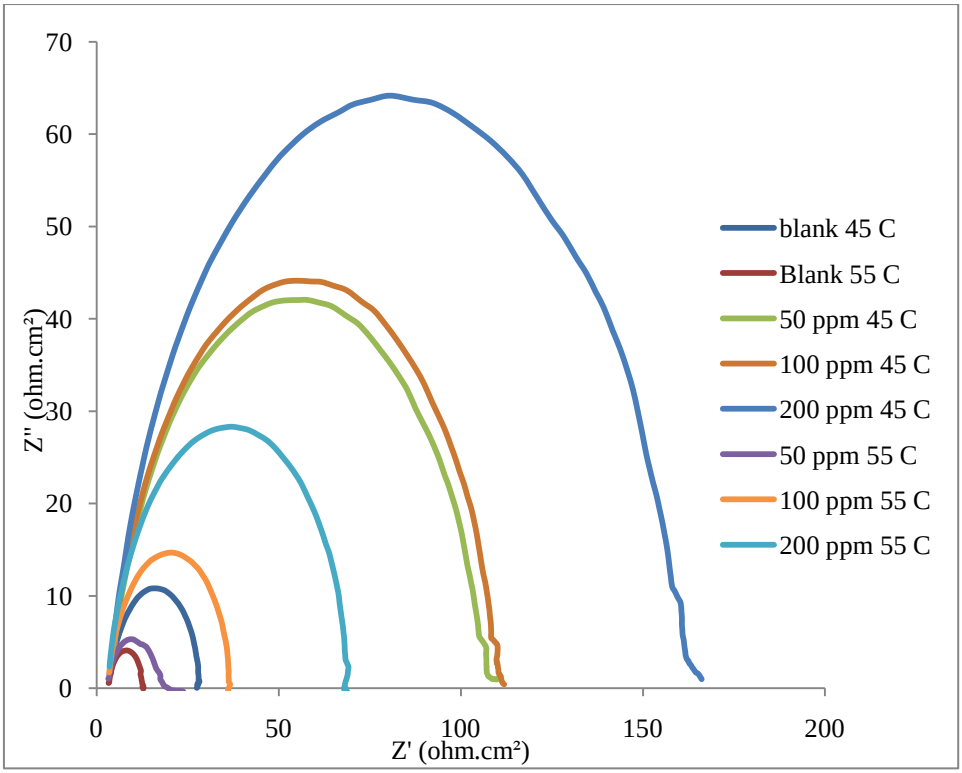

Figure 107: Nyquist plots for mild steel in a 1M HCl solution in the absence and presence of Rosemary plant extract at 25°C, 45°C & 55°C.

Table 54: Impedance parameters and corresponding inhibition efficiency for mild steel in 1M HCl in the absence and presence of Rosemary plant extract at 25°C for specific concentrations.

Con(ppm)	Rsol ($ohm.cm^2$)	Rct ($ohm.cm^2$)	Cd (F)	I corr. (mA/cm^2)	IE%
0	1.542	57.07	0.000431	0.2001	
50	4.357	700.00	0.000154	0.0185	91.85
100	4.506	753.90	0.000152	0.0175	92.43
200	4.517	846.90	0.000150	0.0158	93.26

Table 55: Impedance parameters and corresponding inhibition efficiency for mild steel in 1M HCl in the absence and presence of Rosemary plant extract at 45^{o}C for specific concentrations.

Con(ppm)	Rsol (ohm.cm^2)	Rct (ohm.cm^2)	Cd (F)	I corr. (mA/cm^2)	IE%
0	1.424	24.90	0.000249	0.3230	
50	3.556	78.52	0.000093	0.1788	68.29
100	4.045	84.38	0.000092	0.1748	70.49
200	4.121	95.48	0.000083	0.1601	73.92

Table 56: Impedance parameters and corresponding inhibition efficiency for mild steel in 1M HCl in the absence and presence of Rosemary plant extract at 55^{o}C for specific concentrations.

Con(ppm)	Rsol (ohm.cm^2)	Rct (ohm.cm^2)	Cd (F)	I corr. (mA/cm^2)	IE%
0	1.246	9.43	0.001120	1.2280	
50	3.05	26.67	0.000021	0.5122	64.65
100	3.381	27.87	0.000135	0.5106	66.18
200	3.412	29.23	0.000124	0.5017	67.75

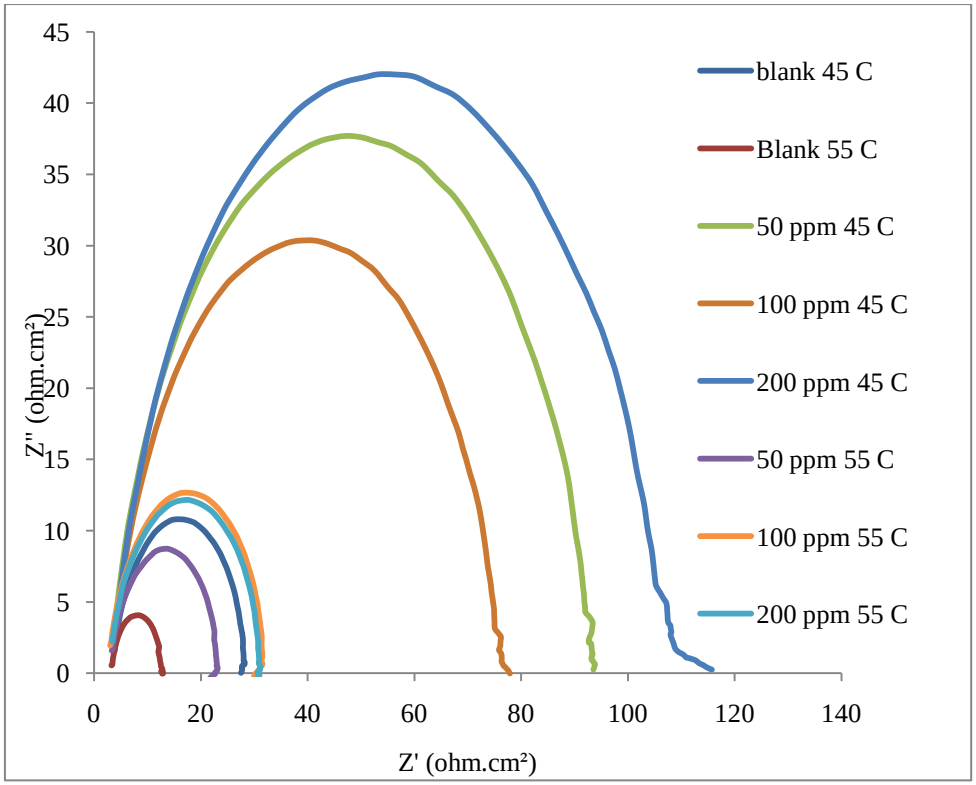

Figure 108: Nyquist plots for mild steel in a 1M HCl solution in the absence and presence of Cypress plant extract at 45°C & 55°C.

Table 57: Impedance parameters and corresponding inhibition efficiency for mild steel in 1M HCl in the absence and presence of Cypress plant extract at 25°C for specific concentrations.

Con(ppm)	Rsol (ohm.cm^2)	Rct (ohm.cm^2)	Cd (F)	I corr. (mA/cm^2)	IE%
0	1.542	57.07	0.000431	0.2001	
50	4.363	554.00	0.000174	0.0280	89.70
100	4.531	758.90	0.000133	0.0266	92.48
200	5.089	908.70	0.000095	0.0174	93.72

Table 58: Impedance parameters and corresponding inhibition efficiency for mild steel in 1M HCl in the absence and presence of Cypress plant extract at 45^{o}C for specific concentrations.

Con(ppm)	Rsol (ohm.cm^2)	Rct (ohm.cm^2)	Cd (F)	I corr. (mA/cm^2)	IE%
0	1.424	24.90	0.000249	0.3230	
50	3.410	74.75	0.000082	0.1796	66.69
100	3.511	78.25	0.000096	0.1780	68.18
200	3.531	85.86	0.000102	0.1767	71.00

Table 59: Impedance parameters and corresponding inhibition efficiency for mild steel in 1M HCl in the absence and presence of Cypress plant extract at 55^{o}C for specific concentrations.

Con(ppm)	Rsol (ohm.cm^2)	Rct (ohm.cm^2)	Cd (F)	I corr. (mA/cm^2)	IE%
0	1.246	9.43	0.001120	1.2280	
50	3.030	25.14	0.000217	0.5655	62.50
100	3.100	26.12	0.000168	0.5588	63.91
200	3.130	26.92	0.000166	0.5585	64.98

4.3.6 Cyclic Sweep Test at Elevated Temperatures

The conditions used for the cyclic sweep tests are the same mentioned in the previous chapter. It can be seen from Figures 110-127 that as the inhibitor is added the corrosion current decreases causing a shift in the curves along the x axis. This indicates a decrease in the corrosion rate and an increase in the inhibition efficiency. The graphs are plotted at each elevated temperature separately and then the three temperatures studied at concentrations of 0-200 ppm. It can also be noticed that there is a shift along the potential after the blank sample at the three recorded temperatures. This shift is due to formation of a layer on the mild steel specimen. The shift is much bigger at a temperature of 25^{o}C than at the elevated temperatures. It can be seen that the cathodic part of the curve does not change in some cases. However, the anodic

part changes slightly after 100 ppm of the inhibitor is added in the case of 25^{o}C. In the other cases, the same conclusion may be drawn; however, the pattern is less clear. The cathodic part of the curves gave rise to parallel lines indicating that the addition of the inhibitor to the 1M HCl solution did not modify the hydrogen evolution mechanism. The inhibitor molecules were adsorbed on the mild steel surface, blocking part of the reaction sites of the mild steel and reducing the corrosion rate [20].

The decrease in the anodic corrosion current density as the inhibitor added proves the formation of protective films containing oxide and inhibitor [20]. All these points prove that the corrosion rate decreases as the inhibitor is added to the solution. However, the decrease in the corrosion current density is more at the lowest temperature. It can be noticed that as the temperature increases the corrosion current density increases. This leads to an increase in the corrosion rate of the metal surface.

The change in the shape of the anodic part of the cyclic sweeps also suggests that some form of a protective (inhibitor) layer is laid on the surface of the metal. The "S" shape is more apparent when higher contractions are used, which is an agreement with all the other test data generated by weight loss, LPR, and impedance spectroscopy. Anodic parts of the sweeps corresponding to lower concentrations as low as 50 ppm were similar to that of the blank

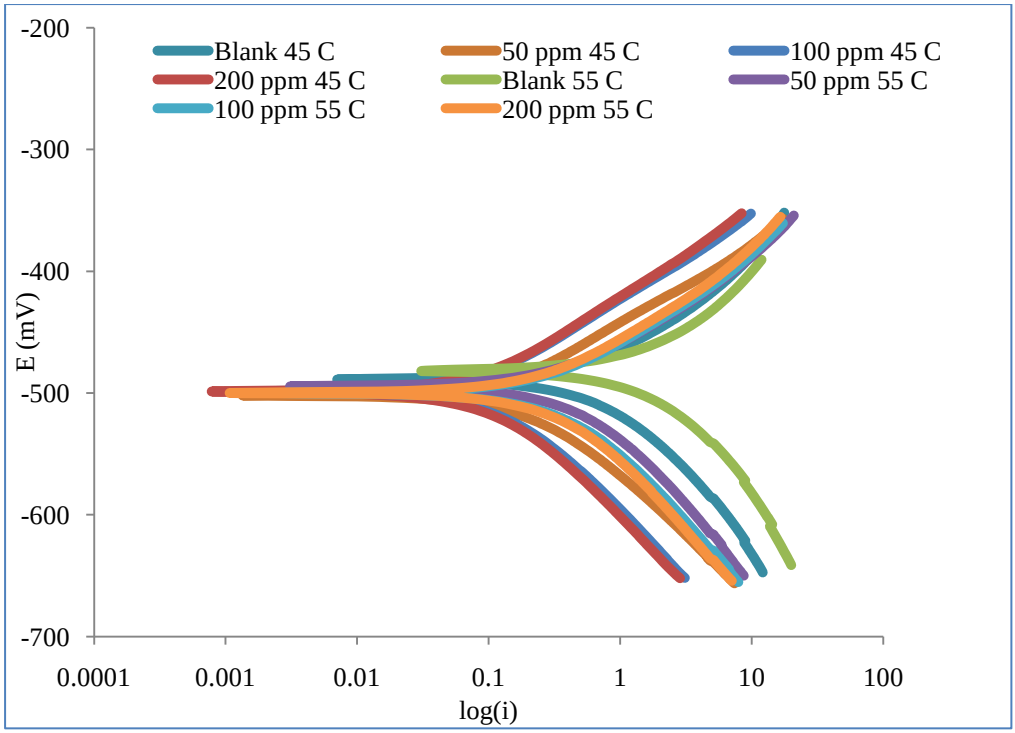

Figure 109: Potential plots of mild steel in a 1M HCl solution in the absence and presence of Fig & Olive (7:1) plant extract at 45^{o}C & 55^{o}C.

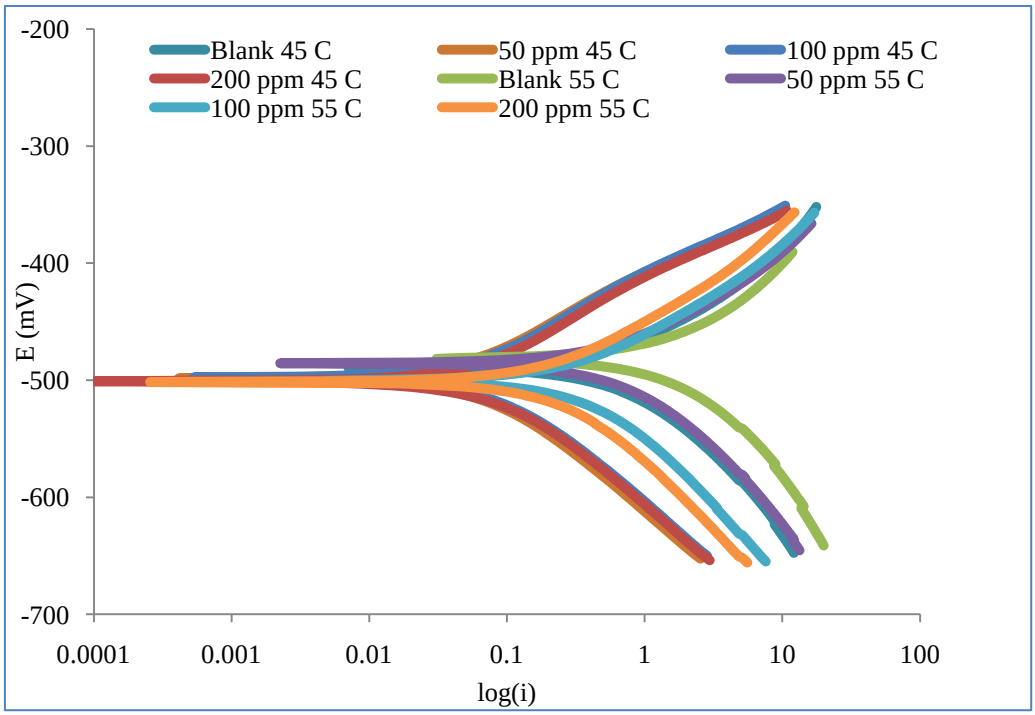

Figure 110: Potential plots of mild steel in a 1M HCl solution in the absence and presence of Fig & Olive (1:7) plant extract at 45^{o}C & 55^{o}C.

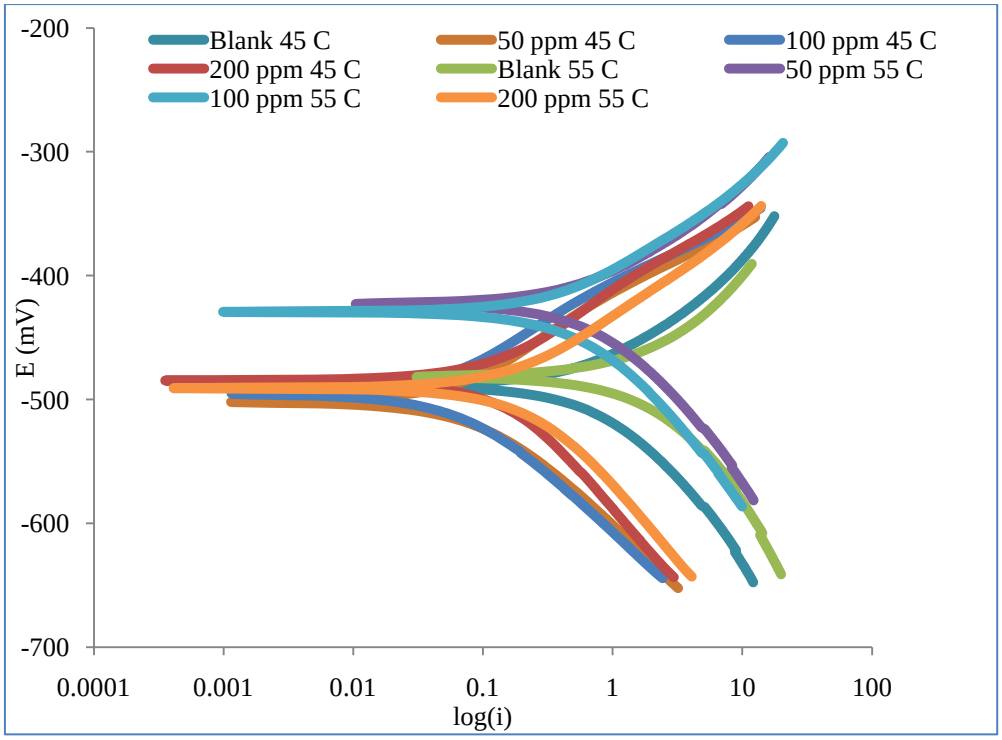

Figure 111: Potential plots of mild steel in a 1M HCl solution in the absence and presence of Fig & Olive (1:1) plant extract at 45^{o}C & 55^{o}C.

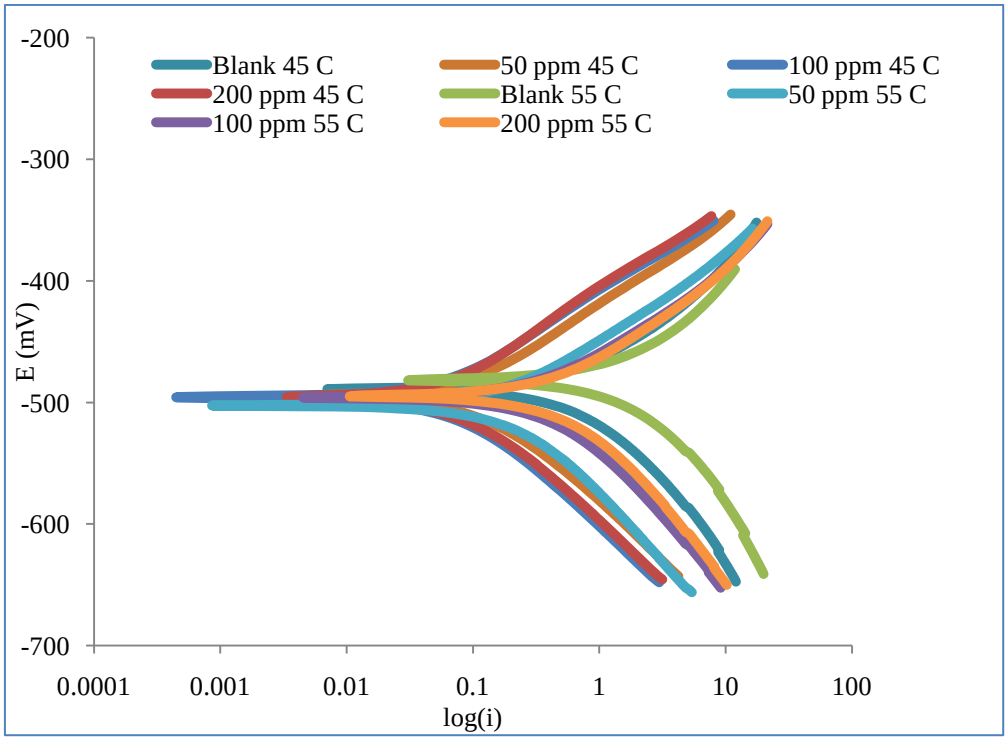

Figure 112: Potential plots of mild steel in a 1M HCl solution in the absence and presence of Fig plant extract at 45^{o}C & 55^{o}C.

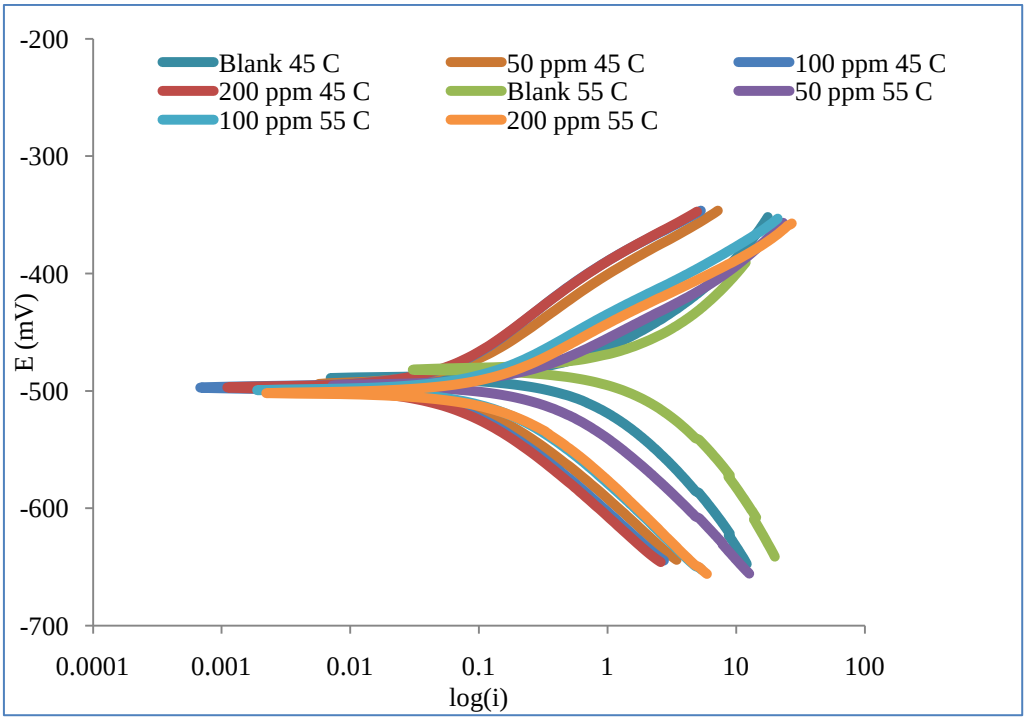

Figure 113: Potential plots of mild steel in a 1M HCl solution in the absence and presence of Olive plant extract 45^{o}C & 55^{o}C.

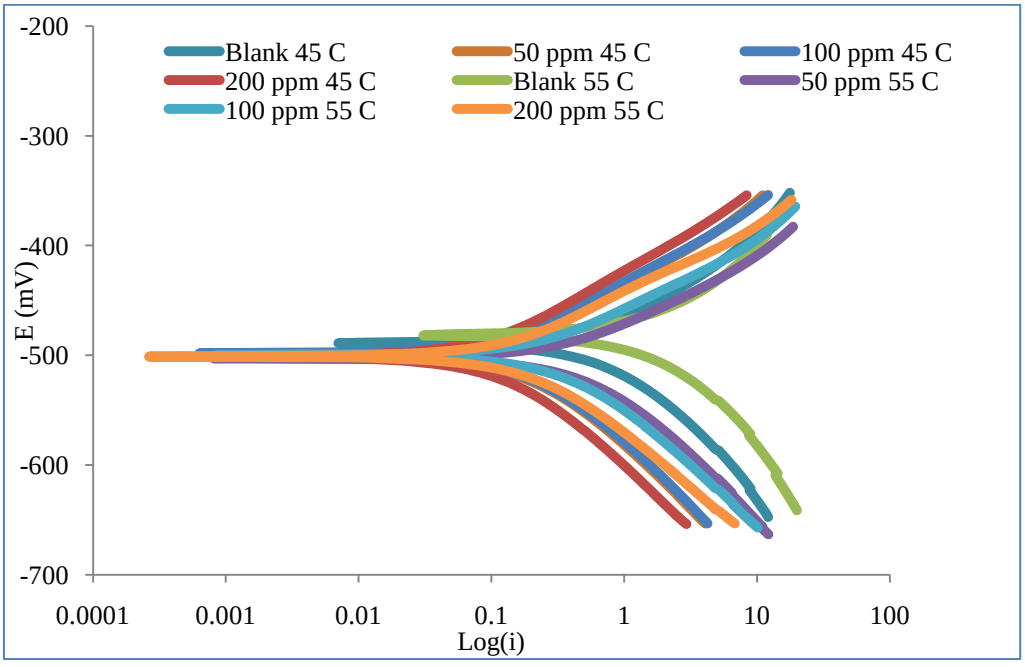

Figure 114: Potential plots of mild steel in a 1M HCl solution in the absence and presence of Rosemary plant extract at 45^{o}C & 55^{o}C.

4.4 Results and Analysis of Adsorption Isotherms by EIS Test

The adsorption isotherm of each of the plants extracts was determined using the EIS testing method. Plotting the concentration of the inhibitor per surface coverage versus the concentration of the inhibitor shows a linear relationship. This proves that the experimental data obtained by the EIS test follows Langmuir Isotherm of adsorption.

The inhibitive action of green extracts towards the acidic corrosion of mild steel could be related to the adsorption of its components onto the mild steel surface. As explained previously, this indicates that the adsorbed layer acts like a barrier between the specimen surface and the corrosive solution, causing the reduction in the corrosion rate. This leads to the fact that the inhibition efficiency is directly proportional to the surface coverage Ɵ.

As seen in the previous sections:-

It is assumed that there is no interaction between the adsorbed species on the surface of the metal and the surface is smooth and saturated. The relationship is explained as viewed by Equations 3.5 & 3.6 [16,21].

The mode of variation of the surface coverage describes the adsorption isotherm that is available in the system. When the extract concentration of the green inhibitor is plotted against (c/Ɵ), a straight line is obtained with an average slope of almost unity as shown in the figures of this section. This behavior suggests that all green inhibitors follow the Langmuir adsorption isotherm. The Langmuir isotherm follows Equations 3.5 and 3.6 of the previous chapter. The intercept of the plotted graphs represents the reciprocal of the adsorption constant k.

The calculated values of the standard free energy of adsorption have negative values. This indicates the spontaneity and stability of the process. It is well known that values of the standard free energy of adsorption on order of – 40 kJ/mol indicates that physical adsorption is occurring [16,21]. The measured values of ΔG^{o}_{ads} suggests a strong physical adsorption of green inhibitors leaves extract onto the surface of mild steel in 1M HCl solution.

Further information on the influence mechanism of the corrosion of mild steel in the 1M HCl environment was found by calculating the activation energies of all plant extracts for the corrosion process using Arrhenius equation [35],

$$\mathrm{Icorr} = \mathrm{K}\exp\left(\frac{-\mathrm{Ea}}{\mathrm{RT}}\right) \tag{4.4}$$

Where Ea is the activation energy, k is the Arrhenius constant, R is the universal gas constant, and T is the absolute temperature. The values of Ea and k could be obtained from the slopes and intercept of the Arrhenius plots below, respectively.

Furthermore, the enthalpy and entropy of adsorption can be calculated from the following equations [35],

$$\Delta\mathrm{H} = \mathrm{Ea} - \mathrm{RT} \tag{4.5}$$

$$\Delta S = \frac{\Delta\mathrm{H}-\Delta\mathrm{G}}{\mathrm{T}} \tag{4.6}$$

The data clearly clarifies that the values of Ea increased with increasing the concentration of plant extracts, while the values of k decreased. This is a well known property of Arrhenius equation that the higher Ea and the lower k lead to a reduction in the corrosion current density and the corrosion rate. The relative increase of the inhibition efficiency causes the increase in the activation energy Ea and suggests that the rate of formation of the adsorbed layer is higher than the rate of dissolution of mild steel surface [35]. The negative values of the enthalpy of adsorption suggest that the process of adsorption of all plant extracts is exothermic. Furthermore, as the concentration increases, the enthalpy values decreases. Moreover, the increase in the concentration causes the values of entropy of adsorption to decrease, rendering the system more ordered. On the other hand, the increase in temperature causes the system to be more disordered and exothermic. As a result, the inhibitors used can be considered effective.

Table 60: Langmuir investigation of Fig & Olive (1:7) leaves extract at elevated temperatures.

ppm	ϴ	C/ϴ	ppm	ϴ	C/ϴ	ppm	ϴ	C/ϴ
25 °C	-	-	45 °C	-	-	55 °C	-	-
50	0.897	55.7	50	0.790	63.3	50	0.717	69.8
100	0.912	109.6	100	0.815	122.7	100	0.722	138.6
200	0.924	216.5	200	0.841	237.9	200	0.752	265.8

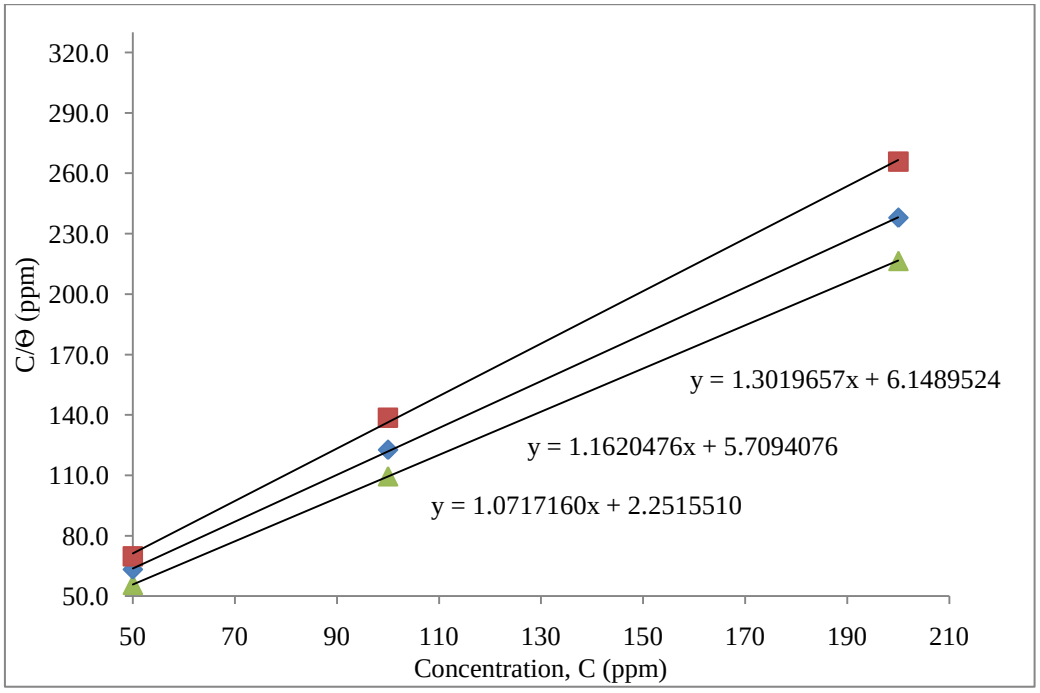

Figure 115: Concentration of the inhibitor per surface coverage versus the concentration of the inhibitor of (1:7) Fig & Olive leaves extract at elevated temperatures.

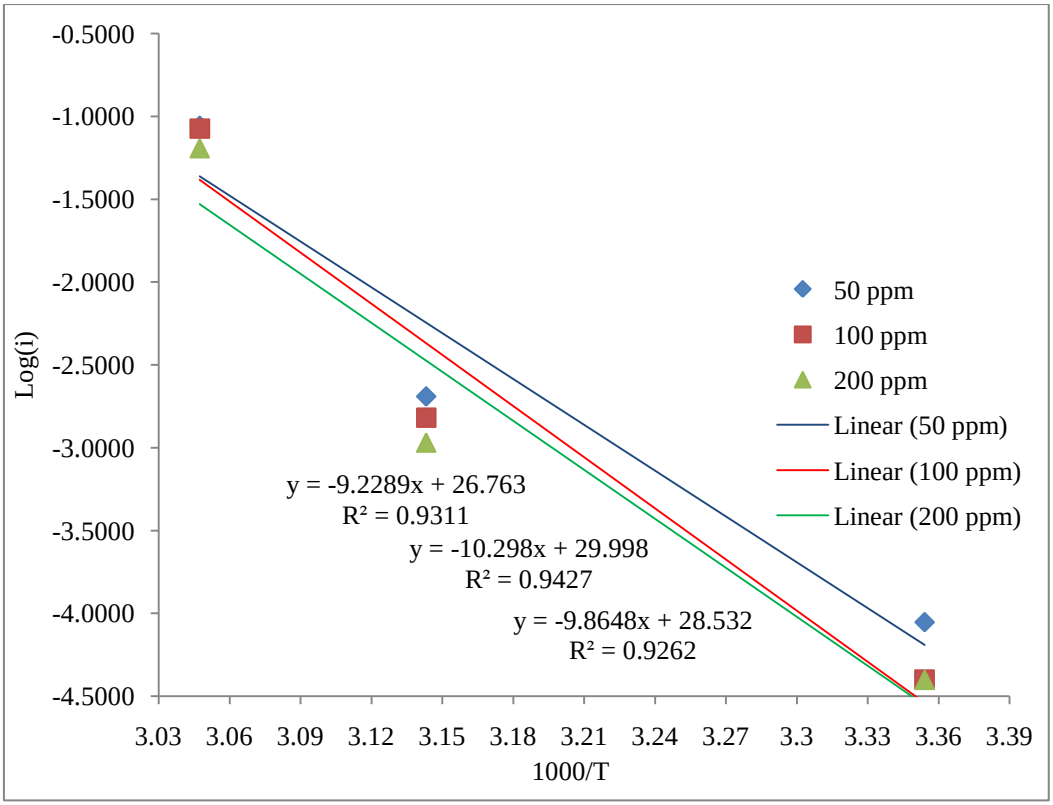

Figure 116: Arrhenius plots of (1:7) Fig & Olive leaves extract at different concentrations.

Table 61: Arrhenius investigation of Fig & Olive (1:7) leaves extract at elevated temperatures.

Ea(KJ/mol)	C(ppm)	Ea(J/mol)
0.07673	50ppm	76.729
0.08202	100ppm	82.016
0.08562	200ppm	85.618

Table 62: Thermodynamic properties investigation of Fig & Olive (1:7) leaves extract at elevated temperatures.

50 ppm				
T (K)	k	ΔG^oads (KJ/mol)	ΔH^oads(KJ/mol)	ΔS^oads(J/mol k)
298.15	0.9325	-34.08	-2.40	106.23
318.15	0.5469	-33.88	-2.57	98.40
328.15	0.4562	-33.59	-2.65	94.29

100 ppm				
T (K)	k	ΔG^oads(KJ/mol)	ΔH^oads(KJ/mol)	ΔS^oads(J/mol k)
298.15	0.9325	-34.08	-2.40	106.25
318.15	0.5469	-33.88	-2.56	98.42
328.15	0.4562	-33.59	-2.65	94.31

200 ppm				
T (K)	k	ΔG^oads(KJ/mol)	ΔH^oads(KJ/mol)	ΔS^oads(J/mol k)
298.15	0.9325	-34.08	-2.39	106.27
318.15	0.5469	-33.88	-2.56	98.43
328.15	0.4562	-33.59	-2.64	94.32

Table 63: Langmuir investigation of Fig & Olive (7:1) leaves extract at elevated temperatures.

ppm	ϴ	C/ ϴ	ppm	ϴ	C/ ϴ	ppm	ϴ	C/ ϴ
25 ^{o}C	-	-	45^{o}C	-	-	55 ^{o}C	-	-
50	0.902	55.4	50	0.829	60.3	50	0.744	67.2
100	0.906	110.4	100	0.857	116.7	100	0.764	130.9
200	0.924	216.4	200	0.878	227.8	200	0.794	251.9

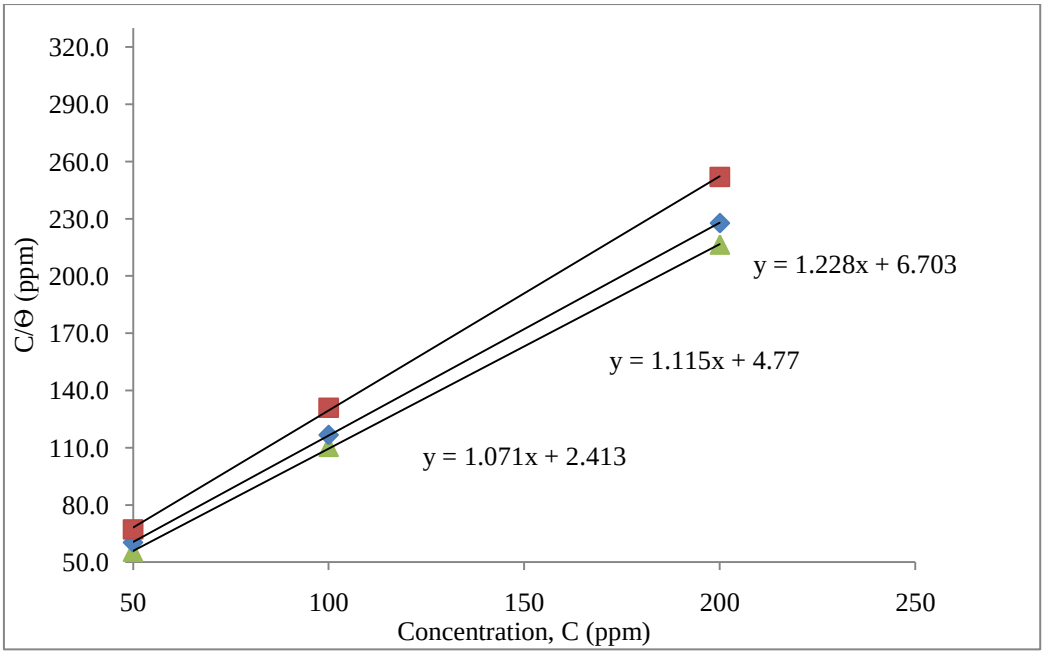

Figure 117: Concentration of the inhibitor per surface coverage versus the concentration of the inhibitor of (7:1) Fig & Olive leaves extract at elevated temperatures.

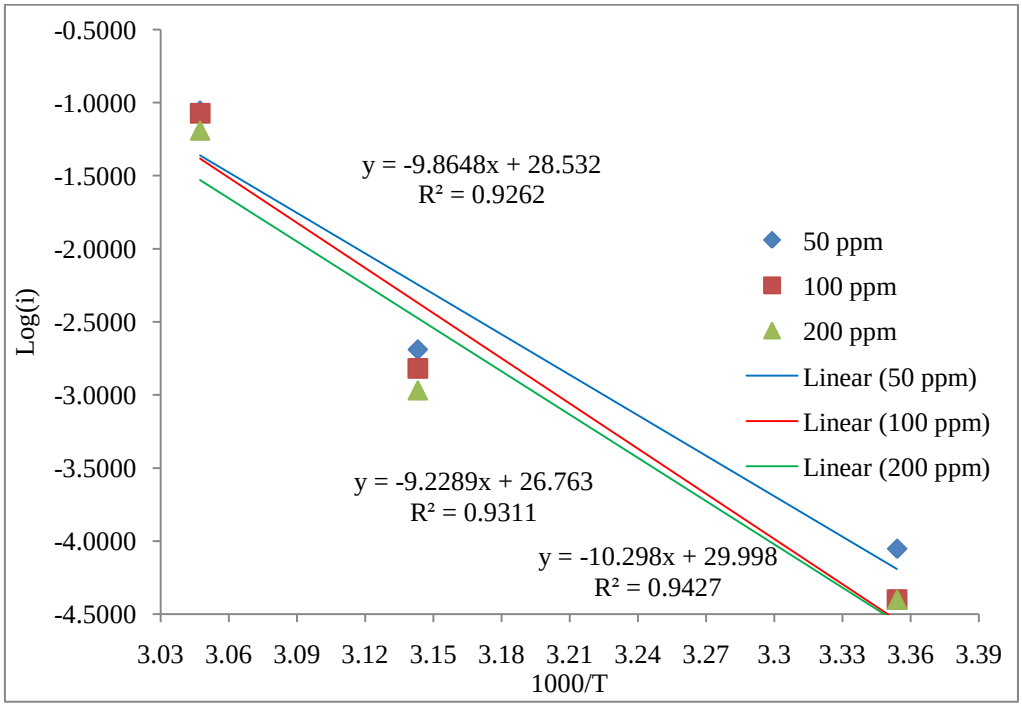

Figure 118: Arrhenius plots of (7:1) Fig & Olive leaves extract at different concentrations.

Table 64: Arrhenius investigation of Fig & Olive (7:1) leaves extract at elevated temperatures.

Ea(KJ/mol)	C(ppm)	Ea(J/mol)
0.07766	50ppm	77.657
0.08277	100ppm	82.769
0.08455	200ppm	84.545

Table 65: Thermodynamic properties investigation of Fig & Olive (7:1) leaves extract at elevated temperatures.

50 ppm				
T (K)	k	ΔG^oads (KJ/mol)	ΔH^oads(KJ/mol)	ΔS^oads(J/mol k)
298.15	0.9325	-34.08	-2.40	106.24
318.15	0.5469	-33.98	-2.57	98.72
328.15	0.4562	-33.74	-2.65	94.74

100 ppm				
T (K)	k	ΔG^oads(KJ/mol)	ΔH^oads(KJ/mol)	ΔS^oads(J/mol k)
298.15	0.9325	-34.08	-2.39	106.26
318.15	0.5469	-33.98	-2.56	98.74
328.15	0.4562	-33.74	-2.65	94.75

200 ppm				
T (K)	k	ΔG^oads(KJ/mol)	ΔH^oads(KJ/mol)	ΔS^oads(J/mol k)
298.15	0.9325	-34.08	-2.39	106.26
318.15	0.5469	-33.98	-2.56	98.75
328.15	0.4562	-33.74	-2.64	94.76

Table 66: Langmuir investigation of Fig & Olive (1:1) leaves extract at elevated temperatures.

ppm	ϴ	C/ϴ	ppm	ϴ	C/ϴ	ppm	ϴ	C/ϴ
25 ^{o}C	-	-	45 ^{o}C	-	-	55 ^{o}C	-	-
50	0.901	55.5	50	0.840	59.5	50	0.752	66.5
100	0.918	108.9	100	0.869	115.1	100	0.770	129.9
200	0.930	215.0	200	0.876	228.3	200	0.750	266.7

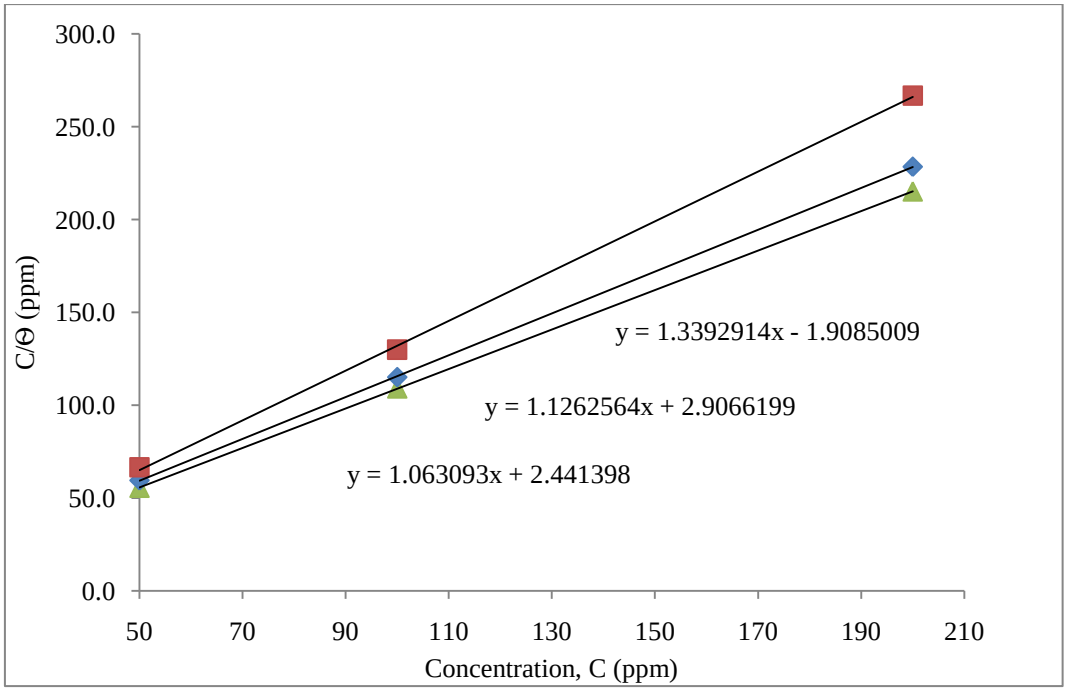

Figure 119: Concentration of the inhibitor per surface coverage versus the concentration of the inhibitor of (1:1) Fig & Olive leaves extract at elevated temperatures.

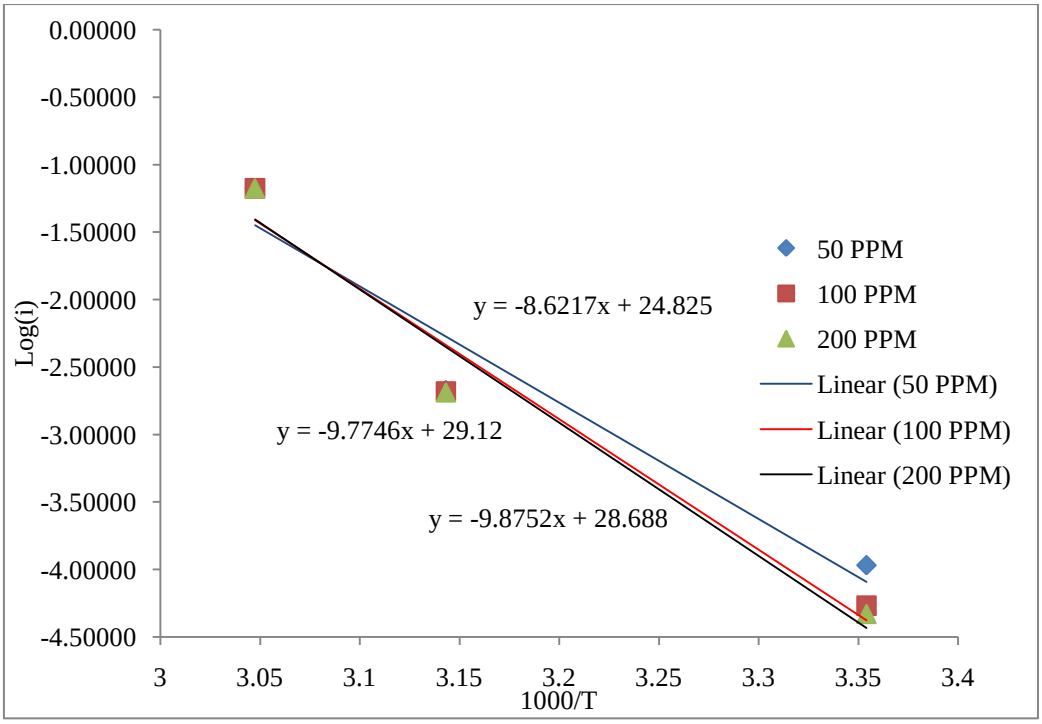

Figure 120: Arrhenius plots of (1:1) Fig & Olive leaves extract at different concentrations.

Table 67: Arrhenius investigation of Fig & Olive (1:1) leaves extract at elevated temperatures.

Ea(KJ/mol)	C(ppm)	Ea(J/mol)
0.08012	50ppm	80.123
0.08127	100ppm	81.266
0.08210	200ppm	82.102

Table 68: Thermodynamic properties investigation of Fig & Olive (1:1) leaves extract at elevated temperatures.

50 ppm				
T (K)	k	ΔG^oads (KJ/mol)	ΔH^oads(KJ/mol)	ΔS^oads(J/mol k)
298.15	0.9407	-34.10	-2.3987	106.3137
318.15	0.8879	-33.95	-2.5650	98.6581
328.15	0.7467	-33.52	-2.6481	94.0895

100 ppm				
T (K)	k	ΔG^oads(KJ/mol)	ΔH^oads(KJ/mol)	ΔS^oads(J/mol k)
298.15	0.9407	-34.10	-2.3976	106.3176
318.15	0.8879	-33.95	-2.5638	98.6617
328.15	0.7467	-33.52	-2.6470	94.0930

200 ppm				
T (K)	k	ΔG^oads(KJ/mol)	ΔH^oads(KJ/mol)	ΔS^oads(J/mol k)
298.15	0.9407	-34.0961	-2.3967	106.3204
318.15	0.8879	-33.9531	-2.5630	98.6643
328.15	0.7467	-33.5236	-2.6461	94.0956

Table 69: Langmuir investigation of Olive leaves extract at elevated temperatures.

ppm	ϴ	C/ϴ	ppm	ϴ	C/ϴ	ppm	ϴ	C/ϴ
25 ^oC	-	-	45 ^oC	-	-	55 ^oC	-	-
50	0.890	56.2	50	0.582	85.9	50	0.595	84.0
100	0.913	109.5	100	0.600	166.7	100	0.602	166.1
200	0.913	219.1	200	0.633	316.2	200	0.635	315.2

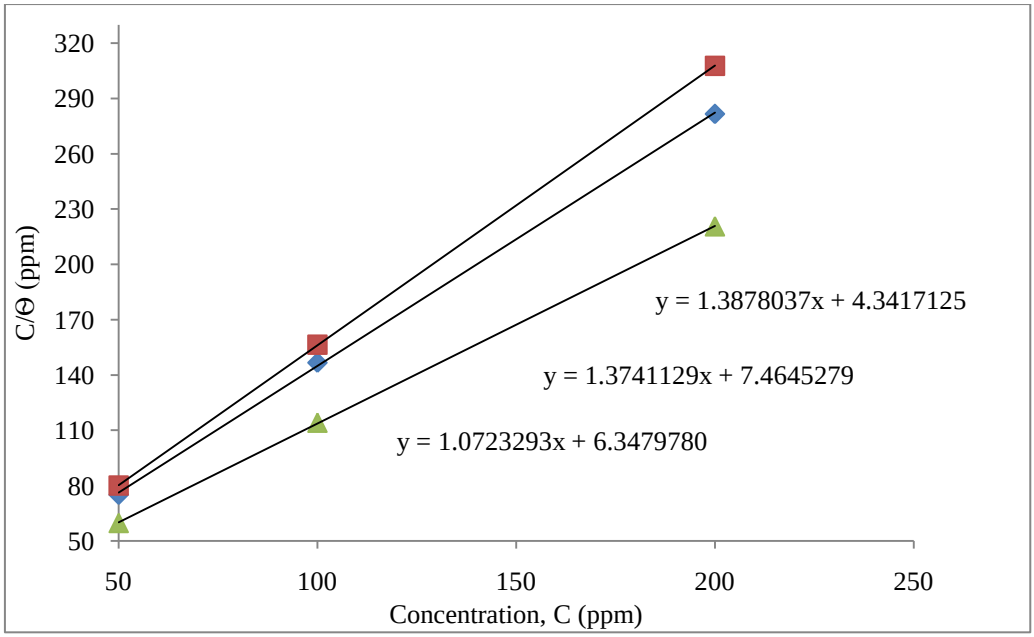

Figure 121: Concentration of the inhibitor per surface coverage versus the concentration of the inhibitor of Olive leaves extract at elevated temperatures.

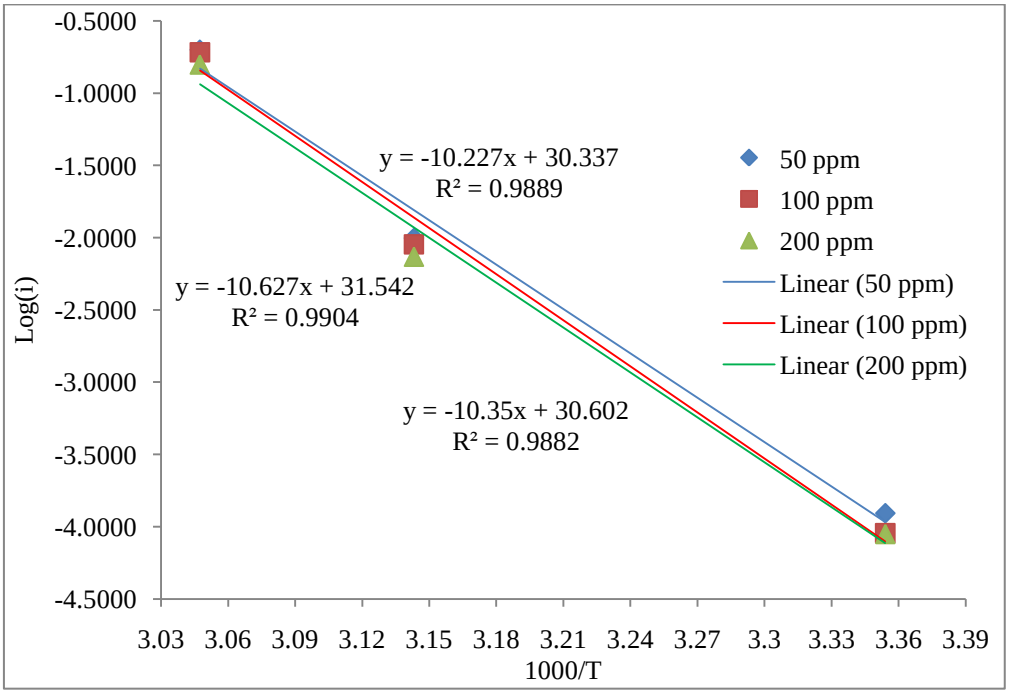

Figure 122: Arrhenius plots of Olive leaves extract at different concentrations.

Table 70: Arrhenius investigation of Olive leaves extract at elevated temperatures.

Ea(KJ/mol)	C(ppm)	Ea(J/mol)
0.08503	50ppm	85.027
0.08605	100ppm	86.050
0.08835	200ppm	88.353

Table 71: Thermodynamic properties investigation of Olive) leaves extract at elevated temperatures.

50 ppm				
T (K)	k	ΔG^oads (KJ/mol)	ΔH^oads(KJ/mol)	ΔS^oads(J/mol k)
298.15	0.9325	-34.0747	-2.3938	106.258
318.15	0.5469	-33.4600	-2.5601	97.124
328.15	0.4562	-33.2134	-2.6432	93.159

100 ppm				
T (K)	k	ΔG^oads(KJ/mol)	ΔH^oads(KJ/mol)	ΔS^oads(J/mol k)
298.15	0.9325	-34.0747	-2.3928	106.262
318.15	0.5469	-33.4600	-2.5590	97.127
328.15	0.4562	-33.2134	-2.6422	93.162

200 ppm				
T (K)	k	ΔG^oads(KJ/mol)	ΔH^oads(KJ/mol)	ΔS^oads(J/mol k)
298.15	0.9325	-34.0747	-2.3905	106.269
318.15	0.5469	-32.7517	-2.5567	94.908
328.15	0.4562	-32.3021	-2.6399	90.392

Table 72: Langmuir investigation of Rosemary leaves extract at elevated temperatures.

ppm	ϴ	C/ϴ	ppm	ϴ	C/ϴ	ppm	ϴ	C/ϴ
25 ^{o}C	-	-	45 ^{o}C	-	-	55 ^{o}C	-	-
50	0.865	57.8	50	0.683	73.2	50	0.647	77.3
100	0.889	112.5	100	0.705	141.9	100	0.662	151.1
200	0.916	218.3	200	0.739	270.6	200	0.677	295.2

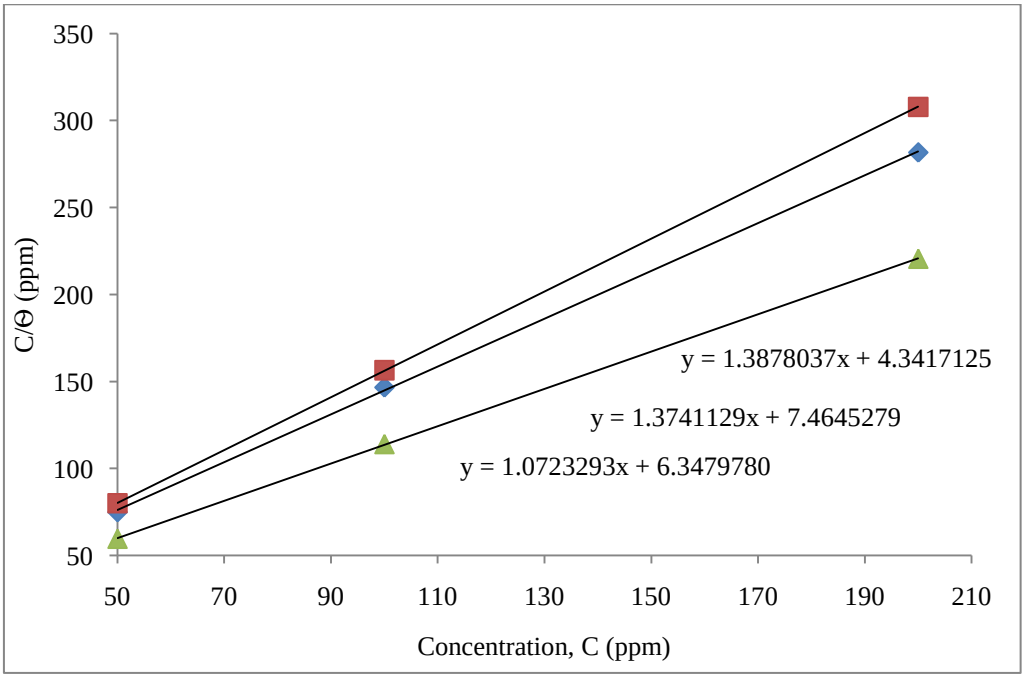

Figure 123: Concentration of the inhibitor per surface coverage versus the concentration of the inhibitor of Rosemary leaves extract at elevated temperatures.

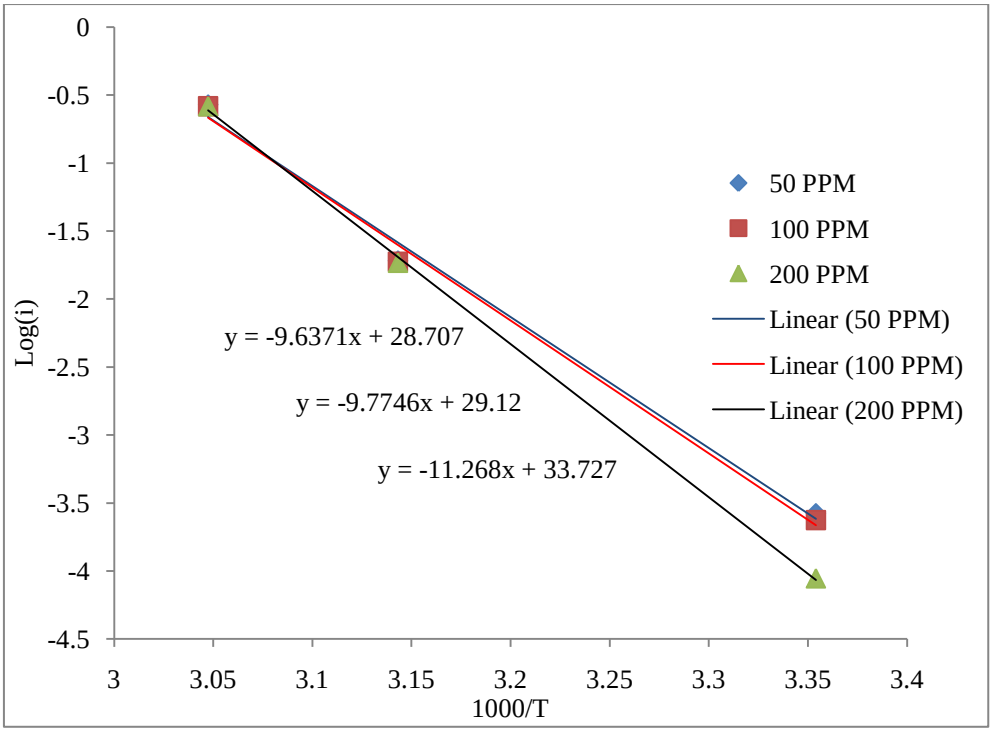

Figure 124: Arrhenius plots of Rosemary leaves extract at different concentrations.

Table 73: Arrhenius investigation of Rosemary leaves extract at elevated temperatures.

Ea(KJ/mol)	C(ppm)	Ea(J/mol)
0.08012	50ppm	80.122
0.08126	100ppm	81.261
0.09368	200ppm	93.682

Table 74: Thermodynamic properties investigation of Rosemary (1:1) leaves extract at elevated temperatures.

50 ppm				
T (K)	k	ΔG^oads (KJ/mol)	ΔH^oads(KJ/mol)	ΔS^oads(J/mol k)
298.15	0.9325	-34.074	-2.3987	106.241
318.15	0.5469	-32.751	-2.5650	94.882
328.15	0.4562	-32.302	-2.6481	90.367

100 ppm				
T (K)	k	ΔG^oads(KJ/mol)	ΔH^oads(KJ/mol)	ΔS^oads(J/mol k)
298.15	0.9325	-34.075	-2.3976	106.246
318.15	0.5469	-32.751	-2.5638	94.886
328.15	0.4562	-32.302	-2.6470	90.371

200 ppm				
T (K)	k	ΔG^oads(KJ/mol)	ΔH^oads(KJ/mol)	ΔS^oads(J/mol k)
298.15	0.9325	-34.075	-2.3851	106.287
318.15	0.5469	-32.751	-2.5514	94.925
328.15	0.4562	-32.302	-2.6345	90.408

Table 75: Langmuir investigation of Cypress leaves extract at elevated temperatures.

ppm	ϴ	C/ϴ	ppm	ϴ	C/ϴ	ppm	ϴ	C/ϴ
25 ^{o}C	-	-	45 ^{o}C	-	-	55 ^{o}C	-	-
50	0.838	59.6	50	0.667	75.0	50	0.625	80.0
100	0.877	114.1	100	0.682	146.7	100	0.639	156.5
200	0.906	220.6	200	0.710	281.7	200	0.650	307.8

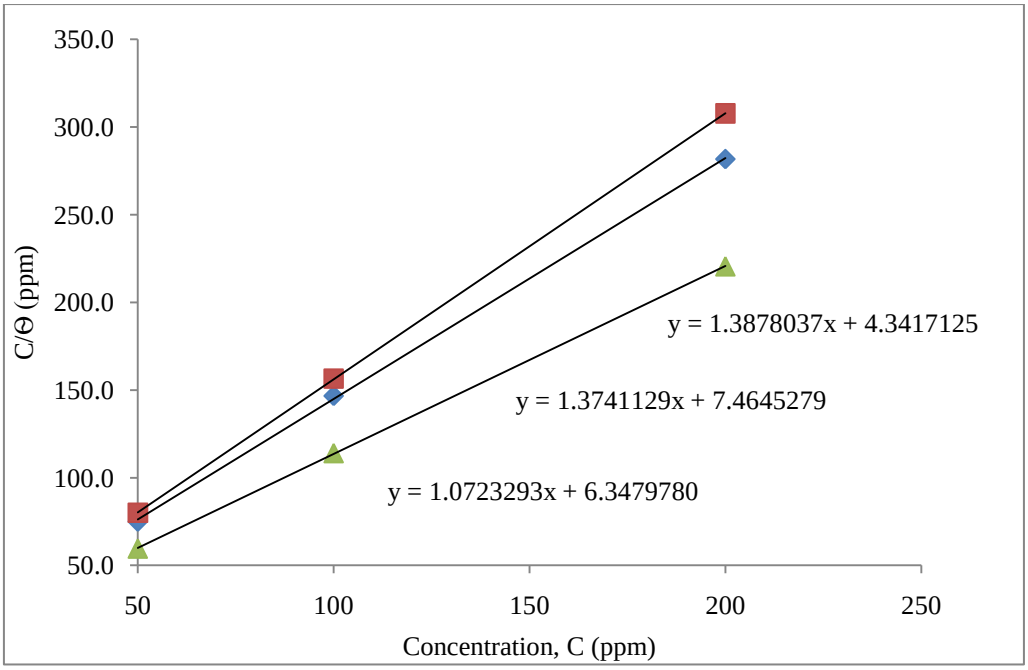

Figure 125: Concentration of the inhibitor per surface coverage versus the concentration of the inhibitor of Cypress leaves extract at elevated temperatures.

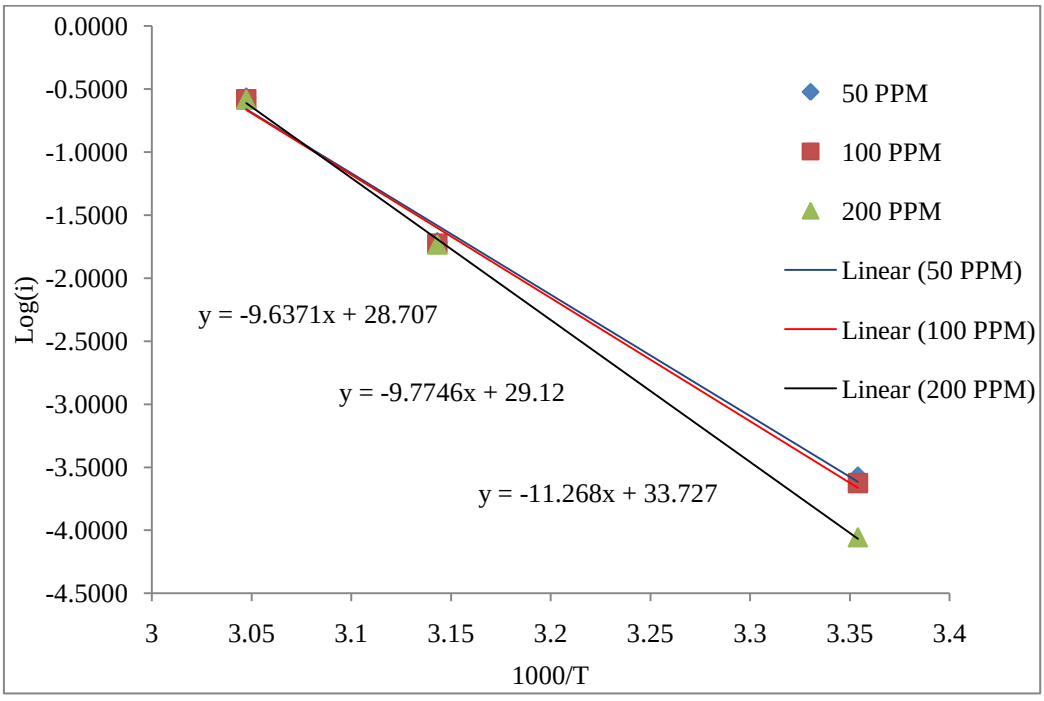

Figure 126: Arrhenius plots of Cypress leaves extract at different concentrations.

Table 76: Arrhenius investigation of Cypress leaves extract at elevated temperatures.

Ea(KJ/mol)	C(ppm)	Ea(J/mol)
0.08012	50ppm	80.122
0.08126	100ppm	81.261
0.09368	200ppm	93.682

Table 77: Thermodynamic properties investigation of Cypress leaves extract at elevated temperatures.

50 ppm				
T (K)	k	ΔG^oads (KJ/mol)	ΔH^oads(KJ/mol)	ΔS^oads(J/mol k)
298.15	0.9325	-34.075	-2.3987	106.2418
318.15	0.7277	-33.460	-2.5650	97.1083
328.15	0.6588	-33.213	-2.6481	93.1443

100 ppm				
T (K)	k	ΔG^oads(KJ/mol)	ΔH^oads(KJ/mol)	ΔS^oads(J/mol k)
298.15	0.9325	-34.075	-2.3976	106.2456
318.15	0.7277	-33.460	-2.5638	97.1118
328.15	0.6588	-33.213	-2.6470	93.1478

200 ppm				
T (K)	k	ΔG^oads(KJ/mol)	ΔH^oads(KJ/mol)	ΔS^oads(J/mol k)
298.15	0.9325	-34.075	-2.3851	106.2873
318.15	0.7277	-32.752	-2.5514	94.9247
328.15	0.6588	-32.302	-2.6346	90.4084

4.5 An Insight Comparison with Commercial Inhibitors

Inhibitors are used in different industries. Commercial inhibitors are known to have high inhibitive action in different media. A commercial inhibitor is usually composed of different components that act to reduce the corrosion rate. HA and EC inhibitors are studied to shed the light on the inhibitive action obtained in 1 M HCl solution. The same mixture ratio used for natural inhibitors is applied using electrochemical analysis, in order to draw a conclusion about the inhibitive action of leaf plant extracts in 1 M HCl environment. The study is conducted on Mild steel specimen of the same composition and dimensions used earlier at 25^{o}C.

4.5.1 Linear Polarization Resistance Measurements (LPR)

A linear polarization test is carried out by a scan from approximately -10mV to +10mV. The polarization resistance can be measured using Equation 3.2.
The resistance is calculated from long term linear polarization resistance curves. The value of the steady state LPR is obtained after running the test for 90 min using (400 & 1000) ppm of pure and mixtures of commercial inhibitors. Tables 14-15 record the parameters obtained by the LPR test. It is obvious that as the inhibitor is injected to the environment, the corrosion current density decreases causing a more pronounced increase in the inhibition efficiency. An increase in the inhibition efficiency indicates a decrease in the corrosion rate of the mild steel specimen. The values of corrosion potential are seen to be far away from the measured value of the blank run indicating the high inhibitive action of the commercial inhibitors.

The order of the best inhibitor efficiency at a concentration range of (400-1000) ppm is as follows:-

- At 25^{o}C : HA & EC (7:1), HA & EC (50:50), HA, HA & EC (1:7).and EC.

The LPR values obtained are much higher than the ones obtained for natural inhibitors. However, the inhibition efficiency of commercial inhibitors is comparable to the inhibition efficiency of natural inhibitors, indicating the high inhibitive action of the plant extracts studied.

Table 78: Different LPR parameters of mild steel immersed in 1 M HCl containing pure commercial inhibitors at 25^{o}C.

Conc. PPM	HA 25 ^{o} C				EC 25 ^{o} C			
	IE (%)	LPR (Ohm.cm^2)	I_{corr} (mA/cm^2)	E(mV)	IE (%)	LPR (Ohm.cm^2)	I_{corr} (mA/cm^2)	E(mV)
0	-	64	0.41523	-442	-	64	0.41523	-442
400	98.12	3348	0.00779	-881	96.44	1766	0.01477	-672
1000	98.77	5126	0.00509	850	97.83	2894	0.00901	-782

Table 79: Different LPR parameters of mild steel immersed in 1 M HCl containing mixtures of commercial inhibitors at 25^{o}C.

Inhibitor	Conc. PPM	Parameter			
		IE (%)	LPR (Ohm.cm^2)	I_{corr} (mA/cm^2)	E(mV)
HA & EC (50:50) 25 ^{o} C	0	-	64	0.41523	-442.80
	400	98.46	4079	0.00640	-802.48
	1000	98.52	3977	0.00616	-872.12
Inhibitor	Conc. PPM	IE (%)	LPR (Ohm.cm^2)	I_{corr} (mA/cm^2)	E(mV)
HA & EC (1:7) 25 ^{o} C	0	-	64	0.41523	-442.80
	400	98.33	3765	0.00693	-839.98
	1000	98.44	4039	0.00646	-817.95
Inhibitor	Conc. PPM	IE (%)	LPR (Ohm.cm^2)	I_{corr} (mA/cm^2)	E(mV)
HA & EC (7:1) 25 ^{o} C	0	-	64	0.41523	-442.80
	400	98.87	5579	0.00468	-864.34
	1000	98.91	5757	0.00453	-863.66

4.5.2 Electrochemical Impedance Spectroscopy Measurements (EIS)

In order to attain information about the kinetics of mild steel corrosion in presence of commercial inhibitors, electrochemical impedance spectroscopy (EIS) process took place at the open-circuit potential. EIS measurements of the mild steel electrode at its open-circuit potential after 20 min of immersion in 1 M HCl solution in

the absence and presence of chosen concentrations of inhibitors were performed over the frequency range from 10 Hz to 1000 Hz. The results of EIS experiments in the Nyquist representation at 25 ^{o}C are seen in Figures 127-128. The shape of the Nyquist plots is approximated by single capacitive semi-circles where the corrosion process was mainly due to charge transfer [23,24,26]. The shape of the semicircles is sustained at all concentrations, indicating that the corrosion mechanism is almost the same upon the addition of commercial inhibitors [20,26]. The radius of Nyquist plots increases on increasing the inhibitors concentration indicating an increase in the resistance to corrosion. As the inhibitor is added to the solution studied, the impedance increases and this indicates a reduction in the corrosion rate. The semicircles obtained in most cases are depressed [22,26,35]. This feature indicates formation of porous layers and adsorption of the inhibitors on the surface of the mild steel specimen [22,26,35]. The inhibition efficiency and the kinetic parameters are recorded in Table 80. Charge transfer resistance R_{ct} and solution resistance increase, where double layer capacitance C_{dl} decreases with the increase of inhibitor concentration. The decrease in C_{dl} suggests that the adsorption of the inhibitor is occurring on the mild steel surface in acidic environment. The increase in the charge transfer resistance leads to an increase of inhibition efficiency and reduction in the corrosion rate. The results indicate good agreement between the values of inhibition efficiency obtained by LPR test and EIS test with an error of $\pm$ 5%. These results suggest the inhibitive behavior of the Commercial inhibitors on corrosion of mild steel in 1 M HCl environment. The R_{ct} values are higher than the one's obtained for natural inhibitors. However, the inhibition efficiency obtained by commercial inhibitors is comparable with the one obtained by the studied plant extracts. This indicates the high inhibitive action of natural inhibitors in the studied environment.

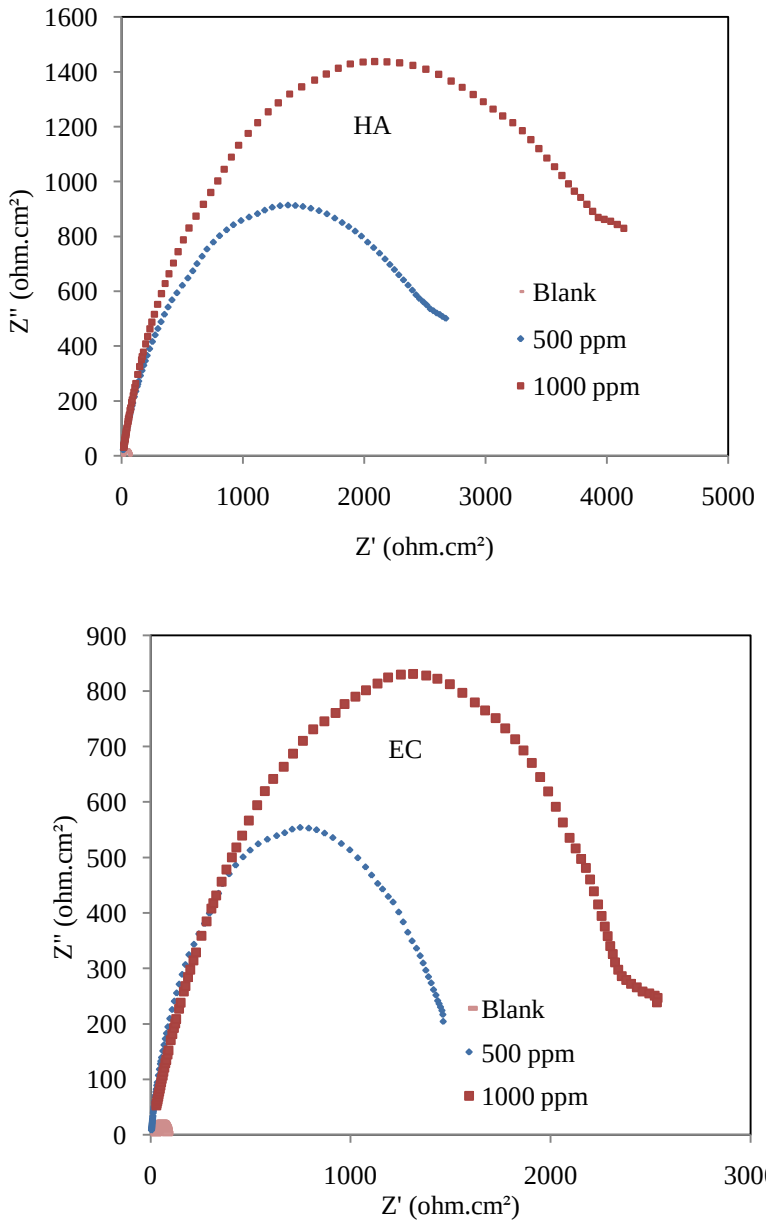

Figure 127: Nyquist plots for mild steel in 1 M HCl at 25^{o}C containing different concentration of pure commercial inhibitors.

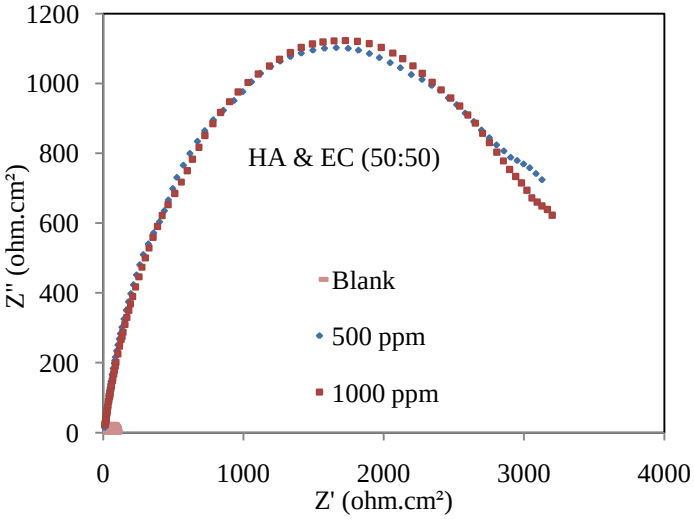

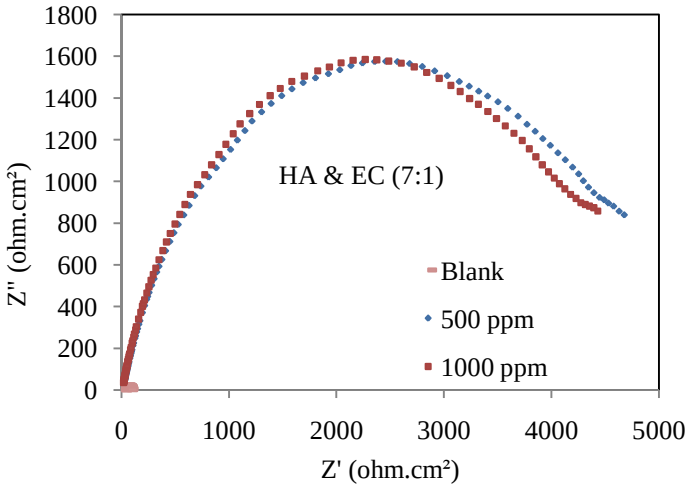

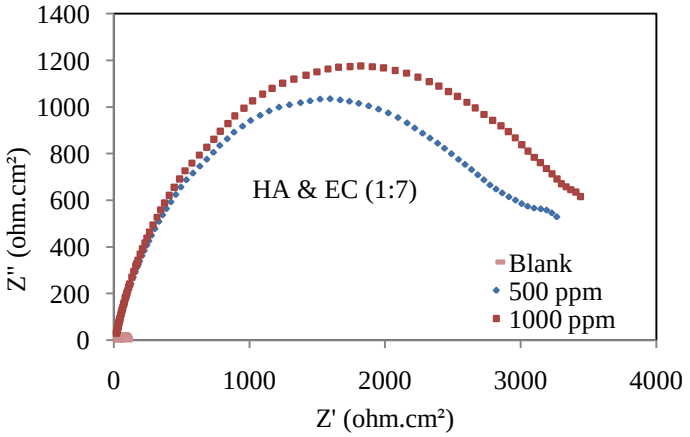

Figure 128: Nyquist plots for mild steel in 1 M HCl at 25^{o}C containing different concentration of mixtures of commercial inhibitors.

Table 80: Different EIS kinetic parameters derived from Nyquist plots of mild steel immersed in 1 M HCl containing pure and mixtures of commercial inhibitors at 25^{o}C.

Plant Extract	Con.(ppm)	Rsol (ohm.cm2)	Rct (ohm.cm2)	Cd (F)	IE%
HA	0	1.54	57.07	0.0004312	-
	400	5.30	3068.86	0.00009568	98.14
	1000	5.40	4755.72	0.00009423	98.80
EC	0	1.54	57.07	0.0004312	-
	400	3.90	1630.59	0.0000514	96.50
	1000	4.00	2481.36	0.0000502	97.70
HA & EC (50:50)	0	1.54	57.07	0.0004312	-
	400	5.51	3566.76	0.0001725	98.40
	1000	5.59	3900.00	0.000124	98.54
HA & EC (7:1)	0	1.54	57.07	0.0004312	-
	400	4.49	5050.34	0.00005283	98.87
	1000	4.68	5140.33	0.00004639	98.89
HA & EC (1:7)	0	1.54	57.07	0.0004312	-
	400	4.20	3170.12	0.0000639	98.20
	1000	4.28	3437.99	0.00006319	98.34

4.5.3 Cyclic Sweep Measurements

Tafel plots that are generated by the cyclic sweep electrochemical test are used in calculating the cathodic and anodic Tafel constants (β) for the studied commercial inhibitors in 1 M HCl solution. The cathodic Tafel plot is scanned on one mild steel sample from approximately 0 to -150 mV vs. OC while the anodic Tafel plot is completed on a second sample of the same composition from approximately 0 to +150 mV *vs.* OC [19,21,23]. The Tafel data are graphed as external potential versus the logarithm of the measured current [Figures 129-130]. The respective tafel constants derived from the above plots are given in Table (81). It is illustrated from the figures plotted and data of Tables (81) that both anodic metal dissolution of iron and cathodic hydrogen evolution reaction were inhibited after the addition of the inhibitors to 1 M HCl environment. In presence of the inhibitors, small change in cathodic Tafel slopes was noticed. The tafel constants changes in all cases suggesting that the presence of commercial inhibitors affect both cathodic and anodic reactions. Therefore, it could be concluded that molecules of extracts adsorb on both anodic and cathodic sites of

the mild steel surface [24,25,26]. This indicates that plant extracts studied act as mixed-type inhibitor. The decrease in corrosion current densities with increasing the inhibitors concentration reflected the formation of anodic protective films containing oxides and molecules of extracts. The films act as a barrier for charge and mass transfer as the case of natural inhibitors [21].

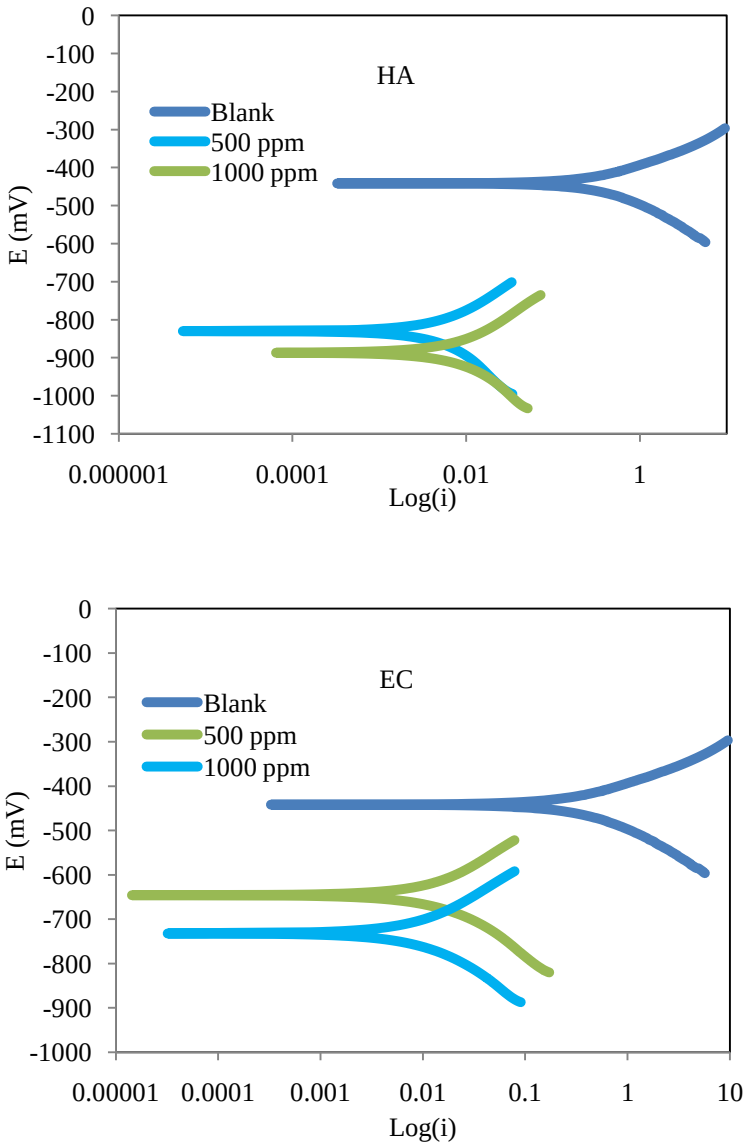

Figure 129: Tafel plots for mild steel in 1 M HCl at 25^{o}C containing different concentrations of pure inhibitors.

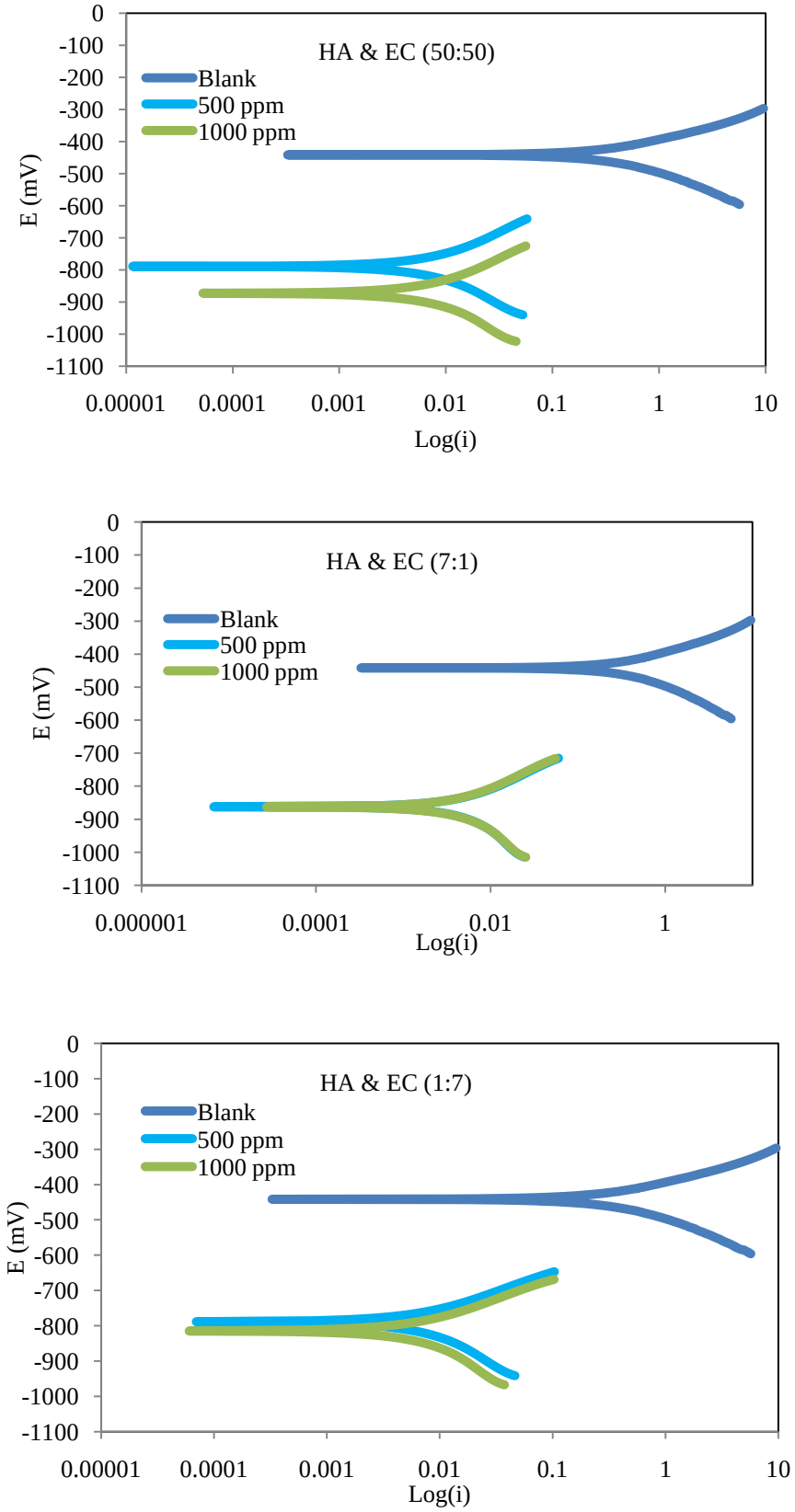

Figure 130: Tafel plots for mild steel in 1 M HCl at 25^{o}C containing different concentrations of mixtures of inhibitors.

Table 81: Tafel constants derived from tafel plots of mild steel immersed in 1 M HCl containing commercial inhibitors at 25^{o}C.

Plant Extract	Con.(ppm)	Ba (mV)	Bc(mV)
HA	0	-	-
	400	73	85
	1000	86	99
EC	0	-	-
	400	87	90
	1000	99	94
HA & EC (50:50)	0	-	-
	400	83	91
	1000	83	95
HA & EC (7:1)	0	-	-
	400	82	101
	1000	83	103
HA & EC (1:7)	0	-	-
	400	83	104
	1000	87	106

Chapter 5: CONCLUSIONS & RECOMMENDATIONS

In conclusion, it was found from the tests conducted that the plant extracts used exhibit good inhibition towards mild steel corrosion in 1M HCL environment. The inhibition efficiency of all plant extracts increased with increasing concentration of the active material. The addition of low concentrations of the inhibitor to the system studied led to significant decrease in the corrosion rate in most cases studied. This proves that the use of pure green inhibitors reduces the corrosion rate in the 1M HCl corrosive media and that the inhibition efficiency of the tested natural inhibitors is promising. The inhibition efficiency changes when changing the ratio of the mixture used. This means that some inhibitors are proven to have more inhibition in corrosive media compared to other green inhibitors. The study proved the high inhibitive effect of all inhibitors used on mild steel sheets.

Electrochemical analysis shows that the natural inhibitors used are of mixed-type inhibitors without modifying the mechanism of hydrogen evolution. AC impedance plots show that the charge transfer resistance increases with the increase of the inhibitor concentration. The decrease in charge density as the concentration of inhibitor increases indicates that the corrosion rate is reduced and the inhibition efficiency of inhibitors increases. It was found that as the concentration of the inhibitor increases, R_{ct} and R_s values increase, whereas values of C_{dl} decrease. The reason is due to adsorption of the inhibitor molecules on the mild steel surface. R_{ct} values are the R_p values, both of which are inversely proportional to the corrosion rate. This proves a reduction in the corrosion rate and an increase in the inhibition efficiency as the inhibitor is added to the solution. The increase in the temperature of the system causes a decrease in the inhibition efficiency and an increase in the corrosion rate of the mild steel specimen. The result may be due to the fact that the film forming at the mild steel surface becomes weaker as the temperature increases. The results obtained from all tests are considered accurate and in agreement with each other with a 93% confidence.

The plant extracts follows Langmuir adsorption isotherm. Moreover, the process of adsorption is spontaneous, stable and considered to be physical adsorption. The thermodynamic properties recorded suggest that the process of film formation is higher than the destruction of the metal surface and that the adsorption process is exothermic. The increase in temperature causes a decrease in the order of the system, making it less stable. The increase in concentration of the inhibitor causes an increase in the activation energy and a decrease in the exponential factor k.

The comparison made at the end of chapter 4 shows the hight inhibitive action of commercial inhibitors. However, the inhibition efficiencies recorded proves the high inhibitive action of green plant extracts used in this study. This can be concluded because the inhibition efficiencies recorded for commercial inhibitors are comparable with the one's obtained for natural inhibitors.

The studies performed are highly sensitive, therefore, the clean sensitivity in performing the experiment is highly recommended. The mixtures used in this study are chosen by the author and can be changed in order to improve the inhibition action of such mixtures. The study can be conducted using different plant extracts; however, the author chose the studied plant extracts with the knowledge of their high useful properties. It is highly suggested to develop a model describing the inhibition of such inhibitors and it is recommended to make a cost analysis of the process.

These findings are worth comparing with availability, performance, cost and environmental impact of the widely used synthetic and commercially applied corrosion inhibitors. It is also worth evaluating the inhibition performance of these natural chemistries and their mixes when combined with some already proven synthetic chemistries. Furthermore, natural chemistries were evaluated in this study as neat extracts. It would be also be worth investigating impact of formulating mixtures of these with some coactives, synergisers, surfactants and in different solvents to serve a wide range of industrial applications.

REFERENCES

[1] H.A. Sorkhabi, D. Seifzadeh, M.G. Hosseini, EN, "EIS and polarization studies to evaluate the inhibition effect of 3H-phenothiazin-3-one, 7-dimethylamine on mild steel corrosion in 1 M HCl solution", *Corrosion Science*, vol.50, p.3363, 2008.

[2] E. E. Oguzie " Evaluation of the inhibitive effect of some plant extracts on the acid corrosion of mild steel", *Corrosion science*, vol.50, p.2993, 2008.

[3] H.A. Sorkhabi, E. Asghari, "Effect of hydrodynamic conditions on the inhibition performance of l-methionine as a green inhibitor", *Electrochimica Acta*, vol.54, p.162, 2008.

[4] E.E. Oguzie, "Studies on the inhibitive effect of Occimum viridis extract on the acid corrosion of mild steel", *Corrosion Science*, vol.99, pp.441-446, 2006.

[5] P.C. Okafor, M.E. Ikpi, I.E. Uwah, E.E. Ebenso, U.J. Ekpe, S.A. Umoren, "Inhibitory action of Phyllanthus amarus extracts on the corrosion of mild steel in acidic media", *Corrosion Science*, vol.50, p.2310, 2008.

[6] I. Radojcic, K. Berkovic, S. Kovac, J.V. Furac, "Natural honey and black radish juice as tin corrosion inhibitors", *Corrosion Science*, vol.50, p.1498, 2008.

[7] K.M. Ismail, "Evaluation of cysteine as environmentally friendly corrosion inhibitor for copper in neutral and acidic chloride solutions", *Electrochimica Acta*, vol.52, p.7811, 2007.

[8] P.B. Raja, M.G. Sethuraman, "Natural products as corrosion inhibitor for metals in corrosive media – a review", *Materials Letters*, vol.62, p.113, 2008.

[9] R.S. Goncalves, L.D. Mello, "Electrochemical investigation of ascorbic acid adsorption on low-carbon steel in 0.50 M Na2SO4 solutions", *Corrosion Science*, vol.43, p.457, 2001.

[10] T. Fallavena, M. Antonow, R.S. Goncalves, "Caffeine as non-toxic corrosion inhibitor for copper in aqueous solutions of potassium nitrate", *Applied Surface Science,* vol.253, p.556, 2006.

[11] A. Bouyanzer, B. Hammouti, L. Majidi, "Pennyroyal oil from Mentha pulegium as corrosion inhibitor for steel in 1 M HCl", *Materials Letters.* vol.60, p.2840, 2006.

[12] D.Q. Zhang, Q.R. Cai, L.X. Gao, K.Y. Lee, "Effect of serine, threonine and glutamic acid on the corrosion of copper in aerated hydrochloric acid", *Corrosion Science,* vol.50, p.3615, 2008.

[13] L. Craig. Brooks, S.P.Domasky, H.Kyle, "Corrosion is a Structural and Economic Problem: Transforming Metrics to a Life Prediction Method", Workshop on *"Fatigue in the Presence of Corrosion",* October 1998.

[14] J.R. Davis. (2000). *Corrosion: Understanding the Basics.* (1st edition) [Online]. Available: www.ebook3000.com/Corrosion--Understanding-the-Basics.

[15] D. Mercier, M.G. Barthés-Labrousse, "The role of chelating agents on the corrosion mechanisms of aluminium in alkaline aqueous solutions", *Corrosion Science,* vol.51, pp.339–348, 2009.

[16] M.A. Brett., *Electrochemistry Principles, Methods and Applications*, New York: Oxford Press, 1993.

[17] M. M. Antonijevic and M. B. Petrovic, "Copper Corrosion Inhibitors.A review", *International Journal of Electrochemical Science,* vol.3, pp.1–28, 2008.

[18] S. Akhtar and M.A.Mumtaz, A. Quraishi, "Use Of Chemical Corrosion Inhibitors For Protection Of Metallic Fiber Reinforcement In Ferrocement Composites", *The Arabian Journal for Science and Engineering,* vol.34, pp.105-113, 2009.

[19].J.Buchweishaija, G.S. Mhinzi. "Natural Products as a Source of Environmentally Friendly Corrosion Inhibitors: The Case of Gum Exudate from Acacia seyal var. seyal, Portugaliae*", Electrochimica Acta,* vol.26, pp.257-265, 2008.

[20] Satapathy, A.K., Gunasekaran, G., Sahoo, S.C., Kumar Amit, and Rodrigues, P.V. "Corrosion inhibition by Justicia gendarussa plant extract in hydrochloric acid solution", *Corrosion Science,* vol. 51, pp.2848-2856, 2009.

[21] El-Etre, A.Y. ” Inhibition of acid corrosion of carbon steel using aqueous extract of olive leaves”, *Journal of Colloid and Interface Science,* vol.314, pp.578-583, 2007.

[22] O.K. Abiola, J.O.E. Otaigbe and O.J. Kio, “Gossipium hirsutum. L extracts as green corrosion inhibitor for aluminum in NaOH solution”, *Corrosion Science,* vol.51, pp.1879–1881, 2009.

[23] El-Etre, A.Y. and El-Tantawi, Z. “Inhibition of metallic corrosion using Ficus extract”, *Portugaliae Electrochimica Acta*, vol.24, pp.347-356, 2006.

[24] Pandian, B.R. and Sethuraman, M.G. “Inhibitive effect of black pepper extract on the sulphuric acid corrosion of mild steel”, *Materials letters*, vol.62, pp.2977-2979, 2009.

[25] Al-Sehaibani, H. “Evaluation of extracts of henna leaves as environmentally friendly corrosion inhibitors for metals”. *Materialwissenschaft und Werkstofftechnik,* vol.12, pp.1060-1063, 2000.

[26] Pandian, B.R. and Sethuraman, M.G.” Studies on the inhibitive effect of Datura Stramonium extract on the acid corrosion of mild steel”, *Surafce Review and Letters,* vol. 14, pp.1157-1164, 2007.

[27] N. S. Patel, S. Jauhari, and G. N. Mehta. “Mild Steel Corrosion Inhibition by Bauhinia Purpurea Leaves Extract Ii 1 N Sulphuric Acid”, *The Arabian Journal for Science and Engineering,* vol.34, pp.61-69, 2009.

[28] A.A. El-Shafei, S.A. Abd El-Maksoud and A.S. Fouda, “The role of indole and its derivatives in the pitting corrosion of Al in neutral chloride solution”, *Corrosion Science,* vol.46, pp. 579–590, 2004.

[29] K.F. Khaled, N.Hackerman, “Investigation of the inhibitive effect of orthosubstituted anilines on corrosion of iron in 1 M HCl solutions”, *Electrochimica Acta*, vol.48, p.2715, 2003.

[30] M. Elayyachy, A. El Idrissi, B. Hammouti, “New thio-compounds as corrosion inhibitor for steel in 1 M HCl”, *Corrosion Science*, vol.48, p.2470, 2006.

[31] C.L. Foley, J. Kruger, C.J. Bechtoldt, "Ellipsometric–potentiostatic studies of iron passivity", *Journal of Electrochemical Society*, vol.114, p.994, 1967.

[32] G.L. Scattergood, Corrosion inhibitors for crude oil refineries, corrosion, ASM Handbook, vol. 13, ASM International, 1992.

[33] J. Flis, T. Zakroczymski, "Impedance study of reinforcing steel in simulated pore solution with tannin", *Journal of Electrochemical Soc*iety, vol.143, p.2458, 1996.

[34] S.V.Ramesh, A.V.Adhikari,"N-[4-(diethylamino) benzylidine]- 3-{[8 (trifluoromethyl) quinolin-4-yl] thio} propane hydrazide) as an effective inhibitor of mild steel corrosion in acidmedia", *Materials Chemistry and Physics*, vol.115, pp. 618–627, 2009.

[35] A.M Badie and K.N Moh.." Corrosion Mechanism of Low-Carbon Steel in Industrial Water and Adsorption Thermodynamics in the Presence of Some Plant Extracts", *Journal of Materials Engineering and Performance*, vol.18, pp.1264-1271, 2009.

VITA

Alaa Shanableh, son of Nidal Shanableh and Jakleen Mohammed Adnan, was born in May 7, 1987, in Abu Dhabi, UAE. He graduated with merit from Al-Mutanabi Secondary school in 2005. He got the award of Sheik Mohammed bin Rashid in IT programming in 2005. He attended the American University of Sharjah in January 2006, and received his Bachelor of Science in Chemical Engineering in August 2009. He received the performance award of British Petroleum for his senior design project. After that, he joined the graduate program at the American University of Sharjah in September 2009 to receive a degree of Master of Science in Chemical Engineering. He got a full assistantship during his studies. He helped in teaching undergraduate levels and supervision of the Chemical Engineering labs. He finished his bachelor in three years and a half, and finished his masters after one year and half.